DIAGNOSIS OF HEPATITIS C USING DRIED BLOOD SPOTS

A thesis submitted to The University of Manchester for the degree of Doctor of Philosophy in the Faculty of Biology, Medicine and Health

2020

BENJAMIN S. BROWN

School of Biological Sciences
Division of Infection, Immunity & Respiratory medicine

CONTENTS

Final word count: 60824

1 LIST OF FIGURES

2 LIST OF TABLES

3 LIST OF ABBREVIATIONS

Aa: Amino acid

AcMNPV: *Autographa Californica* nuclear polyhedrosis virus

ALT: Alanine transaminase

Anti-D: Antibody D immune globulin

Anti-HBc: Hepatitis B Core antibody

Anti-HCV: Hepatitis C Antibody

ARS: autonomously replicating sequence

AST: Aspartate transaminase

AUC: Area under curve

BCIP: 5-bromo-4-chloro-3-indolyl phosphate

BmPNV: Bombyx mori

Bp: base pair

BSA: Bovine serum albumin

BV: budded virus

Cath: v-cathepsin

CCD: Charge coupled device

CD4: Cluster of differentiation 4

CD8: Cluster of differentiation 8

CD81: Cluster of Differentiation 81

CEN: Centromere

ChiA: chitinase

CHO: Chinese hamster ovary

CLDN1: Claudin-1

CPA: Clinical Pathology Accreditation

CPE: Cytopathic effect

DAA: Directly Acting Antivirals

dATP: Deoxyadenosine triphosphate

DBS: Dried Blood Spot

E.coli: *Escherichia coli*

E1: Envelope 1

E2: Envelope 2

EASL: European Association for the Study of Liver

ECL: Electroluminescence

EIA: Enzyme Immunoassay

ELISA: Enzyme-linked immunosorbent assay

EMIT: Enzyme multiplied immunoassay technique

ER: Endoplasmic reticulum

ESLD: End stage liver disease

FCS: Foetal calf serum

GP46: Glycoprotein 46

GST: Glutathione-S-transferase

HBsAg: Hepatitis B surface antigen HBsAg

HBV: Hepatitis B Virus

HCC: hepatocellular carcinoma

HCV: Hepatitis C Virus

Hi5: High Five

HIS: Histidine

HIV: Human immunodeficiency virus

HMPPS: Her Majesty's Prison Probation Service

Hr5: Homologous region 5

HRP: Horse Radish Peroxidase

HRV: Human rhinovirus

HSC: Haematopoetic stem cells

IE1: Immediate early 1

IE1: immediate early gene 1

IEC: ion exchange chromatography

IFN-β: Interferon β

IFN-γ: Interferon γ

IgG: Immunoglobulin G

IL-10: Interleukin 10

IMAC: Immobilized metal ion affinity chromatography

kDaK: Kilodalton

LDL: Low density lipid

lef-1: Late-expression factor 1

lef-2: Late-expression factor 2

lef-3: Late-expression factor 3

LIC: Ligation independent cloning

mAb: Monoclonal antibody

MBP: Maltose binding protein

MOI: Multiplicity of Infection

MSD: Meso Scale Discovery

MSM: Men who have sex with men

MVA: Modified Vaccinia Ankara

NaCL: Sodium Chloride

NAD: Nicotinamide adenine dinucleotide

NBT: Nitro blue tetrazolium

Ng: Nanogram

NHS: National Health Service

NI: Nucleoside analogues

NIBSC: National Institute for Biological Standards and Control

Ni-NTA: Nickel-Nitrilotriacetic acid

NK: Natural killer cells

Nm: Nanometre

NNI: Non-nucleoside inhibitors

NPV: Nucleopolyhedrovirus

NS2: Non-structural 2

NS3: Non-structural 3

NS4a: Non-structural 4a

NS4b: Non-structural 4b

NS5a: Non-structural 5a

NS5b: Non-structural 5b

OCLN: Occludin

OD: Optical density

ODV: Occlusion derived virus

ORF: Open reading frame

PCR: Polymerase chain reaction

Pfu: Plaque forming units

PHE: Public Health England

PWID: People who inject drugs

Rc: Recombinant

RE: Restriction Enzyme

RIBA: Recombinant immunoblot assay

RLU: Relative light units

RNA: Ribose Nucleic Acid

ROC: Receiver operating characteristic

Ru(bpy)32+: Tris(bipyridine) ruthenium(II) chloride

SAP: Shrimp Alkaline Phosphatase

SDS-PAGE: Sodium dodecyl sulphate–polyacrylamide gel electrophoresis

SELEX: Systematic evolution of ligands

SF: Soluble Fraction

Sf9: Spodoptera frugiperda 9

SOD: Superoxide dismutase

SP: Supernatant

SR-BI: Scavenger receptor class B type 1

SVR: Sustained virological response

Trx: Thioredoxin

TF: Total Fraction

TGFβ: Transforming growth factor beta

TLR 3: Toll like receptor 3

TMB: 3,3′,5,5′-Tetramethylbenzidine

TNFβ: Tumour necrosis factor 8

Toll-IL-1: Toll Interleukin 1

TPrA: Tri-n-propylamine

UK: United Kingdom

USA: United States America

UTR: Untranslated region

VLDL: Very low density lipid

VLF-1: Very late factor 1

WASP: Wiscott-Aldrich syndrome protein

WHO: World Health Organization

4 ABSTRACT

Hepatitis C virus (HCV) is a major worldwide health issue, infecting approximately 71.1 million people worldwide, with 143 000 thought to be chronically infected in England. The vast majority of these (92.1%) infections are found in injecting drug users. A major breakthrough in screening has been achieved in the past few years with the introduction of increased screening for HCV, specifically targeting the injecting drug user population. Dried blood spots were shown to be a suitable sample type to use in these circumstances, overcoming previous issues caused by poor venous access and limited availability of sufficiently trained phlebotomists and increasing testing in this population. Despite the improvements brought about through the use of this sample type several issues still remain including:

- A large population of injecting drug users are still unaware of their hepatitis C infection.
- Testing from dried blood spots uses commercial CE marked HCV serological assays, but these assays are not CE marked for use with dried blood spots.
- Optimisation of commercial assays has increased the sensitivity achievable from dried blood spots to a high level (97-100%) this does not match that available from serum samples. Only an assay specifically designed for dried blood spot samples will be able to increase the sensitivity past what is currently achievable.
- Reliable identification of acute HCV infection is not currently possible.

The HCV Core, NS3, NS4, NS5a and NS5b proteins were produced using *flash*BAC™ ultra baculovirus expression system. Low protein yield in NS4, NS5a and NS5b protein production was overcome with the use of a baculovirus transfer vector incorporating an anti-apoptotic vankyrin expression cassette. Proteins were purified using immobilized metal affinity chromatography. Solubility issues in the NS4, NS5a and NS5b proteins were overcome using urea or guanidine based solubilisation.

Purified proteins were optimised in individual ELISAs, and their performance assessed for the detection of anti-HCV in both serum and dried blood spot samples. Results from the individual ELISAs were combined to give a multi analyte array type profile. Performance for detection of anti-HCV in serum samples was high, with a sensitivity of 91.6% while maintaining a specificity of 100%. Performance with DBS samples was higher, giving a sensitivity and specificity of 100%. This matched the performance of the commercial Roche Elecsys® anti-HCV assay and improved on the performance of the commercial Ortho anti-HCV assay for screening of anti-HCV from DBS samples, while removing the need for anti-HCV confirmation testing in the majority (93.5%) of samples.

5 DECLARATION

No portion of the work referred to in the thesis has been submitted in support of an application for another degree or qualification of this or any other university or other institute of learning.

6 COPYRIGHT STATEMENT

7 ACKNOWLEDGEMENT

This work was funded by my employer Public Health England. I would like to express special gratitude to my main supervisor Professor Paul Klapper, who has been a great support throughout my career and this PhD. I would also like to express my gratitude to my other supervisors Professor Ray Borrow and Professor Pamela Vallely for their continued support throughout the project. Thank you to all the University medical virology staff who helped me with my laboratory studies, especially David for all his support during my cell culture work and to Yvonne, Colin and Stuart. Plus, a thanks to all my fellow PhD students, especially to Kiing Aik and Katarina who helped me in the beginning and Mohammed who has been very supportive during the end of my studies. I would like to thank Dr. Eddie McKenzie at the Manchester Institute of Biotechnology for all his help with my protein expression work and wish him a full recovery from recent illness.

From my current employment at Public Health England I would like to thank Dr. Nicholas Machin, Dr. Malcom Guiver, Dr. Louise Hesketh and Dr. Shazad Ahmad for allowing me the necessary time away from work to perform my studies. I would also like to thank everyone in the office at work who have helped provide cover for me while I go to University to study including Peter, Ashley, Emma and Tom.

I would like to give a special thanks to my wife Dr. Layla Faqih, my parents David and Vivian, and to my wider family for their support and patience in completing this PhD over the last few years.

8 AUTHOR

Benjamin Brown

HPC Registered Clinical Scientist. Employed at PHE Manchester Laboratory, Virology department since January 2010.

8.1 CONFERENCE AND PUBLICATIONS

Poster Presentation European Society for Clinical Virology, Stresa Italy, September 13-16th 2017. B. Brown, M. Guiver, J. Moorcroft, H. Gill, A. Viratham. "The Roche Cobas 6000 Analyser and Roche Cobas 6800 Analyser, Hepatitis C diagnosis from Dried Blood Spot Samples".

Oral Presentation at Sixth Network Meeting for Users of Multiplex Immune Assays 16-17 May 2018, Manchester, UK. "Development of a Multi-Analyte Assay for Detection of Hepatitis C from DBS Samples".

9 INTRODUCTION

9.1 HEPATITIS C VIRUS

9.1.1 BACKGROUND

The disease caused by hepatitis C virus was originally described as non-A, non-B viral hepatitis and was associated with the occurrence of hepatitis post transfusion. The agent was shown to be transmissible in 1978[1] but was not actually identified and given the name hepatitis C virus (HCV) until 1989[2]. Since then extensive research into the virus has led to a detailed knowledge of the viral structure and replication strategy; diagnostic screening tests to identify infected patients; therapies to treat patients and epidemiological studies to pinpoint and intervene in high risk populations. Despite significant progress, up to 71 million (1% of the world population) individuals are estimated to be chronically infected with HCV[3], and at increased risk of developing liver cirrhosis and subsequent hepatocellular carcinoma.

9.1.2 STRUCTURE AND REPLICATION

HCV is a member of the genus *Hepacivirus* within the *Flaviviridae* virus family. The virus has a positive sense RNA genome of 9.6kb in length, consisting of a single open reading frame flanked by 5' and 3' untranslated regions. When translated, the single open reading frame produces a polypeptide of around 3000 amino acids in length, which is subsequently cleaved into 3 structural proteins and 7 non- structural proteins (Figure 1).

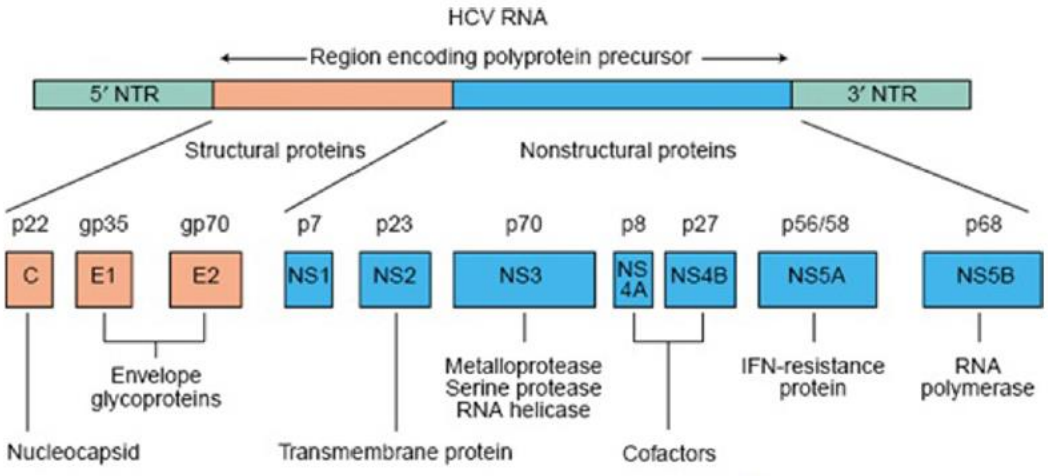

Figure 1 Organisation of the HCV genome. The full 9.6kb genome is translated as a single open reading frame (ORF) into the polyprotein (middle), which if processed to produce 3 structural and 7 non-structural proteins (bottom). Figure taken from[4]

Structural proteins include the 2 envelope proteins E1 and E2 plus the HCV core protein. Non-structural proteins include the p7 ion channel, the NS2 and NS3 proteases, the NS4A polypeptide, the NS4B and NS5A proteins and the HCV RNA dependent RNA polymerase, NS5B[5]. The HCV core protein forms a classical icosahedral structure surrounded by an envelope formed by the E1 and E2 proteins[6], creating a virion of approximately 55 - 65nm in diameter[7] (Figure 2).

Structure of 5' and 3' untranslated region

The 5' UTR region of the HCV genome is highly conserved between different HCV genotypes and plays an essential role in the translation of HCV proteins. It is composed of 4 regions, 1-4, totaling 341 nucleotides in length. Domains 2-4 and the starting 24-40 nucleotide sequence of the HCV core protein make up the internal ribosomal entry site (IRES) complex, responsible for binding to the ribosomal subunit and is essential for the initiation of translation[6]. The 3' UTR is a shorter region involved in virus genome replication. It can be split into 4 regions, starting with a short variable region of 40 nucleotides, followed by a poly U tract and a polypyrimidine tract and finally a highly conserved 98 nucleotide sequence[8].

HCV Core Protein

The HCV core protein is the building block of the HCV nucleocapsid structure, which can be divided into 3 domains. Domain 1, located at the N terminus, is highly basic with numerous arginine and lysine residues and binds to viral RNA via electrostatic interactions[9]. Domain 2, a hydrophobic region located centrally, is responsible for the localisation of core protein onto lipid droplets (LDs)[10]. Domain 3 is a highly hydrophobic region which acts as the signal sequence for the E1 glycoprotein. Domain 3 is removed during processing of protein, with the mature p21 capsid protein comprising only domains 1 and 2[10].

E1 and E2 Glycoproteins

The HCV viral envelope is composed of the proteins E1 and E2. Both proteins are essential for the attachment and entry of the virus into host cells[11], with the receptor binding subunit found in the E2 section of the protein[12]. Both proteins form non-covalently linked heterodimers which are heavily glycosylated, 4 N linked glycan's on the E1 protein and 11 on the E2 protein. Several of these glycan's are critical for virus entry[12]. In addition the glycan's form a shield around the HCV virion aiding it in evasion of the host immune system[13].

p7 protein

The p7 is a hexameric 42kDa viroporin with a flower shaped architecture orientated towards the endoplasmic reticulum (ER) lumen[14]. It is essential for infectivity and is thought to act at a late stage

of the replication cycle [15], likely as an ion channel for the flow of calcium ions from the ER into the cytoplasm[16].

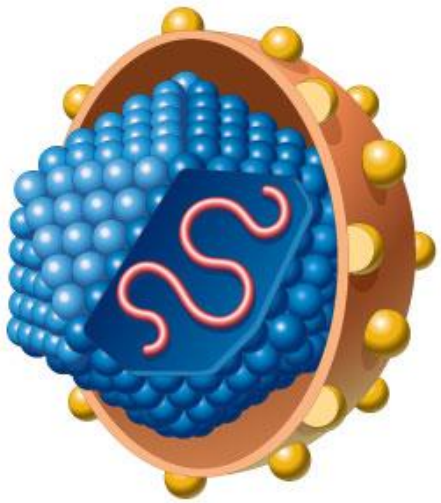

Figure 2 HCV Virion. The viral envelope outer layer consists of the E1 and E2 envelope glycoproteins, with the nucleocapsid composed of repeating units of the single HCV core protein. Taken from http://www.the-scientist.com/?articles.view/articleNo/2433. Accessed 12/02/2014

NS2

The NS2 is a dimeric cysteine protease, consisting of 2 subdomains connected by an extended linker. It contains two composite active sites, which combine with the viral polyprotein and facilitate a single cleavage at the NS2/NS3 junction[17].

NS3/NS4A

The NS3 is a multifunctional protein with protease activity, and through its N-terminal serine protease is involved in the cis-cleavage of NS3/NS4A. It forms a heterodimeric protein with NS4A, and subsequently cleaves at 3 downstream separate sites, NS4A/NS4B, NS4B/NS5A, NS5A/B[18]. In addition to its proteolytic activity the protein is involved in evasion of the immune system through its proteolysis of Toll-IL-1 receptor domain containing adaptor inducing IFN-β[19].

NS4B

The NS4B protein is the least defined of all the HCV proteins, partly due to its highly hydrophobic nature. It is known to reside on the ER and is composed of 4 transmembrane segments [20]. It induces a tight structure consisting of vesicles termed the 'transmembrane web', this web is known to accumulate HCV proteins and forms the viral replication complex in infected cells [21]. In addition to this role the protein is thought to assist in the virus assembly and release processes[22].

NS5A

The NS5A is a membrane associated RNA binding protein with direct involvement in genome replication [23]. The protein contains 3 domains [24] plus an α helix anchor which is embedded in the membrane bilayer [25]. The most well defined is Domain I, this is a highly conserved region which includes an unusual zinc binding motif within the N-terminal, with zinc coordination probably a requirement for function of the NS5A within the viral replication complex[24]. The NS5A protein is a highly phosphorylated protein, with the amount of phosphorylation negatively associated with the level of HCV RNA production [2627]. The domain III c-terminal is not involved in genome replication[28] but has been shown to be essential for HCV particle formation, with the high variability found in this region thought to be a factor in the level of virion production and viral fitness of individual strains[29].

NS5B

The NS5B protein is an RNA dependent RNA polymerase (RdRp) enzyme, approximately 70 Å x 60 Å x 40 Å in dimension. It is composed of 531 residues arranged in the characteristic thumb, palm and finger shape[30], but is given an unusual shape due to the complete encirclement of the palm active site by the finger and thumb domains[31]. The C-terminal acts as a transmembrane anchor for the enzyme [32], which along with other non-structural proteins forms the viral replicase complex[33]. During *de novo* initiation of RNA replication oligomeric interactions between RdRp subunits causes a conformational change in the thumb domain, to open up the closed formation and allow replication to start [34],[35].

9.1.3 HCV REPLICATION

The HCV virion can be found as 3 different forms inside the host termed the very low to low, intermediate, and high density fractions[36]. The classical form is found in the intermediate fraction, the high density fraction contains non-enveloped naked nucleocapsids often bound by immunoglobulins [37] and the low density fraction contains lipid associated virions, as either low density lipid (LDL) or very low density lipid forms(VLDL)[38]. These low forms are associated with a high infectivity and are referred to as 'lipo viro' particles[39].

Numerous host cell proteins are involved in the attachment and entry of these lipo viro particles into cells, including glycosoaminoglycans, CD81, low density lipoprotein receptor, SR-BI and claudin-1[40]. Entry into the cell is pH dependent, with a low pH causing conformational changes in the HCV surface glycoproteins enabling fusion of the membranes and uncoating of the virus [41]. Upon release of the viral RNA into the infected cell translation occurs via the IRES site on the rough endoplasmic reticulum, as one long 3000 amino acid polyprotein. Following translation the polypeptide is cleaved into 10 separate proteins (Figure 1). All the proteins are in some way associated with ER derived

membranes, and via the NS4B membranous web the viral replicase complex is brought together [21]. The RNA genome is replicated by the NS5B RdRp polymerase. A negative strand RNA is copied from the positive strand, from which multiple positive strand copies are produced. These positive strands are then used for further genome replication, viral protein production or viral assembly[41]. The exact steps involved in the late stages of viral assembly are still poorly understood but are likely to involve budding through the ER and exit through a secretory pathway[5].

9.1.4 PATHOGENESIS

Despite a relatively small genome encoding only a few proteins HCV establishes chronic infection in 60-80% of recipients, though a smaller percentage manage to clear the infection naturally. The first line host immune response is interferon based, with IFN-β produced by infected hepatocytes spreading an antiviral state in neighboring non-infected cells. Several HCV proteins play a role in overcoming this initial interferon response, including the NS3/NS4a protein which interferes with the toll like receptor 3 (TLR 3) and retinoic acid inducible gene–1 (Rig-1) pathways, both of which are involved in the downstream IFN signaling and production. Another important IFN pathway, the Jak/Stat pathway induced by IFN-β, is disrupted by overexpression of the HCV core protein (reviewed in [42]). Another important part of the innate immune response, provided by natural killer cells (NK), is affected during infection with HCV. Evidence shows that NK cells, found abundantly in the liver, retain their cytolytic activity but reduce the production of IFN-γ[43], which has important antiviral properties against HCV[44]. The activation of dendritic cells by NK cells in their role as antigen presenting cells, is severely reduced by HCV through an increase in production of the immune regulating cytokines IL-10 and/or TGFβ[45].

The humoral response to HCV does produce neutralising antibodies[46], but these seem to have little effect on clearing the virus from the host. Previous work using chimpanzees highlighted the lack of correlation between antibody levels and clearance of HCV infection, which occurred in several animals despite the poor antibody level[47], with a similar pattern being described in human infections[48]. Due to the very high mutation rate in the RdRp enzyme[49], HCV exists in the host as a quasi-species, with selective pressure exerted by the immune system leading to the emergence of escape mutants which are unaffected by the initial neutralising antibodies[50].

The main immune response in controlling hepatitis C virus infection comes from T-cells. They appear around a month or more after the first appearance of HCV RNA, with the initial T-cell response related to the outcome of acute HCV infection[51]. Patients who formed a strong and lasting CD4+ and CD8+ T cell response clear the HCV infection, while those who have a poor initial or waning T cell response to HCV infection develop chronic infection. CD8+ T-cells are essential to the clearance of infection,

with successful viral clearance linked to sufficient numbers of specific T-cells targeting 8-9 epitopes, compared to only a few epitopes in chronic infection[52]. These specific T-cells can survive for years, improving the chance of clearance if any re-exposure to HCV occurs[53]. A good CD4+ T cell response is seen alongside the CD8+ response in patients who resolve the infection [52,53], and persistence of this initial strong response is required to prevent a rebound of HCV replication and establishment of chronic infection[54]. The ability of HCV to evade and persist in the presence of the cell mediated immune response involves several factors. As with the humoral antibody response, escape mutants with amino acid changes to specific CD8+ T cell epitope targets are created due to selective pressure[55]. However, as chronic infection has developed in patients with a widely targeted T-cell response additional factors such as general impairment in both the CD8+ and CD4+ T cell responses must be considered[56]. Fatigue in CD8+ T cells develops in the establishment of chronic viral infections due to sustained high antigen levels, with the fatigued T cells showing decreased differentiation, proliferation and function[57,58].

The exact mechanism by which HCV causes liver damage is still incompletely understood. Although the majority of damage is thought to be immune mediated, HCV has been shown to induce apoptosis in infected hepatocytes through Bax activated cell stress and pro-apoptotic pathways[5960]. This in turn leads to the activation of Kupfer cells, induction of TNFβ and the deposition of collagen, with repeated cycles leading to fibrosis, cirrhosis and liver failure[61]. Immune mediated damage of the liver is mainly due to cell immunity, whereas in chronic infection the insufficient CD8+ and CD4+ T cell response which cannot clear the virus in the acute phase, is still active enough to significantly contribute to liver injury[62]. Another form of damage is through increased oxidative stress by the induction of reactive oxygen species (ROS) pathways and correlated with increased virus-associated pathologies[63].

9.1.5 CLINICAL

The proportion of patients who develop chronic infection following acquisition of HCV varies widely in different studies and in separate patient groups. Retrospective follow up studies carried out in both Germany and Ireland following administration of a contaminated batch of anti-D immune globulin in the late 1970's found HCV RNA, indicative of chronic infection, in 55% of those positive for anti-HCV[64,65]. Similar rates, 55% developing chronic infection, have been found in follow up studies of children who underwent cardiac surgery in Germany before the introduction of blood borne virus screening[66]. Higher rates of HCV clearance are seen in patients who present with symptoms during the acute phase, with 46% to 66% resolving infection naturally[67--69]. However in studies involving asymptomatic patients, who represent the majority of acute HCV infections, 86% developed chronic infection[70], with similar rates found in community based studies involving predominantly injecting

drug users[71,72]. In the large REVEAL-HCV cohort study carried out in Taiwan, involving around 1000 cases of anti-HCV positive patients there was a significant difference ($p<.001$) in the percentage of developing chronic infection between men and women, 78.8% vs 62.0% respectively, to give an overall rate of 69.3%[73]. A systematic review carried out to provide a better estimate of HCV persistence, involving 31 separate studies, gave a mean value of 74% of HCV infections developing into chronic HCV infection[74].

Acute infection with HCV is predominantly asymptomatic[75], but jaundice can occur in around 15% of patients [76] with or without non-specific symptoms including fatigue, myalgia, low grade fever, right upper quadrant pain, nausea and vomiting[77]. Once HCV becomes established as a chronic infection the possible progression to liver cirrhosis and eventual hepatocellular carcinoma (HCC) depends on several factors, which vary widely according to individual studies. A large study of 2235 untreated HCV infected patients performed in 1997 found that three factors were associated with an increased risk of cirrhosis, age at infection older than 40 years; daily alcohol consumption greater than 50g; and male sex[78]. Another study performed by the same group in 2001 involving 2313 untreated patients confirmed these results[79]. Other factors linked to cirrhosis progression include anti-HBc positive[80], HIV co-infection[81], obesity and diabetes [82], low platelet count and a high AST level [83]. A large systematic review from 2003 aimed to identify significant risk factors from a group of 57 studies, with male gender, heavy alcohol consumption, elevated ALT levels and histological grade of inflammation the significant independent factors identified. Overall risk for developing liver cirrhosis ranged from 10% after 30 years for a woman with no risk factors compared to 25% after 30 years for men who drank heavily, had elevated ALTs and a high histology activity index (HAI) score[84]. Patients who develop liver cirrhosis are at a 4% risk of developing hepatocellular carcinoma at 3 years, 7% at 5 years and 14% at 10 years, with a survival rate of less than 50% after 2 years[85].

Hepatitis C has been linked to several non-hepatic manifestations. The strongest association is with mixed cryoglobulinemia[86] and with an increased risk of non-Hodgkins lymphoma. Other conditions linked to HCV infection include autoimmune thyroid disorders[87], oral lichen planus[88], artherosclerosis[89], membranoproliferative glomerulonephritis[90] and CNS involvement[91].

9.1.6 EPIDEMIOLOGY

Worldwide

The worldwide prevalence of viraemic HCV infection is estimated at 1%, equating to 71.1 million (62.5-79.4) people actively infected[3]. This recent calculation by the Polaris Observatory is lower than the previously estimated 2.2-3.0%[92], with the reduction in estimated prevalence predominantly due to lower than expected rates in Africa. The highest prevalence is found in Africa and the Middle East

at over 10%, while the UK has a low prevalence below 1%. HCV genotypes 1-3 remain the most common representing 46% and 22%, respectively, with genotype 2 and 4 at 12%, genotype 6 at 2% and genotype 5 at 1%[93]. Genotype distribution varies by region, with genotype 1 common worldwide, genotype 4 common in North Africa (due to Egypt) and Genotype 3 common in Asia (due to India and Pakistan)[93].

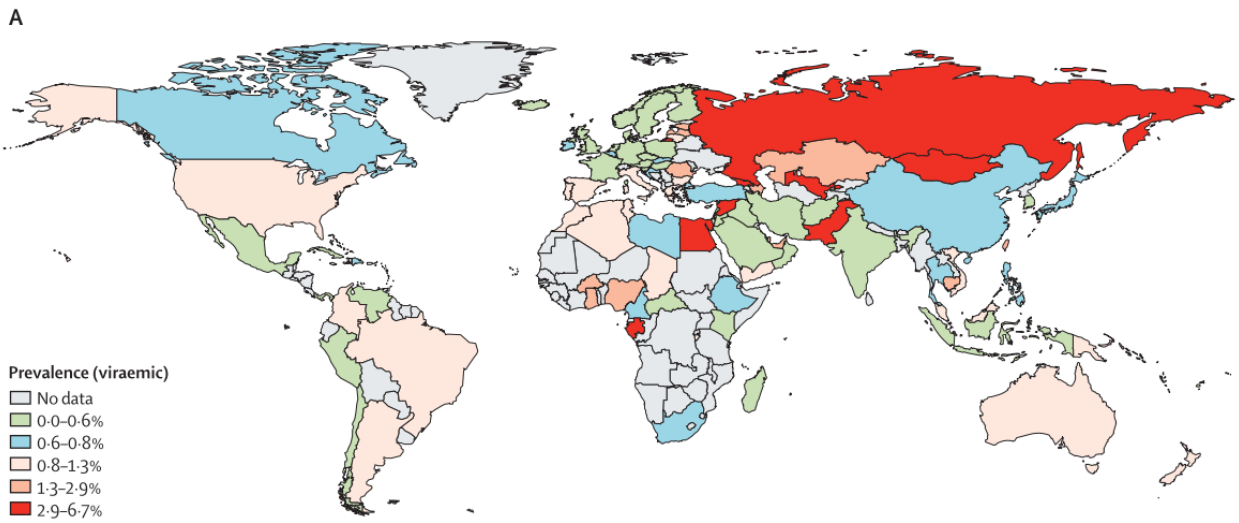

Figure 3 Worldwide prevalence in 2015 of active HCV in countries with approved or estimated models. Taken from [3]

The incidence of new HCV infections was estimated to be 1.75 million new infections worldwide in 2015[94]. The profile of infection varies over geographical areas but can be split into 3 separate patterns of transmission. The pattern seen in the USA and UK involves predominantly infections in the age group 30-49 years old, suggesting relatively recent transmission (10-30 years) in young adults, usually through injecting drug use. Infections in older age groups (Japan, Italy), suggest the majority of infections occurred in the distant past, probably through contaminated blood products and hazardous injecting practices. Infections in all age groups (Egypt) suggest an ongoing risk of transmission, again though contaminated blood products and injecting practices[95]. The picture of transmission changed dramatically in developed countries with the introduction of HCV blood screening in 1992 and the subsequent reduction in risk[96]. Injecting drug use is now the predominant risk factor for HCV transmission in developed countries[97]. However, in developing nations, blood products and unsafe injecting practices are the main route of transmission[98]. The most documented example of this is the high level of HCV in Egypt (15-20% anti-HCV positive) as a result of a mass parenteral anti-schistosomal therapy program introduced in the 1960s and carried out using unsafe injection practices[99]. According to a WHO survey performed in 2008, 39 countries do not routinely screen for blood borne viruses and only 53% of low income countries who do perform screening do

so in a quality assured procedure[100]. However this situation does seem to be improving significantly, with a comparison in transmission of HCV through unsafe injections between 2000 and 2010 showing reduction of 83%[101].

Sexual transmission of HCV is rare, at a rate of 0-0.6% between monogamous heterosexual partners, rising to 0.4-1.8% in those with multiple partners[102]. However certain groups, namely HIV positive homosexual men, are at a significantly increased risk of contracting HCV[102]. Vertical transmission does occur from a HCV infected mother to her baby but the risk is low, with 4-7% of babies acquiring infection during birth[98].

UK

As of 2018 there are an estimated 143000 people chronically infected with HCV currently living in the UK, down from 182400 in 2015[103]. Predominant genotypes are 1 (46%) and 3 (44.2%)[104]. The vast majority of infections, 92.1%, were acquired though injecting drug use[105]. Other populations with a higher incidence include black and ethnic communities with links to high prevalence countries[106].

Injecting Drug Users

The majority of HCV infection resides in the current (44%) or past (43%) injecting drug user population[107]. Data collected anonymously from people who inject psychoactive drugs in England, Wales and Northern Ireland suggest just over half 51% had antibody to HCV in 2018. The HCV RNA (indicating active infection) status was 27% in England, Wales and Northern Ireland[103]. Another group of injecting drug users are those who inject image or performance enhancing drugs (IPEDs), survey data collected in 2014-2015 indicate an anti-HCV positive rate of 5.1%[108]. Data from these anonymous surveys suggest a stable incidence of new infections between 2011 and 2016[109], though there may be a slight increase in incidence in young adults or those who recently started injecting[110].

Progress has been made in trying to improve this situation. The uptake of hepatitis C testing appears to have risen, with those reporting ever being tested for HCV rising from 74% in 2007 to 84% in 2017. However the percentage of those who stated they were aware of their HCV status was 66% in 2017 up from around half in 2016, dropping to only 39% among recent initiates[110], the difference being due in part to the ongoing risk of infection in a proportion of those who have been tested. Another sign of progress is the reduction in the sharing of needles and other injecting paraphernalia, down from 33% in 2002 to 18 % of current injectors in 2017. This has been largely achieved through promotion of needle exchange services and opiate replacement therapy, both of which have been shown to reduce the risk of HCV transmission[111].

Calculating the incidence of new HCV infections can be difficult as the acute phase of HCV infection is predominantly asymptomatic. One way is through the analysis of anti-HCV and HCV RNA results in

survey data, identifying acute HCV infections and with it an estimate of the ongoing incidence of infection. Looking at survey data for young people and recent initiates to drug use is another marker of incidence as most new infections occur in these groups. Using these methods shows transmission in injecting drug users has been relatively stable since 2011, though there has been a slight increase in transmission with recent initiatives to injecting drug use[110].

Other Risk Groups

Previous or current injecting users account for 87% of chronic HCV infections, with the remainder consisting of white/other ethnicity never injecting (7.3%) and South Asian never injectors (5.6%)[107]. The overall prevalence in South Asian never injectors is 0.76%, compared to 0.05% in white/other never injectors. However, when the results are further broken down, the prevalence is 5 times higher in those born in South Asia compared to those born in the UK, with the majority of infection residing in recent immigrants[107]. The prevalence in HIV negative men who have sex with men (MSM) is slightly higher than the overall population, 1.2% vs 0.67%, but rises significantly in MSM who are HIV positive (7.7%), or have had a previous syphilis infection (12.2%)[112]. As the incidence of HIV infection has recently been increasing in London, this may in turn lead to an increase in transmission of HCV between MSMs[113].

Link to Liver Disease

The number of people admitted to hospital with HCV related end stage liver disease (ESLD) or hepatocellular carcinoma (HCC) continued to rise in both England and the UK up to 2014, and modelling predicted a continuing rise in this trend[114]. However, analyses performed on cases between 2011 and 2016 show a tailing off from this rise, with cases remaining relatively stable in those 5 years, at a mean of 1730[115] and dropping off in Scotland. The number of registrations for liver transplants due to HCV cirrhosis has shadowed this rising from 45 in 1996 to 188 in 2013, making up 18% of all liver transplants in 2013[114], before dropping off sharply (40%) in the last three years[105]. Another indicator is the drop off in deaths from ESLD/HCC, which more than doubled between 2005 (209) and 2015 (468), before a fall of 13% between 2015 and 2017 (see Figure 4)[103]. The reduction in ESLD/HCC related transplants and deaths can mainly be attributed to the introduction of new classes of directly acting antivirals for Hepatitis C, which have transformed the success rate for treating HCV, and made it possible to treat advanced cirrhosis negating the need for liver transplants, and reducing deaths.

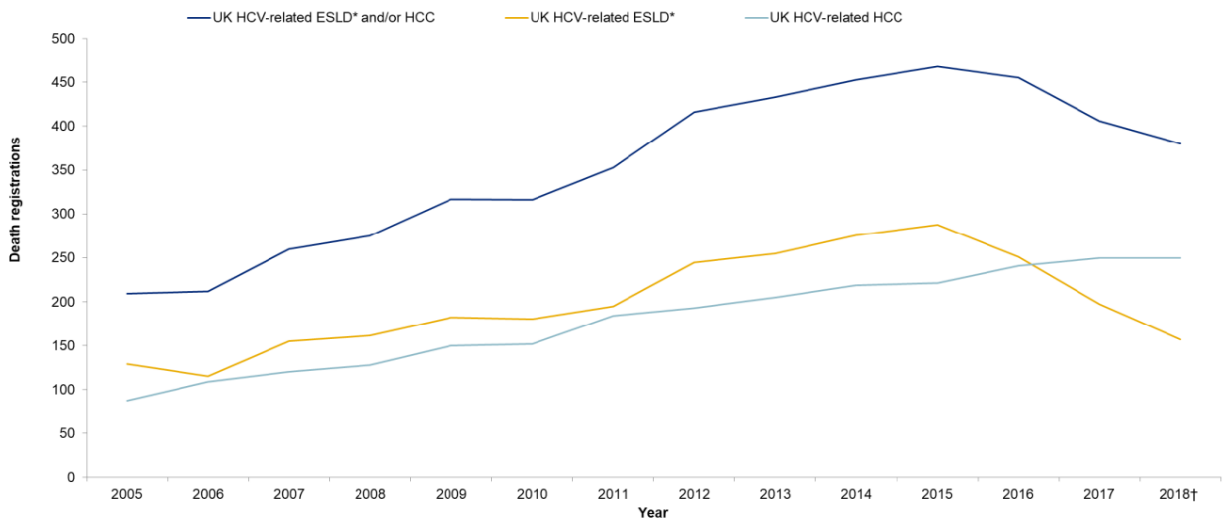

Figure 4 Death registrations* for HCV-related ESLD and HCC in the UK: 2005 to 2018. Taken from**[103]

9.1.6.1 WHO GOAL

In 2016 the World Health Organization (WHO) set out an aim to eliminate Hepatitis B and Hepatitis C by 2030[116]. Currently around 1.7 million people die per year from hepatitis, of which 90% is due to hepatitis B and C viral infection[117]. By eliminating these infections an estimated 7.1 million deaths could be prevented. Elimination of hepatitis B and C as public health concerns means a reduction of new chronic infections by 90% and a reduction in mortality of 65%. The aim is to achieve this by reaching several service coverage targets for hepatitis C, implementing increased screening and

treatment combined with a reduction in transmission through safe blood products and injection equipment (Table 1).

Target areas				Baseline 2015	2020 target	2030 target
Service coverage	Prevention	❶ Three-dose hepatitis B vaccine for infants (coverage %)		82%	90%	90%
		❷ Prevention of mother-to-child transmission of HBV: hepatitis B birth-dose vaccination or other approaches (coverage %)		38%	50%	90%
		❸ Blood and injection safety (coverage %)	Blood safety: donations screened with quality assurance	89%	95%	100%
			Injection safety: use of engineered devices	5%	50%	90%
		❹ Harm reduction (sterile syringe/needle set distributed per person per year for people who inject drugs [PWID])		20	200	300
	❺ Treatment	5a. Diagnosis of HBV and HCV (coverage %)		<5%	30%	90%
		5b. Treatment of HBV and HCV (coverage %)		<1%	5 million (HBV) 3 million (HCV)	80% eligible treated
Impact leading to elimination	Incidence of chronic HBV and HCV infections			6–10 million	30% reduction	90% reduction
	Mortality from chronic HBV and HCV infections			1.46 million	10% reduction	65% reduction

Table 1 Service coverage targets that would eliminate HBV and HCV as public health concerns, 2015-2030[116]

Economic analysis has shown a long-term cost saving by identifying and treating now, over maintaining current levels. Previous interferon based treatments, with efficacy rates of between 42-80%[118,119] were not cost effective for middle and low income countries. The introduction of highly effective DAAs has, however, changed this. Middle income countries can purchase large discounts on new antivirals though national scale purchasing, low income countries may be able to use voluntary licensing agreements for production of generic versions of new HCV medicines, bringing the cost to a viable level. Increases in testing will be needed to identify people for treatment. This will be combined with an increase of testing of blood products to 100%, and 90% of all injections being given with safety engineered devices. All this will need to be combined to reach the target of elimination by 2030.

England

The UK signed up in May 2016 to the WHO target for elimination of HCV by 2030. As part of this the UK has agreed to meet targets in a reduction of incidence in HCV of 80% and a reduction in mortality of 65% by 2030. This will also be achieved by increasing testing and identification of patients,

combined with increased treatments using the new antiviral drugs. NHS England is aiming to treat 15000 people per year up to 2030[109].

Part of the strategy to increase testing was the introduction of "opt out" testing for HCV in prisons. There was an agreement between PHE, NHS England and Her Majesty's Prison Probation Service (HMPPS) to implement a program of 'opt out testing', in a phased implementation, with full implementation by 2017-18[120]. HCV tests are now offered to prisoners when they are admitted or transferred to new prisons. This provides an ideal opportunity to increase testing, as drug users can be tested and treated while in a fixed location. As of November 2017, 75% of prisons in England had implemented testing, with a seven fold increase in testing from 4% to 29%. The target for implementation is an increase in testing to a minimum of 75%[121].

9.1.7 TREATMENT

Treatment for HCV has been based on the use of interferon since discovery of the virus in 1989. Initial treatment consisted of monotherapy with interferon α2b, but even when given 3 times a week for 12 months, only 16% of patients achieved a sustained virological response (SVR; defined as HCV RNA negative after 24 weeks) [122]. A few years later ribavirin was added alongside interferon therapy which improved response rates significantly[123]. Pegylation of the interferon molecule increased its serum half-life and with it further improved response rates when given in combination with ribavirin. However, response to treatment was still variable and was dependent on the HCV genotype. A sustained virological response could be achieved in around 80% of patients with genotypes 2/3, but this dropped to around 43% in patients with genotype 1, and was even lower in patients with cirrhosis or other negative factors[118]. In addition to the variable success rate, unpleasant side effects were common with therapy, including depression, influenza like symptoms, and anaemia[118]. Despite these limitations pegylated interferon/ribavirin remained the only treatment option for HCV for many years. This was partly due to the difficulty in culturing the virus and with it studying its life cycle in the required detail to produce specific antiviral drugs. This remained the case until 1999 when the replicon culturing system for HCV was first introduced[124]. With this came the chance to study the viral life cycle in sufficient detail to identify potential antiviral targets, and this was further improved in 2005 with the discovery of an HCV isolate which undergoes a full life cycle in cell culture[125–127]. In 2011 the first HCV specific antivirals were licensed for use, Boceprevir and Telaprevir, both targeting the NS3 protease. Since their introduction there has been a constant stream of new antivirals, termed directly acting antivirals (DAA), dramatically improving the success rates achieved for treatment of HCV. These antivirals can be classified into 3 main groups based on their specific antiviral targets, NS3/4a, NS5a or NS5b inhibitors.

NS3/4a Inhibitors

The first specific HCV antiviral, named BILN 2061, targeted and inhibited the action of the HCV NS3 serine protease. Though the drug, during preliminary trials from 2003-2005, showed initial success in treating genotype 1 infections it never reached the market due to high relapse rates and safety concerns[128,129]. It was not until 2011 that the first HCV antivirals, Boceprevir and Telaprevir, were licensed for use in combination with pegylated interferon/ribavarin. Both drugs are NS3 protease inhibitors designed for the treatment of genotype 1 infections, in which they improve response rates from 40-50% for pegylated interferon/ribavarin alone, to 70-80% when combined with either drug[130–132]. Despite these improved response rates, both drugs suffer from a low barrier to resistance, a poor toxicity profile, and numerous drug-drug interactions including antiretrovirals, an obvious issue for HCV/HIV co-infected patients. The 2nd generation protease inhibitors, of which Simeprevir was the first to be licensed, promise improved potency against a wider range of genotypes and less toxicity. In clinical trials Simeprevir, again used in combination with ribavirin and pegylated interferon, achieved SVRs of 79-80% in drug naïve and relapsing patients, though the SVR dropped to 31% in non-responders with cirrhosis[133–135]. However, the effectiveness of Simeprevir is limited by the naturally occurring HCV polymorphism Q80K, which leads to a threefold drop in activity[136], and occurs in 25-50% of all genotype 1a isolates[137]. The antiviral was used in combination with other DAA for several years but since the introduction of new antivirals to the market the drug was discontinued in 2018. Currently NS3 protease inhibitors are combined into combination treatments with other classes of DAA, including paritaprevir and grazoprevir.

NS5 Inhibitors

In addition to the protease inhibitors, antiviral drugs have been developed to target the NS5A and NS5B HCV proteins. As the NS5 proteins are relatively conserved over the different genotypes, antivirals inhibiting their action have a wider range of activity than seen with the NS3 protease inhibitors, and have a generally higher barrier to resistance[138].

The exact mode of action of the NS5a inhibitors remains unclear but appear to be involved in inhibition of RNA replication and HCV virion formation (see 9.1.2). Inhibitors of NS5a are generally very potent with good genotype coverage but can have a low barrier to resistance[138]. The first NS5A inhibitor to be licensed was Daclatasvir, which when used in combination with pegylated interferon/ribavirin achieves SVRs of 88% for genotype 2, 87% for genotype 1b, 70% for genotype 3 but only 58% for genotype 1a[139,140]. Newer NS5a inhibitors have been released with better pan-genotypic activity, including valpatasvir and elbasvir, which are given as part of combination DAA therapy.

The NS5b protein is the HCV RNA dependent RNA polymerase, which can be blocked by either nucleoside analogues (NI) or non-nucleoside inhibitors (NNI). As the NS5b is relatively well

conserved, inhibitors have very good cross genotypic activity and are highly effective. The only licensed NS5b inhibitor is Sofosbuvir. It has been shown in numerous trials to be consistently effective for treating HCV infection pan-genotypically in both interferon based and interferon free regimes [141,142,143,144], and now forms the backbone of multiple DAA combination therapies[145]. The alternative type of NS5b inhibitor is a non-nucleoside inhibitor, which binds outside of the nucleoside active site. These are not as potent as NIs and have a lower barrier to resistance. The only currently licensed NNI is dasabuvir, which is given in combination therapies only[138].

Combination Therapies

There has been a series of new antivirals for HCV released since 2011. Some of these such as Simeprevir, were released, used for a couple of years before being removed from the market as new improved antivirals were released. The use of interferon based regimes has decreased over these years and is no longer routinely used in England. All antiviral drugs currently recommended by the European Association for the Study of Liver (EASL) are given as combination therapies, usually combined into a single pill[145]. Sofosbuvir is licensed for use as a single therapy but is not recommended in this format. Some of the combination therapies are pan-genotypic, while others are genotype specific. Treatment duration varies from 8-16 weeks depending on the therapy, genotype, liver cirrhosis score and patient treatment experience. A summary of the current EASL recommendations for treatment of HCV using DAA combinations is shown in Table 2[145].

Commercial Name	NS3 Inhibitor	NS5a Inhibitor	NS5b Inhibitor	Duration	HCV Genotype Indications			
					Non-Cirrhotic		Cirrhotic	
					Naïve	Experienced	Naïve	Experienced
Epclusa		Velpatasvir	Sofosbuvir	12	Pan	Pan	Pan	1a,1b,2,4,5,6
Vosevi	Voxilaprevir	Velpatasvir	Sofosbuvir	12	No	No	No	3
Mavyret	Glecaprevir	Pibrentasvir		8-16	Pan	Pan	Pan	Pan
Harvoni		Ledipasvir	Sofosbuvir	8-12	1a,1b,4,5,6	1b	1a,1b,4,5,6	1b
Viekira Pak	Paritapravir/R+	Ombitasvir	Dasabuvir	8-12	1b	1b	1b	1b
Zepatier	Grazoprevir	Elbasvir		8-12	1a,1b,4	1a,1b	1a,1b,4	1a,1b

Pan = Pan Genotypic, R+ = Ritonavir boosted

Table 2 Summary of EASL recommended DAA treatment for HCV, adapted from [145]

The aim of treating HCV is to eliminate the virus and with it reduce the risk of developing hepatocellular carcinoma. Achieving an SVR has been shown to reduce the rate of decompensation and occurrence of HCC without completely eliminating the risk[145].

Treatment Uptake in England

From 2005 to 2014, when pegylated interferon and ribavirin were used for treatment, an estimated 6326 (21.4%) of those found to be HCV RNA positive were treated[146]. As part of the WHO ambition to eliminate HCV a target of treating 75% of diagnosed patients by 2020 was set[147]. Treatment rates in England have begun to rise since the introduction of the new antivirals. Compared to mean treatment rates between 2008 and 2014 treatment rates rose by 19% in 2015/2016, and 2016/17

rose another 56% compared to the previous year[109]. NHS England has set out targets to continue this rise in treatment, with an aim to treat 15000 people in 2020/21.

9.1.8 VACCINE

Despite the great progress made in treating HCV described in the previous section, for several different reasons, the development of an HCV vaccine could still provide an effective tool for controlling the infection worldwide. A large majority of infected people worldwide are still unaware of their infection; the high cost of the new antivirals may limit their use in resource limited settings and re-infection with HCV can occur even after successful treatment; therefore a vaccine presents an effective way of preventing ongoing transmission of infection[148]. Modelling exercises have predicted a significant reduction in the incidence of infection if an effective vaccine could be developed and targeted at the high risk injecting drug user population[149].

Development of an effective vaccine for HCV has been slow with several difficult challenges to overcome. As stated previously, HCV research was limited by the lack of a cell culture system able to sustain a full HCV life cycle until 2005[127], though progress in this area has continued[150]. Another challenge has been the lack of an easy to use animal model currently, chimpanzees are the only animal known to be susceptible to HCV. As work with chimpanzees is expensive, and using them at all for research purposes is increasingly being questioned on ethical grounds[151], an alternative animal model to work with would be valuable. The ideal animal for laboratory research is mice, but mice are not naturally susceptible to HCV. One approach is to graft hepatocytes into severe combined immunodeficient (SCID) mice, resulting in a full life cycle producing complete HCV virions which can be transmitted between mice[152]. The lack of an adaptive immune system in this animal model limits the research possible, without the ability to study immune reaction and vaccine challenge studies are difficult[153]. More recent approaches have combined the grafting of human hepatocytes with human haemopoietic stem cells (HSC), which produce a human like immune response to HCV. Another alternative is an immunocompetent mouse genetically modified to include the human receptors CD81, SR-BI, CLDN1 and/or OCLN required for HCV entry into cells, however such a model limits study to only a few steps of the HCV life cycle[154].

The second major challenge facing development of an effective vaccine is the ability of the virus to establish chronic infection in the majority of people exposed. As described in the pathogenesis section (1.1.3), HCV evades and manipulates the immune system enabling it to persist in the liver. Vaccines aimed at producing a neutralising antibody response must overcome the variability found in the 2 envelope glycoproteins, including the hyper variable region found in E2[155]. In addition, as CD4+ and

CD8+ responses have been shown to be directly linked to HCV clearance (See 1.1.3), stimulating a good cell mediated response is thought to be important for a vaccine to be effective.

Development of potential vaccines has taken several different approaches. One is the use of recombinant proteins, successfully used for the production of the hepatitis B virus (HBV) vaccine. A vaccine using the E1 and E2 glycoproteins, derived from an HCV genotype 1 viral strain and subsequently expressed in recombinant vaccinia virus grown in HeLa cells, was combined with the adjuvants MF59 and MF75 to improve the immune response[156]. Subsequent trials in chimpanzees have shown some success, with the production of high levels of neutralising antibody and the prevention of chronic infection when challenged with genotype 1 virus strains[156]. Subsequent phase 1 safety trials in humans have been successful[157], with the production of strong neutralising antibody responses to E1/E2 proteins of genotype 1, and at a reduced level to genotype 2[158]. An obvious limitation of these studies was the challenge and protection against only genotype 1 strain viruses, though there is evidence for cross protection against different HCV genotypes from monoclonal antibodies[159]. Further development of this vaccine is warranted[160].

An alternative approach is the use of viral vectors, which offer the possible advantage of stimulating very strong T cell responses, so long as the reduction and blocking of the wanted response by the host immune system to the viral vector can be avoided[161]. Adenovirus is a popular choice as a viral vector due to its protein expression, rapid immune stimulation and known infection profile in humans[162]. To improve the immune response further a prime/boost method can be used, either with 2 distinct viruses[163] or a DNA primer/virus boost combination[164]. One example of this incorporated the NS3, NS4 and NS5 non-structural proteins into 2 distinct rare adenoviruses, one human (Ad6) and one chimpanzee strain (Ad3Ch3)[163]. Rare adenoviruses were chosen in the hope that pre-existing immunity would be low or non-existent. When trialed in humans the vaccine was well tolerated and successfully stimulated a good T-cell response for 1 year, though secondary boosting was limited probably by the initial T cell response[163]. To improve the boosting effect a new vaccine, replacing the Ad6 vector with a MVA viral vector, has been developed and is currently undergoing phase 2 clinical trials as a prophylactic vaccine in high-risk PWIDs[165]. Potentially the most effective vaccine will include both approaches, combining the strong antibody response from the recombinant envelope proteins with the improved cell mediated response provided by a viral vector based vaccine[166].

Vaccines have also been trialed for treatment purposes for chronically infected patients[166], though with the new effective antivirals described in the previous section now coming onto the market (section 1.1.7), the application of this type of vaccine may be limited.

9.2 IMMUNOASSAY

9.2.1 HISTORY OF THE IMMUNOASSAY

The first appearance of immunoassays was in 1960, when Yalow and Berson published a description of a radioimmunoassay for the detection of insulin[167], and Ekins a radioimmunoassay for the detection of thyroxine binding protein[168]. Both assays worked on the same general principles: a detectable antigen (e.g. insulin or thyroxine); a binding agent (antibody or thyroxine-binding protein); a means of separating bound complexes from unbound reactants and a detection method to detect any bound complexes[169]. In the original immunoassays (radioimmunoassays) a radioactive label was used for the detection of any bound antigen/antibody complexes. The first radioactive label was iodine-131, which emitted both β and γ radiation and was hazardous. Safety was improved with the introduction of Iodine-125 as an alternative label, emitting weaker γ radiation than iodine-131, but the use of any radioactive material still presented hazards and required the use of specialised laboratories. Using enzymes as a detection method was initially rejected on the basis that such a large protein would interfere with the steric properties of the binding process, yet despite these reservations, immunoassays using enzymes as the detection agent first appeared in 1971. An Enzyme Immunoassay (EIA) for the detection of IgG in rabbit serum using alkaline phosphatase as a reporter was published by Van Weeman and Schuurs[170], and Engvall and Pearlman described the first Enzyme-linked immunosorbent assay (ELISA) using the enzyme horseradish peroxidase as a reporter[171]. The first assay for a viral target, and the first immunoassay commercialised, was the Abbott AusRIA test for HBsAg developed in 1974[172] followed soon thereafter by the first solid phase EIA for the detection of Hepatitis B surface antigen (HBsAg)[173]. Subsequently a large number of enzyme immunoassays have been introduced for a wide range of targets, using a variety of different techniques.

9.2.2 TYPES OF ENZYME IMMUNOASSAYS

Enzyme immunoassays can be categorised via a range of different criteria. Below is a brief description of the common types of EIA.

ELISA

The ELISA form of immunoassay has been the most common form of immunoassay developed in 1971. These are heterogenous enzyme immunoassays, meaning the antigen-antibody complex must be separated from any free antigen or antibodies before the reporting phase is performed. Below is an outline of the different ELISA formats.

Direct ELISA Format

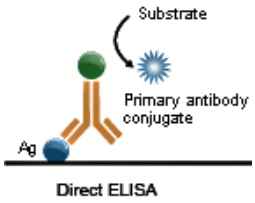

Figure 5 Direct ELISA. Taken from: http://www.abnova.com/support/resources/ELISA.asp. Accessed 12/02/2014

This is the simplest format of ELISA. In the direct assay an antigen is absorbed to a solid phase, usually a 96 well polystyrene plate, to which an antibody specific to the antigen is added and binds to the immobilised antigen. The enzyme for detection is conjugated directly to the primary antibody. Washing removes the unbound antibody after which the enzyme's substrate is added. This form is rarely used in ELISA formats but more commonly used for direct detection of antigens in tissues.

Advantages:

Technique is fast and simple.

Cross reactivity from the 2nd antibody is eliminated.

Disadvantages:

Not suitable for crude samples (blood) as the high level of proteins interferes with the targets absorption to the plastic surface.

Conjugation of the enzyme to the primary antibody may alter its binding properties.

No amplification of the signal.

Primary antibody must be labelled separately for each target.

Indirect ELISA Detection

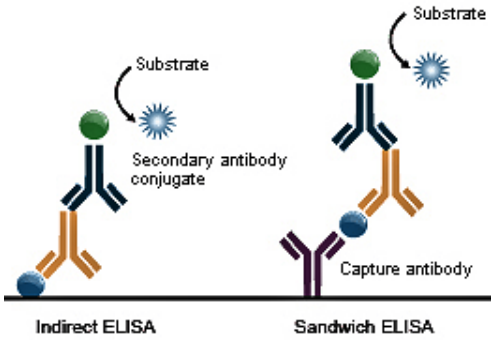

Figure 6 Indirect ELISA. Taken from: http://www.abnova.com/support/resources/ELISA.asp Accessed 12/02/2014

In the indirect format, an antigen is absorbed to a solid phase. The primary antibody specific to the antigen then binds to the antigen before the addition of a secondary antibody conjugated to the enzyme, before addition of an enzyme substrate. Wash steps are performed between each step to remove any unbound antibodies. This is the common format used for the detection of antibodies.

In the capture assay sandwich, an antibody (capture antibody) is bound to the solid phase. Any target antigen in the sample will bind to the capture antibody at a specific epitope site. The primary antibody is then added which binds to a second separate epitope on the antigen. Finally, the secondary antibody with the conjugated enzyme is added, followed by the enzyme substrate. Again, wash steps are performed between each step to remove any unbound antibodies/antigens. This is the most common format used for the detection of antigens.

Advantages:

High sensitivity. Amplification of signal due to multiple bindings of secondary antibody to the primary antibody.

Large quantities of secondary antibody can be conjugated to an enzyme and used in multiple assays.

Wide range of commercially available secondary antibodies.

Binding properties of the primary antibody are not altered by conjugation to the enzyme.

Disadvantages

Extra step involved in the process.

For sandwich assay the antigen must contain 2 suitable epitopes for antibody binding.

Possible cross reactivity from the addition of the second antibody.

Competitive ELISA

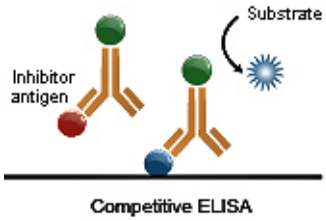

Figure 7 Competitive ELISA. Taken from: http://www.abnova.com/support/resources/ELISA.asp Accessed 12/02/2014

In the competitive assay format, an enzyme conjugated antibody and antibody within the sample compete with each other to bind to the immobilized antigen. The enzyme substrate is then added, with the colour change inversely proportional to the amount of antibody in the sample. The same principle can be used for the detection of antigens, with a capture antibody bound to the solid phase and an enzyme conjugated antigen competing with antigen in the sample. This system, through the use of standards, can be used to quantify the amount of target antigen/antibody in the sample.

Homogenous Enzyme Immunoassay

In homogenous enzyme immunoassays the bound antigen/antibody complex does not require a washing step before the detection phase begins. An example of this is the enzyme multiplied immunoassay technique (EMIT). The assay takes advantage of the changes in the activity of the enzyme, due to steric hindrance, brought about by binding of the antibody to the antigen. For instance, the enzyme glucose 6 hydrogenase will change its absorption at 340nm, due to the conversion of NAD+ to NADH, when the target analyte binds causing a conformational change. The system is fast and simple but is insensitive when compared to heterogenous assays like the ELISA format. This format is commonly used to detect low weight analytes e.g. drugs.

9.2.3 MULTIANALYTE ENZYME IMMUNOASSAYS

Multiplexing of separate immunoassays involves the screening of multiple analytes from a single reaction well. This is an attractive benefit for testing samples of limited volume, obtaining more results and taking less time than running individual assays for each analyte[174]. Different approaches to the multiplexing of immunoassays include variations of standard ELISA techniques and the use of multi-analyte bead array technology.

Multi-analyte ELISA Techniques

The simplest form of multiplexing immunoassays uses the same principles outlined for ELISA techniques above but has numerous defined spots in each well coated with their own capture antigen/antibody.

As standard chemiluminescent signals are generated, for example in a reaction catalyzed by horseradish peroxidase, a normal charge coupled device (CCD) imaging camera can be used to read the plates, no specialised equipment is required.

A modification of this ELISA type approach is the Meso Scale Discovery (MSD) platform. This uses a flat ELISA style plate, with different capture proteins coated onto separate spots within each well. Up to 10 analytes can be screened for in each single well. How this differs from the standard multi-analyte immunoassays described above is in the detection approach employed. The MSD platform uses electroluminescence (ECL) for the detection of analytes. The ECL method was first described in the 1960s[175,176], with the commonly used ruthenium chelates reporter molecules being introduced in the early 1970s[177]. Like chemiluminescence, ECL uses light derived from an electron transfer event, but this is controlled by electric current as opposed to a directed mixing of chemicals. The electric current is used to turn stable precursors into reactive intermediates, which then react together resulting in excited states capable of emitting light. The reactions can be separated into 2 groups based on the pathway used to generate the excited state, the annihilation pathway or the co-reactant pathway. The general principle for an annihilation pathway is listed below.

$$A - e^- \rightarrow A^{\bullet +} \text{ (oxidation at electrode)}$$

$$A + e^- \rightarrow A^{\bullet -} \text{ (reduction at electrode)}$$

$$A^{\bullet -} + A^{\bullet +} \rightarrow A^{\bullet} + A \text{ (excited-state formation)}$$

$$A^{\bullet} \rightarrow A + h\nu \text{ (light emission)}$$

The first 2 reactions outline the oxidation and reduction processes occurring at the surface of the electrode. The 2 products then react together to produce a ground state and an electronically excited state, which return to the ground state through the emission of light. A commonly used ECL luminophore is $Ru(bpy)_3^{2+}$, which, by alternate pulsing of the electrode potential, forms both oxidized and reduced states of the luminophore[177].

$$Ru(bpy)_3^{2+} - e^- \rightarrow Ru(bpy)_3^{3+}$$

$$Ru(bpy)_3^{2+} + e^- \rightarrow Ru(bpy)_3^{+}$$

The 2 forms then react together to give a ground and an excited state.

$$Ru(bpy)_3^{3+} + Ru(bpy)_3^{+} \rightarrow Ru(bpy)_3^{\bullet 2+} + Ru(bpy)_3^{2+}$$

The excited state, $Ru(bpy)_3^{\bullet 2+}$, then returns to a ground state through the emission of a photon of light at 610nm.

$$Ru(bpy)_3^{\bullet 2+} \rightarrow Ru(bpy)_3^{2+} + \text{photon (610nm)}$$

A second alternative is the co-reactant pathway, which is used in many different applications including the MSD platform. In this pathway a co-reactant is used which can undergo oxidation or reduction, this in turn reacts with the ECL luminophore pushing it into an excited state. Using a co-reactant enables the generation of ECL using a single oxidising or reducing potential step, as opposed to the annihilation pathway which requires 2 steps, one for oxidation and one for reduction. The need for only a single potential step is a major advantage. Water has a narrow potential range, too narrow to easily generate both the anion and cation required for electrochemical oxidation and reduction. As a result, annihilation derived ECL must be performed in strictly controlled non-aqueous solvents. Using a co-reactant means only a single potential step in either direction is required, enabling its use in aqueous solutions opening up the possibility of using biological materials in the system[178].

The co-reactant used in the MSD system is tri-n-propylamine (TPrA), in combination with the luminophore $Ru(bpy)_3^{2+}$ [179]. The luminophore is used in the format MSD® TAG-NHS-Ester (Ruthenium (II) tris-bipyridine, N-hydroxysuccinimide) (Figure 8). The N-hydroxysuccinimide esters couple to the primary amine groups in proteins, allowing easy attachment to a wide range of proteins.

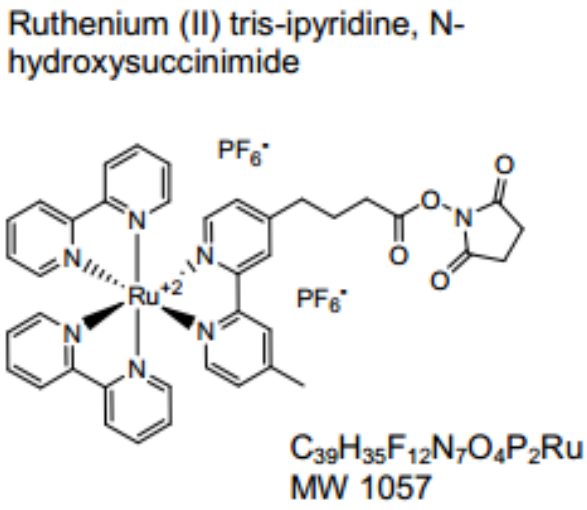

Figure 8 Molecular structure of MSD® TAG-NHS-Ester used for labelling proteins. Take from http://www.meso-scale.com/CatalogSystemWeb/Documents/MSD%20TAG-NHS-Ester.pdf Accessed 12/02/2014

The exact mechanisms of the process of ECL generation via the $Ru(bpy)_3^{2+}$/TPrA pathway has not been fully determined, with several different explanations published[180–182]. A general outline of the process as it is performed in the MSD platform is illustrated in Figure 9.

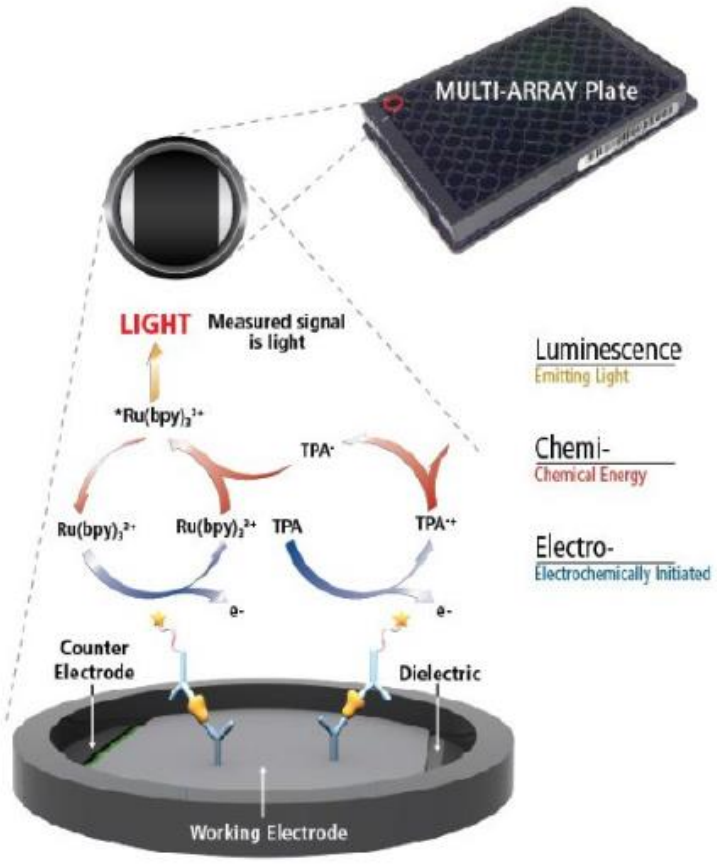

Figure 9 Outline of the Ru(bpy)32+/ TPrA system used in the MSD platform. Taken from http://www.mesoscale.com/CatalogSystemWeb/WebRoot/literature/notes/pdf/Multi_Array_ZF040511A.pdf Accessed 12/02/2014

At the surface of the electrode both $Ru(bpy)_3^{2+}$ and TPrA are oxidized. In the case of the MSD platform the electrode is found on the base of each well and is composed of carbon, onto which immunoglobulins adhere. The $TPrA^{\bullet+}$ radical cation quickly loses a proton to form the reducing intermediate $TPrA^{\bullet}$, which in turn reduces the oxidized $Ru(bpy)_3^{3+}$ to give $Ru(bpy)_3^{\bullet 2+}$. It is from this final excited state that a photon of light at 620nm is emitted. The reaction is energy sufficient, with the electrochemical potential difference between $Ru(bpy)_3^{3+}$ and $TPrA^{\bullet+}$ sufficient to generate the excited state. As a result, at the end of one cycle $Ru(bpy)_3^{2+}$ is produced in its original form ready to start another ECL cycle, meaning that several photons of light can be released in a single measurement cycle[183]. On the modern MSD instruments collection of the light emitted is performed using a CCD camera. This entire process can be performed very quickly, with 96 well plate read times of around 90 seconds.

Advantages of this approach include its flexibility, with both separation and non-separation assays possible, increased sensitivity and dynamic range over standard ELISA formats, speed in obtaining results and the high stability inherent in the MSD® TAG-NHS-Ester [184].

Flow Cytometric Assays

Flow cytometric assays were first used in the 1980's for the measurement of cells in blood[185], followed by its first use as an immunoassay to screen for human IgG[186]. The technique is based on the controlled flow of small polystyrene/latex beads, around 4-6 µm in diameter, past an imaging system for rapid and accurate detection. Capture proteins can be attached to the polystyrene bead, and immunoassays performed in a conventional format. In the final stage the beads are directed past the imaging system and any fluorescent tags on the beads detected.

Attempts to detect multiple analytes using flow cytometry were originally based on using different sized polystyrene beads which the imaging systems could differentiate. By binding different capture proteins to the distinct sized beads, two[187] or up to four analytes[188] could be detected from a single well. Yet this is around the limit of multiplexing if using size to differentiate the beads. To achieve much higher multiplexing capacities a new approach using differentially dyed bead sets was introduced. The FlowMetrix™ system introduced by Luminex in 1997 used 64 distinct bead sets, each identical in size but dyed with different proportions of orange and red fluorescent dyes, giving them a unique profile for identification[189]. Capture molecules, either protein or nucleic acid, are covalently bound to the surface of the beads. A conventional immunosorbent assay is then performed, with a green fluorescent dye used as a reporter (Figure 10).

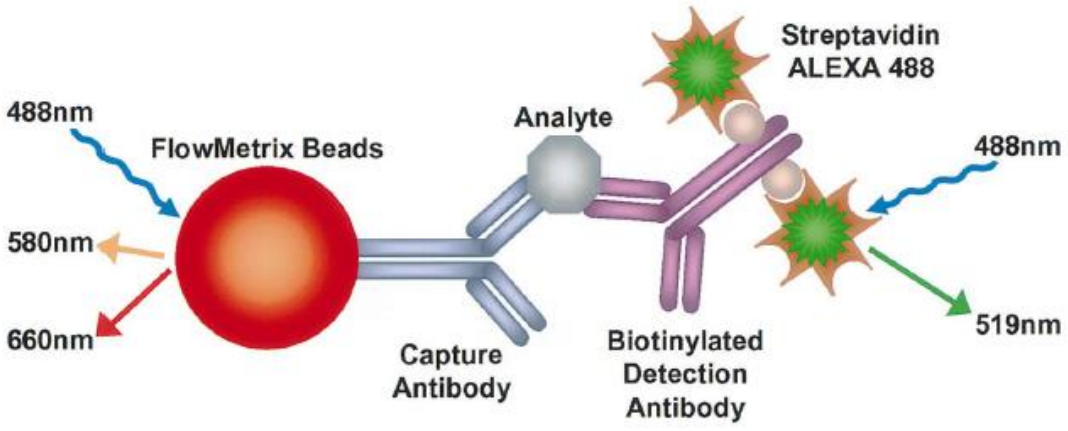

Figure 10 Image of an immunoassay performed using flowmetrix beads. Taken from[190].

In the final stage the beads are placed on the flow cytometer, which passes the beads in a single file past an excitation source, using orange and red fluorescence to identify the bead set and green

fluorescence to identify bound target analyte. The original FlowMetrix™ system used a Becton Dickinson FACScan instrument for flow cytometry purposes, but this was followed by the introduction of an instrument specifically designed for the purpose, the Luminex 100/200. The instrument can identify up to 100 different bead sets based on the proportion of the red and infrared dye sets, termed xMAP technology (Figure 11). The instrument is composed of a flow cytometer and 2 lasers, one at 635nm to identify the beads and the second at 532nm to identify the green fluorescent reporter (Figure 12).

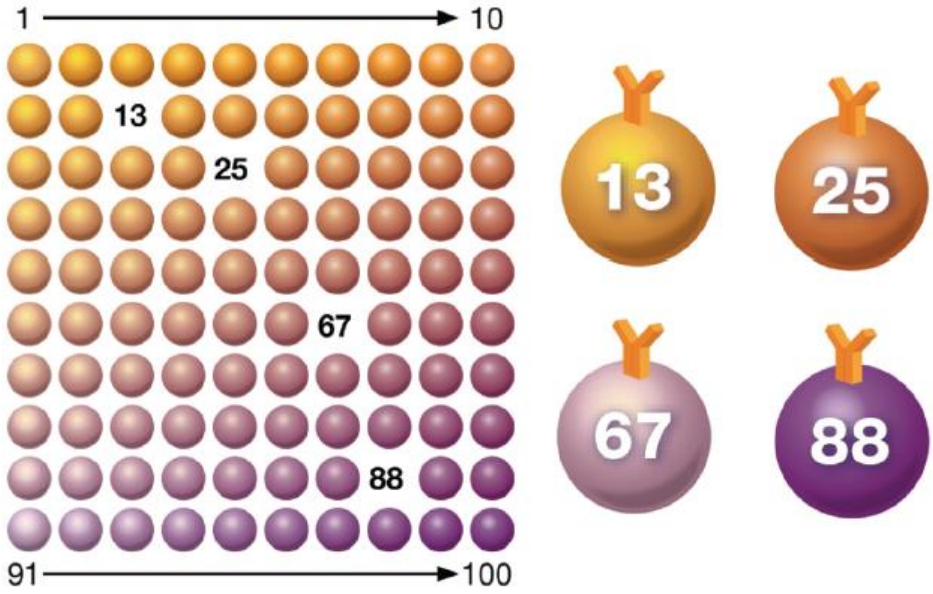

Figure 11 Representation of the xMAP technology bead sets. Each bead set is internally dyed with red and infra-red. Both dyes are used at 10 different concentrations, giving a total of 100 distinct bead sets. Taken from[191]

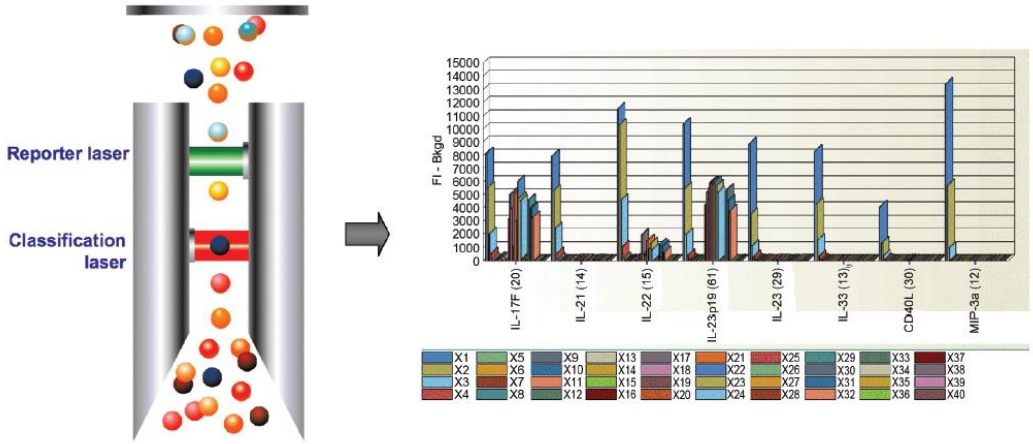

Figure 12 Imaging and data collection from the bead sets. The red laser at 635nm identifies the unique dye set and the reporter laser at 532nm identifies the concentration of analyte. Taken from[191]

Recent developments have increased the number of distinct bead sets up to 500 and introduced a magnetic bead which can be read using a CCD camera avoiding the need for flow cytometry.

The Luminex platform has been a great success since its introduction, with many assays introduced which take advantage of its multiplexing abilities. It offers high sensitivity from a small sample volume, aided by the increased surface area a bead presents over a flat-bottomed plate. There is increased speed of testing as many analytes can be screened for at the same time, and microsphere-based assays allow shorter incubation times and with that use less reagents. Plus almost any type of biological screening assay can be performed using this technology[189].

9.2.4 EIA COMPONENTS

Polyclonal Antibodies

Polyclonal antibodies are produced from the challenge of an animal with an antigen which may be a whole organism, crude fractions of the organism or individual proteins. The polyclonal antibodies produced by the challenged animal are directed against a wide range of epitopes and have a range of avidity. However, the wide range of epitopes targeted may result in target cross-reactivity, leading to a non-specific assay. Specificity can be improved with the use of affinity purification, but this may result in a drop in overall antibody affinity and avidity[169]. Other issues include the variability in individual animals' immune response to different exogenous antigens when challenged, leading to batch to batch variability in quality and quantity of antibodies produced.

Monoclonal Antibodies

Monoclonal antibodies were first described in 1975[192] and feature high specificity and can be manufactured reproducibly. Polyclonal antibody preparations generally have higher average avidities than monoclonal antibody preparations and the high specificity of these antibodies mean that even slight changes in the target epitope may result in the antigen/antibody complex failing to form or binding with significantly reduced affinity. This is likely to be more common with rapidly mutating RNA viruses[169]. Ways around this problem include the use of multiple monoclonal antibodies targeting a variety of epitopes or combining polyclonal and monoclonal antibodies in a sandwich assay format.

Alternatives to antibodies

Alternatives to antibodies produced in animals include the generation of recombinant human antibodies. Peptides[193] and fragments of antibodies[194] can be expressed in *E.coli* through the insertion of DNA fragments into bacteriophages, eventually leading to phage-antibody libraries [195]. The libraries can be very wide ranging, enabling *in-vitro* scanning of a large number of peptides/antibody fragments to identify the most suitable with the highest affinity for the target antigen[196]. This technology is not perfect though, as the antibodies are less stable than those produced in vivo[169].

Rather than using recombinant antibody fragments/peptides, small oligonucleotides have been shown to demonstrate the same epitope binding and mapping abilities. Using systematic evolution of ligands by exponential enrichment (SELEX)[197] the small oligonucleotides produced are termed aptamers. Using combinatorial chemical synthesis of DNA, a random sequence library of aptamers is constructed, each with a unique sequence. On the same principle as screening antigens with random peptide libraries, huge numbers (10^{14} to 10^{15}) of aptamers are used to screen a particular antigen to identify those with the highest affinity. The identified aptamers are subsequently amplified to obtain an enriched library, with the process repeated until saturation is reached[198], resulting in aptamers with a very high specificity[199]. As these are nucleic acids rather than proteins stability can be an issue due to nuclease activity, though modifications to the nucleic acid can be made to address this[200].

9.3 ANTIGEN PRODUCTION

Viral antigens, in this case for hepatitis C, are required to produce an immunoassay to detect infection with HCV. The antigens can either be used for the capture of antibodies in an anti-HCV screening test, or the antigens can be used to produce antibodies for the creation of an HCV antigen screening test. Production of HCV antigens is performed using a variety of recombinant DNA expression systems, where a gene encoding the antigen is cloned into a transfer vector and expressed. The main current technologies for this purpose are either bacterial, yeast, insect or mammalian in origin, each with their own inherent advantages and disadvantages.

9.3.1 BACTERIAL EXPRESSION

Expression of foreign proteins in bacteria, usually *E. coli*, is the most widely established of the protein expression technologies. Advantages of this approach include the relatively low cost, ease of manipulation of the organism, depth of knowledge of the organism, wide availability of vectors and host strains, rapid expression and the possibility of continuous protein production[201]. Due to these advantages many proteins have been produced from *E. coli* based systems, including for commercial use on a large scale. However, a prokaryotic cell cannot perform many of the post translational modifications that are found in eukaryotic cells, including N- and O- linked glycosylation, fatty acid acylation, phosphorylation and disulphide-bond formation, all of which may be required to produce a functional protein[202].

9.3.2 YEAST EXPRESSION

Protein expression in yeasts combines the benefits derived from working with a microorganism to the benefits of expressing protein in a eukaryotic cell. As a unicellular microorganism yeast shares many

of the advantages associated with *E. coli*, including the ease of use, low cost and the possibility of large-scale continuous production. In addition to these benefits yeast can perform many of the post translational modifications *E. coli* is incapable of[203]. *Saccharomyces cerevisiae*, better known as brewer's yeast, is the most commonly used yeast for expression work as it is the most well studied and lacks any known endotoxins for humans. Other common yeasts include *Pichia pastoris* and *Schizosaccharomyces pombe.* Despite the advantages the use of yeast offers, the fact it is a lower eukaryote, results in differences in some post translational modifications compared to mammalian cells, including the formation of N- and O- linked oligosaccharide linkages[202].

9.3.3 MAMMALIAN EXPRESSION

The obvious advantages of using mammalian derived cells is the accurate synthesis, post translational processing and secretion of the desired eukaryotic protein[204]. The most commonly used cell line is Chinese hamster ovary (CHO) derived cells, although many other cell lines exist. The disadvantages inherent in using mammalian cell lines include high cost, complex technology, lower levels of protein expression relative to other protein expression systems, and the potential contamination of the cell lines with human pathogens.

9.3.4 BACULOVIRUS

Baculovirus is a double stranded DNA virus with a closed circular genome between 80-180kb in size[205]. It is part of a diverse family of over 600 species of arthropod insect viruses termed the *Baculoviridae*[206]. The virions are large with a rod like structure, 200µm in length and 40µm in diameter produced in 2 distinct forms, occlusion derived virus (ODV) or budded virus (BV) (Figure 13). Baculovirus can be further separated into 4 genera based on the structure of the occlusion bodies and host species which they infect. Two types of occlusion body exist, the Nucleopolyhedrovirus (NPV) with a polyhedral structure containing many virions, and the Granulovirus genus with ovoid occlusions bodies with a single virion. Viruses which infect leptidopteran species comprise two of the four genera, the alphabaculovirus (leptidopteran-specific NPV) and the betabaculovirus (leptidoptern-specific GV), with the other two genera the gammabaculovirus (hymenopteran-specific NPV) and the deltabaculovirus (dipteran specific NPV)[207]. Using phylogenetic analysis Alphabaculoviruses can be separated into 2 clades[208] , group I and group II, with the most important differences being found in the BV glycoprotein used by the virus to bud from cells and to fuse the viral and cellular membranes. Group I alphabaculoviruses use the GP46 protein for this purpose[209] as opposed to group II alphabaculoviruses, plus the betabaculovirus and the gammabaculovirus all use the non-homologous F protein[210,211]. In addition there are 11 other genes thought to be only found in group I NPVs[212]. The occlusion form is commonly found in soil and on the surface of plants in polyhedral shaped occlusion

bodies termed 'polyhedra'. These occlusion bodies are composed of virions surrounded by a 29-kd protein, polyhedrin, to form a very stable structure which can persist for extended periods in the environment[213]. They remain in this form until ingested by a caterpillar of the host species upon which they dissolve in the high pH (pH10) environment of the midgut and go through the first virus cycle producing the budded virus form which disseminates throughout host tissues[206]. Finally ODV forms are produced in the tissues and disseminate back into the environment[206].

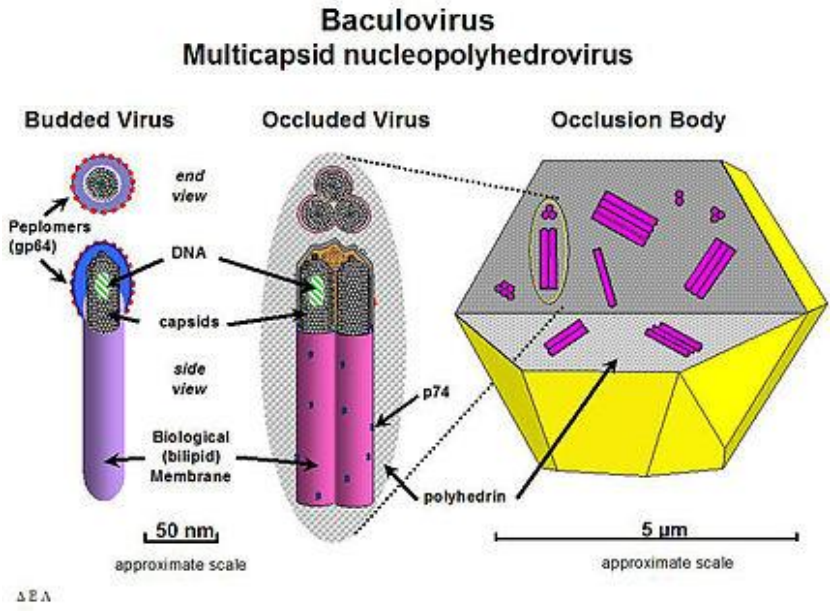

Figure 13 Two distinct forms of baculovirus, the budded virus on the left and the occluded virus in the middle. The occluded virus forms occlusion bodies surrounded by the protein polyhedron. Taken from http://en.wikipedia.org/wiki/Baculovirus Accessed 12/02/2014

The first baculovirus genome to be sequenced was *Autographa Californica* nuclear polyhedrosis virus (AcMNPV)[214], since then the genomes from at least 53 different species have been sequenced[215]. Baculovirus genomes are very diverse but share around 30 common genes involved in RNA transcription and DNA replication, in production of structural proteins, in auxillary proteins and genes to modify host processes[206,216]. The AcMNPV genome contains around 150 open reading frames (ORF)[212], with 62 of these ORFs shared between other lepidopteran specific NPVs and GVs[207].

Baculoviruses are unique among nuclear replicating DNA eukaryotic viruses in that they use both cellular and viral RNA polymerases during the replication cycle[212], and express their genes in 4 different phases[217].

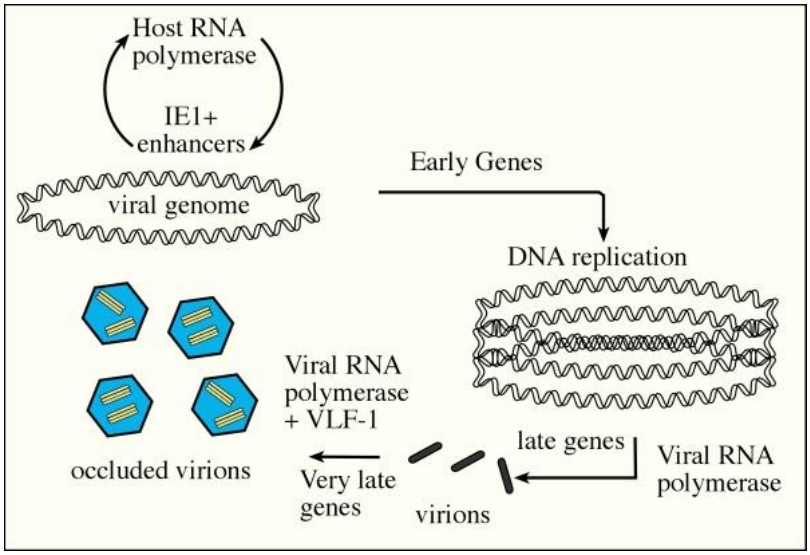

Figure 14 The baculovirus transcriptional cascade showing the interrelationship of host and viral RNA polymerases and DNA replication and VLF-1. Taken from http://www.ncbi.nlm.nih.gov/books/NBK49504/figure/ch04.F1/?report=objectonly Accessed 12/02/2014

The first gene to be transcribed and act is the immediate early gene 1 (IE1), which continues to be transcribed throughout the replication process[218]. It acts as a powerful transcriptional activator[219], through either of 2 possible mechanisms. One involves the direct activation by IE1 and the second involves interaction with the insect host RNA polymerase II and homologous region-bound transcriptional activators[212], recognising baculovirus specific promoters to initiate transcription[220]. Genes transcribed during this early phase include those encoding the viral DNA polymerase, helicase[221], viral DNA dependent RNA polymerase[222], and a collection responsible for initiating late gene expression[223]. Transcription of these early genes is regulated by an unknown factor with the majority switched off early in the virus life cycle[212]. Before transcription of the late genes occurs, the viral DNA must first be replicated. Genes essential for this include the viral DNA polymerase, helicase, late-expression factor 1(lef-1; which acts as a primase), lef-2 (which acts as a primase accessory factor), lef-3 (which is a single stranded DNA binding protein) and IE1 (whose function in DNA replication remains unknown[224,225]). The exact mechanism by which the genome replicates remains unknown but is likely to involve recombination events in a similar process to other large viral DNA genomes e.g. HSV-1[212]. Initial replication of the DNA results in a rapid amplification of the DNA which is then used to transcribe the late genes producing viral proteins required for capsid formation, after which DNA replication and capsid formation fall into synchrony[212]. Transcription of the late genes necessary for capsid formation is performed by the virally encoded RNA polymerase, unusual for viruses which replicate in the nucleus. Following the packaging of viral DNA by capsid proteins to produce the final baculovirus virion, the very late genes are transcribed. During this final very late phase 2 proteins are expressed, the polyhedrin protein[226] and P10. The P10 protein forms a fibular

structure around which the polyhedrin protein can gather to form the occlusion bodies[227], providing a protective shield for the baculovirus virions. Both genes are hyper expressed, producing very large amounts of proteins, a fact which is exploited for the purpose of foreign protein expression. This hyper expression is the result of an interaction between an A/T rich boost sequence and the very late factor 1(VLF-1)[228–230] which have been shown to significantly up regulate the transcription of the very late polyhedrin and p10 proteins[231].

9.3.5 BACULOVIRUS EXPRESSION SYSTEM

As described above baculovirus is produced as 2 separate phenotypes, the ODV and the BV, but from a single genotype. Only the BV type is required for infection of insect cell cultures, meaning the large volumes of polyhedrin and p10 proteins produced to form the ODV are not required[232]. Taking advantage of this fact forms the basis of the baculovirus expression system, as genes to be expressed can be inserted downstream of the powerful polyhedrin and p10 promoters without affecting the infectivity of the virus in cell culture. In addition to this high expression, the baculovirus offers post translational modifications of the protein missing from prokaryotic expression systems; baculoviruses are limited to infections of insects and the insect cells used for culture are not known to be susceptible to any human pathogens; the insect cells, usually lepidopteron derived, are easily cultured in the laboratory and the system can be scaled up to produce large amounts of the required protein[215]. The baculovirus species primarily used for expression work is AcMNPV, with the silk larvae virus *Bombyx mori* (BmPNV), also a member of the genus *Alphabaculovirus*, another effectively used vector[233]. Since the first foreign gene, interferon, was successfully expressed in a Baculovirus by Smith and Summers in 1983[234], many different proteins have been produced using this system. These range from viral proteins used for diagnostic tests[235], viral proteins used for vaccine production[236], proteins produced for the treatment of cancer[237] and recently gene delivery vectors[238].

Genetic Recombination

Originally foreign genes of interest were inserted into the baculovirus genome by the process of homologous recombination[239](Figure 15), with subsequent identification of recombinants by blue white screening and plaque assay purification. The very low level of successful recombination achieved in these early studies led to developments to improve this. Using a linearized plasmid helped to improve the efficiency of the recombination process by up to 30%[240] (Figure 16). This was further improved through the triple digestion of the plasmid in the ORF 1629 gene. The gene is downstream of the polh PP78/83 promoter and encodes the Wiscott-Aldrich syndrome protein (WASP) like PP78/83 protein, which is involved in nuclear actin filament formation and successful completion of the baculovirus life cycle[241,242].The plasmid containing the foreign gene sequence also contains a short sequence to complete the ORF 1629 gene, as a result only viruses which undergo recombination with

the foreign gene will be viable, helping to increase the efficiency up to 99%[243]. Several commercial systems based on this breakthrough have subsequently been released, including Baculogold™ (BD Biosciences) and Bac-N™ (Invitrogen).

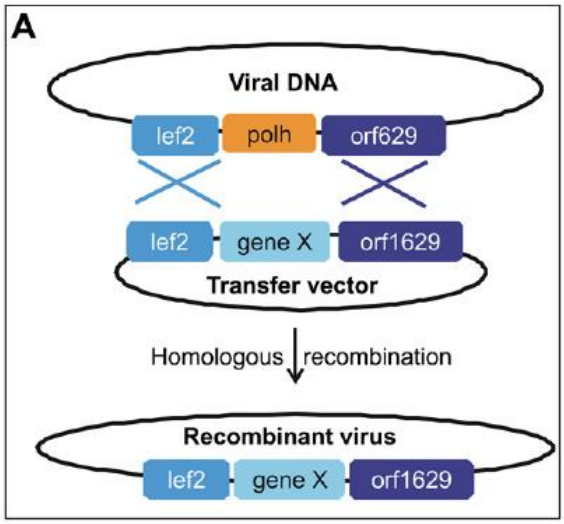

Figure 15 Homologous recombination of Viral DNA and Transfer Vector. Taken from[215]

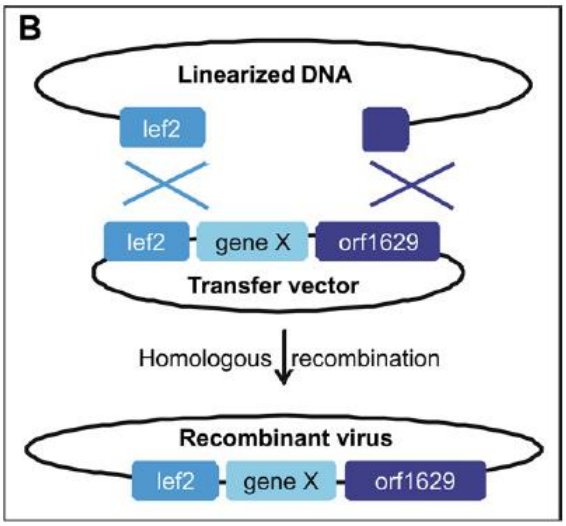

Figure 16 Homologous recombination using Linearised DNA. Taken from[215]

Development of E. coli systems

Despite the developmental improvements to increase recombination efficiency and recovery, the methods described in the previous section still require plaque assay steps to purify and select recombinant virus, a time consuming and complex procedure. In a move to further speed up and simplify the process recombinant baculovirus genomes using a Baculovirus shuttle vector (bacmid) were developed which could be maintained in either yeast or bacterial cells. The first system used the yeast *S. cerevisiae*, the resultant recombinant baculovirus genome containing yeast ARS and CEN

sequences can be replicated and maintained, before successful introduction of the DNA into insect cells[244]. Despite the success in developing a rapid method (10-12 days) which no longer required a time-consuming plaque assay step, it was limited by the lack of compatible transfer vectors. A similar system but replacing the yeast with a special strain of *E. coli* (DH10Bac) was introduced, which used site specific transposition with Tn7 for insertion of foreign genes into the bacmid DNA (Figure 17). This bacmid DNA can be propagated in *E. coli*, and selected through a β-galactosidase selection derived colour change in the colony, further simplifying and speeding up the process (7-10 days from start to finish)[245]. However, only a small percentage of the bacterial colonies contain the recombinant genome. Further improvement was achieved through the incorporation of a lethal gene, *SacB* from *Bacillus amyloliquefaciens,* into a modified donor vector named pBVboost. The *SacB* gene encodes levansucrose which produces levan from sucrose, a lethal substance to the cell. Successful cloning of the foreign gene into the bacmid cassette prevents expression of the *SacB* gene, enabling their selection through growth of the *E. coli* in the presence of sucrose[246]. Though these systems removed the need for plaque purification, recombination in *E. coli* is more complicated compared to homologous recombination in insect cells, requiring several steps in bacterial cells and subsequent DNA purification[247]. The most recent developments in baculovirus systems have used simple homologous recombination without the need for subsequent plaque purification.

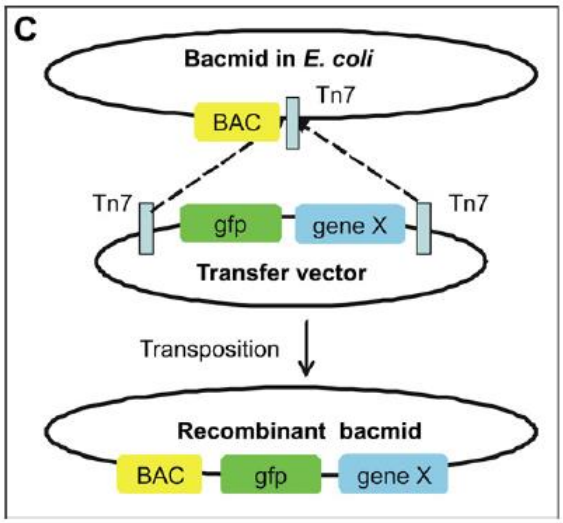

Figure 17 Bacmid system of recombination. Taken from[215]

Combining the principles of homologous recombination with Bacmid technology removes the need for either a selective pressure for identification of recombinants or plaque assay purification. The bacmid technology uses an ACMNPV genome with a cloning site inserted in the essential ORF1629 gene, preventing replication in cell culture. By adding the transfer vector containing the foreign gene and the bacmid DNA directly to the insect cell culture, successful homologous recombination will

remove the BAC gene and replace the orf1629 gene, only recombinant virus will replicate[248] (Figure 18). The virus can then be propagated directly in insect cells, in a process simple enough to enable automation[249]. Commercial systems based on this principle include *flashBAC™* (Oxford Expression Technologies), *BacMagic* (Merck) and *BaculoOne* (PAA).

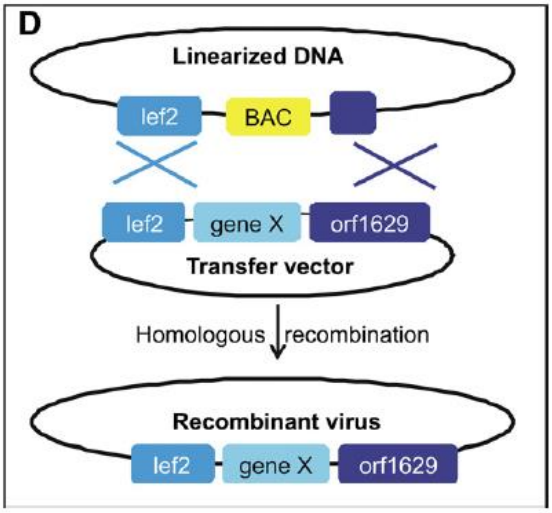

Figure 18 Combination of bacmid and homologous recombination systems. Taken from[215]

Another advantage of this system is the easy removal of non-essential genes. These often encode virulence factors or other functions which are important for insect infections in the wild but have no function related to propagation in cell culture[250,251], the removal of these non-essential genes may improve protein expression and stability[252]. For instance, it has been shown that the removal of the *chitinase* (*chiA*) and *v-cathepsin* (*cath*) genes, both late expressed genes involved in liquefaction of the host insect[253], can improve the stability of the expressed protein[252]. Other proteins identified which are non-essential for propagation in cell culture include *p10*[254], *p74*[255] and *p26*[256]. Deletion of all 5 of these genes, *chiA*, *cath*, *p10*, *p74* and *p26*, from the same bacmid based BEV results in significantly higher levels of protein expression due to a reduction in cellular competition for resources[257]. Commercial kits incorporating these modifications include *flashBAC™* and *BacMagic 3*.

An even more minimalist approach uses an expression vector, pIEx, incorporating the transcriptional elements ie1 and hr5 enhancer for promoting expression of the inserted foreign gene. These elements use endogenous insect transcriptional enzymes to express the foreign gene, without ever producing baculovirus infection of the insect cells[258]. As no recombinant baculovirus need to be produced this method is extremely rapid, with protein produced in a possible 48 hours (around 10 days for BacMagic). This system is commercially available as InsectDirect™ (Merck).

9.4 HEPATITIS C IMMUNOASSAYS

9.4.1 ANTI-HCV

The first specific test for the detection of antibody to HCV was a radioimmunoassay introduced in 1989[259] soon after the virus was first described[2]. The assay was developed from 3 cDNA clones used to first identify HCV. These were expressed as a fusion polypeptide in combination with superoxide dismutase (SOD) in recombinant yeast, giving a 363 amino acid polypeptide termed C100-3. The polypeptide was used as a capture protein, coated onto the wells of a microtitre plate, to which HCV antibodies present in a sample would bind. A second radiolabelled antibody detected any bound HCV antibody in the sample. Though the assay was a successful first attempt at HCV diagnosis, it suffered from poor specificity made worse through the lack of any confirmatory tests[260].

The first alternative assay was the recombinant immunoblot assay (RIBA) for the detection of HCV antibodies[261]. This used the same C100 protein expressed in yeast as the original ELISA plus an additional fragment of the C100 protein (5-1-1) expressed in *E. coli*. As C100 protein is shared between both assays it was not a true confirmatory test for the anti-HCV ELISA, but it did increase specificity over use of the ELISA alone[262].

Following information gathered from sequencing of the whole hepatitis C genome from 8 HCV strains[263–268], new second generation immunoassays started to appear, mainly based on the highly conserved HCV core region. Antibody response to the C100 protein was generally produced late and in only around 74% of HCV infections, as opposed to around 91% for an antibody response to the HCV core region[269].

An improved RIBA was released in 1991, using slightly lower concentrations of the C-100 and 5-1-1 proteins, plus yeast expressed protein from the NS3 region (c33c) and the HCV-core-associated antigen (c22)[270]. Second generation ELISA assays used a similar approach, adding core and NS3 derived antigens to the original NS4 derived C100 antigen[271–273]. Antigens were expressed as recombinant proteins, including the first use of baculovirus for expression of HCV proteins [274], or were produced as synthetic peptides[271]. Generally the 2nd generation assays improved sensitivity while reducing the antibody negative 'window period' and improved specificity[269,275].

Third generation anti-HCV assays added a recombinant antigen from the NS5 region[276] and improved detection from the NS3 region[277]. An improved RIBA III was released which replaced two of the recombinant antigens, for c-22 and c-100, with synthetic peptides [276]. These additional improvements further increased specificity and sensitivity over 2nd generation assays[278–280], though any improvement provided by inclusion of the NS5 antigen remained questionable[280]. The performance of the 3rd

generation assays reduced any additional benefits provided by the RIBA III assay for confirmatory testing, often giving intermediate results in samples with discrepant results[278].

Modern anti-HCV assays remain are similar to the 3rd generation assays, but can be run on high throughput, automated, random access instrumentation and use chemiluminescence detection rather than colorimetric substrate detection. The 4 main commercial platforms are the Architect i2000sr (Abbott) with the Architect anti-HCV assay, the Vitros ECiQ Immunodiagnostic system (Ortho Clinical) with the Vitros anti-HCV assay, the UniCel DxI 800 analyzer (Beckman Coulter) with the Access HCV Ab Plus assay and the Cobas e 411 analyzer (Roche) with the Elecsys anti-HCV assay. Each assay uses antigens derived from the core, NS3 and NS4 regions but the Vitros anti-HCV assay adds in a NS5 derived antigen. It is also the only assay run in a well format, as opposed to the other 3 platforms which use micro particle-based enzyme immunoassays, which theoretically improve assay kinetics through increased surface area. Comparison of all 4 assays showed similar performance characteristics, each recording clinical sensitivities of 100% and clinical specificities of 98.8% for the Elecsys, 98.2% for both the Architect and the Access and 96.5% for the Vitros[281]. The lower sensitivity of the Vitros assay has been found in other studies[282] and could be due to the incorporation of the extra NS5 derived antigen[281]. More recent studies have demonstrated slightly higher sensitivity and a reduced window period with the Elecsys assay but these are very marginal improvements[283].

As none of the assays are completely specific, it is recommended by Public Health England (PHE) that all initial anti-HCV screen positive results should be tested with a second assay for confirmation of the antibody result[284].

9.4.2 HCV ANTIGEN

Assays have been developed to allow the detection and quantification of HCV core antigen[285–287], but the overall sensitivity in comparison to HCV RNA detection by Quantitative real-time PCR has been poor, with a limit of detection around 10^4 - 10^5 RNA copy equivalents/mL. All the assays used monoclonal antibodies directed at conserved epitopes of HCV, one coated on the well of the plate for capture and a second antibody used for detection. One issue which all assays must overcome is the interference caused by patient anti core antibody binding to the antigen and the blocking of the virus antigen by the surrounding viral envelope. Incorporating a pre-testing treatment step with detergents such as Triton X-100 can help disassociate the antibody from the antigen and disrupt the viral envelope, significantly increasing the sensitivity[288]. Modern HCV antigen immunoassays have been developed for automated random-access instrumentation, namely the Abbott Architect platform. The assay uses chemiluminescent micro particle technology, and incorporates a 7 minute pretreatment step to disassociate any patient antibody and disrupt the viral envelope[289]. In numerous studies the

assay has proven to be sensitive, specific and reliable[289–292], yet the exact role of HCV antigen in diagnostics is not exactly clear[293]. Though the modern assay has improved the sensitivity over past HCV antigen assays, a limit of detection of between 500-3000 IU/mL[291] is still more than a 50 fold reduction compared to the most sensitive RT-PCR assays, which can now detect down to 10-15IU/mL[294]. As modern guidelines recommend the use of an assay with a lower limit of detection ≤ 15IU/mL[295], the HCV antigen test is not suitable for monitoring HCV levels during therapy or defining a sustained virological response (SVR) in a patient. Yet there are still several other possible uses for an HCV antigen test. Numerous studies have demonstrated the significantly reduced window period, up to around 35 days less, from using HCV antigen screening when compared to using HCV antibody alone[291,296–299]. This early detection of infection, combined with its speed, simplicity and cost compared to RT-PCR has found use in the monitoring of incident infection in haemodialysis patients[300].

An HCV antigen test would be as a simpler and cheaper alternative to RT-PCR for identifying chronic infection in HCV antibody positive patients. If it is to be used for this purpose the sensitivity must be improved to ensure chronically infected patients with low viral loads are not missed. A recent study in young, HIV negative, untreated IDUs found that 15/60 (20%) had viral loads below 4000 IU/mL[301]. Modern HCV antigen immunoassays would miss the majority of these.

9.4.3 IGM/AVIDITY TESTING

Treatment in the acute stage of hepatitis C has been shown to significantly increase response SVR[302], yet the largely asymptomatic nature of initial infection has meant that identification of new infections has proved problematic. Currently the only definitive way of diagnosing acute infection is through a documented seroconversion event. Past attempts have tried to use IgM detection, successful for diagnosing acute infections in many other viral infections, but its transient appearance in acute HCV infection and its appearance during chronic infection makes it impossible differentiate between the two states[303–305]. Serial dilutions of IgM reactive samples to quantify the IgM response can produce discrimination but would be impractical in a busy diagnostic laboratory[306]. The use of IgG avidity testing has showed more promise[307–309], yet difficulties were still found in differentiating late phase acute infection from past resolved infection[309].

A possible alternative to the use of IgM or avidity testing is to use a RIBA like array (see above) and differentiate acute from chronic infection based on the pattern of antibody binding to peptides and antigens. Previous work has identified that antibody to non-structural proteins appears first, around 6 weeks after infection, followed by antibodies against the structural proteins such as core and then

E1 and E2. Further differentiation can be achieved by measuring the levels of the individually targeted antibodies, with antibodies targeting core protein achieving higher levels quicker than those targeting E1 and E2[310].

9.4.4 RAPID HCV IMMUNOASSAYS

Rapid immunoassays are point of care tests which are performed close to the patient, taking 20-30 minutes or less to obtain a result. They generally utilise lateral flow immunoassay technology where the patient sample is applied directly to the diagnostic device. Antigens are bound to the solid phase of the device, e.g. nitrocellulose membrane, through which a liquid phase including the patient sample e.g. finger prick blood or oral fluid, will pass through by chromatography. Any specific antibodies present in the sample will bind to the antigens, and can subsequently be detected using a chromogenic marker, e.g. protein A labelled colloidal gold. Example rapid care tests currently on the market and CE marked for anti-HCV screening include, the Chembio DPP HCV test, Multiplo Rapid HIV/HCV test (MedMiro) and the Ora-quick HCV Rapid (Orasure). All 3 support use with whole blood, serum/plasma plus the Chembio and Ora-quick test can be used with oral fluid samples. Comparison of the three devices in a laboratory environment gave sensitivities of 96.2%–98.0%, 86.8%–88.3%, and 97.8%–99.3% for the Chembio, Mutilplo and Ora-quick devices respectively[311]. A repeat evaluation but this time performed in field settings gave slightly less impressive result, with the highest sensitivities of 94.0%, 78.9% and 97.4% achieved for the Chembio, Mutilplo and Ora-quick devices[312]. Yet there was high variability between different sites, for instance the sensitivity and specificity for the Ora-quick device varied from 90.8%–94.7% and 92.1%–98.6% with oral fluid samples and 95.9%–97.4% and 98.6%–100.0% with whole blood samples[312]. A consistent finding across the studies was the lower sensitivity reported from HIV co-infected patients, with false negative anti-HCV results ranging from 11.3%[312] to 22.4%[313], the higher results being obtained in co-infected patients but tested in standard ELISAs, ranging from 3.8%-5.5%[314,315].

These generally impressive results demonstrate the suitability of using rapid immunoassays as point of care tests for difficult to reach populations, particularly as the most effective devices can be used with either finger prick whole blood or oral fluid. However, these tests currently only provide an anti-HCV screening test result, any antibody positive must be confirmed using a second test in the laboratory and further testing is required to identify chronic HCV infection.

9.5 ALTERNATIVE SAMPLE TYPES

Screening tests described in the previous sections are designed primarily for use with serum/plasma samples. As the majority of HCV infections reside in the injecting drug user population this presents

a significant problem. As a result of repeated injection of drugs using poor techniques peripheral veins deteriorate and collapse over time, making blood difficult to obtain using conventional venipuncture. In many instances blood can only be obtained from the jugular or femoral vein, a procedure requiring a specifically trained phlebotomist, limiting the number of samples received from IDU population. Alternative sample types include dried blood spots (DBS) and oral fluid samples, both of which are easier and safer to take than venous blood samples. Both have their own inherent advantages, disadvantages and possible uses, which will be explored in more detail in the following section.

9.5.1 DRIED BLOOD SPOTS

Testing using DBS samples for the detection of phenylketonuria in new born infants was first described in 1963[316], and has since become well established as the sample of choice for the neonatal newborn screening program[317]. Since then its use has spread to many other settings including diabetic screening[318], inflammatory markers[319] and blood borne virus screening[320].

Taking of a dried blood spot sample involves the breaking of skin, using a lancet. Resultant capillary blood samples are then dropped onto a collection card, left to dry and sent back to the laboratory for testing. Neonatal screening samples are taken from the heel, while for adults the side of a finger is generally used. The lancets used in this procedure are contact activated and single use. When applied to the skin with sufficient pressure, a spring-loaded needle shoots out a desire length (around 0.5 to 2mm) and breaks the skin, after which it immediately retracts into the body of the lancet. Lancets are single use; once the spring has been activated it will not work again. The procedure is considered relatively painless[321], and is simple and safe without the need to use and dispose of needles and syringes[322].

Collection cards use paper manufactured from high-purity cotton linters which go through strict lot to lot consistency checks for their absorbance properties[323]. Currently 3 types of collection paper are available, Whatman 903, Perkin Elmer 226 and Munktell TFN, which all share equivalent performance characteristics[324,325]. Collected samples are left to dry for around 2 hours, and then placed in a sealed envelope with a desiccant pack included before posting back to the laboratory. Once dry, DBS samples can remain stable at room temperature for extended periods of time[326], and will remain stable in transport as long as they remain dry, which can be ensured by the inclusion of a desiccant pack within the transport packaging. As DBS samples are exempt from UN3373 regulations for the transport of infectious substances[327], standard practices can be used for postage, keeping transport easy and inexpensive.

Processing a DBS sample in the laboratory involves punching out or removing a spot of blood, followed by elution of the spot in an appropriate buffer, most commonly PBS/Tween 20 based. Any biochemical, immunological or molecular markers in the sample should elute out from the spot into the elution buffer. Elution of the spot can vary from hours to overnight incubations, after which the eluate is treated and tested in a similar fashion to any standard serum sample.

Dried Blood Spots and Hepatitis C

As the vast majority of HCV resides in a population with very poor peripheral veins, the IDU population, DBS samples offer an ideal alternative to the collection of serum for the diagnosis of HCV. The first studies using DBS samples for HCV screening were mainly for epidemiological seroprevalence investigations[328–330]. However, the high sensitivity and specificity results obtained in each study, 97%-100% and 87.5%-100% respectively, demonstrated their suitability for use in diagnostic screening. When HCV was recognised as an issue by health authorities in England and Scotland[331,332], DBS testing was identified as a possible measure to increase screening in the IDU population. At that time only around 50% of those infected with HCV had been diagnosed. Several subsequent studies demonstrated the increase in screening for HCV produced by the introduction of DBS testing[333–335], and diagnostic testing was introduced across several laboratories in the UK.

9.5.2 ORAL FLUID

A second alternative sample type to serum/plasma for the diagnosis of HCV is oral fluid. This was first used for blood borne virus screening in 1987, with an assay developed for the detection of HIV antibodies from saliva[336]. Development of diagnostic assays for use with these samples has increased since then, mainly due to the inherent advantages offered by a non-invasive sample type. Oral fluid samples offer an even easier to collect and potentially safer sample than dried blood spots, and is the preferred option of patients when choosing between the 2 sample types[337338].

Saliva is composed of around 99% water, plus a range of proteins/peptides, nucleic acids, hormones and electrolytes, some originating locally and some systemically. It is produced by 4 distinct salivary glands in the mouth plus additional components created separately[339]. One of these components is gingival crevicular fluid, secreted from the shallow crevice around each tooth. This crevicular fluid closely resembles the constituents found in plasma[340], with much higher levels of IgG than found in the general saliva. For instance, IgG is found in human plasma at a mean average of 14730 mg/L, compared to 14.4 mg/L in whole saliva but 3500 mg/L in the crevicular fluid[341]. It is this concentration difference which makes crevicular fluid important for the diagnosis of infectious diseases. General saliva can be used but has been shown to be inferior to devices specifically designed for collection of crevicular fluid, including the Ora sure and Salivette devices [342,343].

Oral Fluid and Hepatitis C

Successful diagnosis of HCV, based on detection of HCV antibodies in crevicular fluid, has been demonstrated in several studies. Methods involve either collection of oral fluid followed by testing using an EIA, usually a commercially available assay which has been modified specifically for oral fluid[330,343,344], or rapid point of care based tests[345–349]. Sensitivity achieved in these studies has generally been high, ranging from 92% - 100% using modified EIA and 85.4%-98.1% for rapid point of care tests, but does not match the performance achievable from DBS samples[330,346,347]. Other factors which affect the sensitivity include the collection device, study center where the sample was taken, and co-infection with HIV. This last factor can have a dramatic effect on the sensitivity of oral fluid testing, with one study recording a drop from 90% to 73% in HIV infected individuals[350]. As HCV has a higher prevalence in HIV infected individuals [112], this is an important issue to consider when using alternative sample types such as oral fluid.

9.5.3 DISADVANTAGES OF DBS/ORAL FLUID SAMPLES

Despite the advantages offered by these 2 samples types several disadvantages must be considered when using them.

Testing from DBS or oral fluid samples commonly uses commercial CE marked HCV serological assays, but these assays are not CE marked for use with DBS or oral fluid samples. CE marked tests licensed specifically for use with these sample types do exist, but they are rapid point of care test such as the Ora-Quick HCV test, which although useful are unlikely to ever completely replace high throughput laboratory automated tests. The United Kingdom Department of Health requires all NHS laboratories to be accredited to medical laboratory accreditation standard ISO 15189. As part of this accreditation process the United Kingdom Accreditation Service (UKAS) expects laboratories to utilise CE marked diagnostic assays within the original protocol set out within the CE license. Deviating from this protocol, i.e. testing dried blood spot samples with a diagnostic assay licensed for serum, requires compliance with European Union *in vitro* diagnostics Directive 98/79/EC and requires a local self-validation of the modified test to overcome this issue but the process is time consuming and expensive. This is further complicated by the modifications manufacturers make to the original assay after release, which requires a repeat of the full validation process for DBS samples. In addition, beginning 25th May 2017 over a 5 year transition period blood borne virus tests will be classified under risk category D and test modification will require specific conformity assessment by a notified body. As test kit manufacturers will not release proprietary information about the tests and their components it will no longer be possible to use such 'self-validated' test procedures. There is a

need to develop an independent test procedure that can undergo conformity assessment and produce a compliant specifically for use with DBS or oral fluid.

Optimisation of commercial assays has increased the sensitivity achievable from dried blood spots to a high level (97.5-99%)[330351] when compared with testing venous blood samples, but given the dilution factor inherent in re-suspending a DBS ready for analysis in a volume suitable for use with a commercial assay, or the lower concentration of analytes found in oral fluid, it will always be difficult to match the performance achievable from a venous sample. This inevitably leads to the occurrence of false negative results, and the possibility of hepatitis C infection going undiagnosed. Only an assay specifically designed for DBS or oral fluid samples will be able to increase the sensitivity beyond what is currently achievable.

The test repertoire currently available from DBS or oral fluid samples is limited when compared to serum. A HCV antigen test would be very desirable as this would significantly reduce the cost of diagnosing active HCV infection, but current assays have proved to be very insensitive when using DBS or oral fluid samples[349].

9.5.4 SELF COLLECTION OF SAMPLES

As both DBS and oral fluid samples are easy and safe to take, they both open up the possibility for self-collection of samples. As a large population of injecting drug users are still unaware of their hepatitis C infection, and with transmission predominantly occurring in young drug users early in their drug taking career[352], despite the progress achieved in increasing HCV testing more must be done to increase testing this difficult to reach population. Self-collection of samples is one option to help address this issue. Patient acceptability of either specimen type is high, with a slight preference for taking oral fluid samples[338]. The major issue with self-collection is the quality of the sample taken, which can vary quite significantly with oral fluid samples[353].

10 AIMS

The aim of the study is to answer several research questions around the development of a multi-analyte serological assay for the diagnosis of hepatitis C using DBS or oral fluid samples.

1) Can baculovirus derived protein expression systems be used for production of capture antigens to be used in an Anti-HCV immunoassay?

2) Which HCV proteins, when expressed in Baculovirus, give the maximum sensitivity for detection of Anti-HCV?

3) Can an HCV Ag/Ab immunoassay run in a multi-analyte format and using DBS samples match the performance of commercial CE marked immunoassays using serum samples for the diagnosis of HCV infection?

4) Can a multiple recombinant protein based array be used to accurately identify the acute stage of HCV infection?

11 MATERIALS AND METHODS

11.1 ETHICS

Ethical approval for the re-use of unlinked and anonymised serum and DBS samples previously tested for anti-HCV, HCV Genotype and HCV RNA was granted by the North of Scotland Research Ethics Service, (IRAS ID: 208004, REC Ref:17/NS/0087).

11.2 CULTURE OF SF9 AND HI5 INSECT CELLS

All transfections and protein expressions using the InsectDirect™ system were performed in Sf9 insect cells. Sf9 cells are derived from the *Spodoptera frugiperda* caterpillar; cell line IPLB Sf21-AE, Novagen® (Merck, New Jersey USA). During InsectDirect™ experiments cells were maintained using Novagen™ BacVector Insect cell medium (Merck).

For transfection to generate recombinant baculovirus using the *flash*BAC™ ULTRA system, and for subsequent virus amplification, the same Sf9 insect cell line was used. For all experiments cells were maintained in Gibco™ SF-900II™ serum free medium (Thermofisher Scientific, Paisley, UK).

For protein expression with *flash*BAC™ ULTRA generated recombinant baculoviruses Hi5 insect cells were used. These are derived from the *Trichoplusia ni* cabbage looper moth, cell line BTI-TN-5B1-4 (Thermofisher Scientific). Cells were maintained in Gibco™ Express Five™ serum free medium (Thermofisher Scientific).

All cell culture work was performed in a Class II Bio Safety Cabinet (ESCO GB, Barnsley, UK).

11.2.1 RECOVERY OF CELLS

A cell ampoule was removed from liquid nitrogen and placed in a beaker of warm water for rapid thawing. When completely thawed, the ampoule was removed from the water and dried, before wiping down with 70% isopropanol (Sigma-Aldrich, Dorset UK). Using a plastic pipette (Sigma-Aldrich), the thawed cells were split between two 25 cm^3 Nunc culture flasks (Thermofisher Scientific) each containing 5 mL of pre-warmed media. The flasks were placed in an incubator (Heraeus, Frankfurt, Germany) set at 28°C for 1 hour to allow the cells to settle. After an hour the media was removed and replaced with 5 mL of fresh media. The flask was placed in a 28ºC incubator and left until cells reached 90-95% confluence.

11.2.2 PASSAGING OF ADHERENT CELL CULTURES

Both Sf9 and Hi5 insect cells were passaged when they reached 85-95% confluence.

To dislodge adherent cells, flasks were tapped 1-2 times until the majority of cells were re-suspended in the media. The cells were counted, and cell viability determined using trypan blue dye. Cells were diluted in pre-warmed media (28°C) to a final concentration of 5 x 10^5 cell/mL, in a total volume of 20 mL. For cell counting 0.1 mL of re-suspended cells was added to 0.9 mL of media. From this dilution at 1:1 dilution, was performed in 0.4%$^{w}/_{v}$ trypan blue dye (Sigma-Aldrich) and mixed, and 50 µL added to a cell of a FastRead counting chamber (Immune systems, Devon UK). The trypan blue dye will be taken up by non-viable cells. Only un-stained cells were counted for the dilution.

Cells were counted in the 4 large corner squares, and the following calculation performed:

Total No. of cells counted in 4 large squares:

e.g. 85

No. of cells per large square:

$\frac{85}{4} = 21.25$

No. of cells per cm^3 of diluted cell suspension:

$\frac{85}{4} x\ 10^5 = 2.125\ x\ 10^6$

No. of cells per cm3 in original suspension allowing for dilution with trypan blue:

$\frac{85}{4} x\ 10^5 x\ \frac{3}{2} = 3.1875\ x\ 10^6$ cell/cm^3

Therefore to create a cell suspension at 5 x 10^5 cell/cm^3 dilution:

$$\frac{\mathbf{0.5}}{\mathbf{3.1875}}\ \boldsymbol{x}\ \mathbf{20} = \mathbf{3.14}\ \boldsymbol{mL\ \ of\ cell\ suspension} + \mathbf{16.86}\ \boldsymbol{mL\ of\ cell\ medium}$$

To determine cell viability the cell counting was repeated including the dyed non-viable cells, and the percentage of viable to overall cell numbers calculated. Only cultures with cell viability above 90% were passaged, cultures dropping below this level were discarded and a new culture set up. Dilutions of cells were prepared in sterile vented capped Nunc 75 cm^3 culture flasks (Thermofisher Scientific). Caps were added tightly, and the culture flasks placed in a 28ºC incubator to grow until 90-95% confluent. Cell cultures were generally passaged around 30 times until a fresh culture was started.

11.2.3 PASSAGING OF SUSPENSION CELL CULTURE

For virus amplification experiments using Sf9 cells, and large protein expressions using Hi5 insect cells, suspension cell cultures were used. Suspension Sf9 cell cultures were prepared by diluting cells

collected from adherent cell cultures to a final concentration of 5 x 10^5 cell/cm^3 in 50 mL of media in 250 mL Erlenmeyer flasks with vented caps (Corning, Tewksbury, USA). Suspension Hi5 cultures were prepared in the same way with 3 x 10^5 cell/cm^3 in 50 mL of media. Suspension cultures were placed in a shaking incubator set at 28°C and 140rpm. Suspension cultures were checked every 2-3 days, counted as described above, and sub-cultured when they had reached a level of 3-6 x 10^6 cell/mL. Cell viability was determined during cell counting, only cells above 90% viability were passaged. Cell cultures were passaged 30 times until a fresh culture was started.

11.3 PROTEIN EXPRESSION USING INSECTDIRECT™ SYSTEM

11.3.1 HCV CORE ANTIGEN

The sequence from the HCV genotype 1a isolate H77 (NCBI Reference Sequence: NC_004102.1) was selected and a TAG stop codon was added to the 3' end of the sequence.

5'ATGAGCACGAATCCTAAACCTCAAAGAAAAACCAAACGTAACACCAACCGTCGCCCACAGGACGTCAAGT TCCCGGGTGGCGGTCAGATCGTTGGTGGAGTTTACTTGTTGCCGCGCAGGGGCCCTAGATTGGGTGTGCGC GCGACGAGGAAGACTTCCGAGCGGTCGCAACCTCGAGGTAGACGTCAGCCTATCCCCAAGGCACGTCGGCC CGAGGGCAGGACCTGGGCTCAGCCCGGGTACCCTTGGCCCCTCTATGGCAATGAGGGTTGCGGGTGGGCG GGATGGCTCCTGTCTCCCCGTGGCTCTCGGCCTAGCTGGGGCCCCACAGACCCCCGGCGTAGGTCGCGCAA TTTGGGTAAGGTCATCGATTAG-3'

11.3.2 DESIGN OF THE PLASMID FOR HCV CORE EXPRESSION

The Novagen® InsectDirect™ (Merck, New Jersey USA) system was used for expression of HCV core antigen.

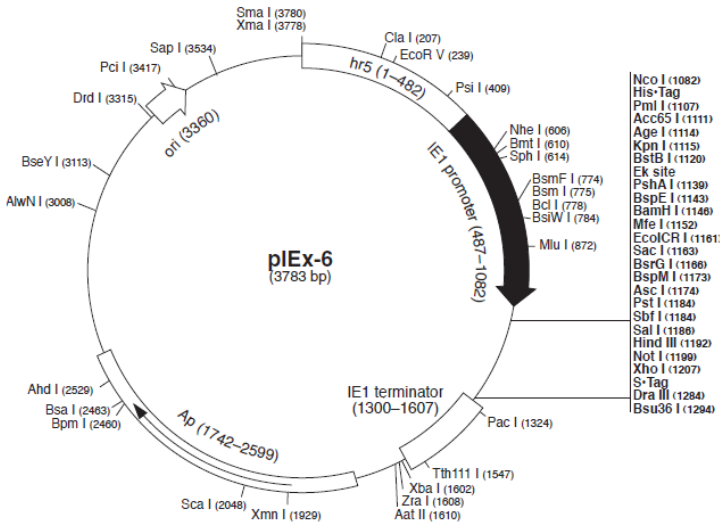

Figure 19 Sequence Map of the pIEx-6 Plasmid. Taken from [354]

The HCV core sequence was synthesised and cloned into a pIEx-6 plasmid by Eurofins Genomics (Ebersberg, Germany). The complete sequence included a NcoI restriction enzyme (RE) site and HISTag sequence at the 5' end, and a Bam H1 RE site at the 3' end.

CCATGGCACATCACCACCACCATCACGTGGGTACCGGTTCGAATGATGACGACGACAAGATGTCCACCAACCCGAAACCT
CAGCGCCAAGACGAGGACCGAGGCTTGGAGTAAGGGCCACACGCAAGACTAGCGAGCGATCGCAACCACGCGGTAGAC
GTCAACCCATTCCCAAAGCGCGTCGTCCTGAAGGTCGCACTTGGGCACAACCTGGCTACCCCTGGCCCTTGTACGGCAAT
GAGGGATGCGGTTGGGCTGGCTGGTTACTCTCTCCACGTGGATCACGTCCTTCCTGGGGTCCGACAGATCCCAGGAGAA
GGAGTCGCAACCTAGGCAAGGTGATCGACTAAGGATCCAAGACGAAGCGCAACACCAATCGCAGACCTCAGGACGTGAA
GTTCCCAGGTGGTGGCCAGATCGTTGGTGGAGTCTATCTGCTGC

Figure 20 Full synthesised gene sequence for insertion into pIEx-6 plasmid. Note RE sites in yellow, HISTag sequence in purple, and HCV core sequence in green.

The gene synthesis/plasmid preparation was ordered as a MIDI prep, resulting in 33 µg of complete plasmid. The plasmid underwent nucleotide sequencing by the manufacturer to ensure the inserted sequence was correct and in the right orientation. Upon arrival the lyophilised plasmid was reconstituted in TE Buffer (Sigma-Aldrich, Dorset UK) to give a concentration of 1 µg/µL and stored at -80ºC until use.

11.3.3 TRANSFECTION OF SF9 CELLS WITH PIEX PLASMID - OPTIMISATION

Rapidly proliferating Sf9 insect cells were used for transfection. The manufacturer's protocol (Merck) for a 6 well transfection format was followed. All cell culture work was performed in a Class II Bio Safety Cabinet placed in a dedicated transfection room to prevent contamination from the general cell culture laboratory.

Serum free BacVector (Merck) insect cell medium was warmed to 28ºC. Rapidly proliferating Sf9 cells were counted as described above (section 5.2.2) and diluted to a cell density of 4×10^5 cells/cm^3 in serum free BacVector insect cell medium. A total volume of 15 mL was required for the transfection experiment. Of this, 2.5 mL of a 4 x 10^5 cells/cm^3 concentration of cells were placed in 4 wells of a 6 well culture cluster flat bottom well plate (Corning, New York USA), giving a final amount of 1 x 10^6 cells per well. A dilution of the pIEx-HCV core plasmid was prepared in BacVector serum free medium, using 2 µL of the suspended pIEx-HCV core (1µg/µl) mixed with 100 µL of BacVector serum free medium. This was performed a total of 4 times. GeneJuice (Merck) was mixed with BacVector serum free medium in 3 different amounts, plus a final mixture for the negative control.

Mix 1: 8 µL of gene juice + 100 µL of BacVector serum free
Mix 2: 12 µL of gene juice + 100 µL of BacVector serum free
Mix 3: 16 µL of gene juice + 100 µL of BacVector serum free
Negative Mix: 12 µL of gene juice + 100 µL of BacVector serum free

The pIEx-HCVcore/BacVector mix (2 µg/100 µL) was added drop wise to the aliquots of Gene Juice/BacVector mix, then gently vortexed for 5 seconds. For the negative control, 100 µL of BacVector serum free medium was added to the negative mix. These mixes were left for 15 minutes at room temperature, then 0.8 mL of BacVector serum free medium was added to all four mixes. All BacVector medium was completely aspirated from each of the 4 wells in the culture plate. Finally, all the pIEx-HCVcore/GeneJuice/BacVector medium mixtures were added to 4 separate wells of the culture plate.

The culture plate was placed in a plastic tray containing a moistened tissue and placed in a 28ºC incubator for 48 hours for the transfection/protein expression to proceed. After 48 hours cell cultures were examined at 10X and 25X magnification, to check the health of the cells and to look for any evidence of transfection. Images of the cells were recorded using a Nikon Coolpix 995 microscope specific camera (Nikon, Tokyo Japan). Before harvesting of the cells, a 250 µL aliquot of the pIEx/GeneJuice/BacVector medium was carefully removed from each of the wells, without disturbing the cells at the bottom of the well and stored in a 2.0ml storage vial for storage at -20ºC. This was repeated for each of the 4 cultures. Finally the cells were harvested using a cell scraper to re-suspend the cells in the remaining pIEx/GeneJuice/BacVector medium, and the complete suspension transferred to a separate 2.0 mL storage vial, then snap frozen in liquid nitrogen and stored at -80°C until use. This was repeated for each of the 4 cultures.

11.3.4 SDS PAGE

The sample to be analysed was mixed 1:1 (30 µL and 30 µL) with Laemmli buffer (Sigma-Aldrich), and heated to 100ºC in a water bath (Grant, Cambridge UK) for 5 minutes. A NuPage 4-12% Bis-Tris SDS-PAGE gel (Thermofisher Scientific) was loaded into an XCell SureLock™ mini cell electrophoresis system (Thermofisher Scientific). Running buffer was prepared from 50 mL of 20x NuPAGE® MES SDS running buffer (Thermofisher Scientific) and 950 mL of deionised water and used to fill the XCell SureLock™ mini cell. Following this 15 µL of each sample/sample buffer mix was loaded into the SDS-PAGE gel. A broad range pre-stained protein ladder was applied to the first well, covering the range 11kDa to 245kDa (New England Biolabs, Hitchin UK). Electrophoresis was then run at 200V for 35 minutes, post electrophoresis the gel was washed with de-ionised water, stained with 20 mL of InstantBlue™ stain (Expedeon, Cambridge UK) and shaken at 150 rpm on an orbital shaker for one hour. Finally, the gel was de-stained with 20 mL of deionised water, and an image of the gel recorded using a digital camera.

11.3.5 WESTERN BLOT

Multiple western blots were performed throughout the study. These used NuPage 4-12% Bis-Tris SDS-PAGE gels, pre-cut 0.45 µm nitrocellulose membrane, and NuPage gel electrophoresis apparatus (Thermofisher Scientific). The primary antibody varied according to the protein to be detected, with a secondary antibody complementary to the primary antibody. The secondary antibody was conjugated, either to alkaline phosphatase (AP) or horse radish peroxidase (HRP). For AP conjugated antibodies the substrate used was FAST™ BCIP/NBT (5-bromo-4-chloro-3'-indolyphosphate/nitro-blue tetrazolium) (Sigma-Aldrich). For HRP conjugated antibodies the substrate used was 1 Step TMB (3,3',5,5'-tetramethylbenzidine) blotting solution (Thermofisher Scientific). Table 3 lists the primary and secondary antibodies used for western blot analysis for each protein.

Protein Target	Primary Antibody	Dilution	Secondary Antibody	Dilution	Substrate
Core 1-124	Mouse mAb Anti-HCV Core (Abcam:ab2740)	1:1000	Rabbit pAb Anti-Mouse IgG [AP] (Abcam:ab6729)	1:1000	FAST™BCIP/NBT
Core 1-124	Mouse mAb Anti-HCV Core (Abcam:ab2740)	1:1000	Rabbit pAb Anti-Mouse IgG [HRP] (Abcam:ab6728)	1:3000	TMB Ultra
Core 3-190	Goat pAb Anti-HCV Core Antigen (Abcam:ab50288)	1:1000	Donkey pAb Anti-Goat IgG[AP] (Abcam:ab6886)	1:2000	FAST™BCIP/NBT
NS3	Mouse mAb Anti-HCV NS3 (Abcam:ab18184)	1:1000	Rabbit pAb Anti-Mouse IgG [HRP] (Abcam:ab6728)	1:3000	TMB Ultra
NS4	Mouse mAb Anti-HIS(6X) (Abcam:ab18184)	1:1000	Rabbit pAb Anti-Mouse IgG [HRP] (Abcam:ab6728)	1:3000	TMB Ultra
NS5a	Mouse mAb Anti-HIS(6X) (Abcam:ab18184)	1:1000	Rabbit pAb Anti-Mouse IgG [HRP] (Abcam:ab6728)	1:3000	TMB Ultra
NS5b	Mouse mAb Anti-HIS(6X) (Abcam:ab18184)	1:1000	Rabbit pAb Anti-Mouse IgG [HRP] (Abcam:ab6728)	1:3000	TMB Ultra

Table 3 List of primary and secondary antibodies and the substrate used for western blot analysis

Buffers were pre-prepared. These included a transblotting buffer composed of 50 mL of 20X NuPAGE® Transfer Buffer (Thermofisher Scientific), 100 mL of 100% methanol (Thermofisher Scientific), and 850 mL of deionised water, wash buffer comprised PBS with 0.05%$^{v}/_{v}$ Tween 20 (Sigma-Aldrich) and blocking buffer comprised of PBS with 0.05%$^{v}/_{v}$ Tween 20 and 5% $^{w}/_{v}$ skimmed milk (Sigma-Aldrich) to 25 mL of wash buffer.

A 0.45 µm pore nitrocellulose pre-cut blotting membrane (Thermofisher Scientific) and 6 blotting pads were soaked in the transblotting buffer for 20 minutes prior to the transfer stage.

An SDS page was performed as described in 11.3.4. The SDS-PAGE gel was then removed but not stained. The pre-soaked blotting pads and nitrocellulose membrane were combined with the SDS PAGE gel in a cassette (Thermofisher Scientific). See Figure 21 for the arrangement in the cassette.

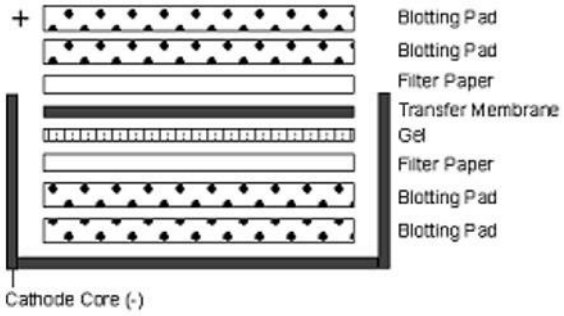

Figure 21 Arrangement of gel/membrane within the cassette. Taken from http://www.lifetechnologies.com/uk/en/home/references/protocols/proteins-expression-isolation-and-analysis/western-blot-protocol/western-blotting-using-polyvinylidene-difluoride-membranes.html Accessed 12/02/2014

The cassette was transferred to the XCell SureLock™ mini cell electrophoresis system and filled with transfer buffer until the gel/membrane was completely covered. The outer chamber was filled to an equal level with deionised water, and electrophoresis run at 100V for 60 minutes. When electrophoresis had finished, the nitrocellulose membrane was carefully separated from the gel and transferred to a Sterilin™ 100 mm square petri-dish (Thermofisher Scientific) containing 25 mL of blocking buffer and placed on an orbital shaker set at 150 rpm for 1 hour. A 1:1000 primary antibody dilution (see Table 3) was prepared in 5 mL of blocking buffer in a 50 mL centrifuge tube. After the blocking stage, the membrane was carefully rolled in on itself and inserted inside a 50 mL centrifuge tube containing the primary antibody dilution. The centrifuge tube was then placed on a roller mixer (Grant, UK) at 4°C for overnight incubation. The following morning the membrane was placed in a square petri dish, 20ml of wash buffer added and put on an orbital shaker for 5 minutes to wash. This was repeated another two times, to give a total of 3 washes. A secondary antibody solution (Table 3) was prepared in 5 mL of blocking buffer in a 50 mL centrifuge tube. After the third wash, the membrane was carefully transferred from the square petri dish to the 50 mL tube containing the secondary antibody and placed on the roller mixer for 1 hour at room temperature. Following the hour incubation the membrane was transferred to a square petri dish and the wash steps repeated 3 times. Finally, 20 mL of substrate was added until distinct bands on the membrane had developed (around 15 minutes) after which the reaction was stopped by washing in distilled water. The image of the developed membrane was taken using a digital camera.

11.4 PROTEIN EXPRESSION USING FLASHBAC™ ULTRA SYSTEM

Protein expression using the *flash*BAC™ ULTRA baculovirus system (Oxford Expressions Ltd) was attempted for HCV Core, NS3, NS4, NS5a and NS5b proteins. This used a variety of *flash*BAC™ ULTRA compatible transfer vector plasmids, including the Novagen pIEx/Bac-3 plasmid (Merck), and the pOET1 and pOET8 plasmids (Oxford Expressions Ltd). Target sequences for each protein to be expressed were amplified by PCR either from HCV positive sera, or from other transfer vectors. Cloning techniques varied according to each transfer vector, the pIEx/Bac-3 vector was a ligation independent cloning (LIC) compatible plasmid, the pOET1 and pOET8 vectors were compatible with restriction enzyme based conventional cloning. All cloned plasmids were transformed into competent *E. coli* cells, selected for, and amplified in antibiotic selective media, purified using column-based plasmid purification and confirmed by nucleotide sequencing.

11.4.1 PCR OF HCV PROTEIN SEQUENCES

11.4.1.1 Primer Design

Primers were designed to amplify HCV protein sequences from synthetically produced plasmids and HCV positive serum. The primers designed included modifications for either ligation independent cloning into a pIEx/Bac-3 transfer vector plasmid or modifications for traditional cloning into pOET1 or pOET8 transfer vector plasmids.

Primers to be used for amplification of a HCV protein sequence for transfer from one plasmid to another were designed using Snapgene software.

Primers for amplification of HCV protein sequences from HCV positive sera were designed using a nucleotide sequence alignment of full-length HCV genomes (>200 sequences), produced using Bioedit Sequence alignment editor, v7.2.6.1. Multiple PCR primers were designed for each target to cover the high sequence variability inherent in the HCV genome. All potential primer sequences were analysed using the Oligo Calc primer calculation tool, located at http://biotools.nubic.northwestern.edu/OligoCalc.html, accessed 25/05/2016. to assess the GC %, melting temperature (T_m), potential hairpin formation, primer dimer and self-annealing. Snapgene software was used in design of primers to simulate cloning of amplified targets into the target plasmid, ensuring inserts were cloned downstream and in frame with the baculovirus promoter and Histag.

All PCR primers were produced by Thermofisher Scientific, UK.

11.4.1.1.1 Primer design for cloning into pIEx/Bac-3 LIC

Primers were designed to amplify the HCV Core gene from the pIEx plasmid, for subsequent cloning into a pIEx-Bac 3 transfer vector plasmid. Primers were designed to amplify specific regions of the NS3 and NS4 genes from wild type HCV strains, for subsequent cloning into the same pIEx-Bac 3 transfer vector plasmid. A map of the plasmid is shown in Figure 22 below.

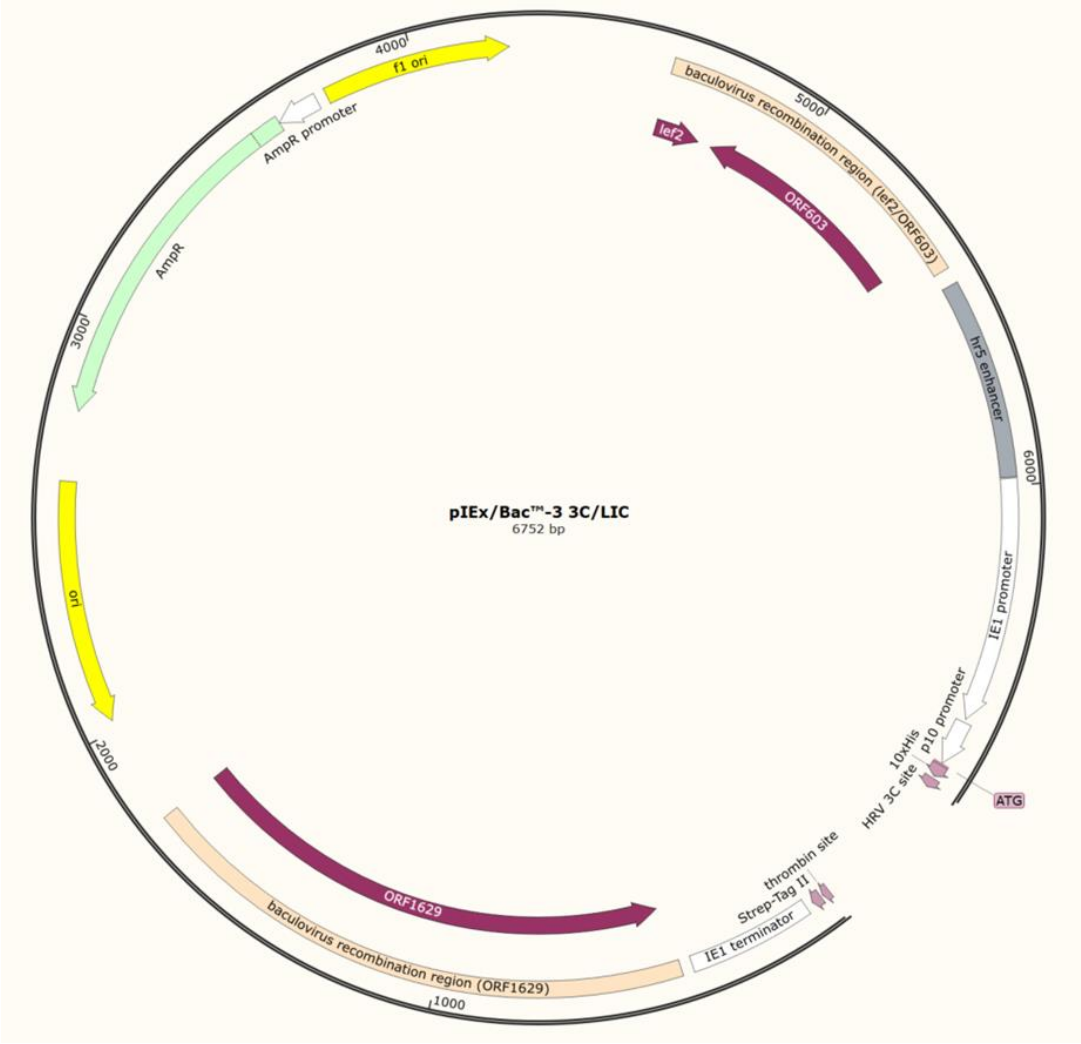

Figure 22 Map of the pIExBac 3 LIC transfer vector. Plasmid is linearized with cut ends enabling ligation independent cloning. Upstream of the LIC site are the IE1 and p10 baculovirus promoters plus sequence encoding a 10XHis site at the 5′ terminus if an expressed protein.

Primers included LIC tags at the 5'end, for cloning into the pIEx-Bac-3 plasmid. All reverse primers included a stop codon sequence to stop expression of the protein at the end of the inserted sequence. Table 4 below lists all the primers designed for cloning into the pIEx-Bac3 plasmid.

For amplification of the NS3 gene a literature search identified amino acids 1225-1456 of the HCV genome as the imuunodominant regions of the NS3 protein. Primers were then designed from a HCV alignment of 960 sequences from HCV isolates ceated in Bioedit 7.2 software to amplify a sequence covering this region. In total 2 forward and 2 reverse primers were designed, to amplify the NS3 protein sequence from HCV genotype 1 strains. The primers were designed with the additional sequence tags at the 5'end to ensure they were comptabible with ligation independent cloning.

The NS4 protein is split into 2 proteins, the NS4a and NS4b. The NS4a protein runs from aa1658-1710 of the HCV genome, NS4b from aa1711-1972. From previous studies using peptides to identify the most immunodominant regions, 1691-1710, 1712-1733 and 1921-1940 were identified as the most important regions to cover. Primers were designed to cover this entire region. Multiple primers were again designed, to help overcome the variability in the HCV genome, with ligation independent cloning tags on the 5' end.

Target	Primer	5'-3' Sequence*
Core	CorePlasFP	CAGGGACCCGGTTCCACCAACCCGAAAC
	CorePlasRP	GGCACCAGAGCGTTTTAGTCGATCACCTTGCCTAG
NS3	NS3502FP	CAGGGACCCGGTGACTTTATCCCCGTAG
	NS3397FP	CAGGGACCCGGTTCTTACTTGAAAGGCTCCTC
	NS31330RP	GGCACCAGAGCGTTCTATGTCTCAATGGTGAAG
	NS31843RP	GGCACCAGAGCGTTCTAGTCATGATGTACTTGGTGAC
NS4	NS44952F	CAGGGACCCGGTACCCTGACGCACCCAATC
	NS45086F	GGCACCAGAGCGTTCTATACAGTGAGGCTGCTGAGTATG
	NS45918R	GGCACCAGAGCGTTCTATACAGTGAGGCTGCTGAGTATG
	NS45954R	GGCACCAGAGCGTTCTAGCTTATCCACTGGTGCAGTC

* Blue sequence denotes LIC Tag, red sequence denotes STOP codon

Table 4 PCR primers for amplification of HCV proteins with ligation independent cloning tags

11.4.1.1.2 Primer design for cloning into pOET1 and pOET8 plasmids

Primers were designed to amplify the full HCV core gene, and sections of the HCV NS5a and NS5b genes from HCV positive serum for cloning into pOET1 plasmid, a map of which is shown below in Figure 23. Primers were designed to amplify the target gene from an HCV alignment of 960 sequences HCV isolates created in Bioedit 7.2 software.

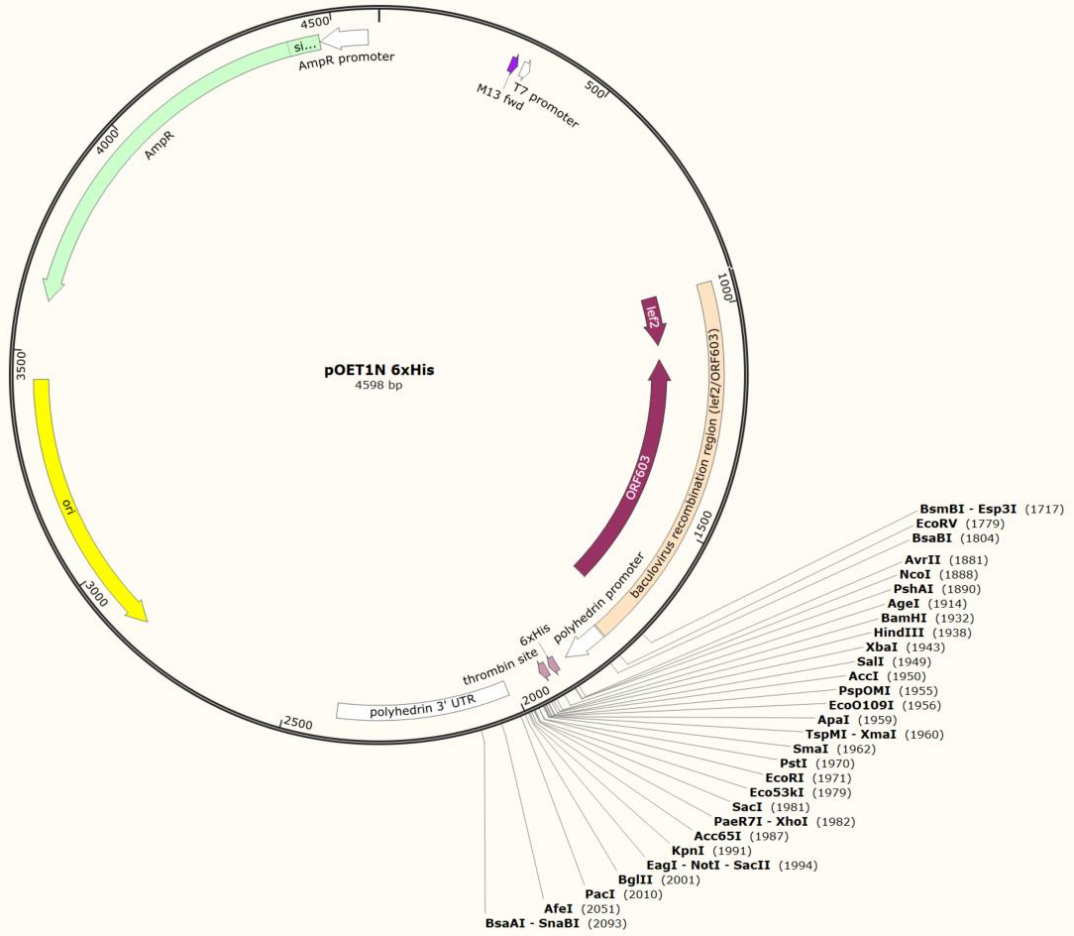

Figure 23 Map of pOET1N 6XHis Transfer Vector. Unique restriction enzyme cut sites shown in and around the multiple cloning site. Primers for amplifying target genes included restriction enzyme tags incorporating cut sites enabling insertion of the amplified target downstream and in frame of the polyhedrin promoter and 8xHis sequence for His tagging of expressed protein at the N- terminus.

Primers were designed to amplify the full core gene (aa1-191). This differed from the previous core plasmids which included the gene sequence for aa1-124. As the genome of HCV is variable, even in the relatively conserved core region, multiple primers sets were designed, including 2 forward and 2 reverse primers. The first forward primer started at nucleotide 1 of the core gene sequence. A second alterative forward primer started at nucleotide 6. The two final reverse primers ended at nucleotide 563, and nucleotide 570. Sequences were chosen which started at the beginning and end of the 191 amino acid sequence and tried to cover the most common sequences. For the NS5a and NS5b genes

primers were designed to amplify most of the genes as the immune reactive regions were spread widely across the sequences. Multiple forward and reverse primers were designed to overcome the variability encountered in these genes.

As PCR amplicons were to be inserted into pOET1 plasmids by conventional restriction enzyme cloning techniques, restriction enzyme cut sites and spacer sequences were inserted into the 5' end of each primer. Restriction enzyme XBaI cut site was included in the forward primer and a BglII cut site in the reverse primer. Snapgene software was used to simulate PCR and cloning using possible primer sets to ensure the resultant cloned plasmid would be in the correct reading frame to express under the control of the polyhedrin promoter and with a 6XHis residue tag at the N termini. Possible primer sequences were then analysed using biotools.nubic.northwestern.edu/OligoCalc.htm to determine primer properties and check for possible primer dimer and self-annealing. See Table 5 for the primers designed.

Target	Primer	Restriction Enzyme	5'-3' Sequence*
Core	Core1FPXb	Xba1	TAAGCATCTAGACATGAGCACAAATCCTAAACCTC
	Core6FPXb	Xba1	TAAGCATCTAGAGTGCACCATGAGCACGAATC
	Core563RPBg	BgiII	TGCTTAAGATCTGGCACAGTCAGGCAAGAG
	Core570RPBg	BgiII	TGCTTAAGATCTTGAAGCGGGCACAGTCAG
NS5a	NS5A1a30FPXB	Xba1	TAAGCATCTAGACTGGATATGCGAGGTGCTG
	NS5A1a73FPXB	Xba1	TAAGCATCTAGAAGCCAAGCTCATGCCACAAC
	NS5A1a1247RP	BgiII	TGCTTAAGATCTCATGGAAGAATAGGACTCAGCGT
	NS5A1a1431RPBg	BgiII	TGCTTAAGATCTCGAGTTGCTCAGTGCGTT
NS5b	NS5A1a1228FPXb	Xba1	TAAGCATCTAGATGAGTCCTATTCTTCCATGC
	NS5A1a1274FPXb	Xba1	TAAGCATCTAGATCCGGATCTCAGCGACG
	NS5B1a3039RPBg	BgiII	TGCTTAAGATCTCACGCTGTGATAAATGTCT
	NS51a3157RPBg	BgiII	TGCTTAAGATCTAGCAAGCAGGAGTAGGCA
	NS51a3195RPBg	BgiII	TGCTTAAGATCTTCGGTTGGGGAGGAGGTAGAT

*Brown sequence denotes spacer sequence, Blue sequence denotes RE sequence

Table 5 Primers designed for amplification of Core, NS5a and NS5b sequences for cloning into pOET1 plasmid.

11.4.1.1.3 Primer design for cloning into POET 8 Plasmid

Primers were designed for amplification of the NS4 protein sequence from a pIEX-Bac3 plasmid for transfer into the pOET8v2 plasmid, and for amplification of the NS5a and NS5b genes from pOET1 plasmids for transfer into the pOET8v2 transfer vector plasmid, a map of which is shown below in Figure 24.

Figure 24 Map of pOET8v2 Transfer Vector. Unique restriction enzyme cut sites are shown in and around the multiple cloning site. Primers for amplifying target genes included restriction enzyme tags incorporating cut sites enabling insertion of the amplified target downstream and in frame of the polyhedrin promoter and 8xHis sequence for His tagging of expressed protein at the N- terminus.

All primers designed for traditional cloning included restriction enzyme sequences plus spacer sequences at the 5' end of the primer. Predicted sequences were checked using Snapgene software to ensure the chosen RE were single cutters within the pOET8 plasmid and amplified target gene. For cloning into the pOET8 plasmid either Pme1 or Not1 were used for cutting the forward primer and Bmt1 was used for the reverse primer. Reverse primers included a stop codon sequence to stop expression of the protein before the C' terminus his sequence. A full list of primers is given in Table 6.

Primers were designed to amplify the NS4 sequence from the pIExBacNS4 plasmid. A plasmid specific primer was used as the forward primer, with NS4 sequence specific reverse primer. This

amplified the N' terminal 10X His tag and NS4 sequence in one product. Restriction enzyme cut sites were added to the forward (PmeI) and reverse (BmtI) primers. Using these restriction enzymes on the pOET8 plasmid excises the HISTag sequence but keeps the melittin signal sequence. The HIStag is taken with the NS4 amplified product and is inserted downstream of the polyhedrin and melittin signal sequence when cloned into the pOET8 plasmid.

For amplification and transfer of the NS5a gene a pOET1 forward primer and a NS5a specific reverse primer were designed. This amplified the NS5a sequence and the HISTag from the pOET1NS5a plasmid and inserted them downstream of the polyhedrin promoter and melittin signal sequence in the cut pOET8 plasmid.

For amplification and transfer of the NS5b gene primers were designed for both a longer and shorter section of the NS5b sequence, to help overcome difficulties in cloning large fragments. The shorter NS5b option would still cover the most important immune reactive regions of the NS5b gene. Both the forward and reverse primers were NS5b specific, not plasmid specific as with the NS5a above. They both used a Not1 RE enzyme sequence, which inserted the NS5b PCR product downstream of the HIStag sequence in the pOET8v2 plasmid. The same reverse primer was used, a NS5b 2902 RP incorporating a Bmt 1 cut sequence.

Target	Primer	Restriction Enzyme	5'-3' Sequence*
pIExBac3NS4	pIExFPPme1	Pme1	TAAGCAGTTTAAACATGGCACATCACCACCATCA
	NS45954RPBmt1	Bmt1	TGCTTAGCTAGCCTAGCTTATCCACTGGTGCAGTC
p0ET1NS5a	pOET1Pme1	Pme1	TAAGCAGTTTAAACATAGGATCTCCTAGGACCATGG
	NS5a1247RPBmt1	Bmt1	TGCTTAGCTAGCCTAGGAAGAATAGGACTCAGCGT
pOET1NS5b	NS5b1731FPPme1	Not1	TAAGCAGCGGCCGCCGCAAAAGACGTAAGATGTC
	NS5b2902RPBmt1	Bmt1	TGCTTAGCTAGCTTATGACGTAATAAGCTCAAGATC
pOETNS5b	NS5b2183FPNot1	Not1	TAAGCAGCGGCCGCCTTGACCGAACGACTGTAT
	NS5b2902RPBmt1	Bmt1	TGCTTAGCTAGCTTATGACGTAATAAGCTCAAGATC

*Brown sequence denotes spacer sequence, Blue sequence denotes RE sequence
Red sequence denotes a Stop Codon

Table 6 Primers designed for amplification of Core, NS4, NS5a and NS5b sequences for cloning into pOET8 plasmid.

11.4.1.2 Nucleic Acid Extraction

The NS3 and NS4 targets were amplified from HCV RNA positive serum. The first stage of this process was to perform nucleic acid extraction on several unlinked and anonymised human sera. Nucleic acid extraction was performed on HCV positive serum using the NucliSENS® EasyMag® instrument (BioMeriéux, Marcy l'Etoile, France) according to the manufacturer's instructions. In total 4 HCV

positive plasma samples were extracted, with an HCV human negative serum included as a negative control.

In short:
For each serum to be extracted 200 µL was added to a reaction vessel. The reaction vessel was placed on the EasyMag® with the corresponding pipette tips, and the extraction protocol set to on-board lysis, 200 µL serum sample and 60 µL eluate. The lysis stage of the extraction process was started. During the 10-minute lysis stage Magnetic silica beads were prepared by mixing 1:1 with molecular grade water. Upon completion of the lysis stage 100 µL of magnetic beads were added to each reaction vessel and mixed. The remainder of the extraction process was then started, which included multiple ethanol-based washes before a final elution step. The final eluate was transferred from each reaction vessel well into a 2.0 mL storage vial and stored at -20˚C until use.

11.4.1.3 Reverse Transcriptase

Reverse transcriptase reactions were performed on all nucleic acid extracts, to convert HCV RNA into DNA. Reverse transcriptase master mix was prepared with final concentrations of PCR Buffer at 1X, $MgCl_2$ 7.5 mM, dNTP at 1.5 mM each, random hexamers at 2.5 µM, 200 units of Moloney murine leukaemia virus (MMLV) reverse transcriptase (MMLV RT) (Thermofisher Scientific), 16 units of RNasin RNAase inhibitor (Promega, Madison USA) and made up to a final volume of 20 µL for each reaction with molecular grade water. The master mix was aliquoted in 20 µL volumes into 0.2 mL reaction tubes (Thermofisher Scientific). Nucleic acid extracts were added in 20 µL volumes to each tube, giving a total reaction volume of 40 µL. Tubes were placed on a Applied Biosystem 9600 thermal cycles (Thermofisher Scientific) and run with conditions of 22˚C for 10:00, 37˚C for 45 minutes and 80˚C for 5 minutes. Tubes were removed and stored at 4˚C until use.

11.4.1.4 PCR Amplification

Multiple PCR amplifications were performed throughout the study. All PCR amplifications were performed using Qiagen HotStart Taq DNA polymerase reagents (Qiagen, Venlo, Netherlands). For amplification of gene targets from plasmids PCR was performed directly on dilutions of purified plasmid DNA. For amplification of gene targets from positive sera the PCR was performed on cDNA created from reverse transcription of nucleic acid extracts. A standard master mix was used for all PCR, comprised of Qiagen PCR Buffer at 1X concentration, $MgCL_2$ at a final concentration of 2.0 mM, 5 units of HotStart Taq DNA polymerase (all supplied by Qiagen), dNTPs at 0.25 mM each and forward and reverse PCR primers at 0.5 µM each, made up to a final volume of 45 µL with molecular grade water and aliquoted into 0.2 mL 8-tube PCR strips. To this was added 5 µL of each target. All PCR

used standard PCR cycling conditions of 95°C for 15:00 as the activation step for the HotStart Taq polymerase, a 95°C for 15 secs denaturation stage, followed by variations in the annealing temperatures and extension times according to the primers used and size of the target.

11.4.1.4.1 Amplification of HCV Core from pIEx Plasmid

The HCV core sequence was amplified from the pIExCore plasmid for subsequent cloning into pIExBac3 plasmids, using the primers listed in Table 4. The pIEx HCV Core plasmid had previously been re-suspended to a concentration of 1 µg/µL. This was diluted to a concentration of 10 ng/µL in molecular grade water, then diluted further to 0.1 ng/µL and 0.01 ng/µL. All 3 concentrations were used in the PCR. See Table 7 below for PCR thermocycling conditions.

Stage	Target	Temperature °C	Time min	Cycles
Taq Activation	pIEXCore	95	15:00	1
Denaturation		95	00:15	40
Annealing		46	00:30	
Extension		72	01:00	
Final Extension		72	05:00	1
Hold		4	∞	

Table 7. PCR Thermal Cycling Conditions for amplification of HCV Core sequence from pIExCore plasmid for cloning into pIExBac3 plasmid.

11.4.1.4.2 Amplification of NS3 and NS4 from HCV Positive Serum

Both the NS3 and NS4 target sequences were amplified with PCR from cDNA produced by reverse transcription of nucleic acid extracted samples, for subsequent cloning into pIExBac3 plasmid. Primers used are listed in Table 4. All cDNA solutions were added neat. In total 3 samples and a negative control were run with the NS3 primers, and 6 samples and a negative control were run with the NS4 primers. Thermal cycling conditions for each target are listed in Table 8 below.

Stage	Target	Temperature °C	Time Minutes	Cycles
Taq Activation	All	95	15:00	1
Denaturation	All	95	00:15	40
Annealing	NS3	50-58	00:30	
	NS4	50-58		
Extension	All	72	02:00	
Final Extension	All	72	05:00	1
Hold	All	4	∞	

Table 8 PCR Thermal Cycling Conditions for amplification of NS3 and NS4 sequences from cDNA for cloning into pIExBac3 plasmid.

11.4.1.4.3 AMPLIFICATION OF FULL CORE, NS5A AND NS5B FROM HCV POSITIVE SERUM

Amplification of the full core, NS5a and NS5b sequences was performed using the cDNA produced from reverse transcription of nucleic acid extracted samples for subsequent cloning into pOET1 transfer vector plasmid.

Primers used are listed in Table 6 Primers designed for amplification of Core, NS4, NS5a and NS5b sequences for cloning into pOET8 plasmid. All cDNA solutions were added neat. In total 6 samples were tested in each PCR plus a negative control. Thermal cycling conditions for each target are listed in
Table 9 below.

Stage	Target	Temperature °C	Time min	Cycles
Taq Activation	All	95	15:00	1
Denaturation	All	95	00:15	40
Annealing	Full Core	54-58	00:30	
	NS5a	60-68		
	NS5b	52-58		
Extension	Full Core	72	01:00	
	NS5a		02:00	
	NS5b		03:00	
Extension	All	72	02:00	
Final Extension	All	72	05:00	1
Hold	All	4	∞	

Table 9 PCR Thermal Cycling Conditions for amplification of Full Core, NS5a and NS5b sequences from cDNA for cloning into pOET1 plasmid

11.4.1.4.4 AMPLIFICATION OF CORE, NS4, NS5A AND NS5B FROM PLASMIDS

All sequences for cloning into pOET8 plasmids were amplified from other plasmids. The core and NS4 sequences were both amplified from pIExBac3 plasmids. The NS5a and NS5b sequences were both amplified from pOET1 plasmids. Primers used are listed in Table 6. All plasmids were diluted 1:100

in molecular grade water. The same annealing temperature of 52°C was used for all PCRs, with varying extension times. Thermal cycling conditions for each target are listed in Table 10 below.

Stage	Target	Temperature °C	Time min	Cycles
Taq Activation	All	95	15:00	1
Denaturation	All	95	00:15	40
Annealing	pIExBac3Core	52	00:30	
	pIExBac3NS4			
	pOET1NS5a			
	pOET1NS5b			
Extension	pIExBac3Core	72	01:00	
	pIExBac3NS4		02:00	
	pOET1NS5a		02:00	
	pOET1NS5b		02:00	
Extension	All	72	02:00	
Final Extension	All	72	05:00	1
Hold	All	4	∞	

Table 10 Thermal Cycling Conditions for amplification of Core, NS4, NS5a and NS5b sequences from cDNA for cloning into pOET8 plasmid

11.4.2 GEL ELECTROPHORESIS

Gel electrophoresis was used for analysis of PCR products. A 1% agarose gel was prepared with 1.25 g of ultrapure agarose added to 125 mL of TBE (Tris borate-buffer EDTA) buffer (both Thermofisher Scientific), and heated until the agarose had completely dissolved. A 1:10000 dilution of Sybrsafe DNA stain (Thermofisher Scientific) was added to the liquid agarose, before pouring into a gel mold to cool and set. For loading 5 µL of each PCR product was mixed with 5 µL of gel loading buffer and all 10 µL added to individual wells of the gel. A low DNA mass ladder size ladder (Thermofisher Scientific) was run alongside the PCR products. The gel was run for a total of 40 minutes at 100 volts. Visualisation of the gel was performed using Alphaimager™2200 imaging system (Alpha Innotech, Cannock).

11.4.3 PCR CLEAN UP

A PCR purification kit (Qiagen) was used to prepare the amplified PCR product for ligation independent cloning. The PCR purification was performed according to the manufacturer's instructions. A volume of 225 µL of Buffer PB was added to 45 µL of PCR product. A pH indicator in the buffer PB turned the solution yellow. To this, 10 µL of Sodium acetate was added, turning the solution blue. The entire solution was added to a QIAquick spin column held in a 2.0 mL tube. The column was centrifuged at 8000g for 1 minute, and the flow through discarded. Next 750 µL of PE wash buffer was added to the column, then centrifuged again as described above. The flow through was then discarded. The centrifuge step was repeated to fully dry the column. The column was moved to a new, clean 1.5 mL centrifuge tube. Finally, elution buffer was added in a 50 µL volume, left to rest for 1 minute, and then centrifuged. The column was discarded. The eluted PCR product was quantified using a UV spectrophotometer (Implen Nanophotometer, Munich, Germany).

11.4.4 LIGATION INDEPENDENT CLONING INTO PIEX/BAC-3 PLASMID

A Novagen 3C/LIC cloning kit (Merck) was used to clone the purified PCR products into the pIExBac-3 LIC plasmid. The process is outlined in Figure 25 below.

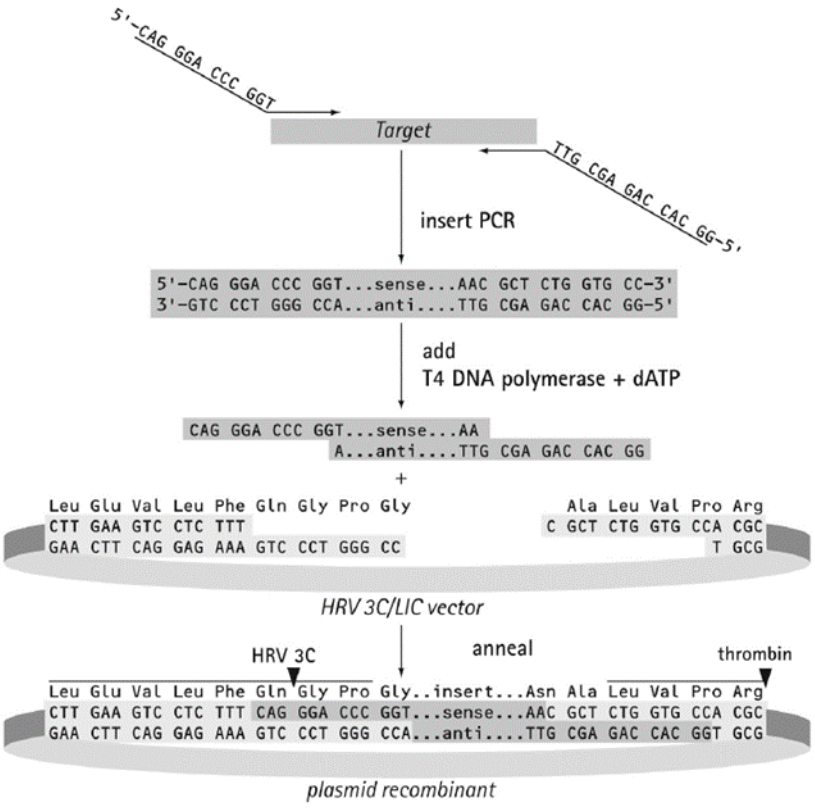

Figure 25 Illustration of ligation independent cloning[355]**.** First the target is amplified by PCR using LIC tagged primers. The first stage in the process involves the treatment of the PCR product with T4 DNA polymerase. Treatment of purified PCR product with T4 DNA polymerase in the presence of dATP creates an overhang which complements the 11-12bp single stranded overhangs in the pIEx/Bac-3 plasmid, enabling cloning without the need for DNA ligase. Cloning is completed when the plasmid was transformed into E. coli, upon which covalent bonds form at the vector insert junction completing a circularised plasmid.

11.4.4.1 T4 Treatment

The volume of PCR product for a total of 0.2 pmol was calculated based on the insert length and the concentration of DNA. In a 0.2 mL PCR tube 0.2 pmol of PCR product was mixed with 2 µL of 10X T4 DNA polymerase buffer, 2 µL of 2 mM dATP, 1 µL of 100 mM DTT and 0.4 µL of T4 DNA polymerase, made up to a total volume of 20 µL with molecular grade water. This was placed on a thermal cycler and run at 22˚C for 30 minutes followed by 75˚C for 20 minutes.

11.4.4.2 Annealing Reaction

The T4 treated PCR products were annealed adding by 2 µL to 1 µL of pIExBac 3 plasmid in a 0.2 mL PCR tube and gently mixing by pipetting. The tubes were placed on a thermal cycler at 22˚C for 5 minutes. After the first incubation 1 µL of 25 mM EDTA was added to each tube and placed back at

22˚C for a further 5 minutes. Annealed vectors were immediately used for transformation into competent *E. coli* cells using the transformation protocol outlined in 11.4.5.2.

11.4.5 TRADITIONAL CLONING USING RESTRICTION ENZYMES INTO POET1 AND POET8 PLASMIDS

Alternative transfer plasmids to the pIEx-Bac-3 described above and compatible with the -system were used in the study, pOET1N_6xHis and pOET8.VE2 (both Oxford Expressions Ltd). Cloning into both these plasmids was performed using traditional cloning techniques with restriction enzymes. An outline of the process is shown in below Figure 26.

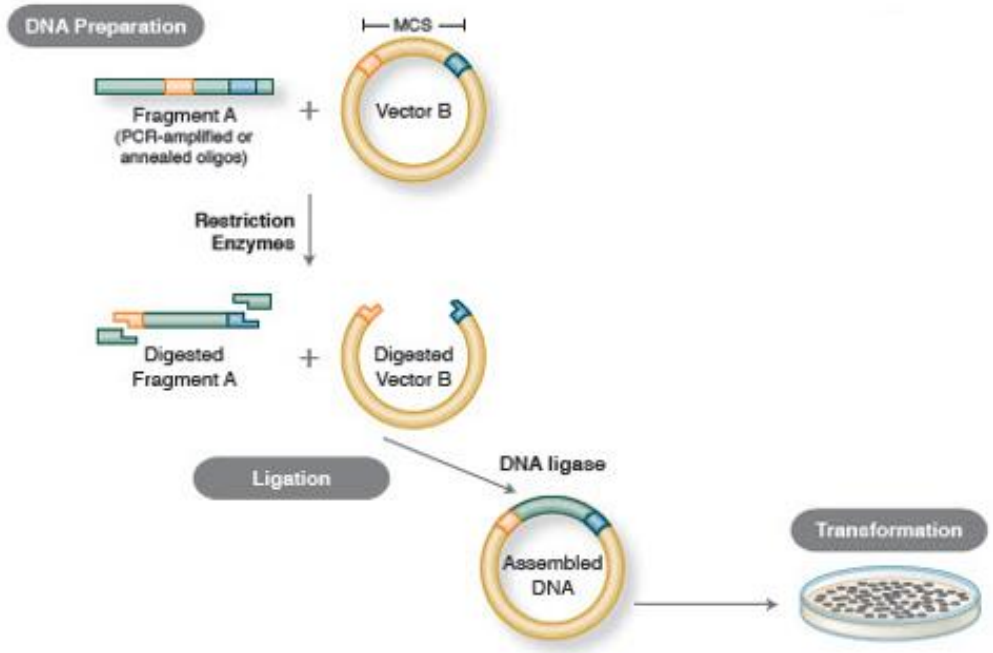

Figure 26 Outline of the traditional cloning process. Target gene is amplified with primers containing restriction enzyme cut sites. These same restriction enzyme cut-sites are located in the multiple cloning site of the target vector. Different restriction enzymes are included in the forward and reverse primers to ensure correct orientation of the inserted amplicon. Both the PCR amplicon and vector are treated with restriction enzymes to cut and create complementary ends. After purification of the PCR amplicon and vector the two are ligated together with DNA ligase. Cloned vector is then transformed into *E.coli* and cultured on selective agar. Discrete colonies are picked, purified and presence of PCR amplicon confirmed by nucleotide sequencing. Taken from **https://www.neb.com/tools-and-resources/feature-articles/foundations-of-molecular-cloning-past-present-and-future Accessed 10/08/2020.**

PCR products were purified using a PCR purification kit before treatment with restriction enzymes, exactly as described in section 11.4.3.

11.4.5.1.1RESTRICTION ENZYME TREATMENT

The quantity of the purified PCR product and plasmid was determined using the nanophotometer. Both the PCR product and the matching plasmid were cut with restriction enzymes in separate 0.2 mL PCR tubes. The NEB cloning tool, http://nebcloner.neb.com, accessed 08/03/2016, was used to choose a compatible buffer for the two restriction enzymes. The full list of restriction enzymes used for each PCR product and matching plasmid is listed in Table 11 below.

Target	PCR Primers	Plasmid	Restriction Enzyme 1	Restriction Enzyme 2	Buffer
Core	Core1a6FPXb Core570RPBglII	pOET1	XbaI	BglII	10X NEBuffer 3.1
NS5a	NS5a30FPXb NS5a1431RPBg	pOET1	XbaI	BglII	10X NEBuffer 3.1
pIExBac3Core	CoreHISFPPmeI CoreRP2BMt1	pOET8	PmeI	BmtI	10X CutSmart Buffer
pIExBac3NS4	pIExFPPmeI NS45954RPBmtI	pOET8	PmeI	BmtI	10X CutSmart Buffer
p0ET1NS5a	pOET1Pme1 NS5a1247RPBmt1	pOET8	PmeI	BmtI	10X CutSmart Buffer
pOET1NS5b	NS5b1731FPPme1 NS5b2902RPBmt1	pOET8	PmeI	BmtI	10X CutSmart Buffer

Table 11 List of RE and Compatible buffer used for cutting PCR products and matching plasmid

Restriction enzymes reactions were set up on ice. The RE mix included the compatible buffer at a final concentration of 1X, 10 units of each RE, 1 µg of PCR product or plasmid and made up to a final volume of 50 µL with molecular grade water. Each tube was then transferred to a thermal cycler at 37°C for 60 minutes. After 30 minutes, shrimp alkaline phosphatase (SAP) was added to the plasmid only, to dephosphorylate the cut ends and reduce the possibility of the plasmid self-annealing. After RE cutting was completed a gel extraction purification was performed to remove enzymes.

11.4.5.1.2GEL EXTRACTION PURIFICATION

A Monarch® DNA gel extraction kit (New England Biosciences). was used for purifying both the RE cut PCR product and plasmid RE cut PCR products and plasmids were electrophoresed on a 1% agarose gel as described in 11.4.2. A large well comb was used to enable the addition of the total volume of 50 µL from the RE reaction. The 1% gel was run for 1 hour at 100v. When the electrophoresis was complete, UV transillumination was used to view the bands, and the DNA fragment was excised from the agarose gel using a sterile scalpel. The gel slice was transferred to a 1.5 mL microcentrifuge tube and weighed. A proportional amount of Monarch Gel dissolving buffer

(400 µL for each 100 mg agarose) was added to the gel slice. The sample was incubated at 50°C, vortexing periodically until the gel slice was completely dissolved (generally 5–10 minutes). The dissolved sample was added to a Monarch® DNA clean up column, and the column placed in a collection tube. The tube was spun for 1 minute at 15000 x g, and the flow through discarded. Next 200 µL of DNA wash buffer was added to the column, and the centrifugation step repeated. This wash stage was repeated a 2nd time. An extra centrifuge step was then performed to completely dry the column. For the final elution step the column was transferred to a 1.5 mL storage tube, 10 µL of elution buffer added to the column, left to incubate for 1 minute, then centrifuged to collect the eluate. The amount of DNA in the collected eluate was then quantified using a nanophotometer. The RE cut and purified PCR product and plasmid were then immediately ligated together.

11.4.5.1.3LIGATION OF PCR PRODUCT AND PLASMID

The purified RE cut PCR product and plasmid were ligated together using Instant sticky end ligase master mix (New England Biosciences). A ligation calculator tool (http://nebiocalculator.neb.com/#!/ligation), 08/03/2016, was used to calculate a 3:1 insert to vector ratio, based on the DNA sequence length (in Kb) of both the insert DNA and vector DNA.

All reagents were kept on ice during the ligation procedure. The volumes required for 30ng of plasmid vector, and the volume for a 3:1 ratio of insert DNA, were mixed together and made up to a total volume of 5 µL. To this was added 5 µL of instant sticky end master mix and mixed thoroughly by pipetting up and down 10 times. Ligated product was then immediately used for transformation into *E. coli*.

Transformation into *E. coli* was performed as described in section 11.4.5.2. All plasmid transfer vectors used contained an ampicillin resistance gene, allowing growth on ampicillin containing selective media. Plasmid preparations were performed on a selection of colonies as described in section 11.4.5.3, with subsequent confirmation by nucleotide sequencing as described in section 11.4.5.4. Only vectors with confirmed insertion of DNA in the correct reading frames were used in subsequent protein expression experiments.

11.4.5.2 Transformation

All cloned plasmid transfer vectors were transformed in competent *E. coli* cells. The competent cells used were NEB® Beta-10 *E.coli* (New England Biolabs). Pre-aliquoted vials (50 µL) of competent cells were taken out of the freezer and immediately placed on ice and left to thaw for 10 minutes. Cells were re-suspended by gently flicking. A volume of 1 µL of the plasmid was added to a vial of competent cells, gently mixed using the pipette and placed back on ice. Tubes were left on ice for 30

minutes. Tubes were then transferred to a hot block at 42˚C for exactly 30 seconds, before placing back on ice for 5 minutes. Keeping the tubes on ice, 450 µL of NEB 10-beta/Stable outgrowth medium was added, then the tubes transferred to a shaking hot block set at 37˚C (300rpm) for 60 minutes. Pre-prepared nutrient agar plates containing the antibiotic ampicillin (50 µg/mL) were taken out and left to warm to room temperature. After the tubes had spent 60 minutes at 37˚C, all 500 µL of medium from each was pipetted onto ampicillin agar plates, spread out evenly and left to dry for 5 minutes at room temperature. Plates were then turned over and transferred to a 37˚C incubator and left overnight to grow. Plates were checked for evidence of transformed colonies after 24 hours.

11.4.5.3 Plasmid Clean Up

Plasmids were purified from isolated colonies using a QIAprep spin miniprep kit (Qiagen), according to the manufacturer's instructions. A single isolated colony was picked from an agar plate and added to 5 mL of LB medium/Ampicillin 50 µg/µL in a 15 mL centrifuge tube, this was incubated at 37˚C for 16 hours in a shaking incubator. This was repeated for 3 separate colonies from each agar plate. After 16 hours incubation cells were centrifuged at 5400g for 10 minutes at 4˚C to pellet the bacterial cells, and the supernatant discarded. The pellet was re-suspended in 250 µL of buffer P1 and transferred to a 1.5 mL centrifuge tube. Buffer P2 was added in a 250 µL volume and the tube mixed thoroughly. Buffer N3 was then added in a 350 µL volume and mixed thoroughly immediately. The homogenous solution was centrifuged at 15000 x g for 10 minutes. The supernatant was then added to a QIAprep spin column, and centrifuged for 1 minute at 15000 x g. The column was washed with 0.75 mL of buffer PE and centrifuged as described above. The flow through was discarded and the centrifuge step repeated to fully dry the column. Elution buffer was added in a 30 µL volume, left for 1 minute, then centrifuged to collect the eluate. The column was then discarded, and the collected eluate quantified using the nanophotometer, before storing at -20˚C until use.

11.4.5.4 NUCLEOTIDE SEQUENCING OF PLASMIDS

Each cleaned up plasmid transfer vectors were checked for successful insertion of PCR amplicon by nucleotide sequencing. Nucleotide sequencing was performed using the Sanger sequencing method with Applied Biosystems™ BigDye™Terminator v1.1 cycle sequencing reagents and an Applied Biosystems™ 3130 genetic analyser (Thermofisher Scientific). Primers used for sequencing included plasmid specific forward and reverse plasmid primer, plus insert specific forward and reverse primers (Table 12).

Primer	Plasmid Target	5'-3' Sequence*
IE	All pIExBac3	TGTTGGATATTGTTTCAGTTGCAAG
ST24 RP		TGGCTCCAAGCGGAACTA
CoreFS	pIExBac3Core/pOET1FCore/ pOET8HCore	TCCACCAACCCGAAAC
CoreRS		TTAGTCGATCACCTTGCCTAG
NS3502FS	pIExBac3NS3	GACTTTATCCCCGTAG
NS31330RS		TGTCTCAATGGTGAAG
NS45086FS	pIExBac3NS4/ pOET8NS4	TACAGTGAGGCTGCTGAGTATG
NS45918RS		TACAGTGAGGCTGCTGAGTATG
pOETFP	All pOET1/ pOET8	CAAACTAATATCACAAACTGGAAATGTCTATC
pOETRP		TACAACAATTGTCTGTAAATCAACAACGC
NS5A73FS	pOET1NS5a/ pOET8NS5a	AGCCAAGCTCATGCCACAAC
NS5A1a711FS		ATCTCTCAAGGCAACTTGCA
NS5a1247RS		CATGGAAGAATAGGACTCAGCGT
NS5b2183FPNot1	pOET8NS5b	CTTGACCGAACGACTGTAT
NS5b2902		ATGACGTAATAAGCTCAAGATC

Table 12 Primers used for sequencing of plasmids

Plasmids were diluted to a final concentration of 50 ng/µL in molecular grade water. Individual sequencing mixes were prepared with 2 µL of BigDye Terminator v1.1, 2 µL of 5X Big dye sequencing buffer, 2 µL of primer at 5 µM and made up to a final volume of 18 µL with molecular grade water. The mix was aliquoted into designated wells of a MicroAmp™ optical 96-well reaction plate. Next 2 µL of each plasmid was added to the corresponding well of the 96 well plate. The plate was sealed with Microamp optical caps. The plate was placed on a thermal cycler and run with 25 cycles of 95˚C for 2 secs, 50˚C for 5 secs and 60˚C for 4 minutes.

11.4.5.4.1 Sequencing product clean up

Sequencing reaction products were cleaned using an ethanol precipitation based protocol. A solution of 50 µL of 100% ethanol plus 2 µL Sodium acetate was added to each well. The wells were sealed with adhesive cover, gently rotated to mix then spun on a plate centrifuge (Eppendorf, Germany) at 2000 X g for 20 minutes. Following this the adhesive cover was removed, the plate turned upside down onto absorbent paper, and spun in the plate centrifuge at 150 X g for 1 minute to dry. The absorbent paper was discarded, the plate turned to face upwards again, and 150 µL of 70% ethanol added to each well. The plate was then spun at 5000 X g for 5 minutes. A repeat centrifugation step was performed to remove the 70% ethanol. The final, dry pellets in each well were re-suspended in 20µl of HiDi formamide (Thermofisher Scientific). Following re-suspension the plate was placed on a 3130 Genetic analyser and run on a 1 hour protocol using a 50 cm capillary.

11.4.5.4.2 Sequencing Analysis

Sequence analysis was performed using the free automated sequence analysis software (RECall)[356] located at http://pssm.cfenet.ubc.ca, accessed 11/05/2015. Reference sequences for each gene were uploaded to the website, and SEQA sequence files for each plasmid aligned against the reference. Sequences were checked for miscalls between different primer sequence files, and a final consensus sequence produced for each plasmid

Each final consensus sequence was then aligned against the predicted plasmid sequence using SNAPgene software. The sequence was checked for the insertion of the gene in the correct reading frame, and for any base sequence errors.

11.4.5.5 DESIGN OF NS5B PLASMID

After multiple failed cloning attempts to clone the amplified NS5b gene into the pOET1 transfer vector, a synthesized NS5b gene was ordered from Eurofins. This covered the entire NS5b gene and arrived cloned into the pOET1 transfer vector.

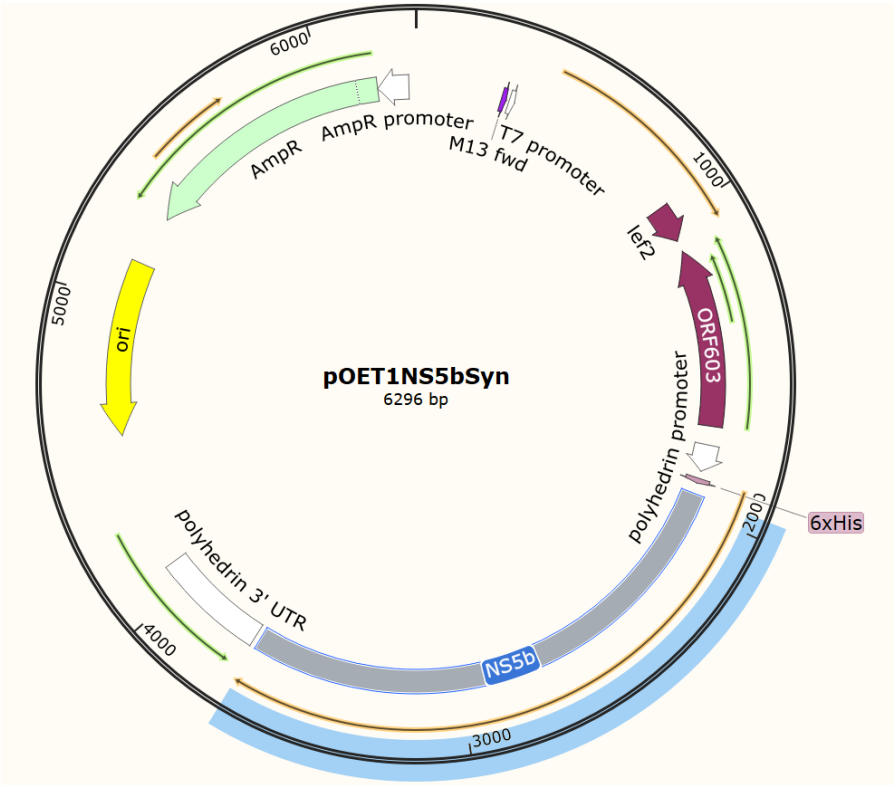

Figure 27 Synthetic NS5b gene inserted into pOET1 transfer vector. The synthetic NS5b gene is highlighted in blue, downstream of the polyhedrin promoter and 6XHis tag. Synthetic NS5b gene was produced by cloned into pOET1 vector by Eurofins.

11.4.6 PROTEIN EXPRESSION USING THE *FLASH*BAC™ ULTRA SYSTEM

Protein expression was performed using *flash*BAC™ ULTRA expression system (Oxford Expressions Ltd). The *flash*BAC™ bacmid was transfected in combination with a plasmid transfer vector into SF9 cells to generate recombinant baculovirus. The recombinant baculovirus was amplified in Sf9 cells before expression of protein in Hi5 cells. An outline is shown in Figure 28 below.

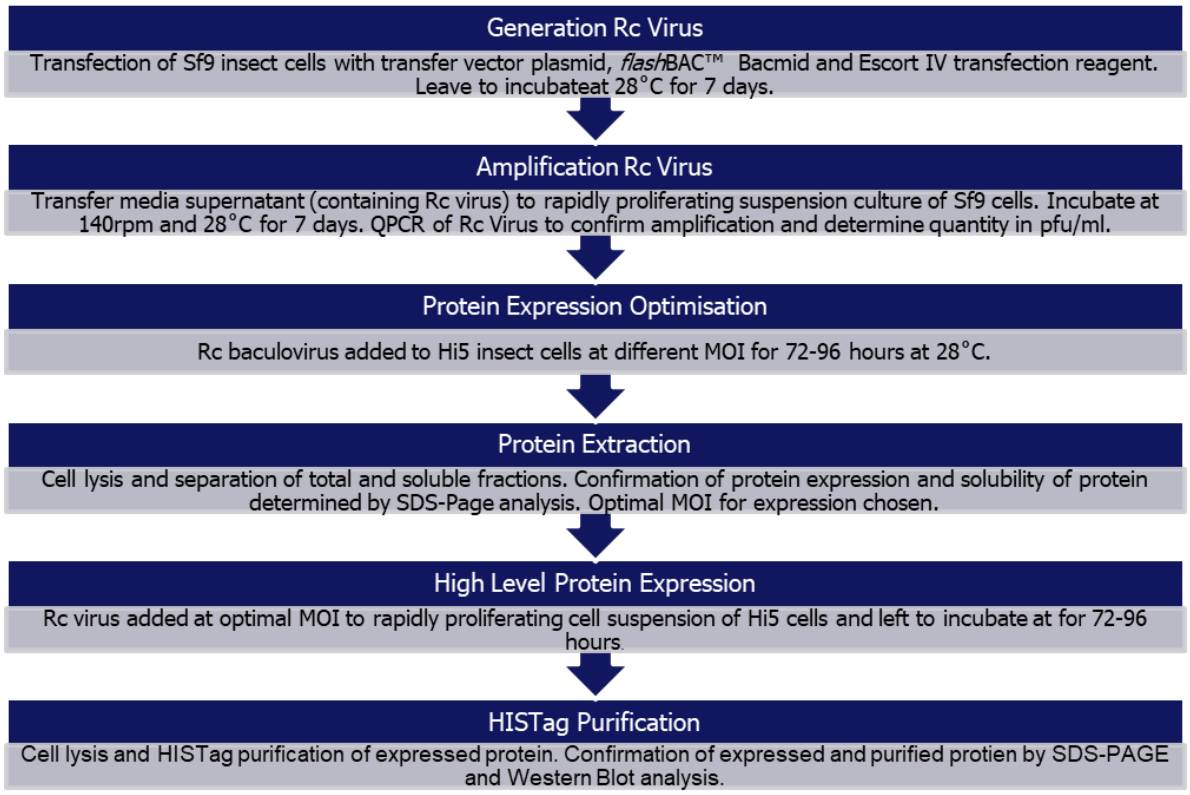

Figure 28 Outline of process for protein expression using *flash*BAC™ ULTRA expression system.

11.4.6.1 GENERATION OF RECOMBINANT BACULOVIRUS

Rapidly proliferating Sf9 insect cells were used for transfection with a plasmid transfer vector and *flash*BAC™ ULTRA bacmid to generate recombinant baculovirus. All cell culture work was performed in a Class II Bio Safety Cabinet.

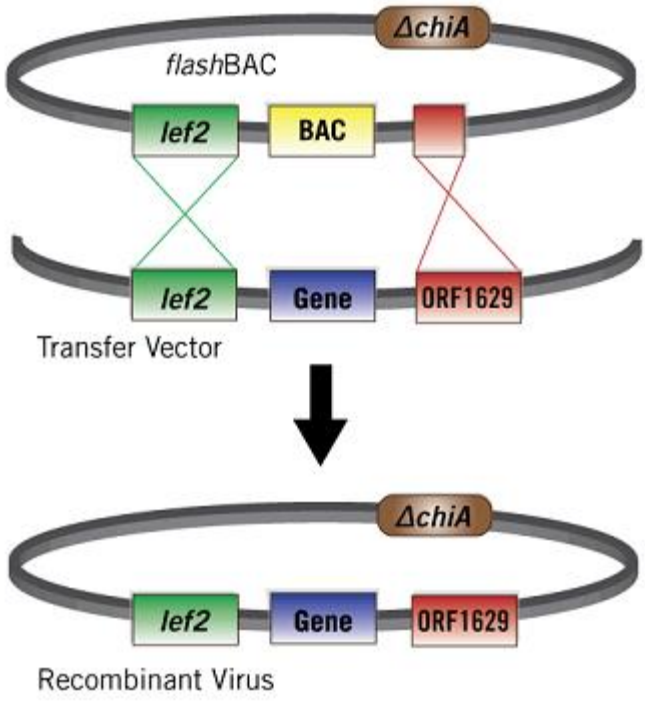

Figure 29 Generation of Rc baculovirus by homologous recombination between *flash*BAC bacmid and complementary transfer vector. The *flash*BAC bacmid is missing the essential orf 1629 gene. When transfected into insect cells in combination with a matching transfer vector containing the orf 1629 gene and the gene to be expressed, homologous recombination occurs and a recombinant baculovirus is produced containing the gene to be expressed. The requirement for the missing essential gene acts as a selection tool, as only the recombinant virus containing the transfer vector will replicate. Taken from https://www.mirusbio.com/products/virus-production/flashbac-baculovirus-expression-system#figure1272. Accessed 20/08/2020.

Wells of a 6 well culture plate were seeded with 2 mL of 5 X 10^5 cells/mL (1 X 10^6 cells total) of Sf9 cells, *flash*BAC™ ULTRA and checked for even distribution. The plate was left for 1 hour at 28°C to allow the cells to settle. During the 1-hour incubation a co-transfection mix was prepared. In a tube labelled 'A' 2.5 µL of *flash*BAC™ ULTRA bacmid and 250 ng of transfer plasmid were combined with 100 µL of SF-900™ media and gently swirled to mix. In a separate tube labelled 'B' 100 µL of SF-900 media was combined with 6 µL of Escort IV™ transfection reagent (Sigma-Aldrich) and gently swirled to mix. Tubes A and B were combined and gently swirled to mix, then left for 45 minutes at room temperature. After 1-hour incubation media was removed from the wells of the culture plate. All 200 µL of tube A/B mix was added dropwise to the wells, followed by 800 µL of SF-900™ media on top. This was incubated at 28°C for 24 hours. After 24 hours an extra 1ml of SF-900 media was added to each well and left to incubate at 28°C for a further 6 days. Following the weeklong incubation images of the cells were recorded using a Nikon Coolpix 995 microscope specific camera before the supernatant containing recombinant baculovirus was carefully aspirated from each well, and immediately transferred into a 50ml SF9 suspension culture for amplification of the virus.

11.4.6.2 AMPLIFICATION OF RECOMBINANT VIRUS

Recombinant virus was amplified in rapidly proliferating Sf9 cells for one week, to generate sufficient virus for subsequent protein expression experiments. The Sf9 cell suspension had been passaged for a minimum 3 times and were >95% viable. Media used for all virus amplification was SF-900.

A 50ml suspension of rapidly proliferating Sf9 cells was prepared in 250 mL Erlenmeyer flasks with vented caps, at a concentration of 2 X 10^6 cells per mL, as described in section 11.2.3. All supernatant collected from the transfection was added to the 50ml cell suspension and incubated in a shaking incubator set at 140rpm and 28°C for 7 days. After 7 days the suspension culture was transferred to a 50 mL centrifuge tube and centrifuged at 700 X g for 3 minutes. Before spinning an aliquout of the cell suspension was added to a counting chamber and images of the cells were recorded using a Nikon Coolpix 995 microscope specific camera. The budded virus containing supernatant was aspirated, being careful not to disturb the cells, and transferred to a separate 50 mL centrifuge tube for storage at 4°C in the dark.

11.4.6.3 QUANTITATIVE PCR OF RECOMBINANT VIRUS

The level of recombinant virus post amplification was determined by quantitative PCR (QPCR). This was performed using a previously published Taqman™ primer and probe set[357]. Nucleic acid extraction was performed using an Invitrogen nucleic acid extraction kit (Thermofisher Scientific), followed by a Taqman based real-time PCR using Applied Biosystems Fast PCR mix and an Applied Biosystems StepOne™ Real-Time PCR System (Thermofisher Scientific).

11.4.6.3.1 Nucleic Acid Extraction

Nucleic acid extraction of the recombinant virus was performed using Invitrogen genomic DNA kit (Thermofisher Scientific UK). A volume of 200 µL of recombinant virus supernatant was aliquoted into a 2.0ml storage vial. To this 20 µL of RNase A and 20 µL of proteinase K was added to the media, and the tube briefly vortexed. Following this 200 µL of genomic lysis/binding buffer was added, vortexed, then placed at 55°C in a heating block for 10 minutes. The tube was removed from the heating block and 200 µL of ethanol added, then vortexed to mix. The total lysate (640 µL) was then transferred to a spin-column and spun at 10000 x g for 1 minute at room temperature. The column was spun at 10000 x g for 1 minute at room temperature, after which the collection tube containing the run through was discarded and the column placed in a new collection tube. A volume of 500 µL of wash buffer 1 was added, and the centrifuge step repeated. A further wash step was performed with wash buffer 2, and the centrifuge step repeated. After removal of wash buffer another spin was performed at 14000 x g for 3 minutes to fully dry the column. The column was transferred to a 1.5

mL Eppendorf tube, 50 uL of elution buffer added to the column and left for 1 minute. A final spin at 14000 x g was performed to collect the eluate, and the column discarded. Extracted eluates were stored at -20°C until use.

11.4.6.3.2 Real-Time PCR

Real-time PCR was performed using Applied Biosystems Taqman™ Fast universal PCR master mix and run on an Applied Biosystems StepOne™ real-time PCR system (Thermofisher scientific). A 10-fold dilution series of a recombinant baculovirus of known quantity (previously quantified by Oxford Expression Ltd) was prepared in SF-900 media and extracted as described above. The dilution series ran from 1 X 10^9 pfu/mL to 1 X 10^4 pfu/mL and run in duplicate alongside the samples. A negative extract control was included on each run.

A real-time PCR master mix was prepared containing 12.5 µL of Fast universal PCR master mix, primers at a final concentration of 0.3 µM and probe at a final concentration of 0.1 µM, made up to a final volume of 20 µL per sample. This was aliquoted into a Microamp™ fast optical 48-well reaction plate (Thermofisher Scientific). Samples and controls were added in 5 µL volumes. All standards and samples were run in duplicate. The plate was placed on a StepOne™ Real-Time PCR System and run with the following conditions, 95°C for 20 secs, 35 cycles of 95°C for 3 secs and 60°C for 30 secs. The run was analysed, and a standard curve produced, giving a quantity in pfu/mL for each sample. A mean value was calculated from the duplicate results for each recombinant virus.

11.4.6.4 PROTEIN EXPRESSION OPTIMISATION IN HI5 INSECT CELLS

Protein expression was first trialled and optimised in HI5 insect cells, at varying multiplicity of infection (MOI) levels. Each recombinant virus was diluted in Express Five media to the desired MOI level. Insect cells, Hi5, used for protein expressions had been passaged a minimum of 3 times, and were a minimum >90% viable. Media used for all protein expression work was Express Five. All protein expression work was performed in a Class II Bio Safety Cabinet.

Cells were seeded into 6 well 35m dish, 2 mL of 5 X 10^5 cells/mL (1 X 10^6 total per well). Cells were left for 1 hour to settle and adhere to the culture plate. Cell medium was removed, then 200 µL of media/RcVirus was added to each well dropwise. The Rc virus was left for 1 hour to absorb, with occasional tipping of the plate. After 1 hour 2 mL of Hi5 media was added to each well, the plates placed in a sandwich box and left in the incubator for the 72 hours at 28°C. After 72 hours the cells were gently re-suspended and transferred to 2.0 mL storage vials.

11.4.6.5 PROTEIN EXTRACTION

The protein extraction method used a Triton x-100 based lysis buffer. Triton x-100 is a non-anionic surfactant detergent. Non-ionic detergents disrupt lipid to lipid and lipid to protein interactions but not protein to protein and are non-denaturing[358].

Protein was extracted from Hi5 insect cells after 72 hours incubation. Cells were lysed in a buffer prepared in sterile distilled water with 25 mM Tris-HCL (Formedium, UK), 150mM NaCL, 1% Triton X-100 (Sigma-Aldrich) Benzonase at 1:10000 dilution (Merck) and a HALT protease inhibitor cocktail at 1:100 dilution (Thermofisher Scientific), adjusted to a final pH of 8. After lysis a total fraction and soluble fraction were collected to identify if protein expression had occurred and if any protein expressed was in a soluble form.

Each cell suspension was centrifuged at 800 X g for 2 minutes, and the supernatant collected. The remaining pellet was re-suspended in 0.5 mL of chilled lysis buffer and left on ice for 30 minutes. Every few minutes the suspension was re-suspended using a pipette to ensure consistent lysis of the suspended cells. A 30 µL aliquot of the lysed suspension was collected and labelled 'Total Fraction'. The suspension was then centrifuged at 15000 X g for 30 minutes at 4˚C. A 30 µL aliquot of the supernatant was taken and labelled 'Soluble Fraction'. The remaining supernatant was separated into a 1.5 mL storage vial and snap frozen in liquid nitrogen. Each aliquot was analysed by SDS-PAGE to determine if protein expression had occurred, to identify if any expressed protein was soluble, and to select the optimum MOI.

11.4.6.6 SCALED UP PROTEIN EXPRESSION

If protein expression had been confirmed, a large-scale protein expression was performed using the optimum MOI of recombinant virus. Large scale protein expression was performed in Hi5 suspension culture, using cells adapted to suspension culture for at least 3 passages and a minimum >95% viable.

An 80 mL suspension of rapidly proliferating Hi5 insect cells was prepared at a concentration of 5 X 10^5 cells/ml in 250 mL Erlenmeyer flasks with vented caps, as described in section 11.2.3. Recombinant virus was added at the desired MOI directly to the cell suspension. This was placed in a shaking incubator set at 140rpm and 28˚C for 72 hours. After 72 hours the suspension was split into 2 x 40 mL in 50 mL Falcon tubes and spun at 800xg for 2 minutes. The supernatant was carefully removed and stored in a separate 50ml Falcon tubes, with the 2 remaining cell pellets snap frozen in liquid nitrogen and stored at -80˚C until use.

11.4.6.7 LARGE SCALE PROTEIN EXTRACTION

Protein extraction of frozen 40 mL cell pellets was performed using the same protocol and lysis buffer described in section 11.4.6.5. The only addition to the lysis buffer was Imidazole at a concentration of 5mM. This was added to prevent nonspecific binding when the lysed solution was added to Ni-NTA beads for purification. The volume of lysis buffer added to each 40 mL cell pellet was increased to 2 mL.

11.4.6.8 PROTEIN PURIFICATION

Purification of expressed proteins was performed using HisTag purification with nickel coated Ni-NTA beads (Thermofisher Scientific). This is an affinity-based protein purification method. The principle involved is the affinity for his residues to metal ions, in this case nickel ions immobilised on agarose beads. A chelating agent, Nitrilotriacetic acid (NTA) is used to immobilise nickel ions onto agarose beads, as can be seen in Figure 30.

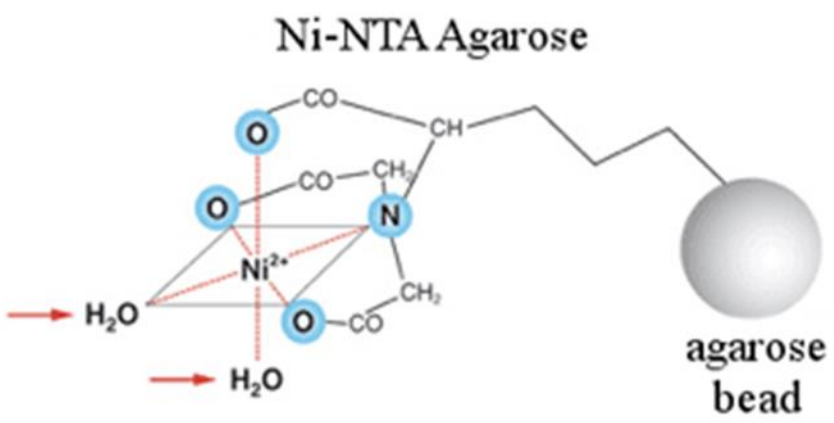

Figure 30 Diagram of Nickel coated agarose beads used for His Tag purification. Binding sites for His residues are highlighted with red arrows.

The pIExBac3, pOET1 and pOET8 plasmids used as transfer vectors all code for N terminus His tags composed of multiple His residues. During protein purification Ni-NTA agarose beads are mixed with the protein solution, and the His residues at the N terminus of the protein bind to the Nickel ions coated on the agarose beads. The His residues have a higher affinity for the nickel ions than other proteins, selectively binding the protein of choice. To further increase the specificity of nickel binding, a salt is included in the binding buffer to prevent non-specific ionic interactions, and low level of competing agent (5 mM Imidazole) included. After a binding incubation has been performed the beads are washed in higher concentrations of imidazole, which removes any low-level binding proteins from the nickel. To increase specificity the imidazole concentration can be increased, generally in a range from 10 mM to 70 mM. The final elution stage uses a high concentration of

imidazole buffer, 250 mM, which out competes any bound His residues and removes the protein from the nickel coated beads into the elution buffer.

All washing and elution imidazole buffers were prepared in PBS at a pH of 8. These included equilibration buffer containing 5mM Imidazole in PBS, wash buffers including a range of Imidazole from 10-70 mM in PBS, and elution buffer containing 250mM imidazole in PBS. All steps were performed on ice and in chilled centrifuges at 4 °C.

The Ni-NTA beads were prepared by placing a volume of 400 µL of Ni-NTA bead suspension (containing 200µl of Ni-NTA beads) into a 15 mL universal tube and centrifuging at 700 x g for 2 minutes. The storage buffer supernatant was removed, and the beads washed with 1 mL of equilibration buffer followed by a repeat centrifugation and supernatant removal step. All 2 mL of lysed pellet solution from the large-scale protein extraction was added to the 200 µL of washed Ni-NTA beads. The bead solution mixture was rotated on a tube roller for 2 hours at 4°C for binding. After 2 hours binding the mixture was spun at 700 x G for 2 minutes. The supernatant was then discarded, with an aliquot taken and labelled as FT ('Full transfer'). A 5 mL volume of 10 mM imidazole wash buffer was added to the beads, rolled for 5 minutes at 4°C, then centrifuged at 700 x g for 2 minutes after which the supernatant was discarded. An extra 4 wash steps were performed, with an incremental imidazole gradient running from 20-50 mM. Aliquots were taken from each wash step. Elution was then performed by adding 200µl of 250 mM imidazole wash buffer, followed by rolling for 5 minutes at 4°C, centrifuged at 700g for 2 minutes and the supernatant removed and placed in 1.5 mL storage tube. Aliquots were taken from each elution step. All eluates were snap frozen in liquid nitrogen and stored at -80°C until use. Aliquots were analysed by SDS-PAGE and western blot analysis.

11.4.6.9 PROTEIN SOLUBILISATION

For proteins which were only expressed in insoluble forms several solubilisation procedures were performed.

11.4.6.9.1 HIGHER SALT LYSIS AND SONICATION AND HISTAG PURIFICATION

The protein extraction was performed as described in section 11.4.6.5, but the NaCL concentration in the lysis buffer was increased from 150 mM to 300 mM. Another modification was the doubling in the concentration of benzonase nuclease added to the lysis buffer to a 1:5000 dilution. All other components of the lysis buffer remained the same. A pellet fraction (from 40 mL of cell suspension) was lysed in 2 mL of lysis buffer with 300mM NaCL. After repeated pipetting up and down on ice for 30 minutes, the lysed cell suspension was sonicated for 10 seconds.

Lysed and sonicated cell suspensions were purified via HIStag purification as described in section 11.4.6.8, except that a higher NaCL concentration of 300 mM was used in both the wash buffers and elution buffers. Washing of beads used an imidazole gradient running from 10 mM to 50 mM, before final elution in 250 mM imidazole. Subsequent SDS PAGE analysis was performed to determine the success of the solubilisation procedure.

11.4.6.9.2UREA/GUANIDINE SOLUBILISATION

Solubilisation using urea or guanidine used the same procedure. Urea solubilisation buffer was prepared with 50 mM Phosphate buffer at pH 8.0, 300 mM NaCL, 10 mM β-mercaptoethanol and 8 M urea. Guanidine solubilisation was prepared with 50 mM Phosphate buffer at pH 8.0, 300 mM NaCL, 10 mM β-mercaptoethanol and 6 M guanidine hydrochloride. All procedures were performed on ice and centrifuges set to 4°C. Preparation of both solubilisation buffers was performed in a fume extraction cupboard.

Standard protein extraction was performed, using 2 mL of lysis buffer for a cell pellet from 40ml of cell suspension. A centrifugation step of 15000 x g for 30 minutes was used to separate the soluble fraction from the insoluble fraction, and the soluble supernatant removed. The remaining insoluble pellet was dissolved in either 1 mL of urea or 1 mL guanidine based solubilisation buffer. The pellet was gently agitated on ice for 30 minutes to dissolve. After 30 minutes a centrifugation step at 15000 x g for 30 minutes was performed to separate remaining soluble and insoluble fractions. The soluble supernatant was then removed, and an aliquot taken for SDS page analysis. The removed soluble fraction was then HISTag purified using either a hybrid denaturing method, or a full denaturing method.

11.4.6.9.3HISTAG PURIFICATION UNDER HYBRID DENATURING CONDITIONS

The solubilised supernatant (around 1ml) was added to 200 µL of washed Ni-NTA beads, and bound for 2 hours at 4°C. After binding the beads were first washed twice in 5 mL non-imidazole denaturing wash buffer, comprised of 50m phosphate buffer at pH 8.0, 500 mM NaCL and 8 M urea. Beads were washed for 5 minutes on a rolling shaker at 4°C, before centrifugation at 800 x g for 2 minutes followed by removal of the wash buffer. After 2 washes in denaturing non-imidazole buffer, an imidazole concentration gradient wash was performed as described in 11.4.6.8. The imidazole wash buffer contained 50mM phosphate buffer at pH8.0, 150 mM NaCL and imidazole running in 10 mM increments from 10-70mM. No urea was added to the wash buffer. For each wash step 5 ml of wash buffer was added to the breads, washed for 5 minutes at 4°C, then centrifuged, wash buffer removed then repeated. After all imidazole washes, standard 250 mM imidazole elution buffer was added in

200 µL volumes, eluted for 5 minutes, then centrifuged before collection of the eluate. A total of 3 elutions were performed. Aliquots were collected at each stage for SDS PAGE analysis.

11.4.6.9.4HISTAG PURIFICATION UNDER DENATURING CONDITIONS

A HISTag purification under denaturing conditions was performed as described for the hybrid purification, except with the addition of 8 M urea into all wash buffers and elution buffers. The same imidazole gradient buffer wash stages were performed, with the same elution procedure, all performed with 8 M urea added to the buffers to maintain denaturing conditions throughout the purification procedure. Aliquots were collected at each stage for SDS PAGE analysis.

11.4.6.10 PROTEIN QUANTITATION

The concentration of protein in each eluate from the His tag purification process was determined using an Invitrogen Qubit 4 fluorometer with Invitrogen Qubit protein assay kit (Thermofisher Scientific). Protein quantitation was determined according to manufacturer's instructions. A working protein solution was prepared by mixing Qubit protein reagent with Qubit buffer, in a 1:200 ratio. Enough working solution was prepared for the 3 control samples and to test the number of eluates in duplicate. The 3 control samples were added in 10 µL volumes to 190 µL of protein working solution in clear 0.5ml PCR tubes, and vortexed for 2-3 seconds. The protein eluates were added in 1 µL volumes to 199 µL of protein working solution, and vortexed for 2-3 seconds. Each protein eluate was set up in duplicate. The samples and controls were left to incubate for 15 minutes at room temperature. Tubes were then placed in the Qubit Fluorometer for reading. First the 3 controls were tested to generate a standard curve, next the samples were tested, setting the volume on the fluorometer to 1 µL. The mean average was calculated from the duplicate values for each protein eluate.

11.5 REFERENCE ASSAYS

11.5.1 ANTI-HCV ASSAYS

11.5.1.1 SERUM SAMPLES

All sera used for subsequent ELISA optimization and validation experiments had been previously tested using the Roche Elecsys® anti-HCV II run on the Roche Cobas® 6000 analyser (Roche Switzerland). This is an electrochemiluminescence immunoassay for the detection of antibodies to hepatitis C. The assay is CE marked for use with sera/plasma and was run as described in the manufacturer's instructions.

Any serum sample which tested anti-HCV positive using the Elecsys anti-HCV II assay was confirmed with a second anti-HCV assay, the Ortho anti-HCV (Ortho Clinical Diagnostics, New Jersey USA) run on the Dynex DS2 (Dynex Technologies, Chantilly USA). The assay is CE marked for use with serum/plasma samples and was run as described in the manufacturer's instructions. Serum samples which were positive with both assays were assigned as anti-HCV positive, samples which were positive in the first Elecsys anti-HCV assay but negative in the second Ortho anti-HCV assay were assigned as anti-HCV equivocal.

11.5.1.2 DBS SAMPLES

DBS samples had previously been collected on a custom designed collection card. The card design uses Ahlstrom 226 grade paper, with 5 spot outlines for collection of dried blood spots. The circumference of the circle outline represents an average dried blood spot of 25 µL in volume. A perforation was included around 4 of the 5 spots, to enable removal using a set of disposable tweezers. A design of the card can be seen in Figure 31 below.

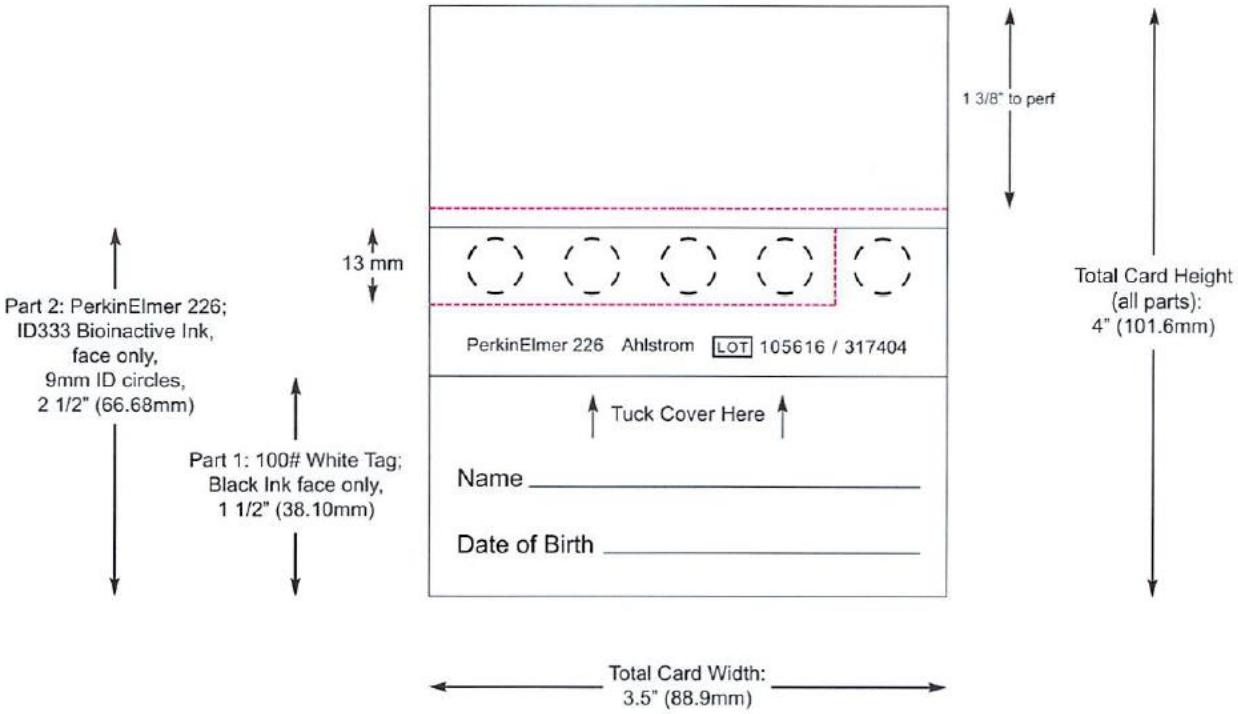

Figure 31 Design of custom DBS Collection Card

All DBS samples were processed using the same method. A disposable set of forceps (Robinson Healthcare Ltd, Nottingham UK) was used to tear off the dried blood spot strip containing the 4 blood spots along the perforated line. The remaining 5th spot was left attached to the card for HCV RNA testing, see section 11.5.2.2. A new disposable set of forceps was used for each dried blood spot card to prevent carry over contamination. The strip was placed in a matched labelled 50 mL skirted centrifuge tube (Eppendorf) and 1.5 mL of PBS/Tween 0.05% elution buffer added to each sample. The tube was sealed and placed flat in a tube rack ensuring the strip was lying at the bottom of the tube and placed on an orbital shaker overnight for elution. The following morning the eluate was removed using a disposable pastette and transferred to a 2.0 mL vial labelled with a matching study number.

Testing of eluted DBS samples for anti-HCV used the same assays as were used for serum samples. A previous optimisation and validation for use with DBS samples had been performed, with positive cut-off values set specifically for use with DBS samples using receiver operating characteristic (ROC) analysis (data not shown). For testing of serum samples both assays used a positive cut-off value of ≥1.0. For testing of DBS samples the Roche Elecsys® anti-HCV II used a DBS specific cut-off of ≥0.5, the Ortho anti-HCV assay used a DBS specific cut-off of ≥0.25. Performance of the re-optimised assays with DBS samples is shown in Table 13 below.

Anti-HCV Assay	Sample Type		Serum		Sensitivity %*	Specificity %*
			Pos	Neg		
Roche Cobas	DBS	Pos	103	0	100 (96.5-100)	100 (97.4-100)
		Neg	0	141		
Ortho Anti-HCV		Pos	72	0	97.4 (87.1-98.6)	100 (96.1-100)
		Neg	4	92		

*95% Confidence Intervals

Table 13 Diagnostic Sensitivity/Specificity results for testing of DBS samples with 2 commercial anti-HCV assays using DBS specific positive cut-off value

11.5.2 HCV RNA ASSAY

11.5.2.1 SERUM SAMPLES

All anti-HCV positive serum samples were tested with the Roche Cobas® HCV RNA assay run on the Cobas 6800 automated analyser according to manufacturer's instructions. This is a CE marked assay for quantitative HCV RNA testing of serum or plasma samples. All testing was performed according to manufacturer's instructions using the 200 µL protocol. This protocol has an analytical sensitivity (Limit of Detection) of 15 IU/mL.

11.5.2.2 DBS SAMPLES

The HCV RNA status of all anti-HCV positive DBS samples had previously been determined using nucleic extraction on the bioMerieux Nuclisens EasyMag followed by 1 step Taqman based RT-PCR. A single 25 µL DBS eluate was added to 2 mL of Nuclisens lysis buffer (bioMerieux France) plus 10µl of MS2 bacteriophage. This was incubated at 37°C on a shaking incubator for 30 minutes. All the lysis buffer was then transferred to a reaction vessel and loaded onto the Nuclisens EasyMag for completion of the extraction process, eluting into a final volume of 40 µL. A Taqman real-time PCR was run using Applied Biosystems Fast 1 step RT master mix (Thermofisher) HCV Taq with primer oligonucleotides FP(GTCTAGCCATGGCGTTAGTA) and HCV Taq RP (GTACTCACCGGTTCCGC) at final concentration of 0.3µM and HCV Taq probe (FAM-CCCTCCCGGGAGAGCCATAGTG-TAMRA) at a final concentration of 0.2µM, MS2 FP (CACTACCCCTCTCCGTATTCACG), MS2 RP (GTACGGGCGACCCCACGATGAC) primers and MS2 Probe (CY5-CACATCGATAGATCAAGGTGCCTACAAGC-BHQ) were at a final concentration of 0.1 µM, with 20 µL of DBS extract. Reactions were set up in a Thermoamp 0.1 mL reaction plate (Thermofisher) and loaded onto an Applied Biosystems Fast 7500 Real-time PCR system.

11.6 ANTI-HCV ELISA OPTIMISATION

The HCV proteins expressed and purified in the preceding sections were trialed and optimised in individual ELISAs for the detection of anti-HCV. In addition to the proteins expressed in baculovirus an additional HCV NS4 protein, expressed in *E.coli*, was purchased from a commercial source (ProSpec Bio, Israel). A list of the proteins used in the ELISA optimisation is given in Table 14.

Protein	Expression System	Form
Core	*flash* BAC Ultra	Native
NS3	*flash* BAC Ultra	Native
NS4	*flash* BAC Ultra	Denatured 8M Urea
NS5a	*flash* BAC Ultra	Denatured 6M Guanidine
NS5b	*flash* BAC Ultra	Denatured 8M Urea
NS4PrSpc	*E. coli*	Denatured Urea

Table 14 List of expressed proteins used for ELISA Optimisation. All proteins were produced in baculovirus expression systems, except the NS4PrSpc protein which was produced commercially in *E.coli*.

11.6.1 ELISA PROCEDURE

Greiner MICROLON 200 medium binding polystyrene 8 well strips (Merck) were used. All wash stages were performed using a Biotek ELx50 automated plate washer (Biotek, Swindon UK). Final plate reading was performed using a Biotek ELx808 plate reader at a wavelength of 450 nm. The wash buffer was PBS/Tween 20 0.05%$^{v}/_{v}$. The enzyme colourimetric substrate was TMB (Sigma Aldrich). Stopping solution in all experiments was 0.5M sulphuric acid.

Antigen was diluted in carbonate/bicarbonate coating buffer to the desired concentration, and added in 50 µL volumes to assigned wells of the 8 well strips, the strips were covered with a plate sealer and incubated overnight at 4° C. The following morning the solution was removed and washed with 200 µL wash buffer for 5 X 2 minutes on the automated plate washer. Next, 300 µL of blocking buffer was added and left to incubate for 1 hour at RT. The wash step was repeated to remove the blocking buffer. Diluted primary antibody solution was added in 100 µL volumes and incubated for 1 hour at RT. The wash step was repeated. Next 100 µL of anti-Human IgG HRP secondary antibody was added to each well, covered and left to incubate at RT for 1 hour. The wash step was repeated. Next 100 µL of TMB solution was added to each well and left to incubate for 30 minutes at room temperature. Finally, 100 µL of stopping solution was added and the plate read at 450nm.

Individual components and steps of this procedure were optimised in a series of experiments. The majority of these experiments were performed using the NS3 protein testing known anti-HCV positive and negative serum samples. The variables optimised for each ELISA are listed below.

11.6.1.1 SECONDARY ANTIBODY SELECTION

A comparison was performed between 2 secondary antibodies, both of which were conjugated with horse radish peroxidase (HRP). The first secondary antibody trialed was a rabbit polyclonal anti-human IgG HRP (Abcam), the second secondary antibody trialed was a mouse monoclonal Human IgG Fc specific monoclonal antibody (Stratech Scientific).

For the comparison the NS3 antigen ELISA was used. The antigen was coated at 2 concentrations, 10 and 5 µg/mL. A 1% Bovine Serum Albumin (BSA) based blocking buffer and diluent were used. A known anti-HCV positive and a known anti-HCV negative serum sample was tested together with a non-serum blank composed of diluent buffer. Serum samples were diluted 1:40 and 1:80 in 1% BSA sample diluent. All samples and blanks were tested in duplicate and an average reading calculated. Both antibodies were diluted in sample diluent, and a dilution series running from 1:10000 to 1:80000 was used to find the optimum secondary antibody dilution level.

11.6.1.2 Primary and Secondary Antibody Dilution

The dilution factor for both the primary and secondary antibodies were optimised at the same time. The primary antibody, known anti-HCV positive and negative serum, were tested in a range of dilutions from 1:10 to 1:80. The secondary antibody, mAb anti-Human IgG HRP, was tested in a range from 1:5000 to 1:40000. All dilutions were trialed with NS3 antigen at a coating concentration of 10 and 5 µg/mL. A 1% BSA based blocking buffer and diluent were used. All samples and blanks were tested in duplicate and an average reading calculated. Both the positive/negative ratio and the positive-negative readings were calculated to help identify the optimum dilutions.

11.6.1.3 BLOCKING AND DILUTION BUFFER

Two different blocking buffers were compared. The first was 1% BSA (Sigma) prepared in PBS. The second was 5% foetal calf serum (Thermofisher) prepared in PBS. The dilution buffer was used for diluting the primary antibody (serum sample) and the secondary antibody solution. The dilution buffer matched the composition of the blocking buffer, plus the addition of Tween 20 at a final concentration of 0.05%$^{v}/_{v}$.

The NS3 antigen was coated at a final concentration of 5 µg/mL. Four known anti-HCV positive and 4 known anti-HCV negative serum samples were tested, plus a non-serum blank composed of diluent buffer. All serum samples were diluted 1:20 in 1% BSA or 5% Foetal calf serum (FCS) based diluent. All samples and blanks were run in duplicate and an average optical density value calculated. The

secondary antibody used was mAb anti-human IgG HRP at a final concentration of 1:20000. The ELISA was performed as described in section 11.6.1.

11.6.1.4 TEMPERATURE OPTIMISATION

A temperature optimisation was performed, comparing incubation at room temperature (range 19-22°C) and 25°C. For the room temperature incubation was performed on a laboratory bench, for the 25°C incubation an incubator was used with intervening wash steps performed at room temperature.

The NS3 antigen was coated at a final concentration of 5 µg/mL. Four known anti-HCV positive and 4 known anti-HCV negative serum samples were tested, plus a non-serum blank composed of diluent buffer. All serum samples were diluted 1:20 in 1% BSA. All samples and blanks were run in duplicate and an average calculated. The secondary antibody used was mAb anti-human IgG HRP at a final concentration of 1:20000. The ELISA was performed as described in 11.6.1

11.6.1.5 TIME OPTIMISATION

A time optimisation was performed for the substrate reaction. The time started with the addition of TMB substrate and stopped with the addition of 0.5 M sulphuric acid. The optimisation tested 3 substrate reaction times, 10, 20 and 30 minutes.

The NS3 antigen was coated at a final concentration of 5 µg/mL. Three known anti-HCV positive and 3 known anti-HCV negative serum samples were tested, plus a non-serum blank composed of diluent buffer. All serum samples were diluted 1:20 in 1% BSA. All samples and blanks were run in duplicate and an average calculated. The secondary antibody used was mAb anti-human IgG HRP at a final concentration of 1:20000. For all incubations the ELISA plate was placed in an incubator at 25°C. The ELISA was performed as described in section 11.6.1

11.6.1.6 ANTIGEN COATING OPTIMISATION

Antigen coating optimisations were performed for each expressed HCV protein. The NS3 antigen was optimised at a coating concentration of 10 or 5 µg/mL. The Core, NS4, NS5a and NS5b proteins were tested at coating concentrations of 10, 5, 2.5 and 1.25 µg/mL. The commercially purchased Pro Spec NS4 protein was tested at coating concentrations 5, 2.5, 1.25 and 0.625 µg/mL. All proteins were diluted in 0.2 M carbonate/bicarbonate coating buffer at pH9.4, prepared from individual sachets (Thermofisher) dissolved into 500 mL of de-ionised and autoclaved water.

For each coating optimisation a total of 3 known anti-HCV positive and 3 known anti-HCV negative samples were tested. Due to insufficient sample volumes the same samples were not run with each

protein optimisation. All serum samples were diluted 1:20 in 1% BSA. All samples and blanks were run in duplicate and an average calculated. The secondary antibody used was mAb anti-human IgG HRP at a final concentration of 1:20000. For all incubations the ELISA plate was placed in an incubator at 25°C, and the final TMB substrate reaction was run for 20 minutes. The ELISA was performed as described in section 11.6.1

11.6.1.7 DBS DILUTION OPTIMISATION

Once the ELISA for each protein had been optimised with serum samples, a final optimisation was performed for DBS samples as the source of primary antibody solution. Three known anti-HCV positive and 3 known anti-HCV negative DBS samples were tested. Each DBS sample was tested at final dilutions of 1:1, 1:2, 1:5 and 1:10. All dilutions were performed in 1% BSA diluent. All samples and blanks were run in duplicate and an average calculated.

The optimisation used both the NS3 antigen assay and the NS5a antigen assay, using the optimum conditions determined in the previous experiments. The NS3 assay used a final coating concentration of 5 µg/ml, the NS5a assay used a final coating concentration of 1.25 µg/mL. The secondary antibody used was mAb anti-human IgG HRP at a final concentration of 1:20000. For all incubations the ELISA plate was placed in an incubator at 25°C, and the final TMB substrate reaction was run for 20 minutes. The ELISA was performed as described in section 11.6.1.

11.7 ANTI-HCV ELISA VALIDATION

11.7.1.1 OPTIMISED ELISA

Validation experiments were performed for each HCV protein ELISA using a panel of known anti-HCV positive and anti-HCV negative samples. Separate validations were performed for serum samples and DBS samples. All ELISA validation experiments used the optimum reagents and conditions finalised in the optimisation experiments, listed below.

Antigen Coating Concentration: Each antigen was diluted out in carbonate/bicarbonate coating buffer to the concentration listed in Table 15 below.

Protein	Final Concentration µg/ml
HCV Core	5
NS3	5
NS4	2.5
NS5a	1.25
NS5b	5
NS4C	1.25

Table 15 Final coating concentration for each HCV protein and final ELISA reagents

Wash Buffer: PBS/Tween20 0.05%.

Blocking Buffer: PBS/1%BSA

Primary Antibody: Serum diluted 1:20 in PBS/1%BSA/Tween 20 0.05% or DBS diluted 1:2 in PBS/1%BSA/Tween 20 0.05%

Secondary Antibody: Mouse mAb anti-Human IgG HRP diluted 1:20000 in PBS/1% BSA/Tween 20

Substrate: TMB

Stopping Solution**: 0.5 M sulphuric acid**

ELISA Procedure:

Antigen was added in 50 µL volumes to assigned wells of the 8 well strips, the strips covered with a plate sealer and placed overnight at 4°C. The following morning the solution was removed and washed with wash buffer for 5 X 2 minutes on the automated plate washer; 300 µL of blocking buffer was added and left to incubate at 25°C for 1 hour. The wash step was then repeated to remove the blocking buffer. Diluted samples were then added in 100 µL volumes to the plate and incubated 25°C for 1 hour. The wash step was then repeated. Secondary antibody was added to each well, covered and left to incubate at 25°C for 1 hour. The wash step was then repeated. Next 100 µL of TMB solution was added to each well and left to incubate at 25°C for 1 hour. Finally, 100 µL of stopping solution was added and the plate read at a wavelength of 450 nm.

11.7.2 SAMPLE SELECTION

For validation of each optimised ELISA a selection of unlinked, anonymised, surplus residual clinical samples with known anti-HCV status were used. Samples were defined as anti-HCV positive if they had previously tested positive with both the Roche Elecsys® anti-HCV II assay run on the Roche Cobas® 6000 analyser and the Ortho anti-HCV assay run on the Dynex DS2, see section 11.5.1. Samples were defined as anti-HCV equivocal if they had tested positive with the Elecsys® anti-HCV

II but negative with the Ortho anti-HCV assay. Samples were defined as anti-HCV negative if they had previously tested negative with the Elecsys® anti-HCV II assay.

For validation with serum samples a total of 95 anti-HCV positive, 92 anti-HCV negative and 1 anti-HCV equivocal samples were used. Of the 95 anti-HCV positive samples, 50 were HCV RNA positive and 45 were HCV RNA negative. Of the HCV RNA positive samples, 38 were genotype 1, 3 were genotype 2, 48 were genotype 3, 2 were genotype 4, 1 was genotype 6 and 3 were mixed 1/3 genotypes. The single anti-HCV equivocal sample was HCV RNA negative.

For validation with DBS samples a total of 92 anti-HCV positive, 89 anti-HCV negative and 7 anti-HCV equivocal samples were tested. Of the 92 anti-HCV positive samples 39 were HCV RNA positive and 53 were HCV RNA negative. The HCV genotype of the DBS samples was unknown. Of the 7 anti-HCV equivocal samples 1 was HCV RNA positive (genotype unknown) while the remaining 6 were HCV RNA negative.

11.7.2.1 RECEIVER OPERATING CHARACTERISTIC ANALYSIS

Receiver operating characteristic (ROC) analysis was performed on the results for each ELISA to assign the threshold for the positive/negative 'cut-off' value and for comparison of the ELISAs through the calculated area under the curve (AUC). All anti-HCV equivocal profiles were removed before ROC analysis, only the results from confirmed anti-HCV positive serum and DBS samples were included. ROC Analysis was performed using R software running the pROC statistical package[359]. The package was used to generate a ROC curve for each set of ELISA results. The positive cut-off value was assigned using 3 separate methods, the first set threshold for the positive cut-off at the minimum required to maintain a specificity of 100%; the second method assigned the positive cut-off using the Youden index[360], which is the threshold which maximizes the distance to the diagonal line, and the third method used the closest top left, which calculates the threshold closest to the top left part of the plot[361]. The corresponding sensitivities and specificities at each threshold were calculated.

The total AUC was calculated for each set of results[362], to a significance of p0.05 and the corresponding power listed. Confidence intervals, 95%, for the AUC were calculated and used to compare the performance of different ELISAs using the Delong method[363]. If no statistical significance was determined using the total AUC, a partial AUC was calculated using the McClish method[364] covering the 90% specificity area and above of the ROC curve and a comparison performed using a bootstrap method[359](replicates 2000).

12 RESULTS

12.1.1 TRANSFECTION OF SF9 CELLS WITH PIEX HCV CORE PLASMID – OPTIMISATION

The first expression experiments involved the transfection of Sf9 cells with the pIEx HCV core plasmid for expression of the HCV Core protein. The transfection reagent GeneJuice was used, a proprietary transfection reagent composed of a non-toxic cellular protein and a novel polyamine. The recommended volume of gene juice is 5 µL per µg of plasmid, though optimisation should occur between the range of 4-8 µL per µg. Based on these recommendations the optimisation experiment used 3 concentrations of Gene Juice, 4, 6 and 8 µL per ug of plasmid, to span the entire optional range. As 2µg of the pIEx HCV core plasmid were transfected the actual amounts of gene juice used were 8, 12 and 16µl total. An additional negative control was set up, incorporating 6 µL of gene juice with the cultured cells but with no plasmid added.

The Sf9 insect cells were incubated for 48 hours at 28ºC and observed at 24 hours and 48 hours under a microscope to look for evidence of transfection. Transfected cells look larger and granulated, with possible inclusion bodies.

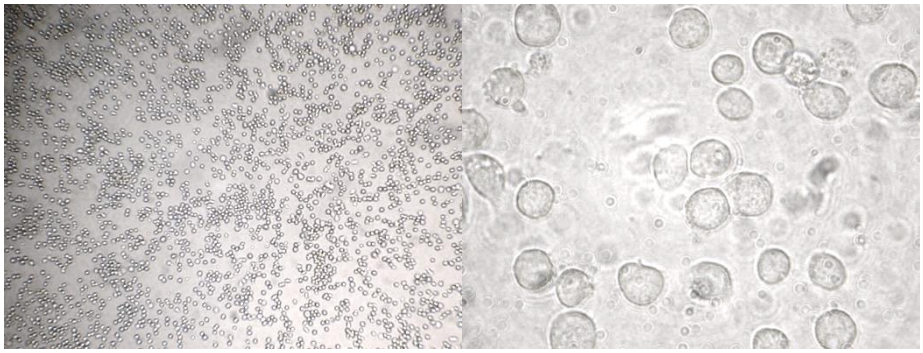

Figure 32 pIExHCV Core transfection of Sf9 insect cells 24 hours. Sf9 insect cells ($1x10^6$ cells) transfected with 8µl of gene juice, 2µg of pIExHCV Core plasmid and 200µl of BacVector serum free medium, made up to a total volume of 2ml with BacVector serum free media and incubated at 28°C. Images taken at 24 hours post transfection, left at 10X Magnification, right at 25X Magnification. Cells look healthy showing no granulation or inclusion bodies.

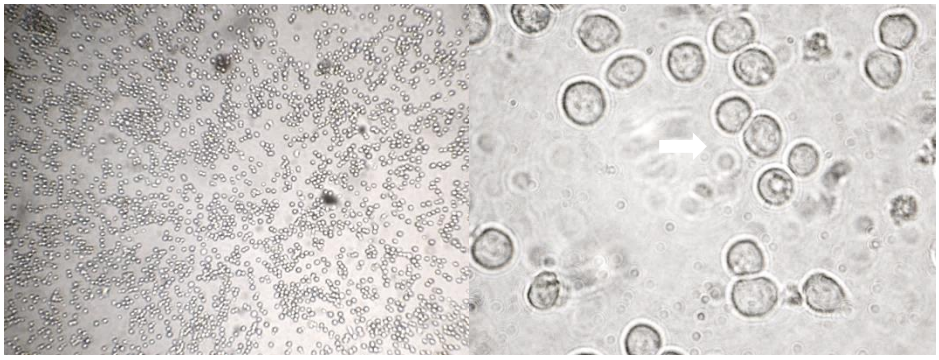

Figure 33 pIEx transfection negative control Sf9 cells 24 hours. Sf9 insect negative control cells ($1x10^6$ cells) transfected with 6µl of gene juice and 200µl of BacVector serum free media, made up to a total volume of 2ml with BacVector serum free media and incubated at 28°C. Images taken at 24 hours post transfection, left at 10X magnification, right at 25X magnification. Cells look healthy and are indistinguishable from transfected cells shown above in Figure 32 above.

Figure 32 above shows the 10X magnification and 25X magnification of the pIEx HCV Core infected Sf9 cells after 24 hours, using 4 µL of Gene juice transfection reagent per µg of pIEx HCV Core plasmid. The images for infections using 6 µL and 8µl of gene juice per µg of plasmid were very similar but are not shown. The 10X magnification images taken at 24 hours show a relatively low cell density across the different culture wells. The 25X magnification images taken at 24 hours do not show any conclusive evidence that transfection of the Sf9 cells with the pIEx HCV core plasmid has occurred. The cells appear healthy with clear cell walls and no granulation or shrinking. There is no discernible difference with the negative control cells shown in Figure 33 above.

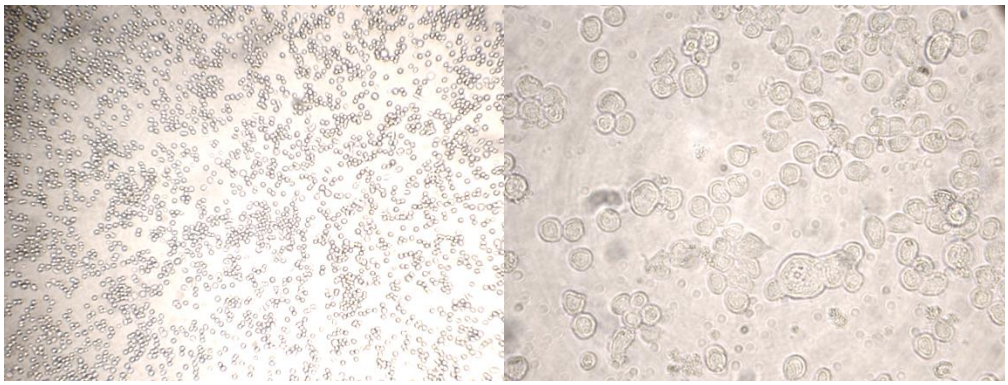

Figure 34 pIExHCV Core transfection of Sf9 insect cells 48 hours. Sf9 insect cells ($1x10^6$ cells) transfected with 8µl of gene juice, 2µg of pIExHCV Core plasmid and 200µl of BacVector serum free medium, made up to a total volume of 2ml with BacVector serum free media and incubated at 28°C. Images taken at 48 hours post transfection, left at 10X magnification, right at 25X magnification. Cells look healthy showing no granulation or inclusion bodies.

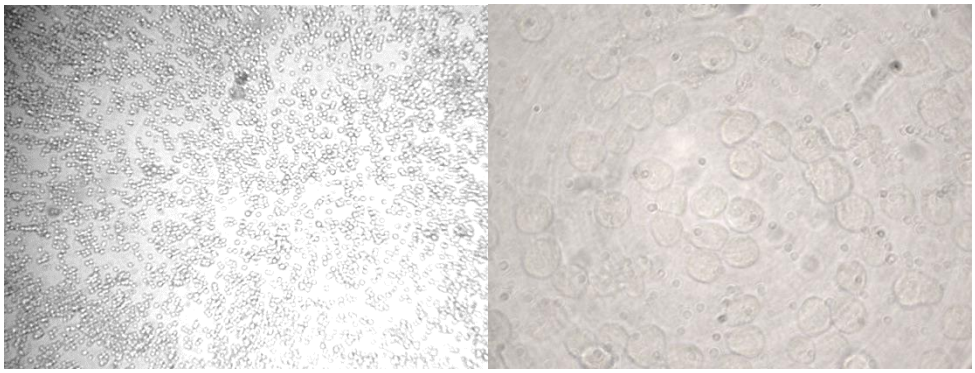

Figure 35 pIEx transfection negative control Sf9 cells 48 hours. Sf9 insect negative control cells (1x10^6 cells) transfected with 6µl of gene juice and 200µl of BacVector serum free media, made up to a total volume of 2ml with BacVector serum free media and incubated at 28°C. Images taken at 48 hours post transfection, left at 10X magnification, right at 25X magnification. Cells look healthy and are indistinguishable from transfected cells shown above in Figure 34 above.

Figure 34 above shows the same pIEx HCV Core infected Sf9 cells using 4 µL gene juice per µg of plasmid 48 hours post-infection. Again, the images for both the infections using 6 µL and 8 µL of gene juice were very similar and are not shown. The 10X magnification images taken at 48 hours show a similar cell density to the images taken at 24 hours, suggesting very little cell proliferation has occurred. The 24X magnification images taken at 48 hours do not show clear evidence of infection. There is a large cell in the middle, but this is a dividing cell. The cell wall is still defined, and there is little to no granulation. Compared to the negative control shown in Figure 35 there is no clear difference. The lack of any obvious cell cytopathic effect (CPE) does not mean the cells have not been transfected with the pIExHCV Core plasmid. As transfection of the plasmid into Sf9 cells does not lead to replicating virus, the CPE seen with the InsectDirectTM system is reduced compared to baculovirus based expression systems which produce a full recombinant virus life cycle leading to granular formations combined with cell shrinking and ultimately cell lysis.

After 48 hours of transfection, the insect cells from each well were harvested before undergoing further tests to determine if protein expression in the transfected Sf9 cells had occurred.

12.1.2 SDS PAGE

SDS-PAGE analysis, sodium dodecyl sulphate polyacrylamide gel electrophoresis, is a technique used to accurately differentiate proteins based on their size. The NuPAGE® system used in these experiments has a modified buffer which maintains a neutral pH during electrophoresis increasing the resolution compared to standard SDS-PAGE approaches[365]. After the electrophoresis was completed the gel was stained using InstantBlue™ to highlight any protein bands present in the gel.

Both the cell medium and harvested cells collected after 48 hours of the transfection experiment were analyzed using the NuPAGE® system. A high range molecular weight marker was run either side of the samples to help easily identify the molecular weight of any bands present in the gel.

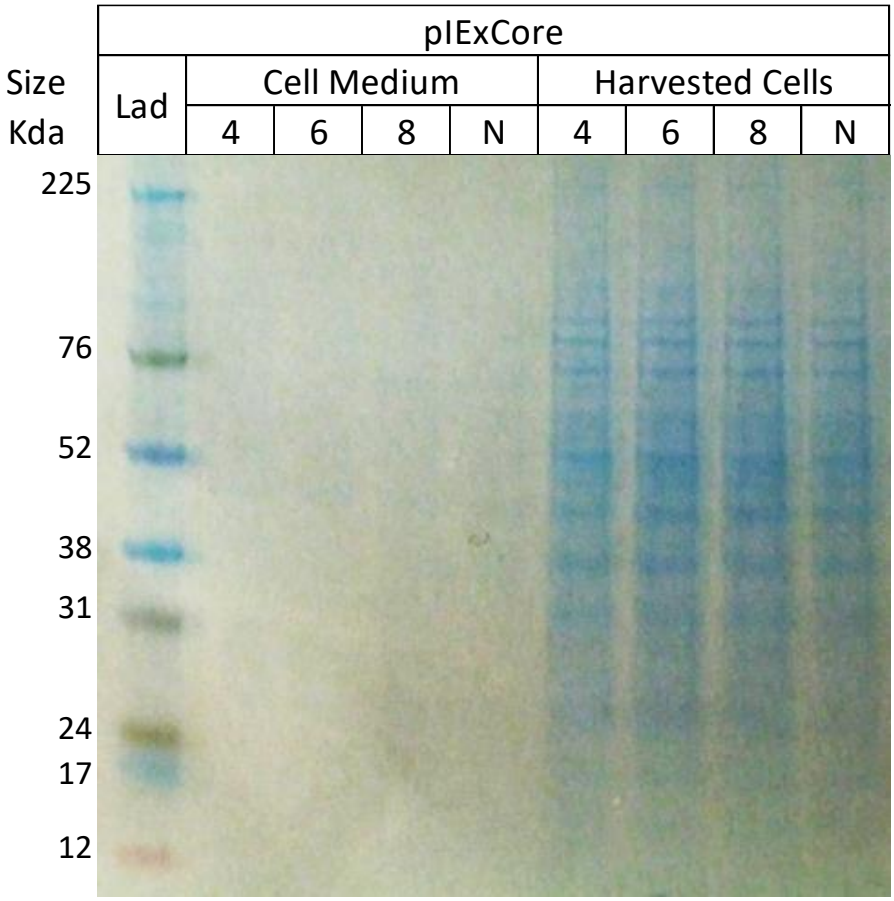

Figure 36 Gel image of SDS-PAGE analysis for cell medium and SF9 insect cells harvested 48 hours post-transfection with pIExHCV Core plasmid. NuPage 4-12% Bis-Tris PAGE gel run for 200V for 35 minutes, post electrophoresis stained with InstantBlue and image taken with digital camera. Number in the 3rd row (4,6,8) refers to µl of gene juice used per µg of pIExHCV Core plasmid for transfection, N refers to the non-transfected negative control. Left side of image shows cell medium from each transfection, right hand side shows harvested cells.

Figure 36 is an image of the gel post SDS-PAGE analysis. The first 4 columns (three pIEx HCV core cultures and the negative culture) contained no visible bands. This suggested that if there was any HCV core protein was expressed in the Sf9 cells, it was not excreted into the medium.

The last 4 columns of the gel represent the harvested cells from the three pIEx HCV core cultures and the negative culture. The HCV core protein should have a relative molecular weight of 22 kDa; larger molecular weights may be seen if the core protein is glycosylated (50 kDa) or if the core protein self assembles into virus like particles. Looking at the gel there seems no obvious band at 22 kDa, though there is a potentially a very faint band around this region. The NuPage 4-12% acrylamide gel used in the SDS-PAGE analysis should have offered enough resolution to visualise this band. The

pIEx HCV core cultures were further examined by western blot which offered a higher sensitivity of detection for any bands present.

12.1.3 WESTERN BLOT

To investigate if the transfection and expression of the HCV Core protein had occurred an anti-HCV core monoclonal antibody (mAb) was purchased. The use of a mAb which targets only a single epitope of the HCV core protein should significantly reduce the risk of non-specific binding to other proteins present in the cultures, though this does leave the risk of missing the detection of expressed protein if the single epitope targeted is not present.

As the cell medium collected from each culture showed no evidence of protein excretion in the SDS-PAGE analysis, it was decided to run only the harvested cells through the Western Blot. An NIBSC WHO 4th HCV RNA international standard was included to control for the performance of the Western Blot. The standard is composed of a whole HCV genotype 1a virus which is diluted in human plasma to a concentration of 260 000 IU/mL. The control was tested neat, and at dilutions of 1:10 and 1:100,

A rabbit anti-mouse IgG alkaline phosphatase antibody was used to identify any bound HCV core mAb. FAST™BCIP/NBT was used as the substrate for the antibody, which upon reaction produces an insoluble black purple precipitate.

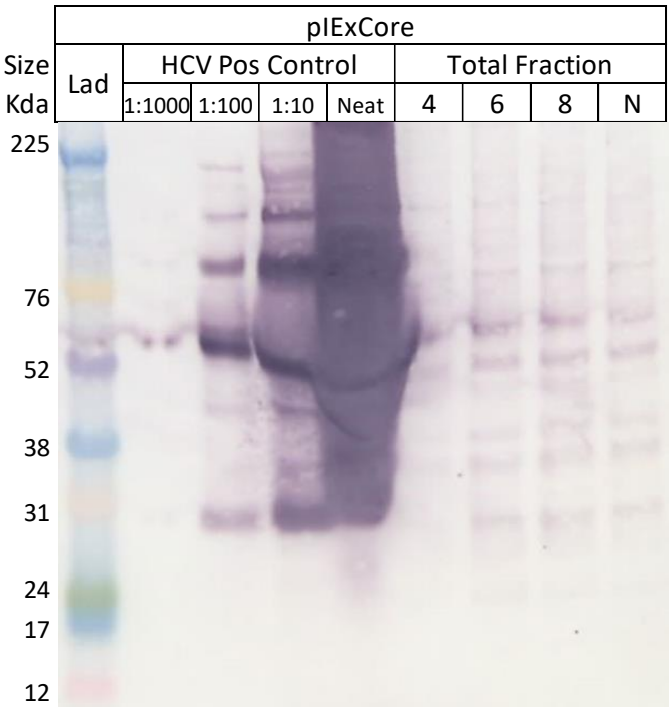

Figure 37 Image of Western Blot analysis of SF9 insect cells harvested 48 hours post-transfection with pIExHCV Core plasmid. Western blot used NuPage 4-12% Bis-Tris gels transferred to 0.45µm Nitrocellulose

membrane. Mouse mAb Anti-HCV Core used as primary antibody at 1:000 dilution, rabbit pAb-Anti-mouse IgG (AP) used as secondary antibody, substrate was FastBCIP/NBT. Left hand side of gel shows NIBSC HCV international standard run at 1:1000, 1:100, 1:10 and neat dilutions, right hand side of gel shows harvested cells, number in 3rd row (4,6,8) refers to µl of gene juice used per µg of pIExHCV Core plasmid for transfection, N refers to the non-transfected negative control.

The most striking element of the image in Figure 37, is the solid purple band in the middle, the neat HCV standard. Significant non-specific binding of the monoclonal antibody was apparent. The 1:100 dilution of the HCV standard gave a clearer picture, with multiple defined and clear bands. All three of the plasmid infected harvested cells produced multiple bands, but these were very light and did not fully mirror those seen with the positive control. These same bands appeared in the non-infected control, suggesting this was non-specific binding of the anti-HCV mAb and not evidence of HCV core expression. The expected size of the expressed HCV core protein was 22 kDa. There was no clear band at this size seen in the Western blot. There was a very faint band at this size in the 3 and 10 MOI infected cells but was so faint it cannot be seen clearly in the image. This may represent some expression of the HCV core protein, but insufficient for any downstream protein work.
As the InsectDirect™ system had failed to produce a suitable amount of HCV core protein, it was decided to move expression to an alternative baculovirus expression system.

12.1.4 EXPRESSION OF PROTEINS USING FLASHBAC™ ULTRA SYSTEM AND PIEX-BAC 3 TRANSFER PLASMID

The HCV core antigen gene from the pIEx plasmid was transferred to a *flash*BAC™ compatible transfer vector plasmid. As opposed to the InsectDirect™ system which expresses protein directly from a transfected plasmid, the *flash*BAC™ expression system involves the creation of a recombinant baculovirus. As the *flash*BAC™ expression system uses recombinant virus infection of insect cells for expression of proteins, it is a slower system than the InsectDirect™ system. However, it was expected that higher levels of protein would be produced, overcoming the low expression seen with the InsectDirect™ system. There are several variants of the *flash*BAC™ expression system, of which the flashBAC™ ULTRA was chosen. This includes numerous gene deletions in the baculovirus genome, including chiA (chitinase) and v-cath (cathepsin), plus the p10, p74 and p26 genes. These deletions combine to increase the level of protein expression and stability of expressed protein.

Multiple transfer vectors are available for use with the *flash*BAC™ ULTRA expression system. The first transfer vector chosen was the pIEx-Bac 3 plasmid (Merck) as this had been used with some success within the department. The transfer vector has the required baculovirus homologous recombination region required for use with the *flash*BAC™ ULTRA expression system, plus a combination of immediate early (IE) and p10 promoters for high level expression. The inclusion of the IE promoter directs expression early in the insect cell life cycle, while the p10 promoter is one of the 2 highly expressed late promoters (alongside the polyhedrin promoter) ensuring high level expression of the

desired protein. There is a 10 X His tag sequence downstream of the two promoters, so any expressed proteins will be produced with a HISTag at the N' termini of the protein for subsequent protein purification.

12.1.4.1 PCR AMPLIFICATION OF HCV CORE ANTIGEN GENE FROM PIEX 6 CORE PLASMID

Primers were designed for the amplification of the HCV Core antigen gene from the pIEx Core plasmid, with the necessary overhangs to perform LIC into the pIEx-Bac-3 plasmid, see Table 4. Snapgene software was used to assist with the design of the primers, and to ensure the amplified product would be in the correct reading frame when inserted into the new pIEx-Bac-3 plasmid. The PCR was run as described in section 11.4.1 and the plasmid run at 3 dilutions, from 1:100 to 1:1000. The PCR was successful at all 3 dilutions, producing a clear strong band on the agarose gel, see Figure 38.

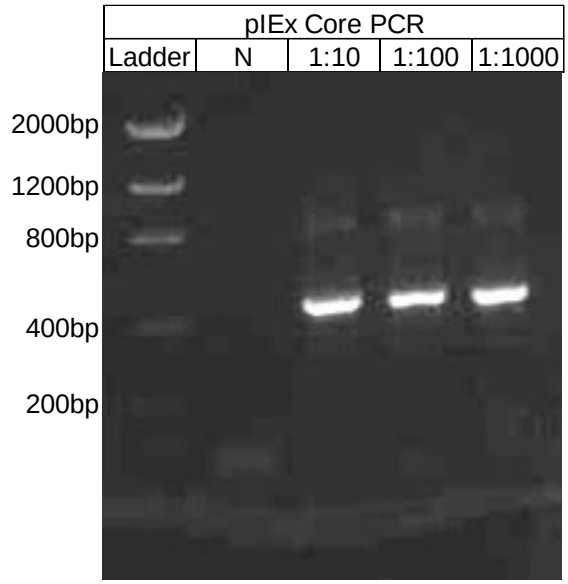

Figure 38 Gel electrophoresis image for PCR of Core antigen gene from pIExHCV Core plasmid. Agarose 1% gel with 1:10000 dilution of SyBr safe DNA stain run at 100 V for 40 minutes, post electrophoresis imaged using Alphaimager 2200 imaging system under UV. Loading order of gel: DNA size ladder, negative PCR control, 1:10 dilution, 1:100 dilution and 1:1000 dilutions of pIExHCV Core plasmid.

The PCR products were purified using a QIAquick purification kit, see section 11.4.3, to remove excess reagents left over from the reaction. The quantity of DNA in the PCR products was determined using the nanophotometer, these were in the range 133 ng/µL to 155 ng/µL. The 1:100 cleaned up PCR product was then selected for ligation independent cloning into the pIEx-Bac3 plasmid.

12.1.4.2 LIGATION INDEPENDENT CLONING

The amplified HCV products were cloned into the pIEx-Bac 3 plasmid using ligation independent cloning, using the method described in section 11.4.4.

12.1.4.2.1 Transformation into *E.coli*

The heat shock protocol outlined in 11.4.5.2 was used for transformation of the cloned plasmid into *E.coli* followed by overnight culture on ampicillin selective agar plates. Around 40 discrete colonies grew on the selective agar, from which 6 of the most discrete colonies were selected and plasmid extracted using a QIAprep mini plasmid purification kit. A high level of plasmid DNA was obtained in all 6 plasmids preparations, varying from 371 to 769 ng/µL.

Plasmid Prep No.	Name	Conc. µg/µl	Total Vol.	Amt µg
1	pIExHCVCorePP1	0.371	50	18.55
2	pIExHCVCorePP2	0.443	50	22.15
3	pIExHCVCorePP3	0.624	50	31.2
4	pIExHCVCorePP4	0.769	50	38.45
5	pIExHCVCorePP5	0.532	50	26.6
6	pIExHCVCorePP6	0.719	50	35.95

Table 16 Concentration of plasmid DNA post purification in µg/µl. Determined by nanophotometer, total amount of each plasmid given in µg,

12.1.4.3 Nucleotide Sequencing of plasmids

All 6 plasmid preparations were sequenced to confirm insertion of the HCV core DNA in the correct reading frame. Sanger sequencing, using Applied Biosystems BigDye v1.1 sequencing reagent and a 3130XL genetic analyzer, was performed following the protocol set out in section 11.4.5.4.

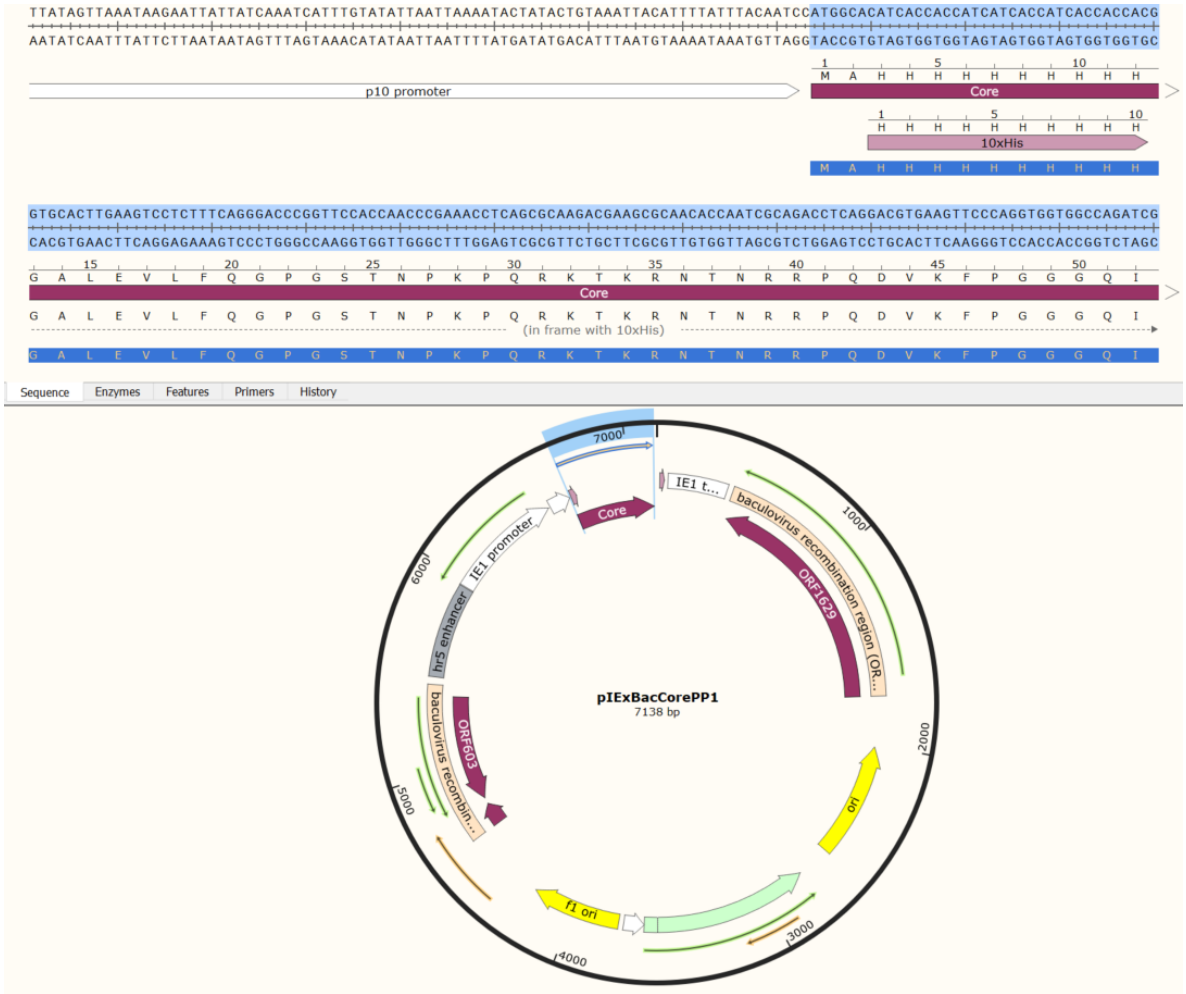

Figure 39 Plasmid map of pIExBacCore viewed in Snapgene software. Highlighted in blue is the inserted Core gene, the top segment of the figure shows the sequence inserted downstream and aligned for expression under control of the IE1 and p10 promoters with a 10XHistag incorporated at the N terminus.

Figure 39 shows the plasmid map for the pIExBacCore transfer vector plasmid, with the sequenced core gene highlighted in blue. The core gene is under the expression of both the IE1 and p10 promoter and incorporates a 10X His sequence at the N termini, all within the same reading frame of the HCV core gene.

12.1.4.4 GENERATION OF RECOMBINANT BACULOVIRUS

Transfection took place in using the protocol listed in section 11.4.6.1. Rapidly proliferating Sf9 cells were seeded into wells of a 6 well culture plate, transfection reagents added and left for 7 days for the homologous recombination and initial replication of the recombinant virus to take place. After 1 week the media containing the budded recombinant virus was removed from the cells and used for subsequent virus amplification. Cytopathic effects (CPE) are only discernible 7 days post transfection, the difference between transfected cells and the negative control cells is not obvious due to the low titre of virus at this stage, see Figure 40 below.

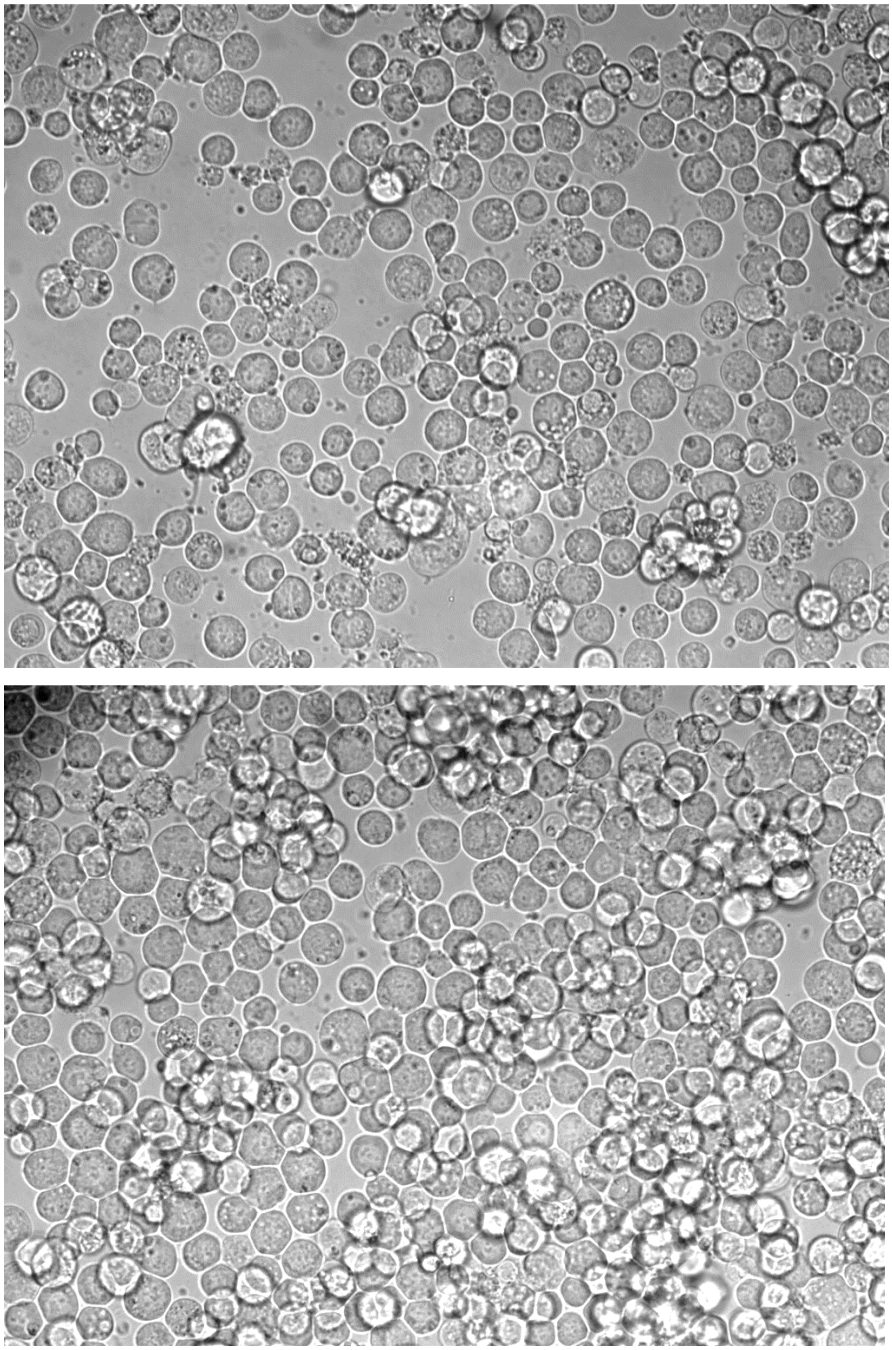

Figure 40 Comparison of transfected Sf9 cells (Top) for generation of recombinant baculovirus and non-infected Sf9 cells (Bottom) after 7 day culture. Generation of recombinant baculovirus by transfection of Sf9 insect cells (1x106 cells) with 2.5µl of *flash*BAC ULTRA, 250ng of pIExBac3 Core plasmid, 6 µl of Escort IV transfection reagent and 1ml of SF-900 insect media and incubated at 28°C for 24 hours, after which an additional 1ml of SF-900 media was added and incubated for a further 6 days at 28°C. Non-infected control cells followed the same procedure minus the 250ng of pIExBac3 core plasmid. Images taken after 7 days at 25X magnification, no discernable difference between top image showing transfected cells and lower image showing non-infected control cells.

12.1.4.5 AMPLIFICATION OF RECOMBINANT VIRUS

Media containing recombinant virus collected from the transfection stage was immediately transferred to a 50 mL suspension culture of Sf9 cells for virus amplification, following the protocol described in section 11.4.6.2. The rapidly proliferating Sf9 suspension was prepared as described in section 5.4.6.1 and cells counted to ensure they had been doubling every 24 hours and were >90% viable. All the recombinant virus media (around 1ml) was transferred to the suspension culture. After culture in a shaking incubator at 28°C for 7 days an aliquot of the suspension was removed to look for evidence of infection under a light microscope. The difference between the transfected and non-transfected cells is obvious, the infected cells appear smaller and granular with disintegrating cell walls, as opposed to the non-infected cells which appear relatively clear and healthy (Figure 41).

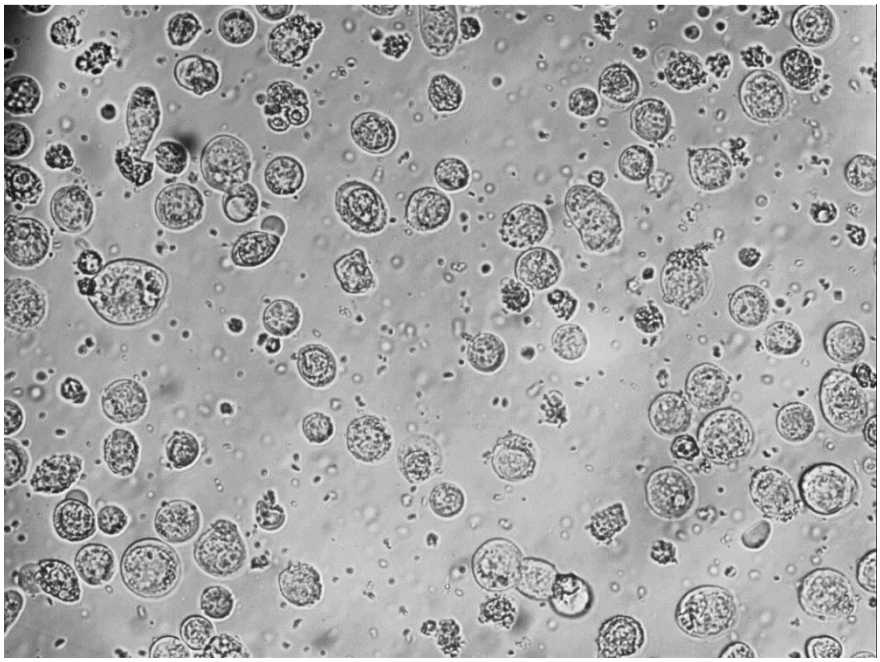

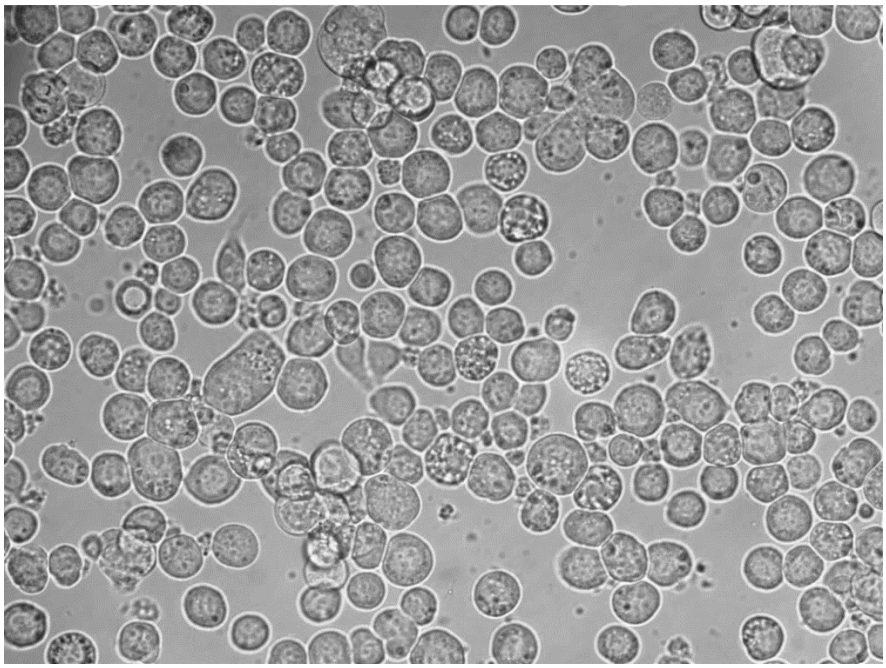

Figure 41 Comparison of infected Sf9 cells (Top) and non-infected cells (Bottom) after 7 day suspension culture. Amplification of recombinant pIExBac 3 Core baculovirus by addition of cell medium from recombinant generation to 50ml Sf9 insect cell suspension ($2x10^6$ cells per ml) incubated at 28°C and shaken at 140rpm for 7 days. Non-infected control cells followed the same procedure but with addition of cell medium from control cells. Images taken after 7 days at 25X magnification, top image showing recombinant virus infected cells demonstrate granulation, shrunken size and widespread cell lysis, non-infected control cells look healthier and in higher numbers.

12.1.4.6 QPCR OF RECOMBINANT BACULOVIRUS

The amplification stage aims to increase the level of recombinant virus to $>10^7$ pfu/mL, the minimum quantity for use in subsequent protein expression experiments. Additional passages can be performed to increase the level, but with increased passages comes increased risk of mutations occurring in the virus and so should be avoided if possible. The level of recombinant baculovirus post amplification was determined to confirm it had reached the required level. Methods available to determine the quantity of virus include plaque assay or quantitative PCR (QPCR). Plaque assay is the gold standard for determining the quantity of recombinant virus but is a time consuming and complex procedure. An alternative is the use of QPCR. This method tests samples alongside a dilution series of known quantity by Taqman based real-time PCR. The dilution series is used to produce a standard curve, from which the results of the samples can be read against to give a quantity, in this case in plaque forming units (pfu)/mL.

The baculovirus real-time QPCR used a previously published Taqman PCR primer and probe set and was tested following the protocol set out 11.4.6.3. For the standard curve to be accepted, the slope of the curve (x value) must be between -3.0 and -3.6 and the R^2 value (coefficient of determination) must be >0.95. When the calibration of the standard curve was deemed accurate, the amplified

pIExBac3Core Rc baculovirus was extracted and run through the QPCR alongside the standard curve dilution series, see Figure 42 below. The pIExBac3Core Rc baculovirus was tested in duplicate and tested positive at aCt. values of 11.3 and 11.4, this calculated out from the standard curve as a mean average quantity of 9.85X 10^7pfu/mL. All recombinant viruses produced for other proteins were tested with this QPCR.

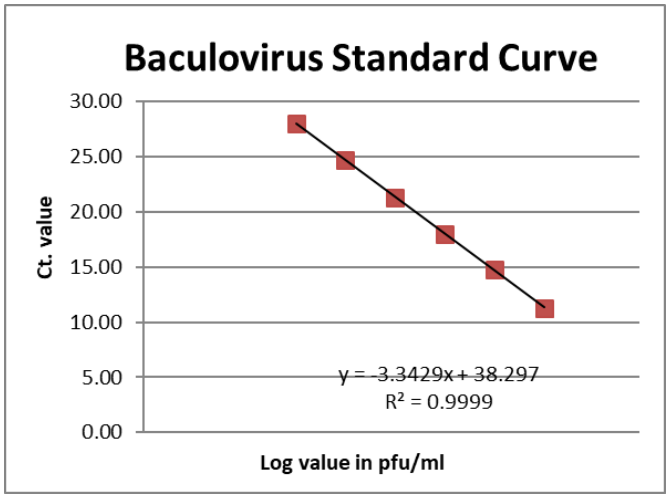

Figure 42 Baculovirus QPCR Standard Curve used for determining quantity of recombinant pIExBac HCV core baculovirus. Standard curve produced by testing tenfold dilution series of baculovirus standard from 1 X 10^8 pfu/mL to 1 X 10^3 pfu/mL by Taqman based real-time PCR. The -3.34x value shows a slope within the -3.0 to -3.6 target and with a high correlation of 0.99. This equation listed on the chart area is used to calculate the quantity (x) in pfu/ml from the Ct. value (y). The pIExBac3Core Rc baculovirus was tested in duplicate and tested positive at Ct. values of 11.61 and 11.54, this calculated out as a mean average of 9.85 X 10^7pfu/m.

12.1.4.7 PROTEIN EXPRESSION OPTIMISATION

The recombinant HCV Core protein baculovirus was expressed in high five (Hi5) insect cells offering potentially higher levels of expression than Sf9 cells.

An experiment was performed to determine the optimum amount of virus to add to Hi5 cells as described in 11.4.6.4. The optimisation of protein expression used five different MOI, ranging between 1-10, plus a non-infected negative control. As seen in Figure 43 below CPE was evident in the infected cells when compared to the non-infected cells. All infected cells at each different MOI showed a shrunken granular appearance with disintegrating cell membranes and cell lysis increasing in relation to increasing MOI.

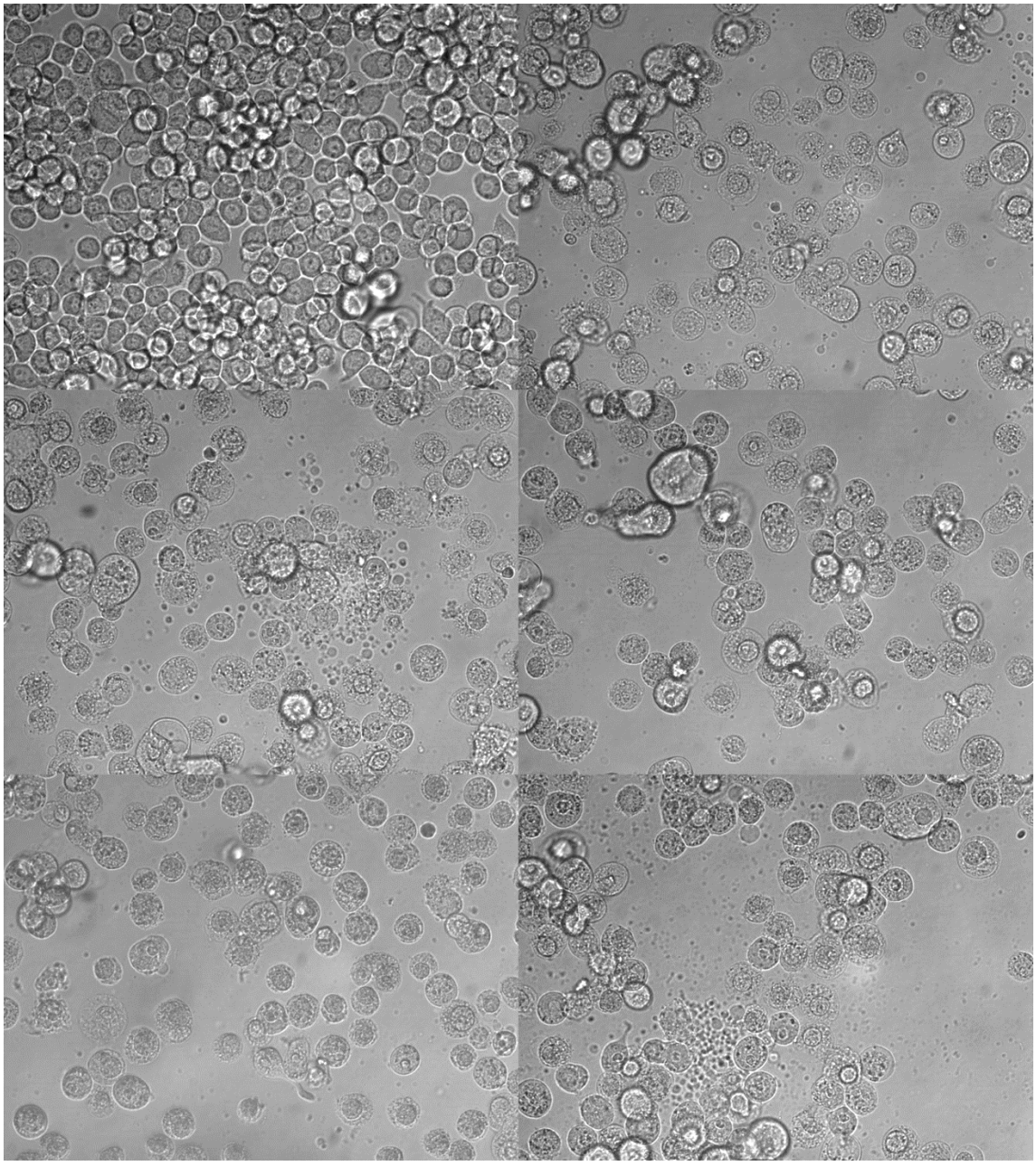

Figure 43 HI5 cells 72 hours post infection with recombinant pIExBac HCV Core baculovirus. Hi5 cells ($1x10^6$ cells) were infected with pIExBac3 HCV core baculovirus at 5 different MOI ranging from 1-10, and left to incubate at 28°C for 72 hours for protein expression to occur. Images taken at 72 hours at 25X magnification. The top left picture is an image of the non-infected control cells, top right is infected with an MOI of 1, middle left an MOI of 3, middle right an MOI of 5, bottom left an MOI of 8 and bottom right an MOI of 10. Non infected control cells look healthy after 72 hours, infected cells look granular, shrunken and show evidence of cell lysis increasing in relation to the MOI.

12.1.4.8 PROTEIN EXTRACTION AND SDS PAGE

Cells were harvested after 72 hours. The supernatant was discarded with retention of an aliquot. The remaining cells were then extracted as described in section 11.4.6.5. The lysis solution was prepared in TE buffer at a pH of 8, with NaCl at a concentration of 150 mM and Triton X-100 at 1%. In addition,

protease inhibitors were added to prevent degradation of protein from proteases released during cell lysis, and benzonase nuclease to degrade nucleic acids. All extraction procedures were performed on ice and with refrigerated centrifugation (4°C) to prevent protein degradation.

The protein extraction procedure involves the incubation of cells in lysis buffer with gentle pipetting over a 30-minute period to aid in the total lysis of cells. An aliquot was taken from the lysed solution and termed Total Fraction (TF). The total fraction contains all the proteins released from the cell, including both insoluble and soluble forms. Following this the lysed suspension was spun at a high speed to pull the insoluble proteins out of the solution, with the remaining supernatant termed Soluble Fraction (SF). An aliquot was taken of this. Both the TF and SF were run through SDS page analysis to determine if protein expression had occurred and if the protein was in a soluble form.

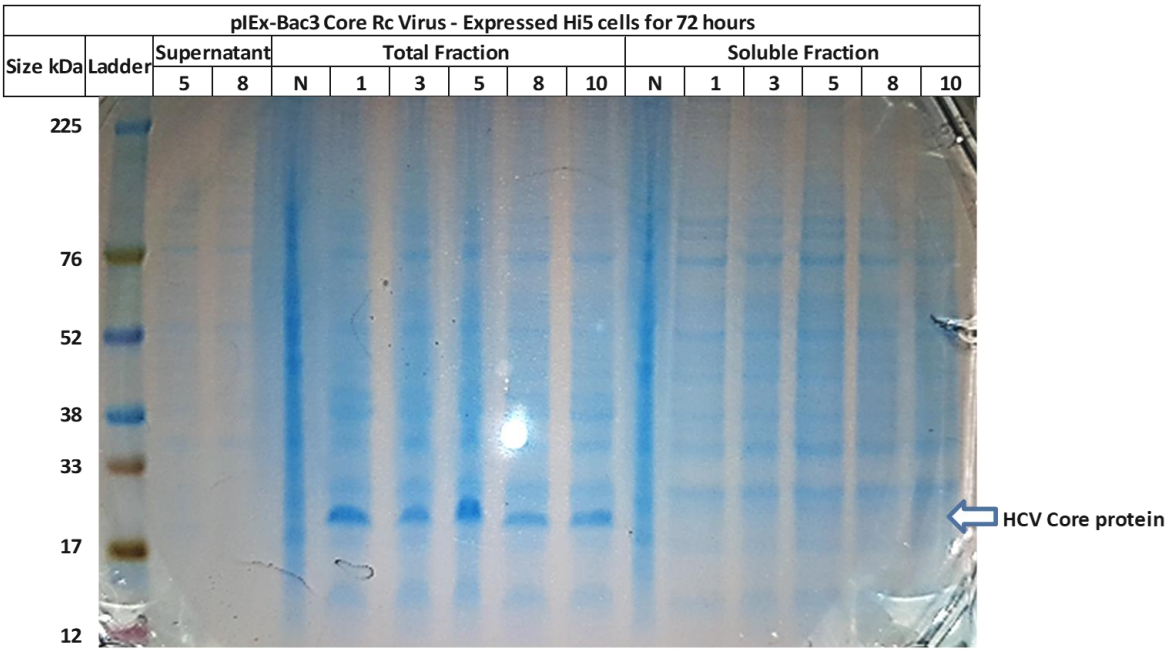

Figure 44 SDS Page Gel of 72 Hour pIEx-Bac 3 Core Rc virus insect cell expression in Hi5 cells. NuPage 4-12% Bis-Tris PAGE gel run for 200V for 35 minutes, post electrophoresis stained with InstantBlue and image taken with digital camera. Loading order: Protein size ladder, Supernatant 5 and 8 = media collected from cells infected at MOI of 5 and 8, Total Fraction N = non-infected cell total fraction, Toral Fraction 1-10 = total fractions collected from cells infected at MOI ranging from 1-10, Soluble Fraction N = non-infected cell soluble fraction, Soluble fractions 1-10 = soluble fractions collected from cells infected at MOI ranging from 1-10. Clear band can be seen in the total fractions for all cells infected with MOI between 1-10 at the expected size of 22kDa for core protein, this band is not seen in non-infected control cells. Band is not seen in any of the soluble fractions for the infected celsl indicating the Core protein has been expressed but not in a soluble form.

Figure 44 above shows the SDS page results from the pIExBac3 Core expression. The expected size of the expressed core protein is 22 KDa. No band is seen in the supernatant at this size showing no core protein was secreted from the cells. In the Total Fraction aliquots there was a clear band in all 5 lanes, showing a good level of core protein expression at all 5 MOI. In all lanes representing the

soluble fractions the same band was not seen. This suggests the expression of core protein from the pIEx-Bac3 Core Rc virus was successful but did not produce any soluble protein. To double check there was no soluble protein produced, a HIS Tag purification and subsequent western blot was performed.

12.1.4.9 HISTAG PURIFICATION

This purification procedure was performed on the soluble fraction of the pIExBac3 core expression. Despite no soluble protein being visible on SDS page, performing a Histag purification should pick out and concentrate any soluble protein present, even in a very low amount. The Histag purification was performed as described in section 511.4.6.8. This included 2 washes using two 10mM imidazole wash buffer followed by 3 of 20 mM washes. A low concentration imidazole wash used to prevent any loss of core protein and maximise the chances of recovering any soluble protein. Aliquots were taken from each of the wash stages and final elution stages, and run through a western blot as described previously, using the same anti-HCV monoclonal antibody used in 12.1.3.

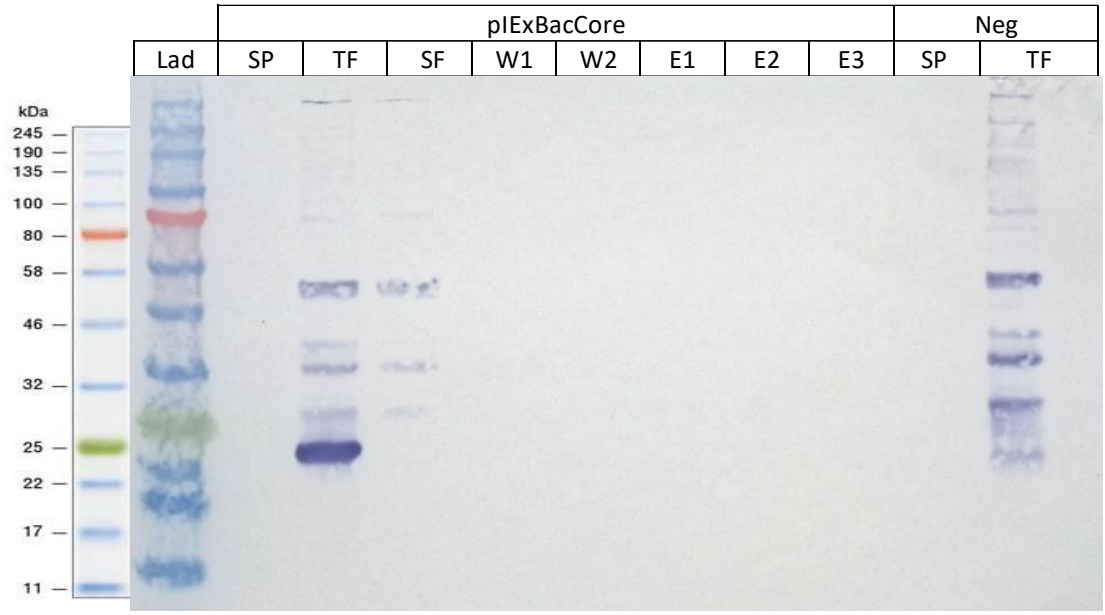

Figure 45 Western blot of pIExBacCore HISTag purification. Western blot used NuPage 4-12% Bis-Tris gels transferred to 0.45µm Nitrocellulose membrane. Primary antibody mouse mAb Anti-HCV Core at 1:1000 dilution, secondary antibody rabbit pAb-Anti-mouse IgG (HRP) used at 1:3000, substrate TMB Ultra. Loading order: Lad = Protein size ladder, SP=supernatant, TF=Total fraction, SF=Soluble Fraction, W1-W2 = Wash 10 and 20mM Imidazole, E1-E3 = 3 elutions 250mM imidazole. Neg TF = Negative Total Fraction, Neg SF = Negative Soluble Fraction. Strong band at the predicted core size of 22kDa is seen in total fraction but is missing from soluble fraction and any of the elutions suggesting Core protein was expressed but not in a soluble form suitable for HIStag purification.

Figure 45 shows the results of the western blot of the purified pIExBac core expression, using an anti-HCV mAb at 1:1000. The supernatant (SP) was included to see if any core protein was excreted from the Hi5 cells, which the blank lane clearly shows did not occur. The total fraction (TF) shows a

clear strong band at the expected size, confirming the expression of core protein. Comparison with the negative control (protein extracted non-infected Hi5 cells) shows some non-specific binding of the total fraction, but no clear band at the expected size and no bands of the same intensity. The soluble fraction (SF) shows no band at the expected size, and no band is seen in any of the wash steps (W1-W2) and any of the elution steps (E1-E3), confirming the lack of any soluble core protein even at a very low level. Expressed protein must be in a soluble form to be purified and for subsequent use in immunoassays. Insoluble expressed protein can be solubilised using urea or guanidine. However, these procedures denature the protein and it loses its native form, and with it the post translational modifications produced by a higher eukaryotic cell like the Hi5 insect cells. To avoid the need for denaturing of the protein an alternative approach was attempted expressing the full core protein, rather than the truncated version expressed in the pIExBac core protein.

12.1.5 EXPRESSION OF FULL CORE PROTEIN USING POET1 PLASMID

As opposed to the pIEx core plasmid, which was bought as a synthesised plasmid, the full core gene was amplified from HCV positive sera and cloned into a suitable transfer vector. The pIEx-Bac3 transfer plasmid originally chosen for use with the *flash*BAC™ ULTRA expression system became unavailable to purchase mid-way through the study. Therefore, an alternative plasmid had to be chosen, the pOET1 plasmid from Oxford expressions Ltd. This is a *flash*BAC™ ULTRA compatible transfer vector with restriction enzyme cloning site, a N' terminus HIS Tag and a polyhedrin baculovirus promoter. This transfer vector was not available in a ligation independent cloning form, so conventional cloning was used for insertion of amplified inserts.

12.1.5.1 PCR AMPLIFICATION OF FULL CORE GENE

A total of 6 serum samples known to be HCV RNA positive were selected from surplus residual, unlinked and anonymised samples used in this study. Primers designed for amplification of the whole core gene were used as described in 11.4.1.1.2. Nucleic acid extraction was performed using the bioMerieux Nuclisens Easymag semi-automated nucleic acid extraction instrument, as described in section 11.4.1.2. Reverse transcription was performed to convert extracted viral RNA to cDNA, followed by PCR amplification using multiple annealing temperatures ranging from 50°C to 58°C as described in 11.4.1.4. Gel electrophoresis was performed on amplified products as described in 11.4.1.

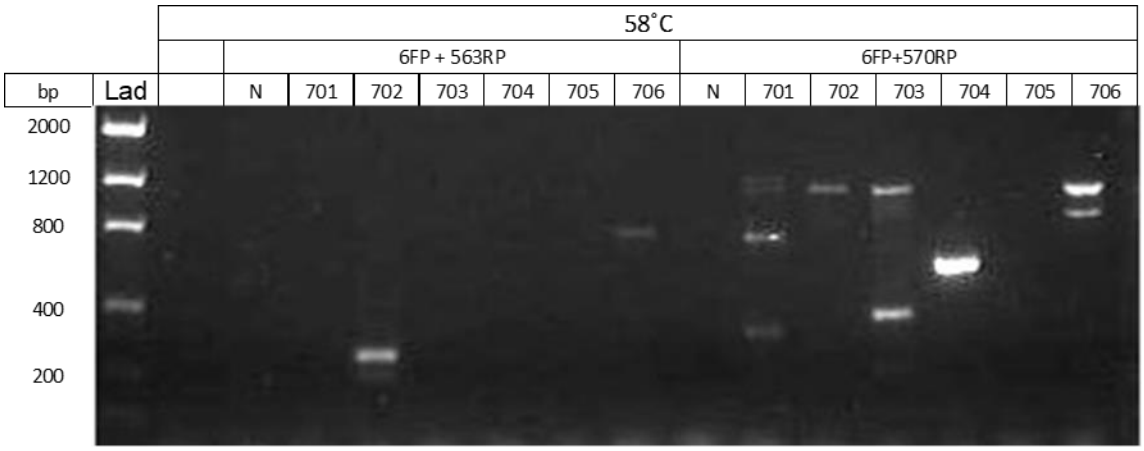

Figure 46 Gel electrophoresis of Full Core PCR. Agarose 1% gel with 1:10000 dilution of SyBr safe DNA stain run at 100 V for 40 minutes, post electrophoresis imaged using Alphaimager 2200 imaging system under UV. Top row lists the annealing temperature, the middle row the forward and reverse primers. Bottom row lists the sample loading order, N = negative control, 701-706 = study samples.

Figure 46 is a gel electrophoresis image from the most successful PCR. None of the PCRs using the Core 1FP or Core 563RP worked, an example of this can be seen on the left-hand side of the gel image above. Results from annealing at 54°C are not shown but led to multiple non-specific bands in the PCR. Running the annealing temperature at 58°C led to cleaner bands as seen above, when combined with the Core 6FP and 570RP primers. Serum sample study no. 704 gave a very clear single band using this combination and was chosen for subsequent cloning into pOET1 plasmids. This primer combination covers the sequence for aa3-190 of the core gene.

12.1.5.2 CLONING INTO POET1 PLASMID

Cloning the amplified full core gene into the pOET 1 plasmid was performed by conventional cloning using restriction enzymes (RE) as described in 11.4.5. The resultant cloned plasmid was then transformed into competent *E. coli* as exactly as described in section 11.4.4. A possible 3 plasmid containing colonies were picked, amplified, plasmid purified, and quantified, before confirmation by nucleotide sequencing. Primers specific for the POET1 plasmid and HCV Core specific primers were used, see Table 12. The 4 sequening files were analysed and combined to produce a fasta file for each plasmid. Snapgene software was used to align the sequenced fast file against the simulated plasmid map previously created during primer design.

Table 17 below lists the quantity and confirmation by nucleotide sequencing of the 3 plasmid preparations.

Plasmid Prep No	Name	Conc. µg/µl	Total Vol.	Amt µg	Confirmed Sequence
1	pOET1FCorepp1	0.381	30	11.43	Yes
2	pOET1FCorepp2	0.324	30	9.72	Yes
3	pOET1FCorepp3	0.349	30	10.47	Yes

Table 17 Concentration of pOET1Core plasmids 1-3DNA post purification in µg/µl. Determined by nanophotometer and confirmed by sanger nucleotide sequencing.

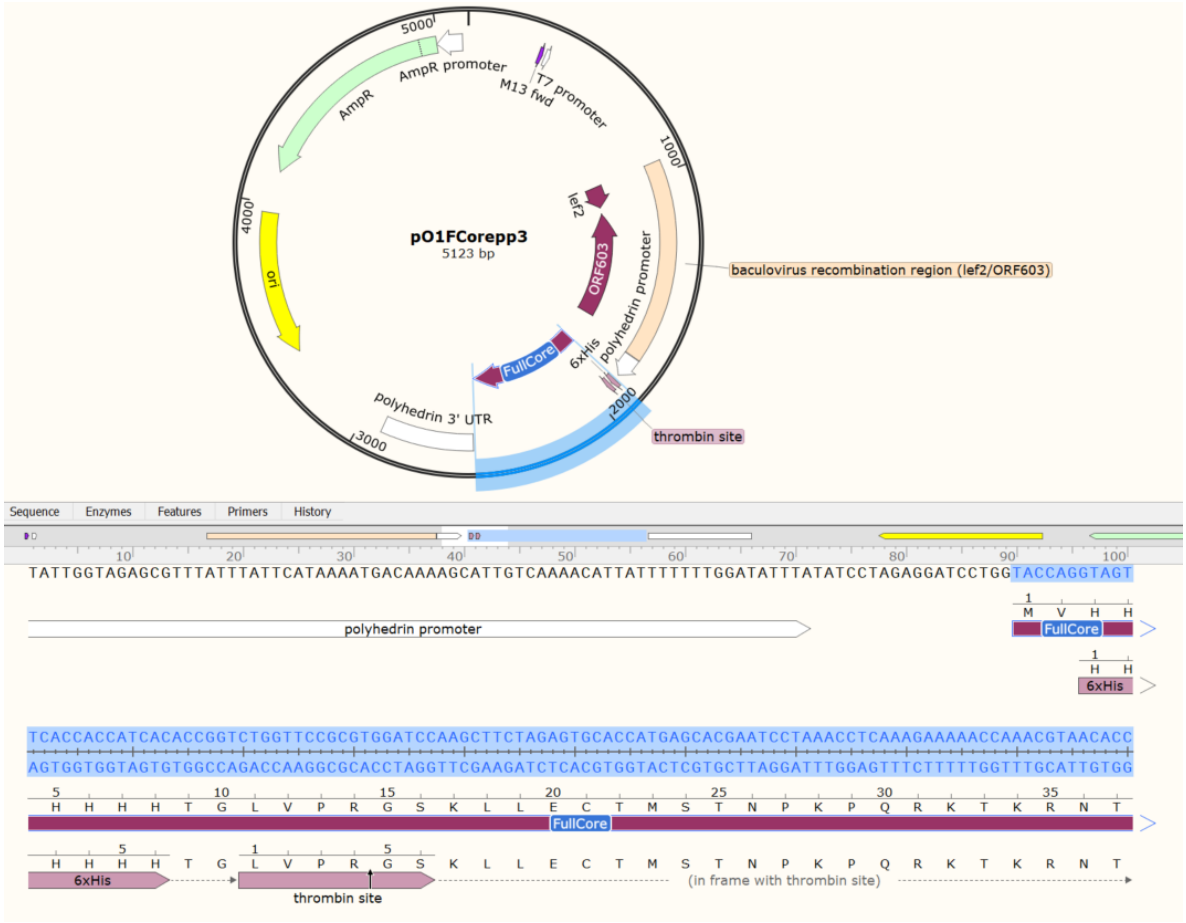

Figure 47 Plasmid map of pOET1FCorepp3 viewed in Snapgene software. Highlighted in blue is the Full core inserted sequence, aligned for expression under the polyhedrin promoter, and with a 6XHistag incorporated at the N terminus.

Figure 47 above shows the plasmid map for the pOET1 full core plasmid preparation 3. The inserted core sequence is highlighted in blue, downstream and in frame of the polyhedrin promoter and 6X His tag. This plasmid was used for subsequent recombinant baculovirus generation and protein expression.

12.1.5.3 TRANSFECTION AND GENERATION OF RECOMBINANT BACULVIRUS

Generation of recombinant baculovirusincorporating the pOET1Corepp3 followed the same procedure as described in section 12.1.4.4. After one-week incubation the medium was transferred into a 50ml

suspension culture and amplified as described in 11.4.6.2. After amplification the pOET1FCoreRc virus was tested by QPCR as described in 11.4.6.3, showing the virus had amplified to a level of $5.12X10^7$ pfu/mL.

12.1.5.4 EXPRESSION OF POET1 CORE RC VIRUS

A protein optimisation experiment was performed in Hi5 cells in a 6 well culture plate as described in section 12.1.4.7. Hi5 cells were seeded at $1x10^6$ into 6 well culture plate, and Rc virus added at a MOI of 1, 3 and 10. The expression was again run for 72 hours at 28°C. After 72 hours infected cells show the same signs of viral replication as shown in Figure 43, with the non-infected control looking comparatively healthy. The cells were collected, separated from the medium supernatant, and extracted exactly as described previously. The results of SDS page analysis are shown below in Figure 48 below.

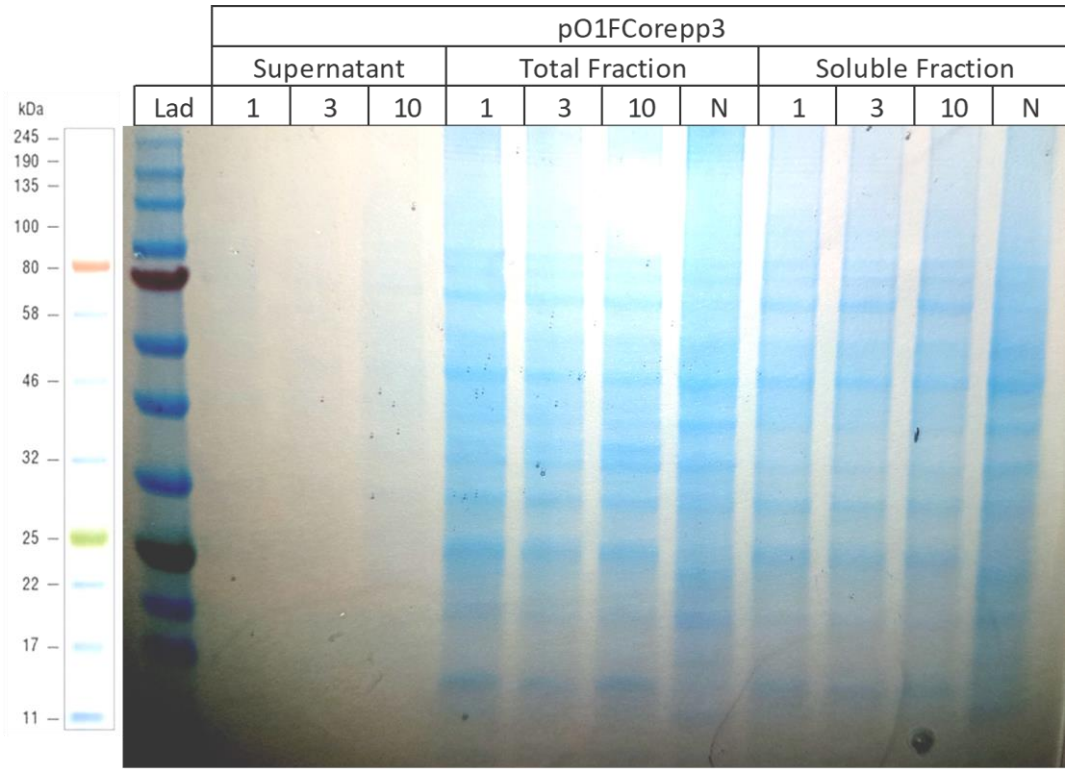

Figure 48 SDS page analysis of pOET1 Core pp3 expression in Hi5 cells. NuPage 4-12% Bis-Tris PAGE gel run for 200V for 35 minutes, post electrophoresis stained with InstantBlue. Loading order: Lane 1 = Protein size ladder; Lane 2-4 = Supernatant media from cells infected at MOI of 1, 3 and 10; Lane 5-7 = Total Fraction from cells infected MOI of 1, 3 and 10; Lane 8 = Total fraction from non-infected cells; Lane 9-11 = Total Fraction from cells infected MOI of 1, 3 and 10; Lane 12 = Soluble Fraction from non-infected cells. In all 3 MOI total fractions a band can be seen at 25kDa which is absent from non-infected cells, this same band can be seen in all 3 MOI soluble fractions again absent from the non-infected soluble fraction.

The SDS page analysis shows a possible band at around 25kDa at all three MOI wells, which is missing from the non-infected control wells. This band can also be seen in the soluble fraction for all three MOI wells, again missing from the non-infected control wells. The supernatant collected from all three MOI wells show no visible bands at all, showing no excretion of protein from infected cells has occurred.

The results suggested that possible expression of the full core protein has been achieved with the pOET1FCore Rc virus, but the band was not as strong as seen in the previous experiment using the pIExBacCore plasmid, see section 612.1.4.8. A large-scale protein expression was performed in suspension cell culture, as outlined in section 5.3.6.6. As all expressions using all three MOI gave the same possible band, the middle MOI of 3 was chosen for an 80 mL suspension culture expression. The expression was again run for 72 hours at 28°C in a shaking incubator set at 140 rpm.

12.1.5.5 HISTAG PURIFICATION AND SDS PAGE ANALYSIS

The 80ml suspension culture was separated into two 40ml tubes, spun down to separate cells from the medium supernatant, and the resultant pellet snap frozen in liquid nitrogen. A large-scale protein purification was then performed, as outlined in section 11.4.6.8. Aliquots collected from each stage were analysed by SDS page electrophoresis.

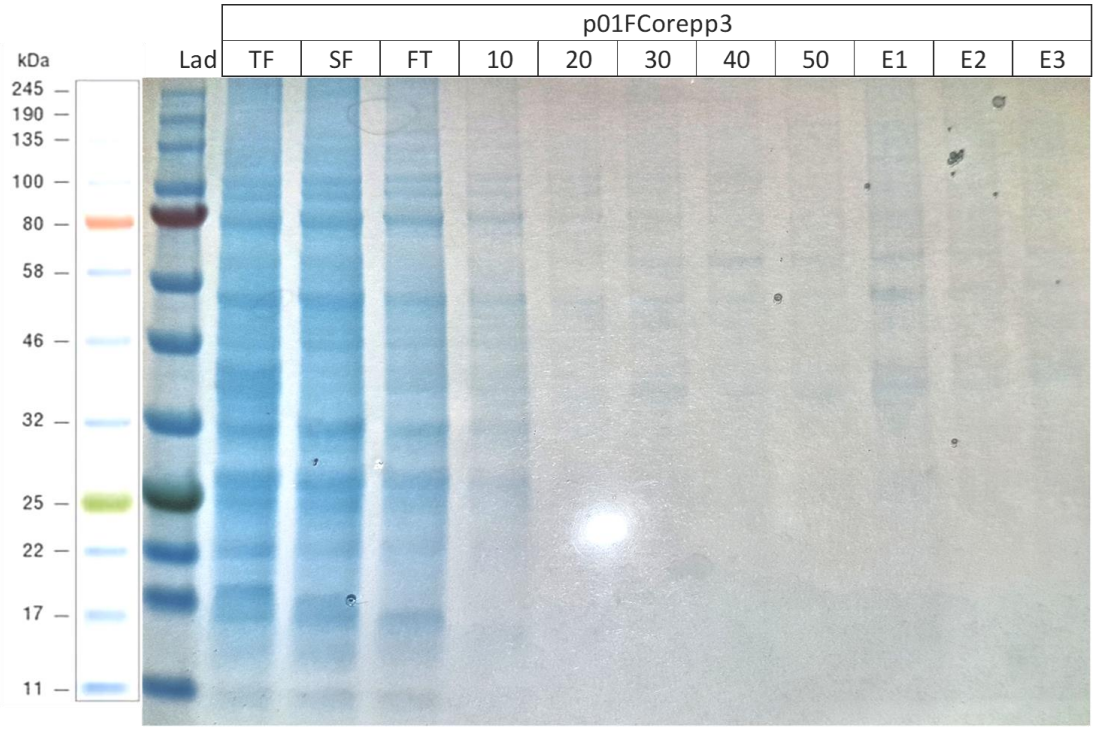

Figure 49 SDS-PAFE gel image of HISTag purification of pOET1Core Rc Virus expression. NuPage 4-12% Bis-Tris PAGE gel run for 200V for 35 minutes, post electrophoresis stained with InstantBlue. Loading order: Lad = Protein size ladder; TF = Total Fraction, SF = Soluble Fraction, FT = Full Transfer, 10 - 50 = 5 Washes in Imidazole gradient from 10-50mM, E1-E3 = 3 X 250mM Imidazole Elutions.

As seen in Figure 49 there is no clear band at the expected size in any of the aliquot lanes, E1-E3. This suggests HIStag purification was not a success. To double check if any core protein expression had occurred, a western blot was performed on a selection of aliquots run through the SDS-page.

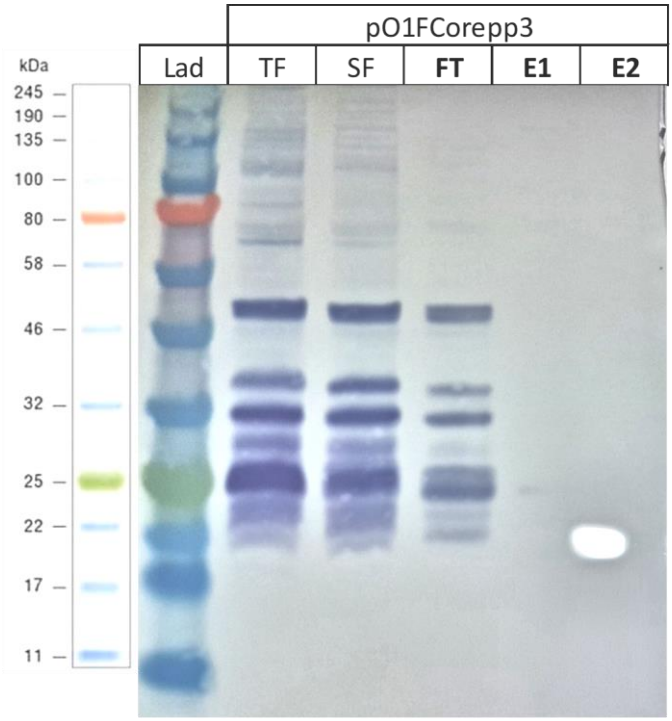

Figure 50 Western Blot of HISTag purification of pOET1Core Rc Virus expression. Western blot used NuPage 4-12% Bis-Tris gels transferred to 0.45µm Nitrocellulose membrane. Primary antibody mouse mAb Anti-HCV Core at 1:1000 dilution, secondary antibody rabbit pAb-Anti-mouse IgG (HRP) used at 1:3000, substrate TMB Ultra. Image taken with digital camera. Loading order: Lad = Protein size ladder; TF = Total Fraction, SF = Soluble Fraction, FT = Full Transfer, E1-E2 = 2 X 250mM Imidazole Elutions. A clear band around 25kDa in the total fraction, soluble fraction, and full transfer but this is missing from both elutions showing no core protein was purified through the HISTag purification process.

The western blot results shown in Figure 50 clearly shows a strongly defined band at around 25kDa, the expected size of the core protein, in both the total fraction and the soluble fraction, however no band is seen in either of the eluates E1 and E2. This suggests expression of the core protein has occurred but was not purified through the HISTag purification process. Possible reasons for the failure of the purification process include non-expression of the HIStag; if the cloning of the core gene removed some or all of the his sequence from the plasmid; folding of the protein which results in the his residues not being available for binding; or wash steps during the purification process removing protein before the elution stage. The pOET1FCore plasmid had been sequenced, and the nucleotide sequence checked to ensure both the His tag and core protein were properly aligned downstream of the polyhedrin promoter. It is possible the protein folded in some way to block the availability of the HIS residues to bind to nickel, but as it was also possible the imidazole wash gradient used in the purification process had removed the core protein before the elution stage. It was therefore decided to check to see if the washing stages had indeed removed the protein This was easier to investigate and correct than the possibility of protein folding hiding the binding site. Aliquots of each wash stage were analysed by SDS page electrophoresis but as the wash stage uses a large volume, especially compared to the elution stage, it is possible the core protein was washed off gradually over several

stages and was not detected with the SDS page or western blot. A further protein purification was performed using up to a concentration of 20 mM for the imidazole washes. All other steps in the elution process remained the same as before, this time using another of the frozen pellets of cells saved from the large-scale protein expression.

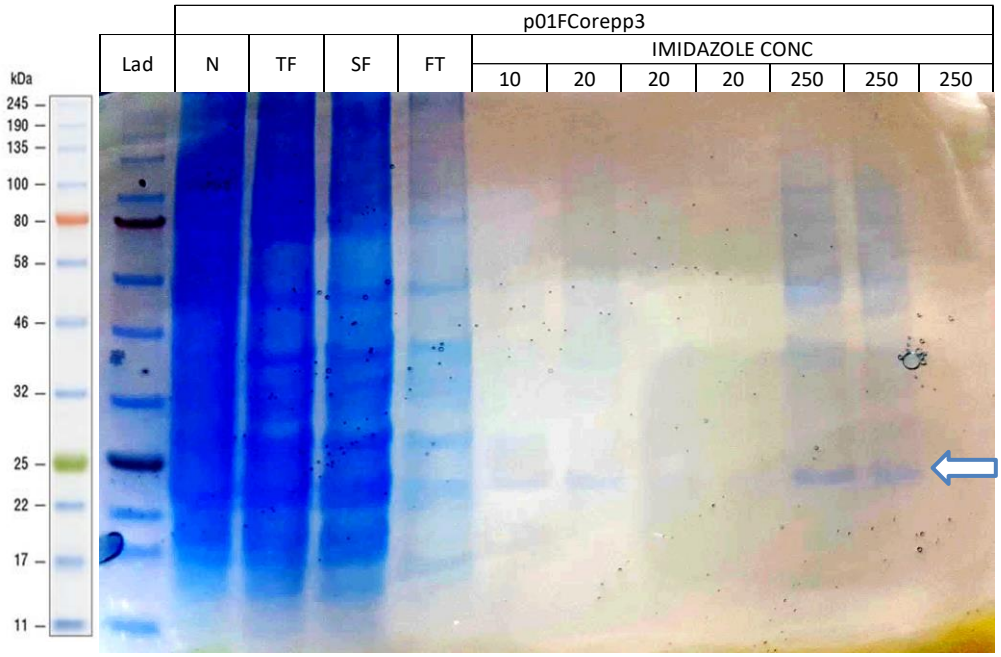

Figure 51 SDS-PAFE gel image of HISTag purification of pOET1Core Rc Virus expression using lower strength imidazole washes. NuPage 4-12% Bis-Tris PAGE gel run for 200V for 35 minutes, post electrophoresis stained with InstantBlue. Image taken with digital camera Loading order: Lad = Protein size ladder; N = non-infected control, TF = Total Fraction, SF = Soluble Fraction, FT = Full Transfer, 10 = 10mM imidazole wash, 20 = 4 X 20 mM imidazole washes, 250 = 3 X 250mM imidazole elutions. Arrow indicates band at 25kDa in the 250mM elutions suggesting expressed core protein was purified through HISTag purification.

Figure 51 shows SDS page results from the alternate purification process, using 1x10 mM imidazole wash, followed by 4X20 mM washes, before the final 3x 250 mM elutions. The SDS page shows a positive band in the first two eluates at the expected size. The bands were quite faint but could be seen with the naked eye. The bands are of the correct size, indicating expressed and purified full core protein.

A western blot was repeated on the selection of the aliquots, to confirm if this was the core protein. Unfortunately, subsequent western blots using the previously used anti-HCV Core mAb were blank (not shown). The western blot was repeated to ensure this was not due to a procedural error, but the result was the same again. Another western blot was then tried, using a different anti-HCV core polyclonal antibody. Note this polyclonal antibody was conjugated to alkaline phosphatase (AP), as opposed to the previous antibody which was conjugated to horseradish peroxidase, hence the use of 5-Bromo-4-chloro-3-indolyl phosphate (BCIP) substrate and the different colour of the developed western blot.

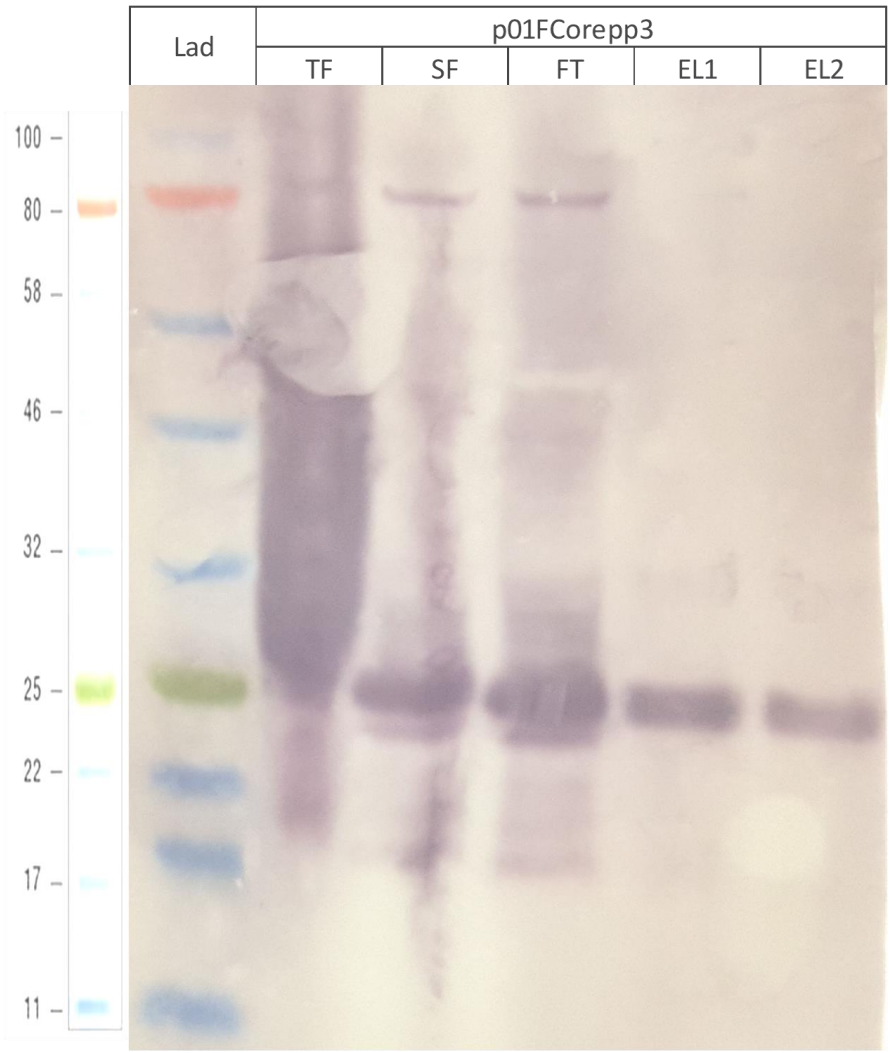

Figure 52 Western Blot of HISTag purification of pOET1Core Rc Virus expression. Western blot used NuPage 4-12% Bis-Tris gels transferred to 0.45µm Nitrocellulose membrane. Primary antibody goat pAb Anti-HCV Core at 1:1000 dilution, secondary antibody donkey pAb Anti-rabbit IgG (AP) used at 1:2000, substrate Fast BCIP/NBT. Image taken with digital camera. Loading order: Lad = Protein size ladder; TF = Total Fraction, SF = Soluble Fraction, FT = Full Transfer, EL1-EL2 = 2 X 250mM imidazole elutions. A clear band around 25kDa in the total fraction, soluble fraction and full transfer can be seen in both elutions 1 and 2 confirming expressed core protein was purified through HISTag purification process using 10-20mM imidazole washes.

Figure 52 shows the results of the western blot using the anti-HCV core pAb from the second HIStag purification using 10-20mM imidazole washes. The western blot shows a band of the expected size, 25kDa, in all the total fraction (TF), soluble fraction (SF) full transfer (FT) and importantly in both the eluates 1 and 2 (EL1-2). Such a strong band in the full transfer shows that not all the expressed protein had sufficiently bound to the nickel coated beads, but some did to give clear bands in the eluates.

This demonstrated successful expression and purification of the HCV core protein, in a soluble native form. This purified protein could now be used in subsequent ELISAs.

12.1.6 NS3 PROTEIN

Production of the HCV NS3 protein was first trialled using a combination of the pIExBac3 transfer vector and the *flash*BAC™ ULTRA system. This followed the same method used for HCV core production using this combination of transfer vector and expression system, see section 12.1.4.

12.1.6.1 PCR AMPLIFICATION

Primers were designed as described in 11.4.1.1.1. A total of 3 serum samples known to be HCV RNA positive were used. Nucleic acid extraction was performed using the bioMerieux Nuclisens Easymag semi-automated nucleic acid extraction instrument. Reverse transcription was performed to convert extracted viral RNA to DNA, followed by PCR amplification using multiple annealing temperatures ranging from 50°C to 58°C. A detailed procedure is outlined in section 11.4.1.

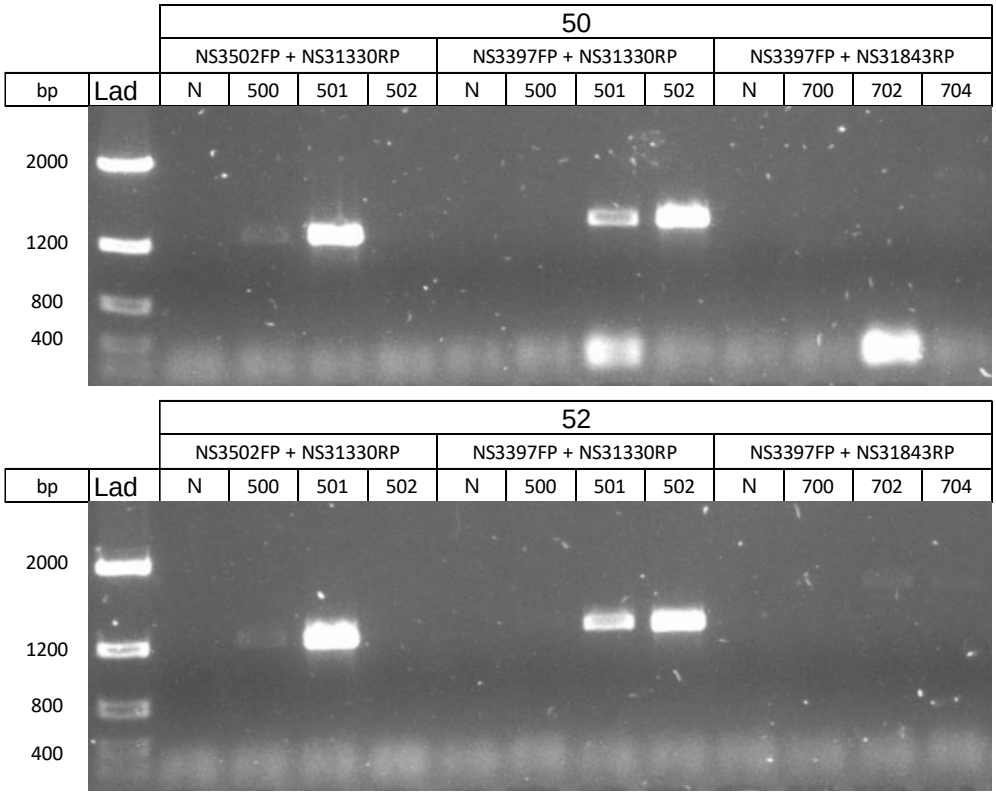

Figure 53 Gel electrophoresis of NS3 gene PCR. Agarose 1% gel with 1:10000 dilution of SyBr safe DNA stain run at 100 V for 40 minutes, post electrophoresis imaged using Alphaimager 2200 imaging system under UV. Top row lists the annealing temperature, the middle row the forward and reverse primers used for PCR. Bottom row lists the sample loading order, N = negative control, 500-501 = study samples.

Figure 53 is a gel image from the PCR amplification of the NS3 gene. Three samples were tested with a combination of 2 forward and 2 reverse primers. Only the gels from PCRs using an annealing temperature of 50°C and 52°C are shown, as any higher temperatures did not produce amplified products. The NS31843RP did not work with in any primer combination at any annealing temperature. The two forward primers, NS3502FP and NS3 397FP both worked in combination with the NS1330RP. It was decided to use the larger of these 2 products, using the primer combination NS3397FP and NS31330RP. Serum sample study number 502 at an annealing temperature at 52°C gave the strongest band with this primer combination and was chosen for subsequent cloning into the pIEx-Bac 3 plasmid.

12.1.6.2 LIGATION INDEPENDENT CLONING

Ligation independent cloning was performed as outlined in section 5.3.4, and as discussed earlier for the HCV core protein in section 6.1.1. The purified NS3 PCR product was successfully cloned into the pIExBac3 plasmid, and nucleotide sequencing performed as described in 12.1.4.3, using the sequencing primers listed in Table 12, to confirm the insertion of the NS3 DNA in the correct reading frame. In total 3 plasmids were purified and sequenced, see Table 18 below.

Plasmid Prep No.	Name	Conc. µg/µl	Total Vol.	Amt µg	Confirmed Sequence
1	pIExBac3NS3pp1	0.686	30	20.58	Yes
2	pIExBac3NS3pp2	0.687	30	20.61	Yes
3	pIExBac3NS3pp3	0.818	30	24.54	Yes

Table 18 Concentration of pIExBac3NS3 plasmids 1-3 DNA post purification in µg/µl. Determined by nanophotometer and confirmed by sanger nucleotide sequencing.

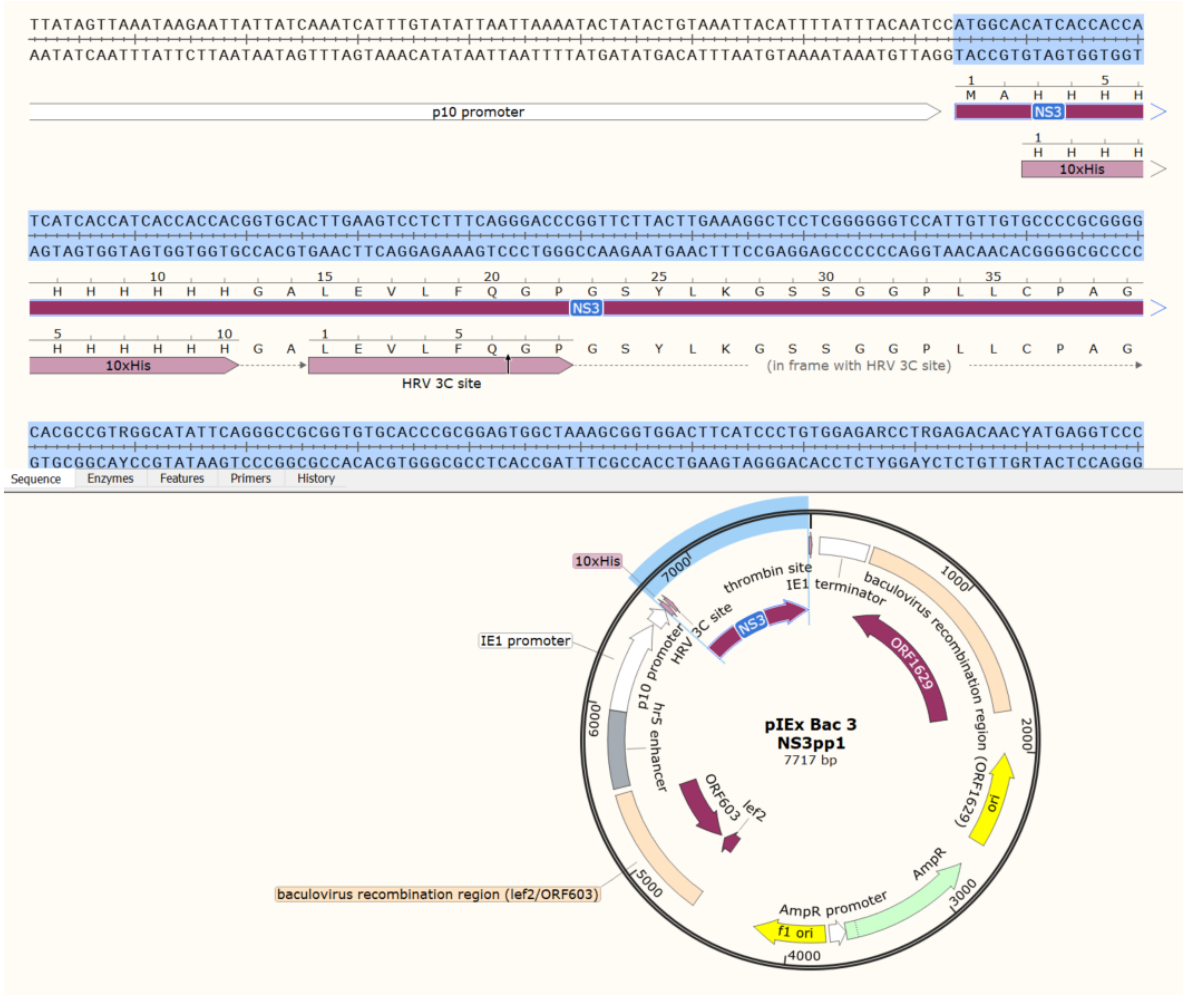

Figure 54 Plasmid map of pIExBac3NS3 viewed in Snapgene software. Highlighted in blue is the NS3 inserted sequence, aligned for expression under the control of the IE1 and p10 promoters, and with a 10XHistag incorporated at the N terminus.

The 4 sequencing files were analysed and combined to produce a fasta file for each plasmid. Snapgene software was used to align the sequenced fasta file against the simulated plasmid map previously created during primer design.

Figure 54 is a plasmid map of the pIExBac3pp1 containing the aligned fasta sequence. The succesfully inserted NS3 sequence is highlighted in blue, downstream and inframe of the IE1 and p10 promoter, and the 10X HisTag. Of the 3 plasmid preperations sequenced all were confirmed to contain the NS3 sequence inserted in the correct reading frame. The pIExBac3pp1 was chosen for subsequent protein expression experiments.

12.1.6.3 NS3 PROTEIN EXPRESSION USING *FLASH*BAC™ ULTRA SYSTEM

Expression of the NS3 protein using the *flash*BAC™ ULTRA system followed the same procedure as decribed section 12.1.4., using the pIExBac3pp1 transfer vector plasmid. Transfected Sf9 cells showed the same CPE as shown previously (Figure 40). After a week of virus amplification Sf9 cells showed a high level CPE suggesting virus amplification had been succesful. Quantity of the Rcvirus was determined by QPCR, the level was $7.96X10^7$ pfu/mL.

A protein optimisation experiment was then performed in Hi5 cells, as described previously. Adherent Hi5 cells in a 6 well culture plate were infected with Rc virus at MOIs of 1, 3, 5, 10 and 20 for 72 hours. A mock infected control well was included alongside the 5 infected wells.

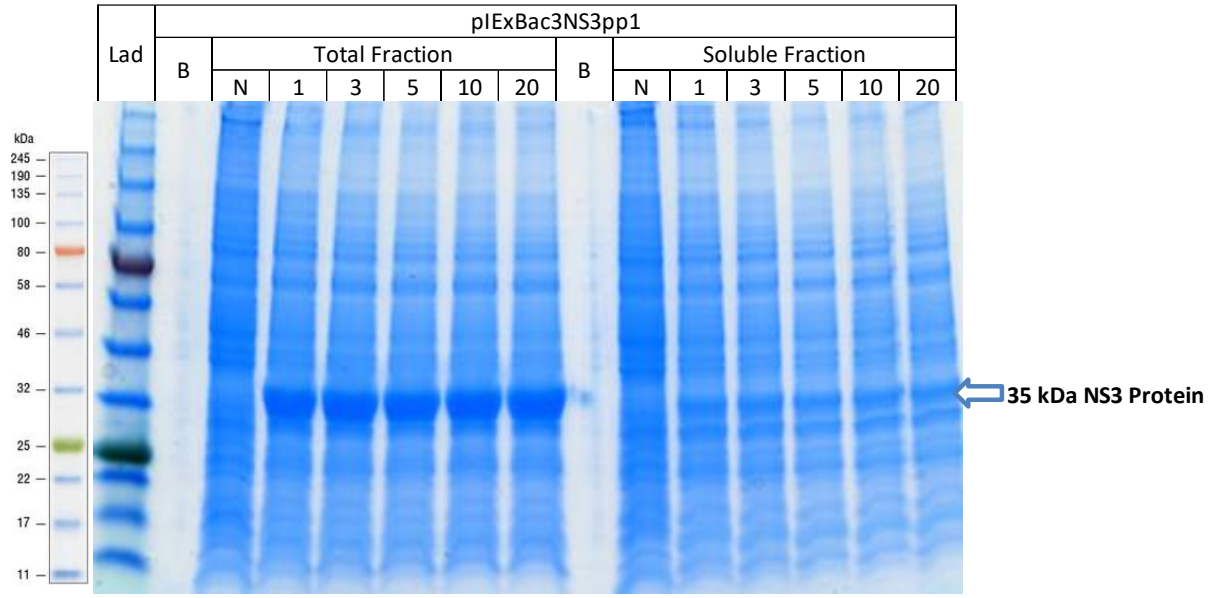

Figure 55 SDS page analysis of pIExBac3NS3 expression in Hi5 cells for 72 hours. NuPage 4-12% Bis-Tris PAGE gel run for 200V for 35 minutes, post electrophoresis stained with InstantBlue. Image taken with digital camera. Loading order: Protein size ladder, B = blank well, Total Fraction N= non-infected cells, Total Fraction 1-20 = total fraction from cell infected with MOI of 1-20, Soluble Fraction N = non-infected cell soluble fraction, Soluble fractions 1-20 = soluble fractions collected from cells infected at MOI ranging from 1-20. Clear band can be seen in the total fractions for all cells infected with MOI between 1-20 at the expected size of 35kDa for the NS3 protein, this band is not seen in non-infected control cells. The same band, slightly less strong but still present can be seen in all the soluble fractions suggesting the NS3 protein was expressed in a soluble form.

Figure 55 shows the SDS page analysis of the NS3 expression in Hi5 cells. The total fraction had a prominent band in all 5 infected wells at the expected size of 35 kDa. This band is missing from the negative control cells. In the soluble fraction lanes, the same band at 35 kDa appears, not as strong as in the total fraction, but defiinitely present. This suggested expression of the NS3 protein was successful, and was produced in a soluble form. There was no obvious difference between the different MOI used for cell infection, with all successfully expressing.

After the success of the optimization experiment a large scale protein expression was performed in 80ml suspension culture of Hi5 cells, infecting with recombinant virus at an MOI of 3. After 72 hours the cell suspension was collected, split into 2 X 40 mL aliquots, the cells pelleted and snap frozen. One of these aliquots was used for large scale protein extraction and HIStag purification as described in 11.4.6.8.

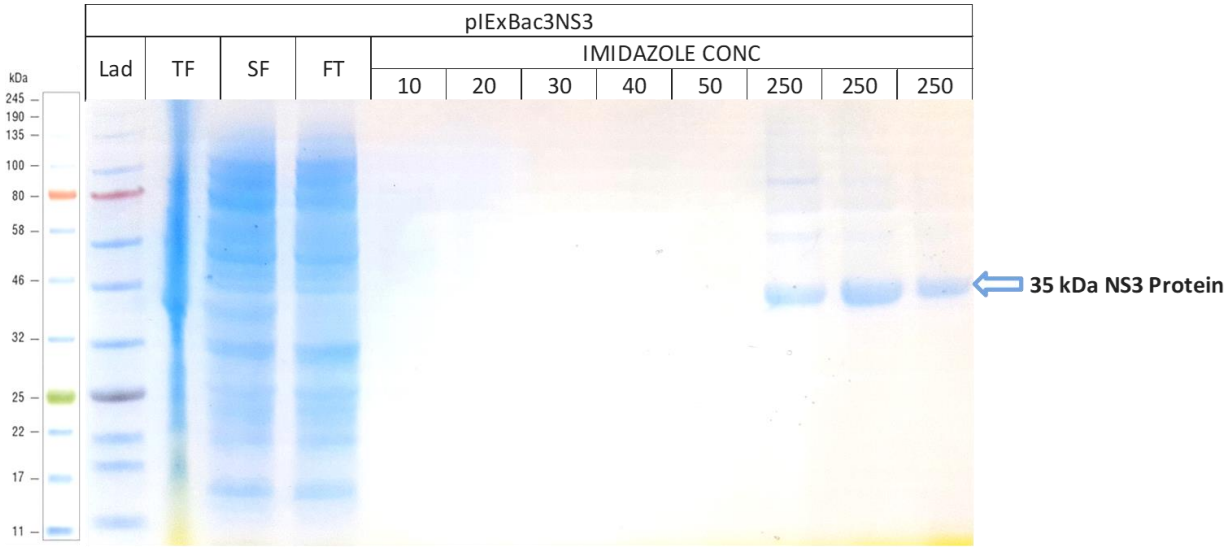

Figure 56 SDS-PAGE gel image of HISTag purification products from pIExBac3 NS3 Rc virus expression. NuPage 4-12% Bis-Tris PAGE gel run for 200V for 35 minutes, post electrophoresis stained with InstantBlue. Image taken with digital camera. Loading order: Lad = Protein size ladder; TF = Total Fraction, SF = Soluble Fraction, FT = Full Transfer, 10 - 50 = 5 Washes in Imidazole gradient from 10-50mM, E1-E3 = 3 X 250mM Imidazole Elutions. Arrow highlights strong band at 35kDa in all 3 X 250mM imidazole elutions indicating purification of the NS3 protein through the HISTag purification process.

Figure 56 shows the successful HISTag purification of the NS3 protein. There is no evidence of NS3 protein removal from the nickel coated beads in any of the imidazole washes. In the 3 final 250 mM imidazole elutions these is a clear band of the expected size of 35 kDa. A western blot was then performed as a final confirmation of the succesful expression and purification of the NS3 protein.

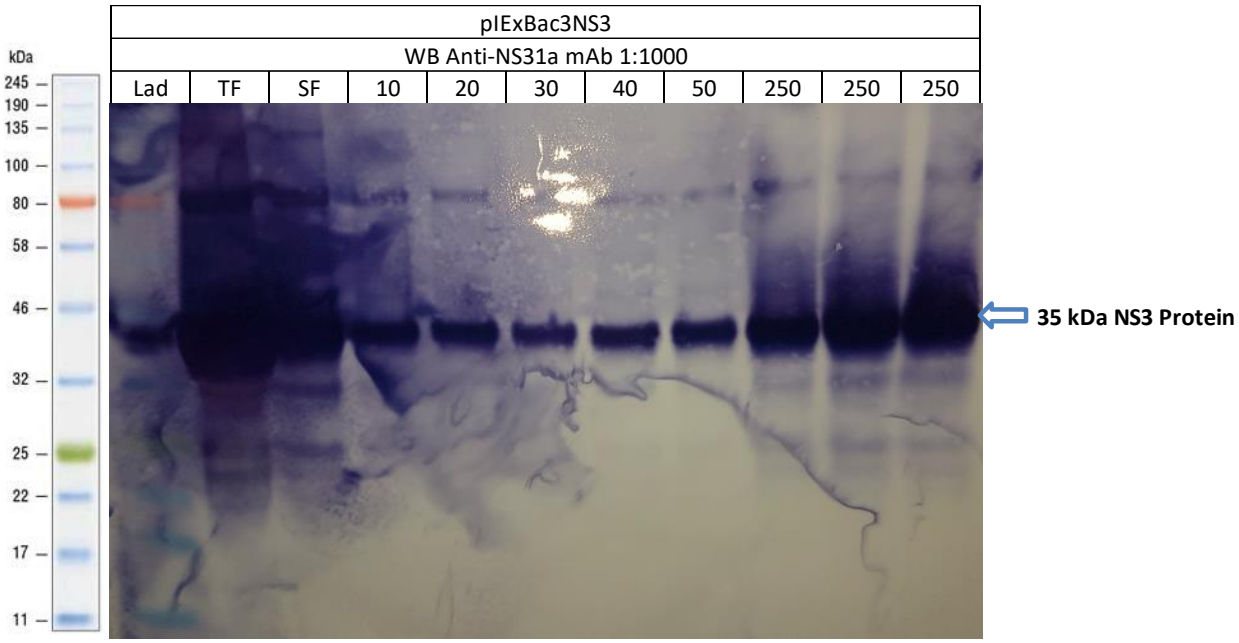

Figure 57 Western Blot of HISTag purification products from pIExBac3 NS3 Rc Virus expression. Western blot used NuPage 4-12% Bis-Tris gels transferred to 0.45µm Nitrocellulose membrane. Primary antibody mouse mAb Anti-NS3 at 1:1000 dilution, secondary antibody rabbit pAb-Anti-mouse IgG (HRP) used at 1:3000, substrate TMB Ultra. Image taken with digital camera. Loading order: Lad = Protein size ladder; TF = Total Fraction, SF = Soluble Fraction, 10-50 = 10-50mM imidazole washes, 250 = 3 X 250mM imidazole elutions. Gel was overstained giving high back ground levels, despite this strong band can be seen in all 3 X 250mM imidazole elutions at 35kDa proving the purification of NS3 protein.

A western blot was run with the aliquots collected during the NS3 protein purification procedure. Figure 57 above is an image of the western blot. The western blot clearly shows a large amount of NS3 protein in the total fraction and soluble fraction. Unfortunately the gel was stained for slightly too long, however the bands at each size can still be clearly seen. The imidazole wash gradient from 10-50 mM shows some loss of protein, though in the 3 X 250 mM elutions there is a much stronger band at the correct size. This confirms the expression and purification of NS3 protein using the combination of pIExBac3 transfer vector and *flash*BAC™ ULTRAexpression system, in a soluble native form.

12.1.7 NS4 PROTEIN

Expression of the HCV NS4 protein followed the same approach used for the NS3 protein. The immunodminant regions of the protein were amplifed from HCV RNA positive serum, and using ligation independent cloning inserted into a pIExBAc3 plasmid. Rc virus was then generated with the *flash*BAC™ ULTRA 3 system in Sf9 cells, before expression optimisation in Hi5 cells.

12.1.7.1 PCR AMPLIFICATION

Primers were designed for amplification of the NS4 immunodominant regions and to enable cloning into the pIExBac3 plasmid as described in 11.4.1.1.1. A total of 6 HCV positive sera were used for

amplification of the NS4. The samples were nucleic acid extracted and reverse transcribed as described in 11.4.1. The PCR was run using a range of annealing temperatures from 53°C and 56°C as described in 11.4.1.4.2.

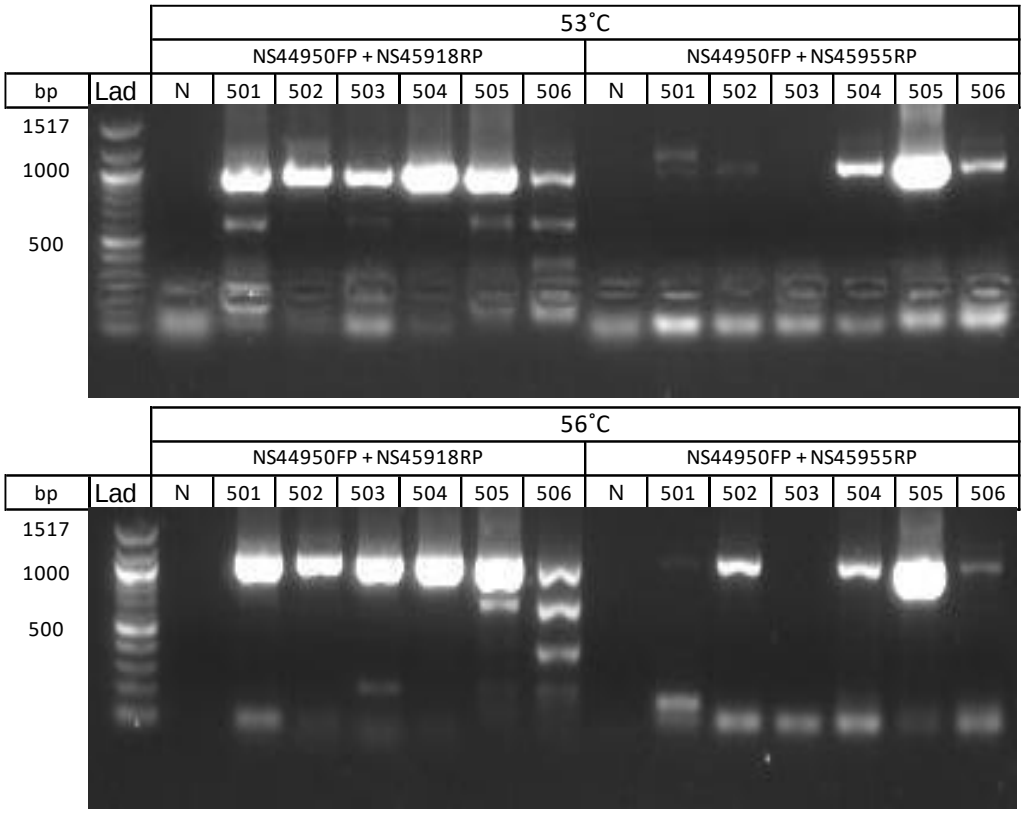

Figure 58 Gel electrophoresis image for PCR amplification of NS4 gene. Agarose 1% gel with 1:10000 dilution of SyBr safe DNA stain run at 100 V for 40 minutes, post electrophoresis imaged using Alphaimager 2200 imaging system under UV. Top row lists the annealing temperature, the middle row lists the forward and reverse primers used for PCR. Bottom row lists the sample loading order, N = negative control, 501-506 = study samples.

Figure 58 shows the gel electrophoresis image for the best performing primer combinations, at the two annealing temperatures giving the strongest and cleanest bands. Of these successfully amplified products, study number 505, with the primer combination NS44950FP and NS45955RP at an annealing temperature of 56°C was chosen for subsequent cloning into pIEx-Bac3 transfer vector.

12.1.7.2 LIGATION INDEPENDENT CLONING

Ligation independent cloning was used to insert the NS4 PCR product into a pIEx-Bac3 transfer vector, as described 11.4.4. After transformation in *E. coli* and plasmid preparation, nucleotide sequencing was used for confirmation of successful cloning. The primers used for nucleotide sequencing of the pIExBac3 NS4 plasmid are listed in Table 12 and followed the protocol described in 11.4.5.4.

Plasmid Prep No.	Name	Conc. µg/µl	Total Vol.	Amt µg	Confirmed Sequence
1	pIExBac3NS4pp1	0.626	30	18.78	No
2	pIExBac3NS4pp2	0.561	30	16.83	Yes
3	pIExBac3NS4pp3	0.522	30	15.66	Yes

Table 19 NS4 Plasmid preparation concentrations and confirmation of NS4 sequence insertion by nucleotide sequencing

Of the 3 plasmids purified post transformation, 2 contained the expected sequence in the correct reading frame. The other plasmid had the correct sequence but had a one base pair deletion mid-way through the NS4 insertion taking the remaining sequence out of frame.

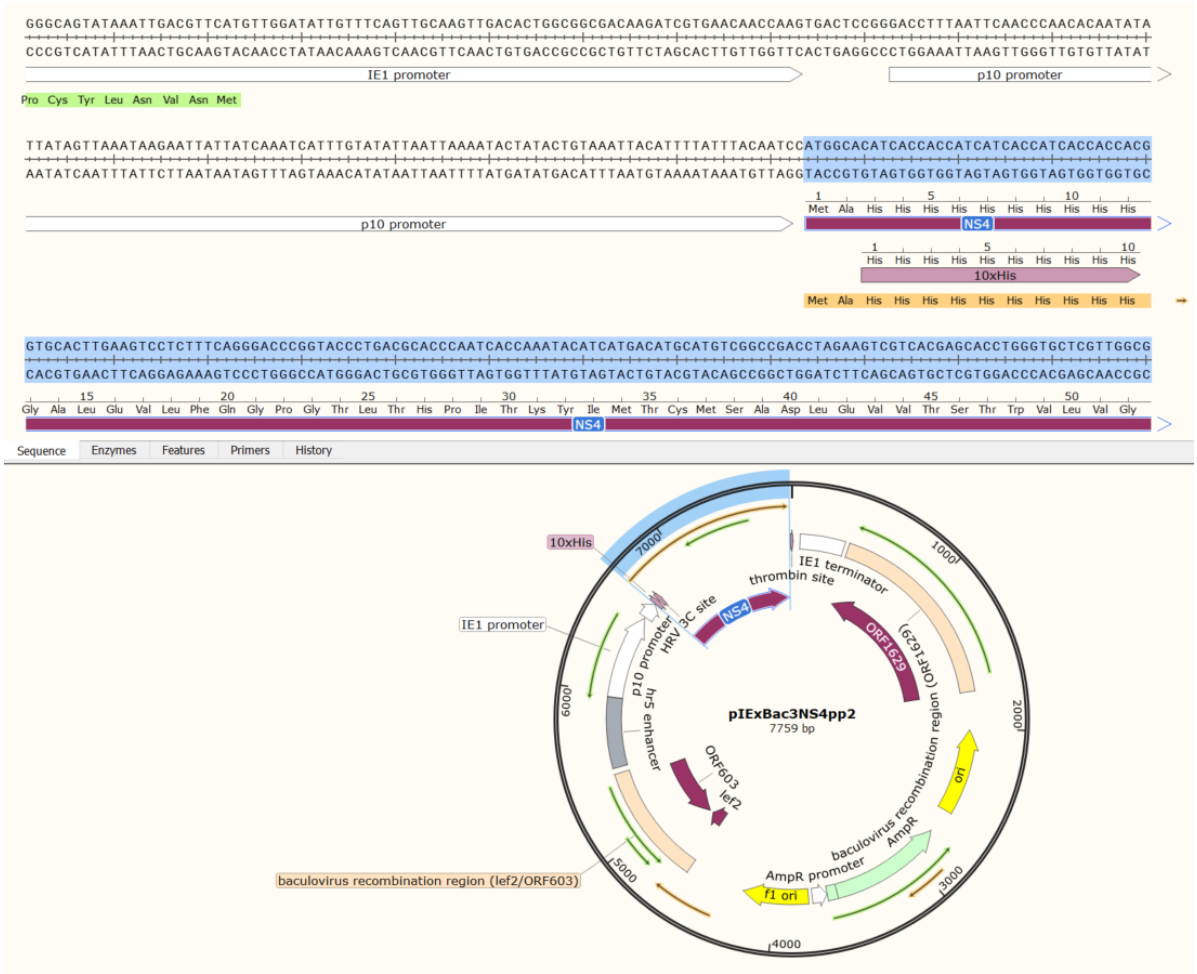

Figure 59 Plasmid map of pIExBac3NS4 viewed in Snapgene software. Highlighted in blue is the NS4 inserted sequence, aligned for expression under the control of the IE1 and p10 promoters, and with a 10XHistag incorporated at the N terminus.

Figure 59 shows the successful insertion of the amplified NS4 PCR product (highlighted in blue) into the pIExBac3 transfer vector, downstream and in-frame with the IE1 and p10 promoter and including a 10XHis tag at the N' terminus.

12.1.7.3 PROTEIN EXPRESSION

Rc virus was generated as described previously using the pIExBac3NS4pp2 transfer vector plasmid. After a week of viral amplification in 50ml of Sf9 suspension culture, QPCR of the Rc virus showed a level of 3.28 X 10^7 pfu/mL. This recombinant virus was then used for protein expression optimization experiment in adherent Hi5 cells as described in 11.4.6.4, infecting with pIExBac3NS4 recombinant virus at MOI of 1, 3, 5, 10 and 20, plus a negative control well. The incubation was left for 72 hours, after which cells were collected and a protein extraction performed as described in 11.4.6.5.

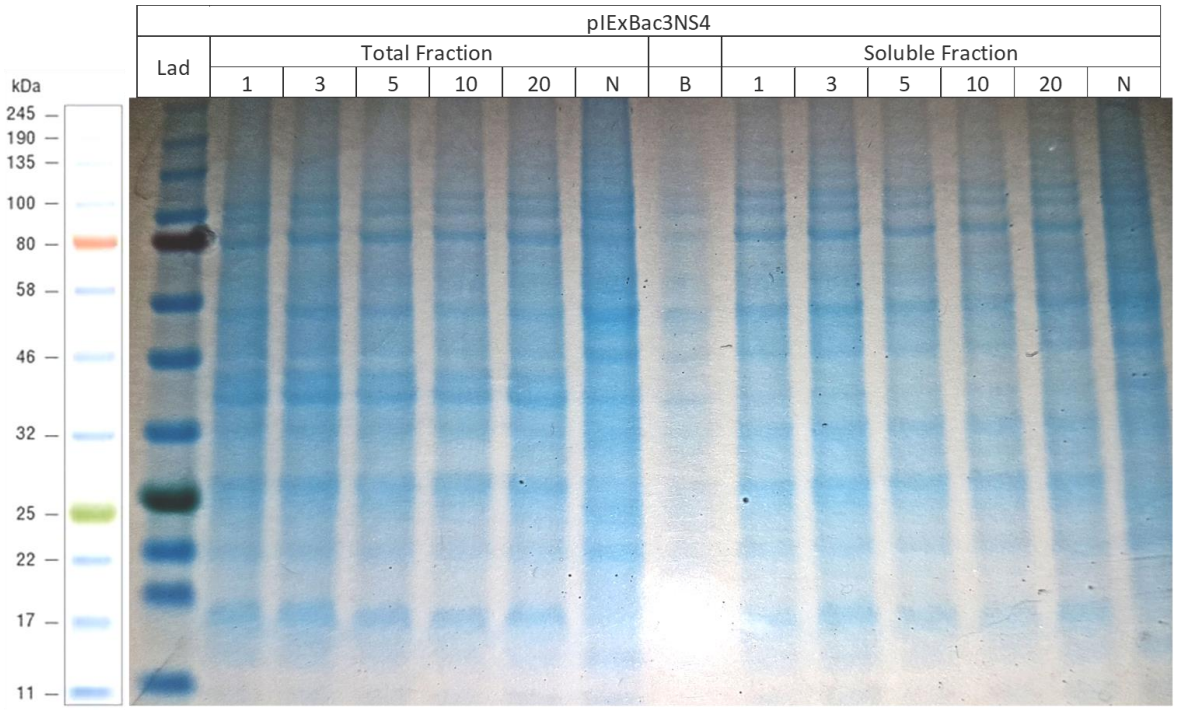

Figure 60 SDS Page Gel of 72 Hour pIExBac3 NS4 Rc virus insect cell expression in Hi5 cells. NuPage 4-12% Bis-Tris PAGE gel run for 200V for 35 minutes, post electrophoresis stained with InstantBlue. Image taken with digital cameraLoading order: Lane 1 = Protein size ladder, Lanes 2-6 = Total Fraction from cells infected with MOI between 1-20, Lane 7 = Total Fraction from non-infected cells, Lane 8 = Blank lane, Lanes 9-13 = Soluble Fractions from cells infected with MOI between 1-20, Lane 14 = Soluble Fraction from non-infected cells. No obvious band at the expected size of 37.4kDa indicating little or no expression of the NS4 protein occurred.

Figure 60 shows the SDS page analysis of NS4 protein expression optimisation in Hi5 cells. The expected size of the expressed NS4 protein is 37.4kDa. There was no obvious band seen on the SDS page gel image at this size, either in the soluble or total fraction. When compared to the negative control wells all the infected Hi5 cells showed obvious signs of Rc virus infection, with reduced cell numbers, shrunken size and deteriorated cell walls. The protein expression optimization was repeated, this time running the experiment for both 72 and 96 hours, to see if increasing the incubation time increased protein production, but again the SDS page analysis showed no obvious band at the right size.

To determine if protein production was occurring at a low level, protein purification was performed followed by western blot analysis. This would concentrate any protein present and western blot analysis would detect to this to a very low level.

The protein purification was performed as described in section 11.4.6.8. As no large-scale protein expression had been performed, all the protein extracts from the 5 infected wells, 1, 3, 5, 10 and 20 MOI, were combined and purified using a small 50 µL aliquot of nickel coated beads. To reduce the loss of protein during the washing stages higher imidazole strength washes were not used. Instead washing of the beads included 2 washes with 10 mM imidazole buffer and 3 washes with 20 mM. The final elution stage used only 50 µL of 250 mM imidazole wash buffer. A western blot was performed on the aliquots taken from each stage.

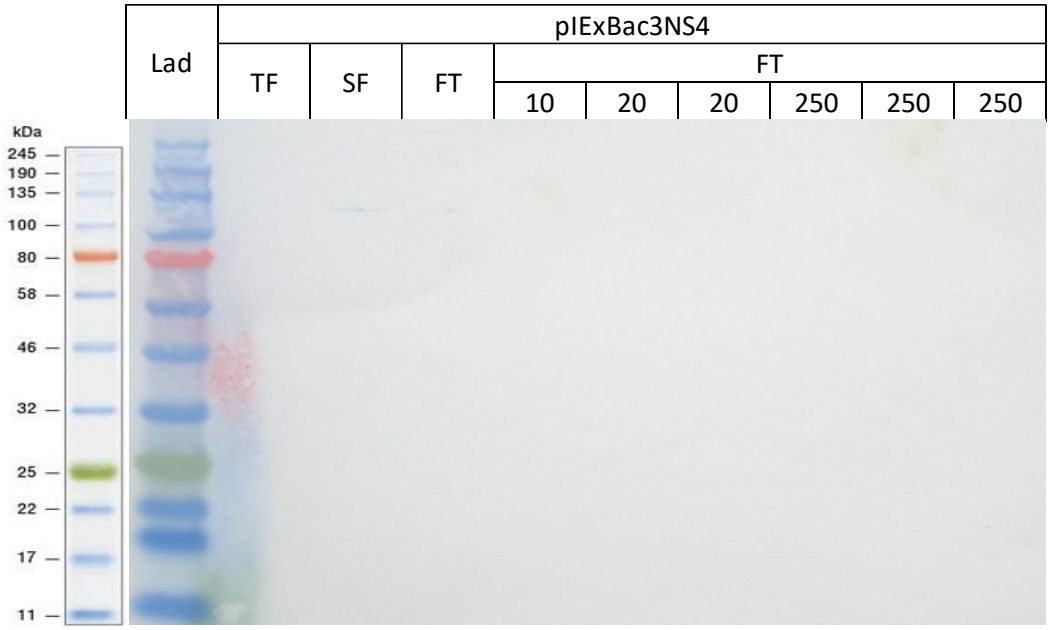

Figure 61 Western Blot of HISTag purification products from pIExBac3 NS4 Rc Virus expression. Western blot used NuPage 4-12% Bis-Tris gels transferred to 0.45µm Nitrocellulose membrane. Primary antibody mouse mAb Anti-NS4 at 1:1000 dilution, secondary antibody rabbit pAb-Anti-mouse IgG (HRP) used at 1:3000, substrate TMB Ultra. Image taken with digital camera. Loading order: Lad = Protein size ladder; TF = Total Fraction, SF = Soluble Fraction, FT = Full Transfer, 10 = 10 mM imidazole wash, 20 = 2 X 20 mM imidazole washes, 250 = 3 X 250mM imidazole elutions. Completely clear image suggests no expression of NS4 protein occurred.

Results of the western blot can be seen in Figure 61. The image is blank, showing no evidence of NS4 protein production. The image was so clean, even in the total fraction, that it is possible the western blot did not work, not because no NS4 protein was produced. Therefore, a repeat western blot was performed, but this time using an anti-6X His mouse monoclonal antibody. This monoclonal antibody should bind to any Histag present at the N termini of the NS4 protein. A positive control was included in this western blot, the total and soluble fractions from the protein

expression using pIExBac3Core, see Figure 44. This protein includes the same 10X Histag at the N' termini as any expressed NS4 protein should contain.

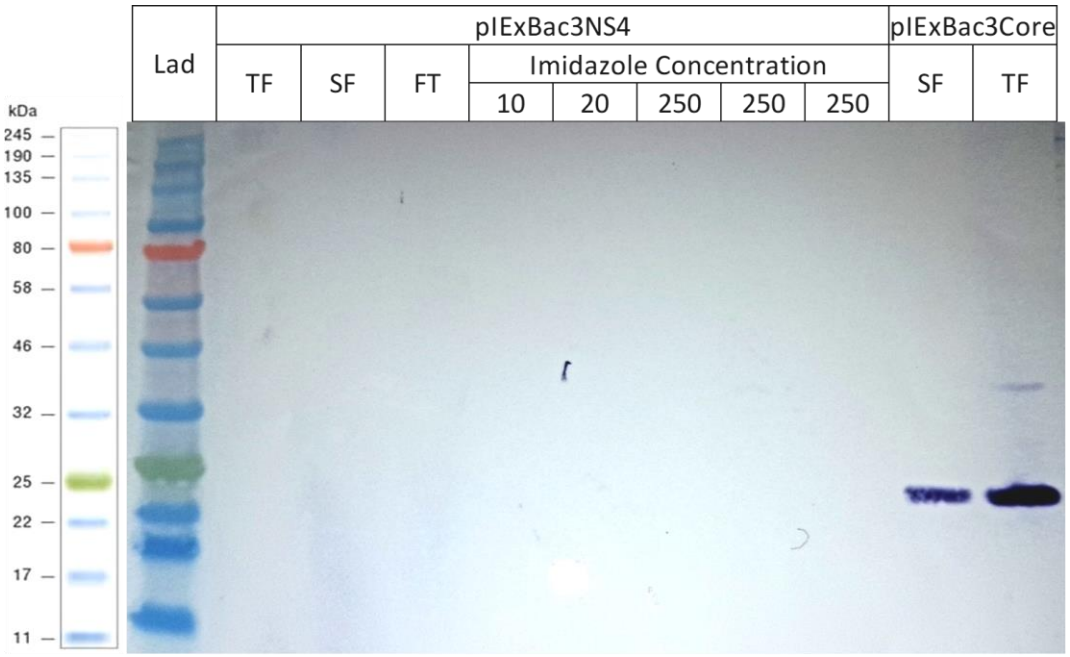

Figure 62 Western Blot of HISTag purification products from pIExBac3 NS4 Rc Virus expression with Anti-HIS mAb. Western blot used NuPage 4-12% Bis-Tris gels transferred to 0.45µm Nitrocellulose membrane. Primary antibody mouse mAb Anti-HIS(6X) at 1:1000 dilution, secondary antibody rabbit pAb-Anti-mouse IgG (HRP) used at 1:3000, substrate TMB Ultra. Image taken with digital camera. Loading order: Lad = Protein size ladder; TF = Total Fraction, SF = Soluble Fraction, FT = Full Transfer, 10 = 10 mM imidazole wash, 20 = 2 X 20 mM imidazole washes, 250 = 3 X 250mM imidazole elutions, final two lanes are soluble and total fractions from previous pOET1Core expressions added as positive control. Strong bands at 25 kDa in core positive control bands show Anti-HIS western blot worked, complete lack of any bands in the pIExBac3NS4 lanes confirm that no NS4 protein was expressed.

The results of the western blot using the anti-6XHis mAb are shown in Figure 62. The presence of strong bands on both the core total and soluble fractions at the expected size prove the anti-His western blot worked and should also pick up any expressed NS4 protein if present. As there was no band in any the lanes from the NS4 protein purification, no protein expression occurred with the pIExBac3NS4 Rcvirus.

It is possible the lack of protein expression could be due to a mutation in the Rcvirus, in the promoter site or NS4 sequence. To check this, a PCR of the recombinant virus was performed using the primers IEFP and ST24RP used for sequencing of the plasmids, see Table 12. The PCR amplification was performed on nucleic extracts of the Rcvirus as described in section 11.4.6.3. Nucleotide sequencing of the PCR amplicons showed the NS4 sequence still in-frame with the promoter and Histag, and with no obvious mutations which would prevent protein expression. It was possible the mutation occurred outside of the area amplified by PCR. To help rule this out it was decided to repeat the entire protein expression experiment, from generation of Rcvirus to protein expression opimisation. This time

pIEXBac3NS4pp3 was used for generation of Rc virus, with *flash*BAC™ ULTRA bacmid. The virus was amplified to a level of 2.75 X 10^7 pfu/mL. The same protein expression optimisation experiment was performed using multiple MOI ranging from 1-20, but subsequent SDS page analysis showed no obvious NS4 protein production. It was then decided to try an alternative approach to producing the NS4 protein in baculovirus.

12.1.7.4 NS4 EXPRESSION USING POET8 TRANSFER VECTOR

The pOET8 plasmid is a similar plasmid to the pOET1, in that it uses protein expression under a polyhedrin promoter combined with a N terminus Histag. It differs from the pOET1 plasmid with the addition of the vankyrin gene (encoding an anti-apoptotic protein) under the expression of a p10 promoter. The expressed vankyrin protein acts to inhibit lysis of the infected insect cells, in the hope of allowing more protein to be expressed and recovered from intact cells. The 2nd difference with the pOET8 plasmid is the inclusion of a melittin signal sequence at the N' terminus of the protein sequence. The encoded melittin sequence is derived from honeybees and induces secretion of any expressed protein into the media.

12.1.7.4.1 TRANSFER OF NS4 GENE FROM PIEXBAC 3 TO POET8

Transfer of the NS4 gene from the pIExBac3 transfer vector to the pOET8v2 transfer vector was achieved using a combination of PCR and conventional cloning, using the method described in 12.1.5.2 for transfer of the HCV core gene from the pIExBac3 plasmid to the pOET8v2. Section 11.4.5 outlines the procedure.

12.1.7.4.2 PCR AMPLIFICATION

The PCR was performed as described in 11.4.1.4.4. A 1:100 dilution of purified pIExBac3NS4pp2 plasmid was performed to reduce the concentration to 5.6 ng/µL. Of this 2 µL was added to the PCR mix containing the pIExPmeI and NS45954BmtI forward and reverse primers. The PCR was run with an annealing temperature of 52°C.

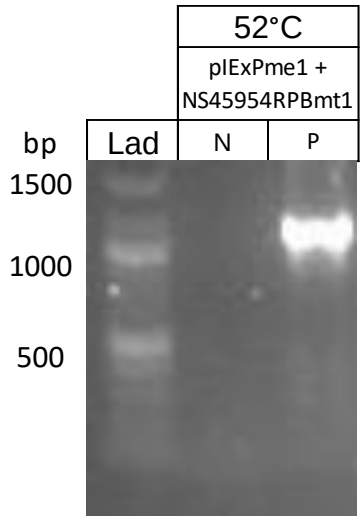

Figure 63 Gel electrophoresis for PCR Amplification of NS4 gene from pIExBac3NS4pp2 plasmid. Agarose 1% gel with 1:10000 dilution of SyBr safe DNA stain run at 100 V for 40 minutes, post electrophoresis imaged using Alphaimager 2200 imaging system under UV. Top row lists the annealing temperature, the middle row lists the forward and reverse primers used for PCR. Bottom row lists the sample loading order, N = negative control, P = pIExBac3NS4pp2 plasmid. Strong band between 1000-1500bp show the successful amplification of NS4 gene from pIExBac3NS4pp2 plasmid.

Figure 63 shows a gel image from amplification of the NS4 gene from the pIExBac3NS4pp2. The PCR successfully amplified the NS4 gene, producing a single band.

12.1.7.4.3CLONING AND TRANSFORMATION INTO POET8

The amplified NS4 PCR product was successfully cloned into the pOET8 plasmid, using the restriction enzyme cloning technique described in 11.4.5. Nucleotide sequencing of the pOET8NS4 plasmids confirmed the successful insertion of the NS4 PCR product into the pOET8 plasmid, see Figure 64 below.

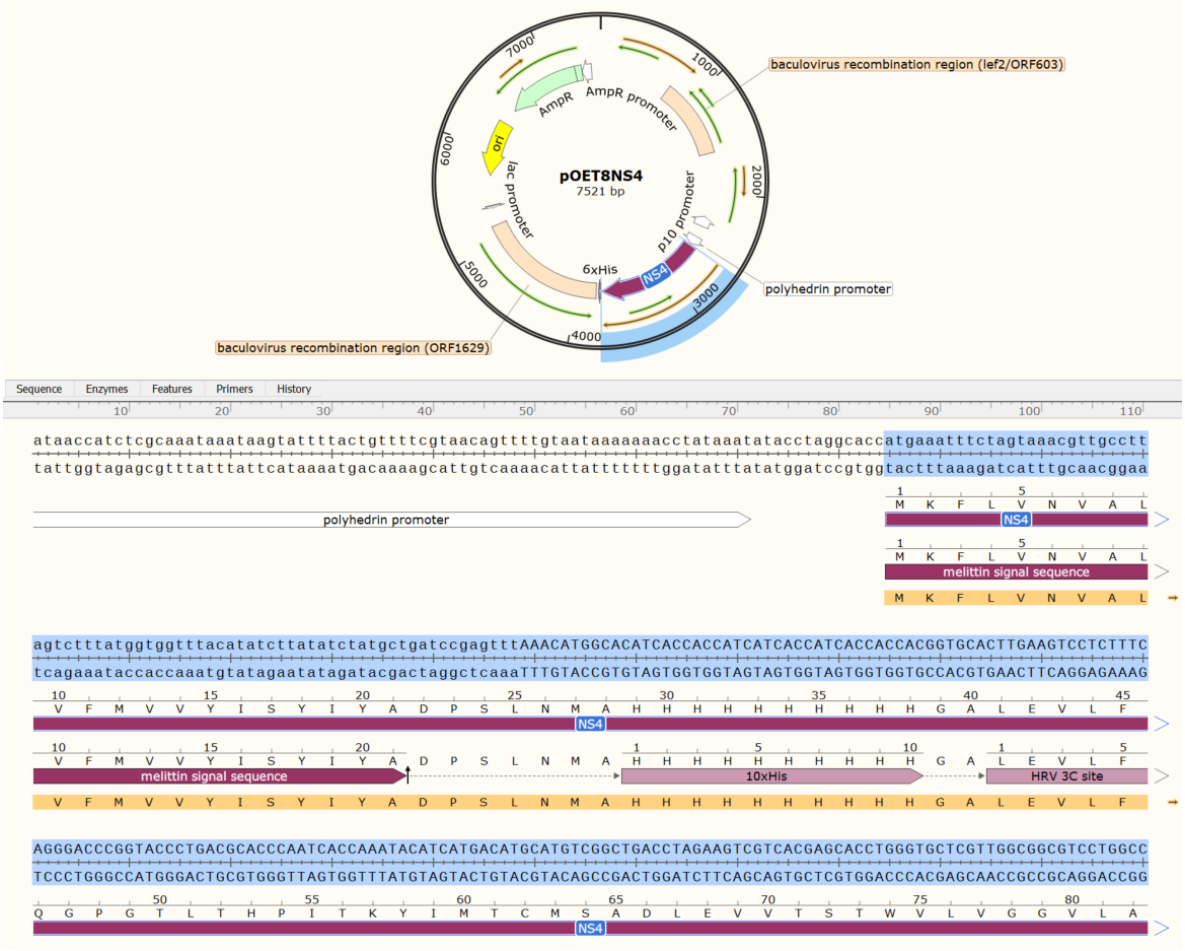

Figure 64 Plasmid map of pOET8NS4 viewed in Snapgene software. Highlighted in blue is the NS4 inserted sequence, aligned for expression under the polyhedrin promoter, and with a melittin sequence and 10XHistag incorporated at the N terminus.

The plasmid map shows the inserted NS4 sequence with the 10X Histag at the N termini, downstream and in frame with the polyhedrin promoter and melittin signal sequence.

12.1.7.4.4PROTEIN EXPRESSION OPTIMISATION POET8 NS4

Protein expression optimisation was performed in Hi5 cells as described in 11.4.6.4. Hi5 cells were infected with a MOI of 1,3,5,10 and 20.

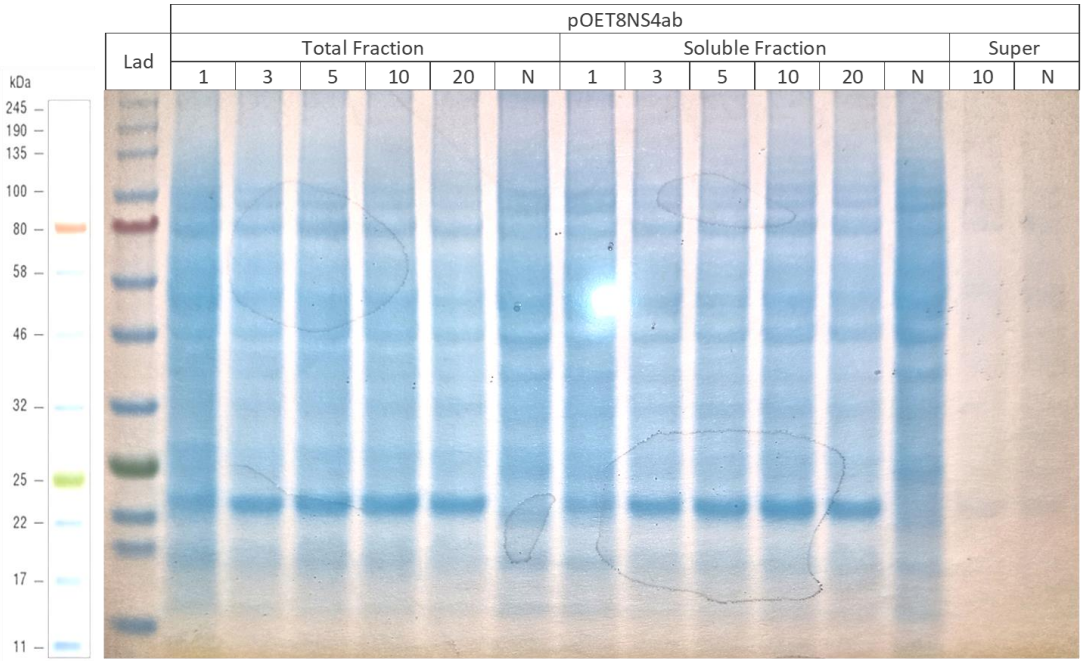

Figure 65 SDS page analysis of pOET8NS4 Rc virus expression in Hi5 cells. 4-12% Bis-Tris PAGE gel run for 200V for 35 minutes, post electrophoresis stained with InstantBlue. Image taken with digital camera. Loading order: Lane 1 = Protein size ladder; Lane 2-6 = Total Fraction from cells infected with MOI between 1-20; Lane 7 = Total fraction from non-infected cells; Lane 8-12 = Total Fraction from cells infected with MOI between 1-20; Lane 13 = Soluble Fraction from non-infected cells, Lane 14 = Supernatant media from cells infected at MOI of 10, Lane 15 = Supernatant media from non-infected cells. Gel image shows no obvious band at the expected size for the NS4 protein suggesting no expression of the protein occurred.

Figure 65 shows the protein optimisation results. There was no obvious band seen on the SDS PAGE at the expected size, in either the total fraction or soluble fraction. To check if protein expression had occurred a protein purification was performed.

The protein purification was performed as described in section 11.4.6.8. As no large scale protein expression had been performed, all the protein extracts from the 5 infected wells, 1, 3, 5, 10 and 20 MOI, were combined and purified using a small 50 µL aliquot of nickel coated beads. To reduce the loss of protein during the washing stages higher imidazole strength washes were not used. Instead washing of the beads included 2 washes with 10 mM imidazole buffer followed by 3 washes with 20 mM. The final elution stage used only 50 µL of 250 mM imidazole wash buffer. A western blot was performed on the aliquots taken from each stage, using an anti-NS4 mouse monoclonal antibody as the primary detection antibody.

The western blot using the anti-NS4b monoclonal antibody was negative, as with the previous NS4 protein expression using the pIEx vector. The image is not shown.

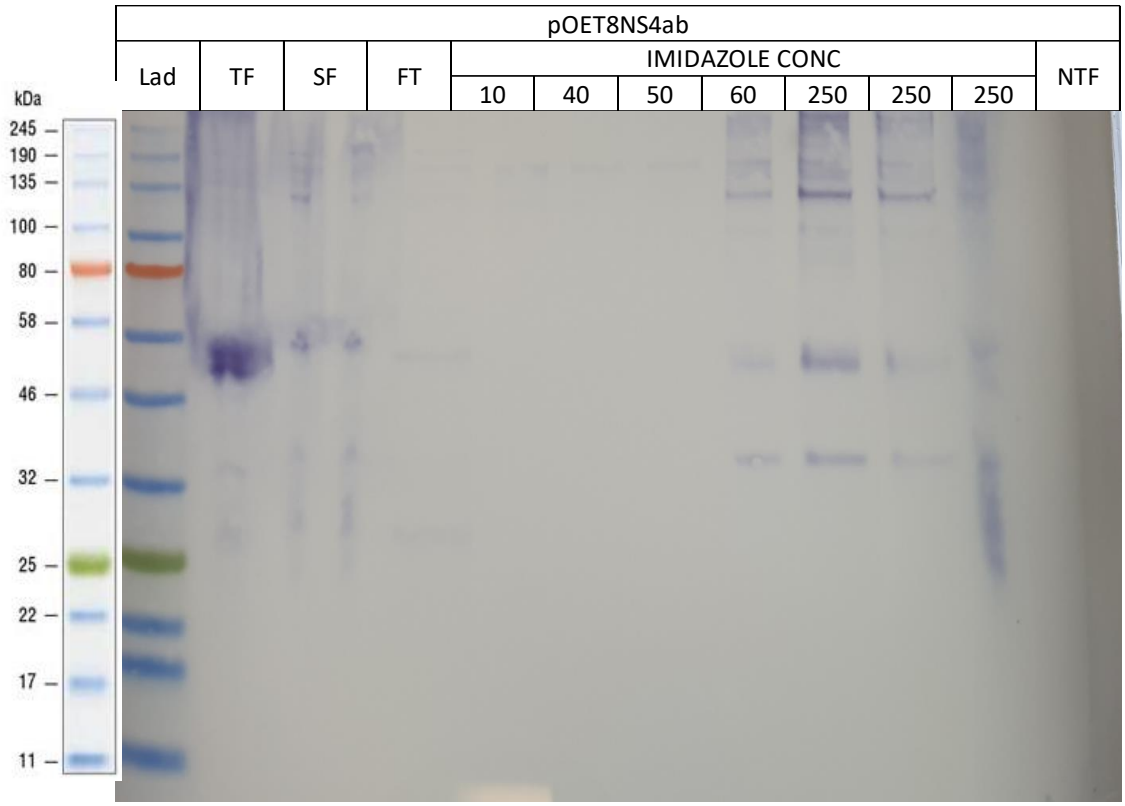

Figure 66 Western Blot of HISTag purification of pOET8NS4 Rc virus expression. Western blot used NuPage 4-12% Bis-Tris gels transferred to 0.45µm Nitrocellulose membrane. Primary antibody mouse mAb Anti-His (6X) at 1:1000 dilution, secondary antibody rabbit pAb-Anti-mouse IgG (HRP) used at 1:3000, substrate TMB Ultra. Image taken with digital camera. Loading order: Lad = Protein size ladder; TF = Total Fraction, SF = Soluble Fraction, FT = Full Transfer, 10 = 10mM Imidazole wash, 40-60 = 40-60 mM Imidazole washes, 250 = 3 X 250mM Elutions, NTF= non-infected cells total fraction. A band is visible at around 46 kDa in the total fraction, soluble fraction and in the 3 X 250mM elutions, this is bigger than the predicted size of 40.4kDa but was still thought to be the expressed NS4 protein.

The membrane was re-probed with anti-6X His monoclonal antibody, see Figure 66 above. The anti-6X His western blot does show positive bands, in the total fraction and in the eluates, slightly higher than the expected size of 40.4 kDa. Unfortunately, the image is not clear and had to be left longer than 20 minutes to develop; suggesting the amount of protein in the eluates was low. As expression did seem to have occurred a large-scale protein expression was performed.

12.1.7.4.5LARGE SCALE PROTEIN EXPRESSION POETNS4

A large scale protein expression was performed using an MOI of 10 in an 80ml Hi5 suspension culture, as described in section 11.4.6.6. To try and maximize the amount of protein expressed the culture was left for 96 hours. The vankyrin protein expressed in the pOET8 plasmid delays cell lysis in recombinant baculovirus infected cells, and thereby allows increased expression incubation periods.

After 96 hours cells were collected as described previously in section 11.4.6.7, and SDS PAGE analysis performed.

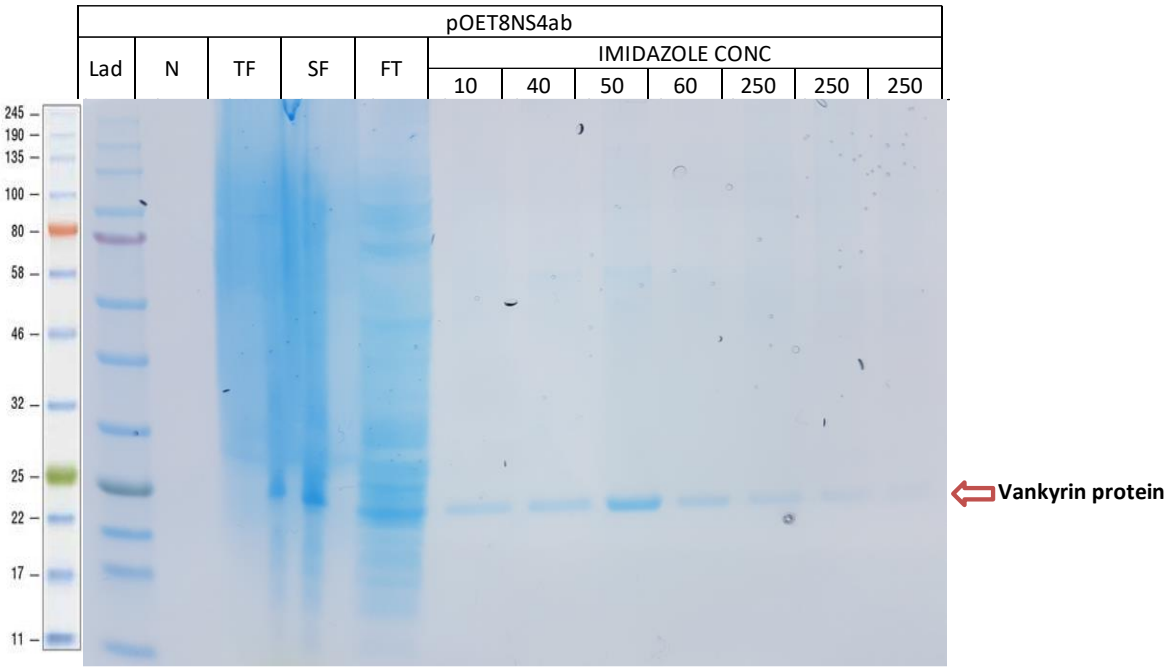

Figure 67 SDS-PAGE gel image of HISTag purification products from pOET8NS4 Rc virus expression. NuPage 4-12% Bis-Tris PAGE gel run for 200V for 35 minutes, post electrophoresis stained with InstantBlue. Image taken with digital camera. Loading order: Lad = Protein size ladder, N = non-infected cells, TF = Total Fraction, SF = Soluble Fraction, FT = Full Transfer, 10 = 10mM Imidazole wash, 40-60 = 40-60mM Imidazole washes, 250 = 3 X 250mM Imidazole Elutions. Arrow highlights strong band at 22kDa is contaminating vankyrin expression protein, expected band at around 40kDa for the NS4 protein is missing suggesting the protein was not purified through HISTag procedure possibly due to low solubility.

Figure 67 shows the image from the SDS page analysis of pOET8NS4 purification. The image is smeared in both the total and soluble fractions. In the eluates there is no protein around the expected size of 40.4 kDa. It is possible the protein is only in the eluate in a very low amount and was not detected using SDS page analysis. This could be due to either a low level of protein expression or the protein had poor solubility leading to poor purification.

The only band which can be seen in the eluates is a band between 22 and 25 kDa. It is likely this protein is the vankyrin protein, included in the plasmid to prevent the cells from lysing and thereby increase the expression of protein. The predicted size of the vankyrin protein is 19.9kDa, similar to the size of the band seen on the image above. The vankyrin protein is expressed under the control of a p10 promoter, a very strong late baculovirus promoter. As a result, the vankyrin protein is expressed at a high level. However, the vankyrin protein is expressed without a HIS Tag, so should not be purified through the nickel purification process. The SDS page analysis shows this was not the case, and there must have been non-specific binding of the vankyrin protein to the nickel beads, possibly due to the high level of protein present.

To try and resolve these issues a denaturing solubilisation and purification of the NS4 protein was attempted. This used a urea based solubilisation of the cell pellet, followed by purification under hybrid conditions as described in section 11.4.6.9.3.

12.1.7.4.6NS4 SOLUBILISATION AND PURIFICATION

The urea solubilisation was performed on the insoluble cell pellet produced during the previous cell lysis and purification of the pOET8NS4 protein. The insoluble cell pellet was solubilised using 8M urea lysis buffer, as described in 11.4.6.9.2. This was followed by purification under hybrid conditions as described in 11.4.6.9.3.

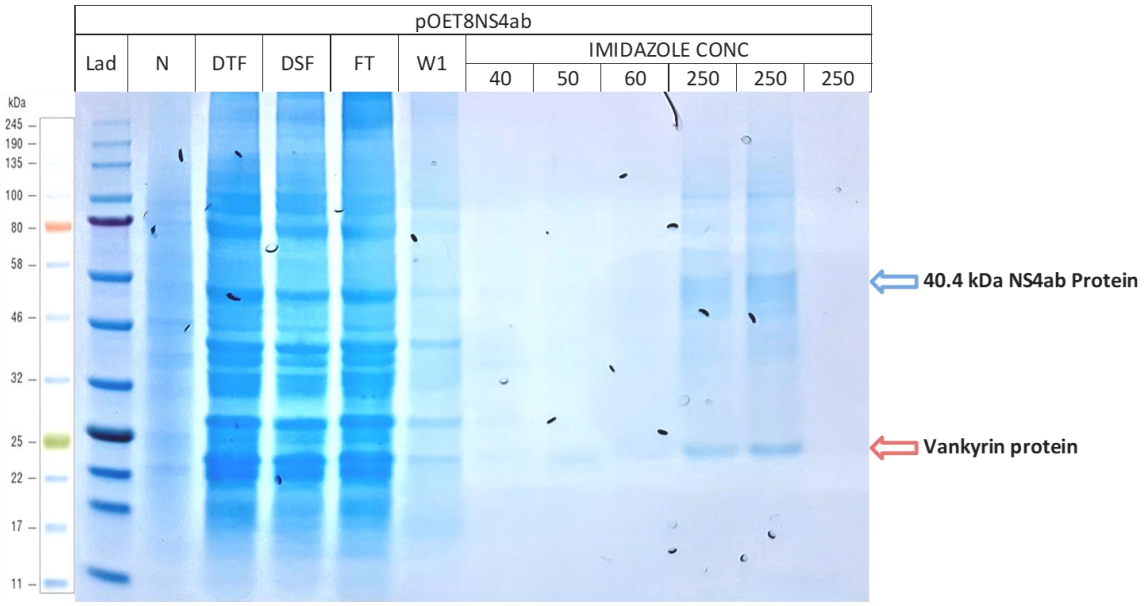

Figure 68 SDS-PAGE gel image of HISTag purification products under hybrid denaturing conditions from pOET8NS4 Rc virus expression. NuPage 4-12% Bis-Tris PAGE gel run for 200V for 35 minutes, post electrophoresis stained with InstantBlue. Image taken with digital camera. Loading order: Lad = Protein size ladder, N = non-infected cells, DTF = Urea Denatured Total Fraction, SF = Urea Denatured Soluble Fraction, FT = Full Transfer, 40-60 = 40-60mM Imidazole washes, 250 = 3 X 250mM Imidazole Elutions. Arrow highlights strong band at 22kDa is contaminating vankyrin expression protein plus band around 46kDa thought to be NS4 protein.

The result of the urea solubilisation and purification under hybrid conditions can be seen in Figure 68 above. A band can be seen in the first two 250 mM eluates between the 46 – 58 kDa markers. This is larger than the predicted 40.4 kDa size for the NS4 protein but could be due to post translational modifications produced by the Hi5 cells. There is a second clear band in the 250 mM elutes which can be seen between 22-25 kDa. This is the same band seen previously in Figure 67. This is most likely the vankyrin protein, non-specifically binding to the nickel beads. The washing steps included higher strength imidazole, up to 60 mM, in an attempt to remove this contaminating protein but this did not prove enough to remove it all. A western blot was performed to confirm the expression of the NS4 protein.

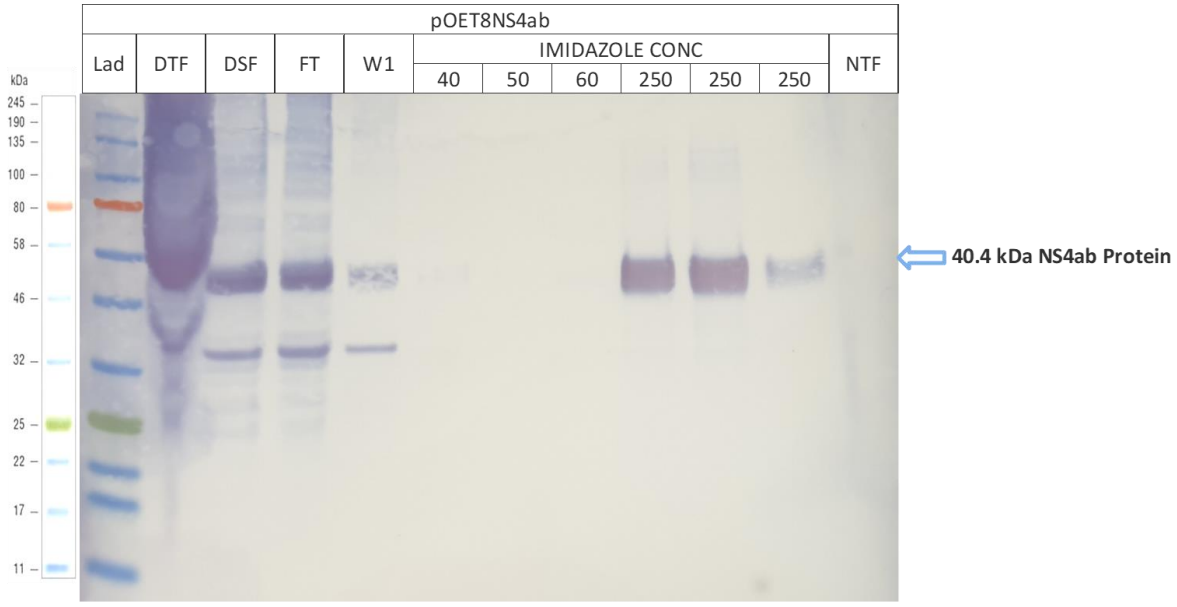

Figure 69 Western Blot of HISTag purification products under hybrid denaturing conditions from pOET8NS4 Rc Virus expression. Western blot used NuPage 4-12% Bis-Tris gels transferred to 0.45µm Nitrocellulose membrane. Primary antibody mouse mAb Anti-His (6X) at 1:1000 dilution, secondary antibody rabbit pAb-Anti-mouse IgG (HRP) used at 1:3000, substrate TMB Ultra. Image taken with digital camera. Loading order: Lad = Protein size ladder, DTF = Urea denatured total fraction, DSF = Urea denatured soluble fraction, 40-60 = 40-50mM imidazole washes, 250 = 3 X 250mM imidazole elutions, NTF=Non-infected cells total fraction. Image clearly shows strong band in all 3 X 250mM elutions confirming the expression and purification of NS4 protein under hybrid denaturing conditions.

Figure 69 shows the western blot analysis of the pOET8NS4ab protein purified under hybrid denaturing conditions. There is a strong band in the total fraction, soluble fraction, full transfer and in each of the 250 mM elutions. This is the same size as the suspected NS4ab protein band seen with SDS PAGE analysis. This suggests purification of the His tagged NS4ab protein, under hybrid denaturing conditions. The band seen between 22-25 kDa with SDS PAGE analysis, the suspected vankyrin protein, does not appear on the western blot image. The contaminating protein is not His tagged but is binding to the nickel beads non-specifically.

12.1.8 NS5 EXPRESSION

The HCV NS5 is made up of two proteins, NS5a and NS5b, both strongly involved in the replication of the HCV genome. The NS5a protein is a membrane associated RNA binding protein, the NS5b is an RNA dependent RNA polymerase. The aim was to express both the NS5a and NS5b proteins as 2 separate proteins, using the pOET1 transfer vector and *flash*BAC™ ULTRA expression system.

12.1.8.1.1PCR AMPLIFICATION

Primers were designed for amplification of the NS5a and NS5b genes and for transfer into the pOET1 plasmid as described in 11.4.1.1.2. The amplification of NS5a and NS5b targets followed the same method used for amplifying other protein targets from HCV positive sera, see section 11.4.1.4.3.

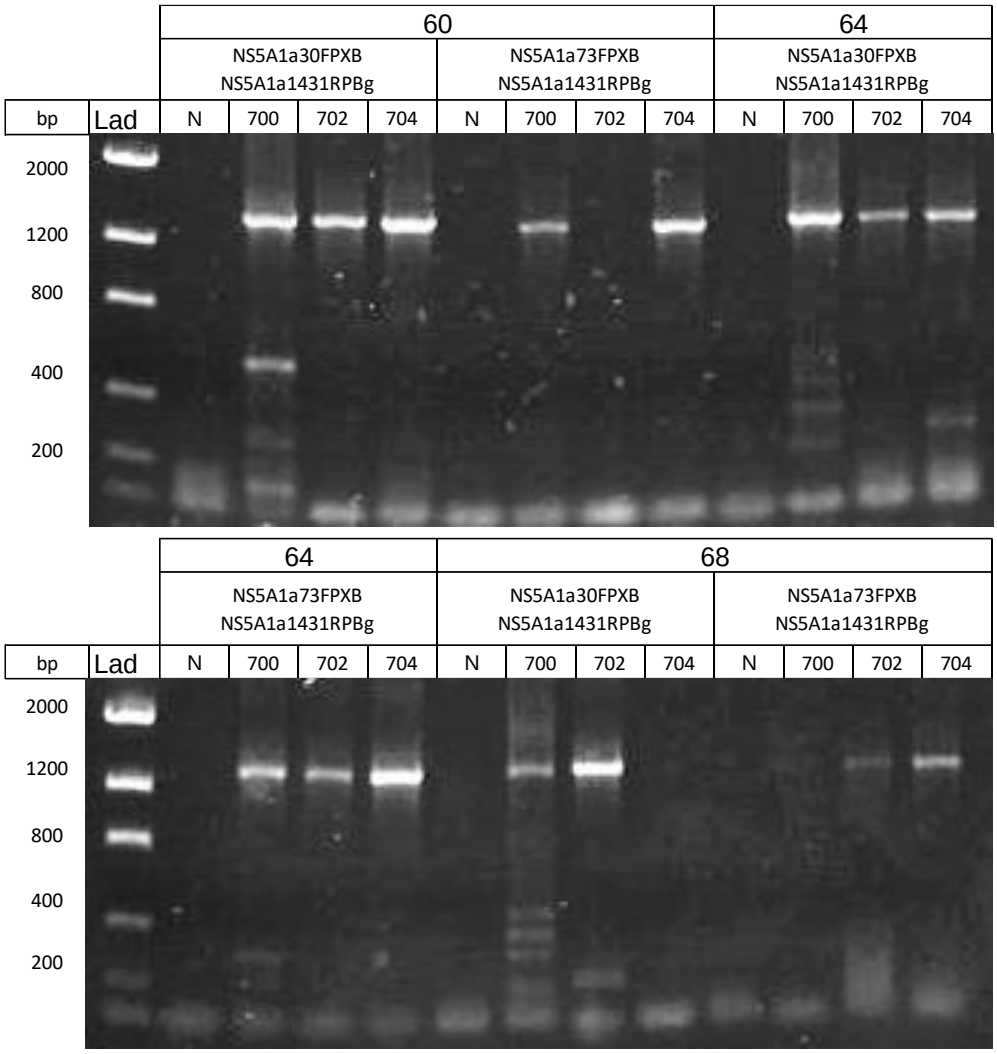

Figure 70 Gel electrophoresis image for PCR amplification of NS5a gene. Agarose 1% gel with 1:10000 dilution of SyBr safe DNA stain run at 100 V for 40 minutes. Top row lists the annealing temperature, the middle row lists the forward and reverse primers used for PCR, post electrophoresis imaged using Alphaimager 2200 imaging system under UV. Bottom row lists the sample loading order, N = negative control, 700, 702, 704 = study samples. Gel image shows band at the predicted amplicon size in multiple samples using the 3 primer combinations and annealing temperatures.

Figure 70 shows the gel images of NS5a PCR. A previous optimisation used primer sets at annealing temperatures ranging from 54°C to 62°C for 6 samples (not shown). Lower annealing temperatures showed multiple bands suggesting non-specific binding of the primers. The image shown in Figure 70 is the 2nd PCR, used 3 annealing temperatures, 60-68°C, and 3 samples (Samples 700,702 and

704). Sample 704, amplified with primers NS5a30FPXb and 1431RPBg, was used for subsequent cloning into pOET1 plasmid.

Amplification of the NS5b gene target proved more difficult. The size of the amplicons produced by the various primer combinations were around 1800 bp. Despite trialing multiple annealing temperatures ranging from 50°C to 60°C, with 6 different samples, a band of the predicted size could not be produced. It is possible the restriction enzyme primer extensions prevented the primers from working optimally. To try and overcome this issue a nested PCR was performed with standard outer primers for the first round, 702FP and NS53157RP, followed by a 2nd round using the restriction enzyme primers. Various combinations of primers were trialed in the 2nd round, and multiple annealing temperatures were used for both the 1st and 2nd round.

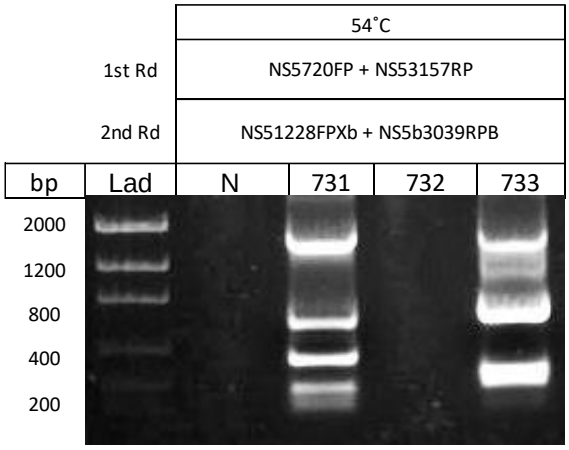

Figure 71 Gel electrophoresis image of nested NS5b PCR. Agarose 1% gel with 1:10000 dilution of SyBr safe DNA stain run at 100 V for 40 minutes, post electrophoresis imaged using Alphaimager 2200 imaging system under UV. Top row lists the annealing temperature, the middle rows list the forward and reverse primers used for 1st and 2nd round nested PCR. Bottom row lists the sample loading order, N = negative control, 731-733 = study samples. Gel image shows bands of the expected size below the 2000bp marker but there are multiple bands below this showing non-specific amplification.

Figure 71 shows the best results achieved for PCR of the NS5b gene. There were multiple non-specific bands, however, the top band represents the expected size for that primer combination. Using the gel extraction technique described in section 11.4.5.1.2, the top band was excised from the gel with a scalpel, leaving the other non-specific PCR products behind. The excised fragment was then purified using the Monarch gel extraction purification kit.

12.1.8.1.2CLONING IN POET1

Both the NS5a and NS5b products were cloned into the pOET1 plasmid transfer vector using conventional cloning techniques, described in 11.4.5.

Plasmid Prep No.	Name	Conc. µg/µl	Total Vol.	Amt µg	Confirmed Sequence
1	pOET1NS5app1	0.466	30	13.98	Yes
2	pOET1NS5app2	0.493	30	14.79	Yes
3	pOET1NS5app3	0.523	30	15.69	No

Table 20 Concentration of pOETNS5a plasmids 1-3 DNA post purification in µg/µl. Determined by nanophotometer and confirmed by sanger nucleotide sequencing.

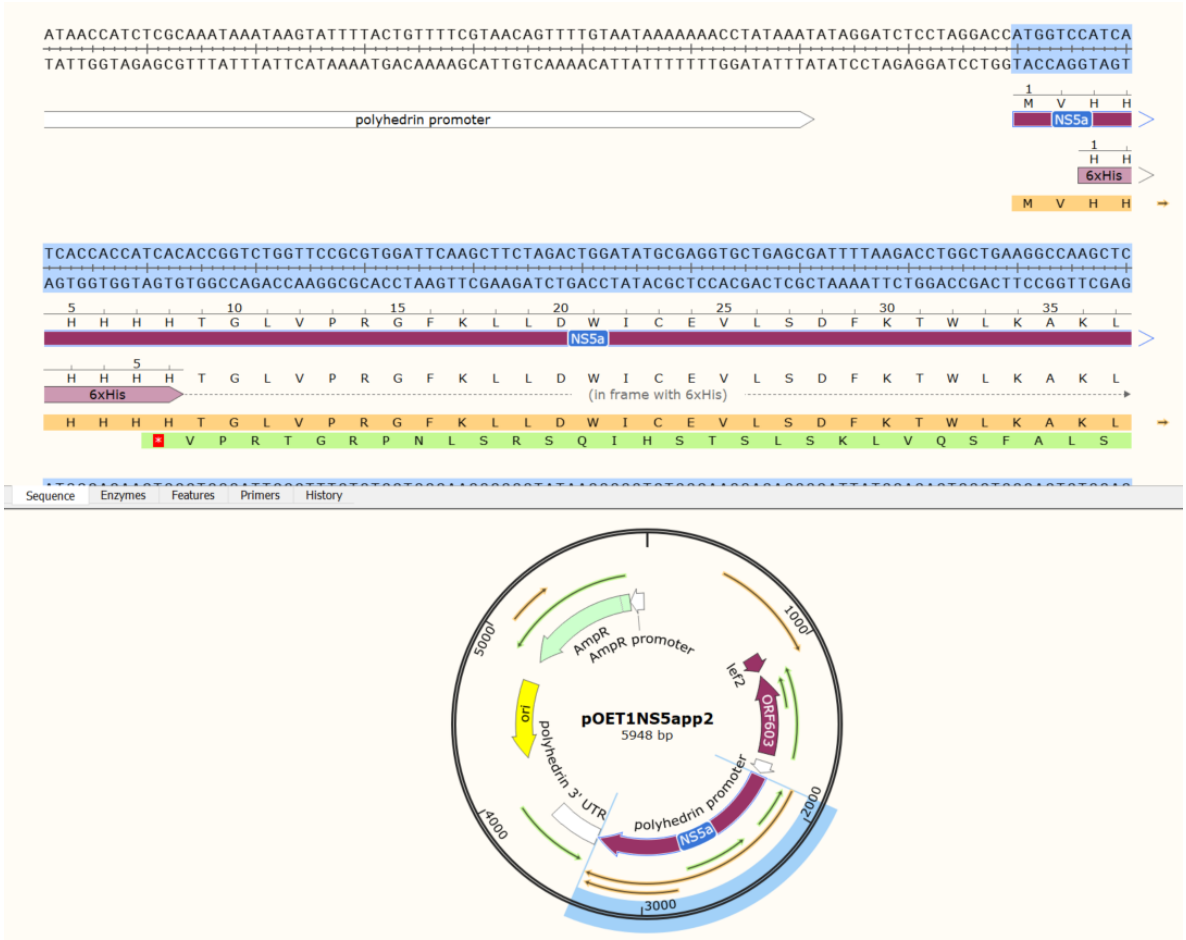

Figure 72 Plasmid map of pOET1NS5a viewed in Snapgene software. Highlighted in blue is the NS5a inserted sequence, aligned for expression under the polyhedrin promoter, and with a 6XHistag incorporated at the N terminus.

Of the pOET1NS5a plasmid preparations, 2 were confirmed by nucleotide sequencing to contain the NS5a sequence. Figure 72 shows plasmid preparation 2, with the NS5a sequence inserted downstream of the polyhedrin promoter and 6X His tag. This plasmid was used for further protein expression experiments.

Cloning of the amplified NS5b PCR amplicon was less successful. Despite multiple attempts to clone the PCR product into the pOET1 plasmid, none were successful. The restriction enzyme cut times were increased to 2 hours, different proportions of insert to vector were attempted (1:3, 1:4 and 1:5) and up to 6 plasmids were purified and sequenced to increase the chances of successful cloning.

None of these attempts worked. Of the cloning and transformations which did produce colonies after overnight growth on selective ampicillin agar, nucleotide sequencing showed none of them contained the NS5b insert. The NS5b PCR amplicon was sequenced and confirmed the excised band from the gel was correct sequence, but despite this successful cloning could not be achieved. To overcome this, it was decided to purchase the NS5b gene as a synthetic plasmid from Eurofins, cloned into the pOET1 plasmid.

12.1.8.1.3DESIGN OF SYNTHETIC NS5B POET1 PLASMID

As designing the plasmid to be produced synthetically removed the restrictions of finding suitable primer binding sites, the entire NS5b gene sequence was purchased and cloned into the pOET1 plasmid by Eurofins as described in 11.4.5.5 The sequence was an HCV genotype 1a strain, selected as the most representative from a HCV NS5b sequence alignment.

12.1.8.1.4PROTEIN EXPRESSION OF NS5A AND NS5B

Protein expression of both NS5a and NS5b protein using the *flash*BAC™ ULTRAsystem followed the same procedure as decribed for the other HCV proteins above. The pOET1NS5app2 plasmid was used as the transfer vector for NS5a, and pOET1NS5bSyn plasmid as the transfer vector for NS5b.Transfected Sf9 cells showed the same CPE as shown previously in Figure 40. After a week of virus amplification, Sf9 cells showed a high level CPE suggesting virus amplification had been succesful. The quantity of the Rc virus was determined by QPCR. The pOET1NS5a Rc virus had a level of 1.57×10^8 pfu/mL. The pOET1NS5b Rc virus had a level of 4.79×10^7 pfu/mL.

A protein opimisation experiment was then performed in Hi5 cells, as described in 11.4.6.4, infecting cells with an MOI of 1, 3, 5, 10 and 20 for 72 hours. A mock infected control well was included alongside the 5 infected wells.

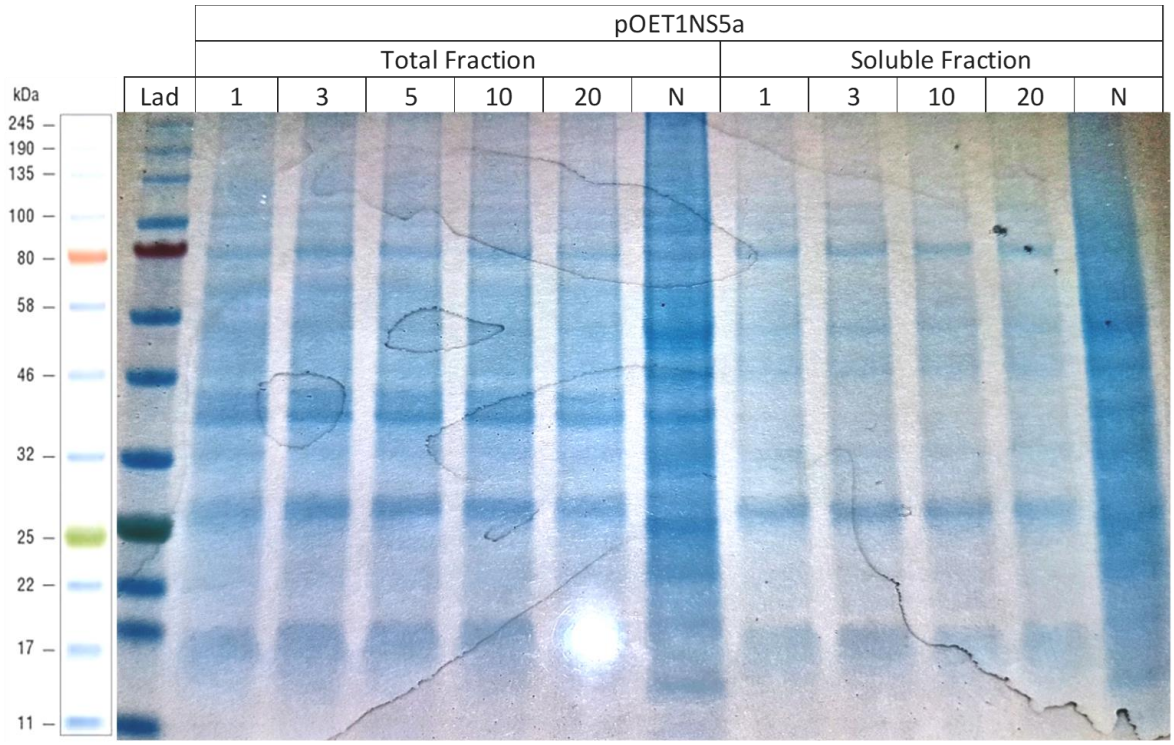

Figure 73 SDS Page Gel of 72 Hour pOET1NS5a Rc virus expression in Hi5 cells. NuPage 4-12% Bis-Tris PAGE gel run for 200V for 35 minutes, post electrophoresis stained with InstantBlue. Image taken with digital camera. Loading order: Lane 1 = Protein size ladder, Lane 2-6 = Total fraction from cells infected with MOI of 1-20, Lane 7 = Total fraction from non-infected cells, Lane 8-11 = Soluble fraction from cells infected with MOI of 1-20, Lane 12 = Soluble Fraction from non-infected cells. There is no obvious band of the expected 53.5 kDa NS5a protein size in any of the total and soluble fractions suggesting little or no protein expression had occurred.

Figure 73 shows the results of the pOET1NS5a expression in Hi5 cells. Note the 5 MOI is missing from the soluble fraction as there were insufficient wells in the SDS gel used. As there was no obvious expression of the NS5a this did not prove to be an issue. The predicted size of the expressed NS5a protein is 53.5 kDa. There was no obvious band at this size in either the total or soluble fractions, suggesting no or only low-level protein expression occurred. This was despite the Hi5 cells showing a high level of infection at all MOIs.

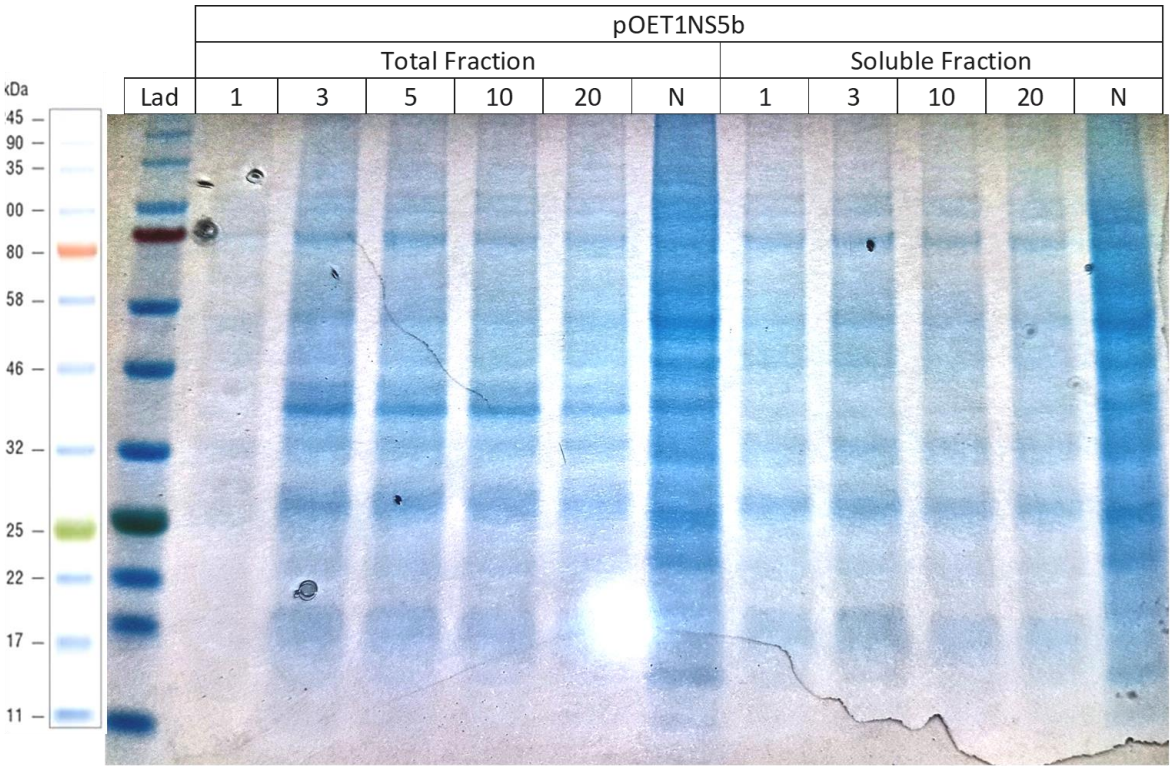

Figure 74 SDS Page Gel of 72 Hour pOET1NS5b Rc virus expression in Hi5 cells. NuPage 4-12% Bis-Tris PAGE gel run for 200V for 35 minutes, post electrophoresis stained with InstantBlue. Image taken with digital camera Loading order: Lane 1 = Protein size ladder, Lane 2-6 = Total fraction from cells infected with MOI of 1-20, Lane 7 = Total fraction from non-infected cells, Lane 8-11 = Soluble fraction from cells infected with MOI of 1-20, Lane 12 = Soluble fraction from non-infected cells. There is no obvious band of the expected 67.4 kDa NS5b protein size in any of the total and soluble fractions suggesting little or no protein expression had occurred.

Figure 74 shows the results of the pOET1NS5b expression in Hi5 cells at various MOI. Again the 5 MOI is missing from the soluble fraction as there were insufficient wells in the SDS gel used. As with the NS5a above, there was no obvious expression of the NS5b protein. The predicted size of the protein was 67.4kDa. There are no bands in either the total or soluble fraction at this size, suggesting no or very low amounts of protein were produced.

Both the pOET1NS5a and pOET1NS5b optimisation experiments were repeated and run for 96 hours. The SDS page analysis showed no obvious expression; they are not shown here as they showed the same pattern of results as seen above. Despite trialing multiple MOI for both 72 and 96 hours, no obvious expression of the NS5a or NS5b protein has been achieved using the pOET1 transfer vector. It was decided to attempt to overcome this issue by using the pOET8v2 transfer vector.

12.1.8.2 NS5 EXPRESSION USING POET8 TRANSFER VECTOR

12.1.8.2.1CLONING INTO POET8 TRANSFER VECTOR

Cloning both the NS5a and NS5b genes followed the same protocol as described for the NS4 above. Primers were designed for amplification of the respective genes from the pOET1 plasmid as described in 11.4.1.1.2., and PCR amplification performed as described in 11.4.1.4.4.

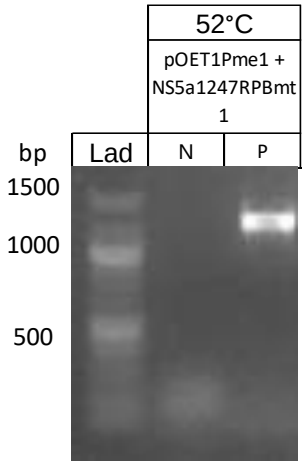

Figure 75 Gel electrophoresis image of NS5a PCR from pOET1NS5app2. Agarose 1% gel with 1:10000 dilution of SyBr safe DNA stain run at 100 V for 40 minutes, post electrophoresis imaged using Alphaimager 2200 imaging system under UV. Top row lists the annealing temperature, the middle row lists the forward and reverse primers used for PCR. Bottom row lists the sample loading order, N = negative control, P = 1:100 dilution of pOET1NS5app2 plasmid. Band at the expected size of 1250bp shows successful amplification of the NS5a gene from the pOET1NS5a plasmid.

Figure 75 shows the gel electrophoresis image for the PCR of the NS5a gene from the pOET1NS5app2 plasmid. The PCR was as described in section 11.4.1.4.4, with an annealing temperature of 52°C, and a 1:100 dilution of the pOET1NS5app2 plasmid giving a final concentration of 4.6ng/µL. The PCR was a success, with a bright band produced at the expected size.

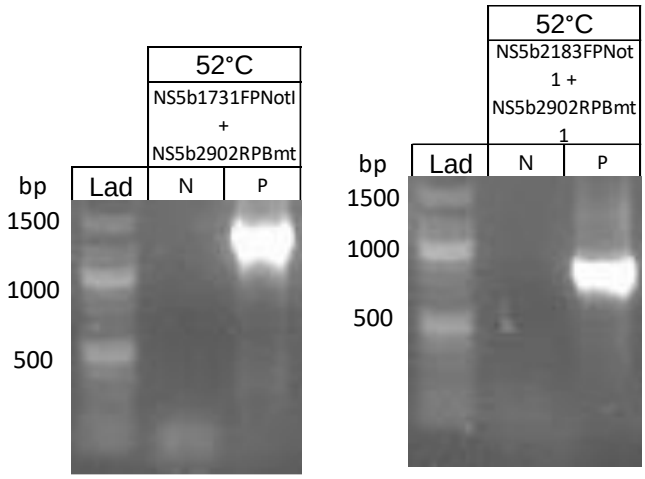

Figure 76 Gel electrophoresis images for NS5b PCR from pOET1NS5b plasmid. Agarose 1% gel with 1:10000 dilution of SyBr safe DNA stain run at 100 V for 40 minutes, post electrophoresis imaged using Alphaimager 2200 imaging system under UV. Left image is from PCR amplifying full NS5b gene, right image is from PCR amplifying smaller segment of NS5b gene. Top row lists the annealing temperature, the middle row lists the forward and reverse primers used for PCR. Bottom row lists the sample loading order, N = negative control, P = 1:100 dilution of pOET1NS5b plasmid. The left image shows successful amplification of the full NS5b gene, the right side shows successful amplification of a shortened region of the NS5b gene.

As shown in Figure 76 the NS5b was successfully amplified with both the longer and shorter PCR primer sets, both producing strong bands.

Both the NS5a and NS5b PCR products were cloned into pOET8v2 plasmid as described in section 11.4.5. Nucleotide sequencing was used to confirm the correct insertion of NS5a PCR amplicon into the pOET8 plasmid. Figure 77 shows the plasmid map for the pOET8NS5app1 plasmid, with the NS5a sequence successfully inserted downstream of the polyhedrin promoter, and the 6X Histag sequence.

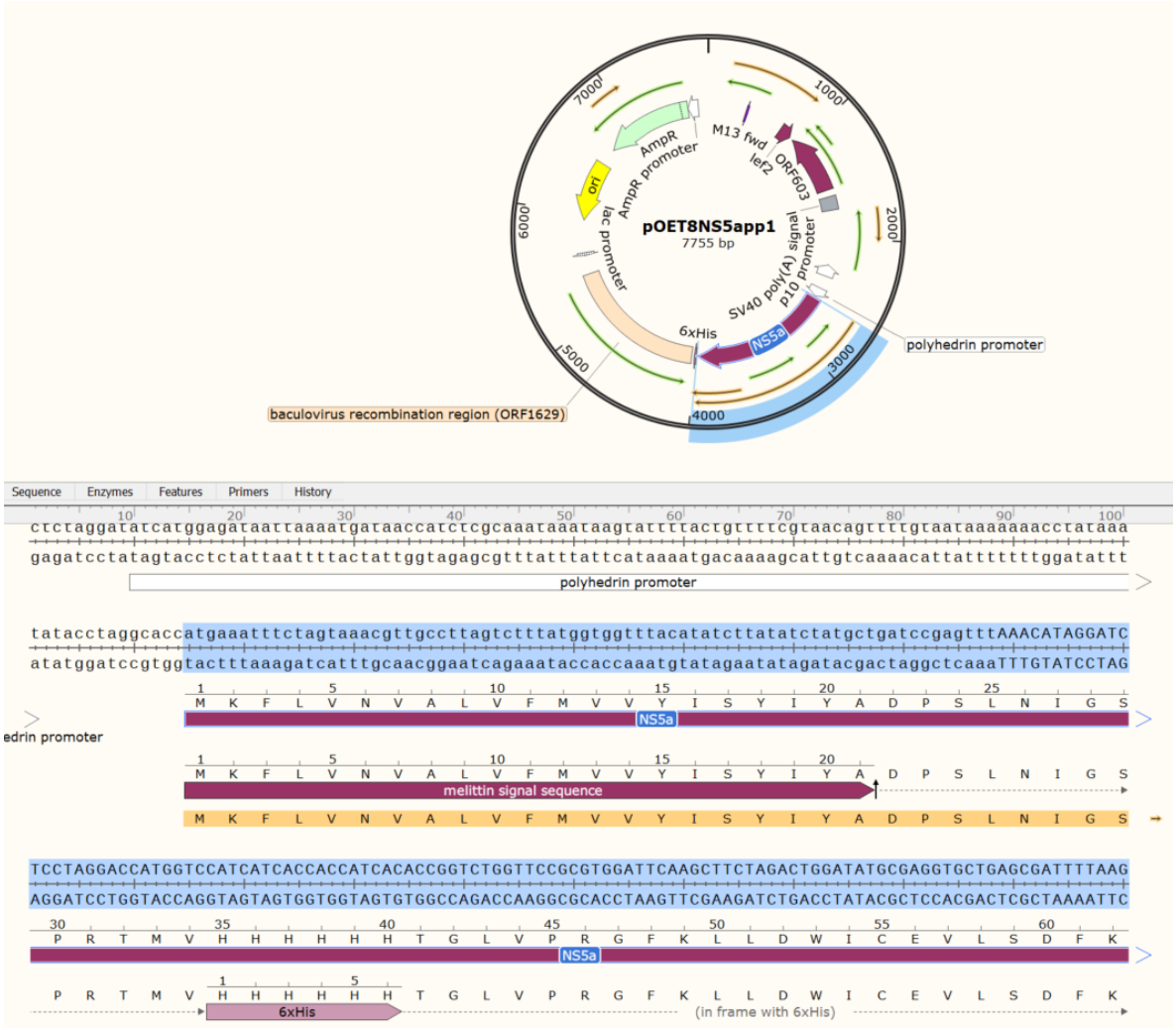

Figure 77 Plasmid map of pOET8NS5a viewed in Snapgene software. Highlighted in blue is the NS5a inserted sequence, aligned for expression under the polyhedrin promoter, and with a melittin sequence and 10XHistag incorporated at the N terminus.

Cloning of the NS5b inserts into the pOET8 plasmid proved more difficult. The shorter NS5b PCR amplicon, from the primer combination NS5b2183FP and NS5b2902RP, was successfully cloned into the pOET8 plasmid. This was confirmed by nucleotide sequencing. The plasmid map is shown in Figure 78.

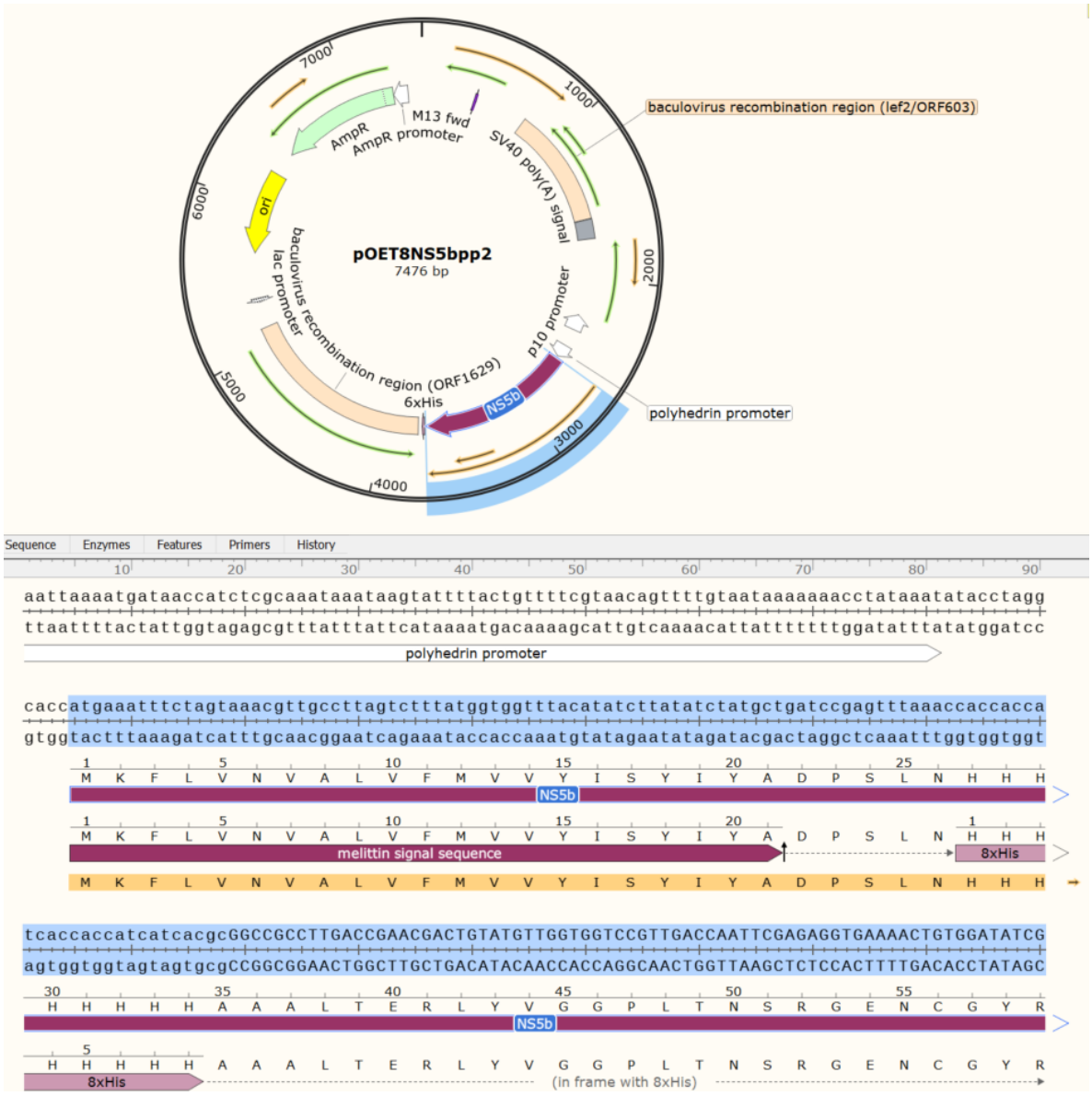

Figure 78 Plasmid map of pOET8NS5b viewed in Snapgene software. Highlighted in blue is the NS5b inserted sequence, aligned for expression under the polyhedrin promoter, and with a melittin sequence and 10XHistag incorporated at the N terminus.

The 2nd larger NS5b PCR product, from the primer combination NS5b1731FP and 2902RP, did not clone successfully into the pOET8 plasmid. The exact reason for this was not identified. Only a few colonies were grown after overnight culture on selective agar, and sequencing of these showed no insertion of the NS5b PCR amplicon.

12.1.8.2.2TRANSFECTION AND GENERATION OF RC VIRUS

The pOET8NS5a and pOET8NS5b1 were used for generation of recombinant baculovirus as described in 11.4.6.1. After a week's amplification QPCR was run as described in section 11.4.6.3. The Rc pOET8NS5a virus and the Rc pOET8NS5b1 virus had both reached a level of 7.43 X 10^7 pfu/mL.

12.1.8.2.3PROTEIN EXPRESSION OPTIMISATION POET8 NS5A AND NS5B

Protein expression optimisation was performed for both the pOET8 NS5a and NS5b, using an MOI of 1,3,5 and 10, in Hi5 cells as described previously in section 11.4.6.4.

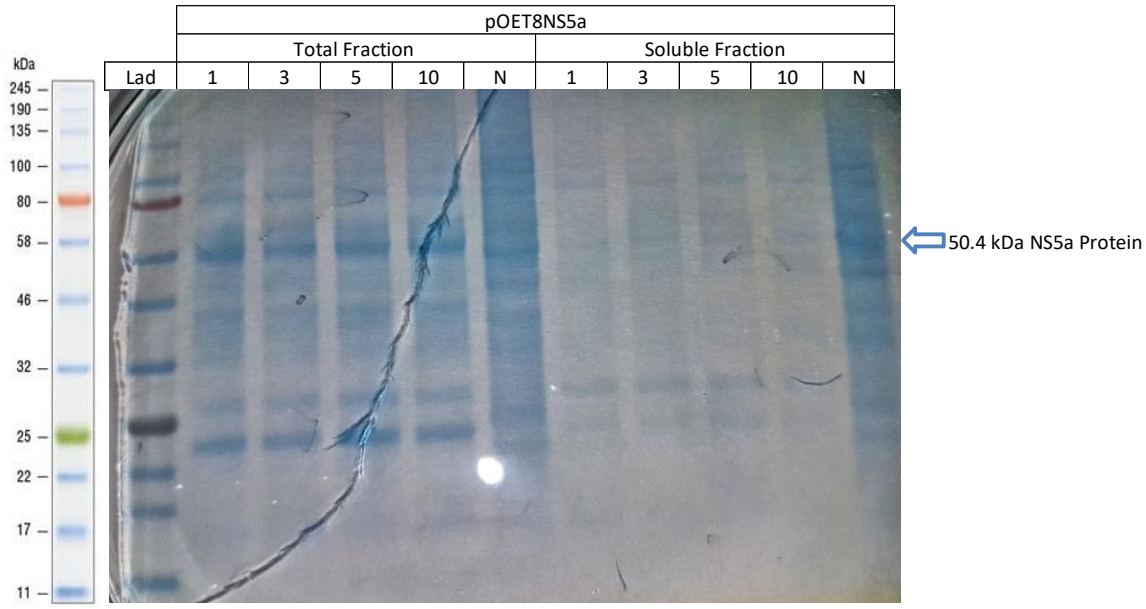

Figure 79 SDS Page Gel of 96 Hour pOET8NS5a Rc virus expression in Hi5 cells. NuPage 4-12% Bis-Tris PAGE gel run for 200V for 35 minutes, post electrophoresis stained with InstantBlue. Image taken with digital camera. Loading order: Lane 1 = Protein size ladder, Lane 2-5 = Total fraction from cells infected with MOI of 1-10, Lane 6 = Total fraction from non-infected cells, Lane 7-10 = Soluble fraction from cells infected with MOI of 1-10, Lane 11 = Soluble Fraction from non-infected cells. There is a strong band at 58 kDa in infected cells at all MOI not seen in the non-infected controls, this was likely the 50.4 kDa NS5a protein, this band is not seen in any of the soluble fractions suggesting expression of the NS5a protein occurred but the protein was not soluble.

Figure 79 shows the SDS page analysis of the pOET8NS5a expression optimisation. In the total fraction there is a strong band around 58 kDa, which is not seen in the negative control. The expected size of the pOET8NS5a expressed protein was 50.4 kDa. The size of the strong band was bigger than this, possibly due to post translational modifications. The fact that an equivalent band was not seen in the non-infected control suggests this was the expressed NS5a protein. This band is not seen in the soluble fraction, so was expressed only in an insoluble form.

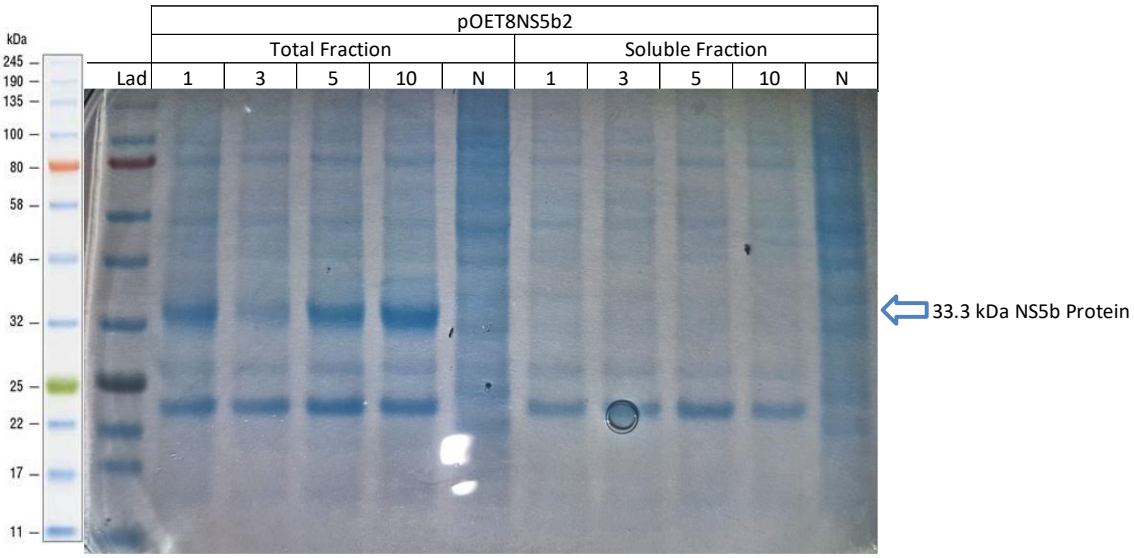

Figure 80 SDS Page Gel of 96 Hour pOET8NS5b2 Rc virus expression in Hi5 cells. NuPage 4-12% Bis-Tris PAGE gel run for 200V for 35 minutes, post electrophoresis stained with InstantBlue. Image taken with digital camera. Loading order: Lane 1 = Protein size ladder, Lane 2-5 = Total fraction from cells infected with MOI of 1-10, Lane 6 = Total fraction from non-infected cells, Lane 7-10 = Soluble fraction from cells infected with MOI of 1-10, Lane 11 = Soluble Fraction from non-infected cells. There is a strong band at around 33 kDa in infected cells at all MOI not seen in the non-infected controls, this was likely the 33.3 kDa NS5b protein, this band is not seen in any of the soluble fractions suggesting expression of the NS5b protein occurred but the protein was not soluble.

Figure 80 shows the SDS page analysis of the pOET8NS5b1 expression optimisation. In the total fraction there is a very strong band around 33.3 kDa, which is not in the negative control. This was the expected size of the expressed pOET8NS5b1 protein. The band was strong, was missing from the negative control, and of the correct size suggesting that this was the expressed NS5b protein. As with the NS5a protein above, the strong band was completely missing from the soluble fraction.

The other common strong band seen in both the NS5a and NS5b SDS gels was the strong band around 20kDa. This size was consistent with vankyrin protein which was observed with expression of NS4 protein with this transfer vector. Delay of cell lysis leads to higher amounts protein expression with this transfer vector.

The results of the NS5a and NS5b expressions using the pOET8 transfer vector resulted in expressed protein at a high level. Both proteins were produced in insoluble forms. A range of solubility experiments were then performed. This commenced with non-denaturing methods using higher salt, then progressed to urea solubilisation and guanidine hydrochloride solubilisation.

12.1.8.2.4HIGHER SALT SOLUBILISATION

A higher salt protein extraction was the first solubilisation attempted for both the NS5a and NS5b as described in 11.4.6.9.1. This method is a gentle solubilisation method which would not denature the

proteins and keeps them in a native expressed form. The NaCL was increased from 150mM to 300mM in both the lysis buffers, wash buffers and elution buffers. As both the NS5a and NS5b are nucleic acid binding proteins the concentration of benzonase nuclease was doubled.

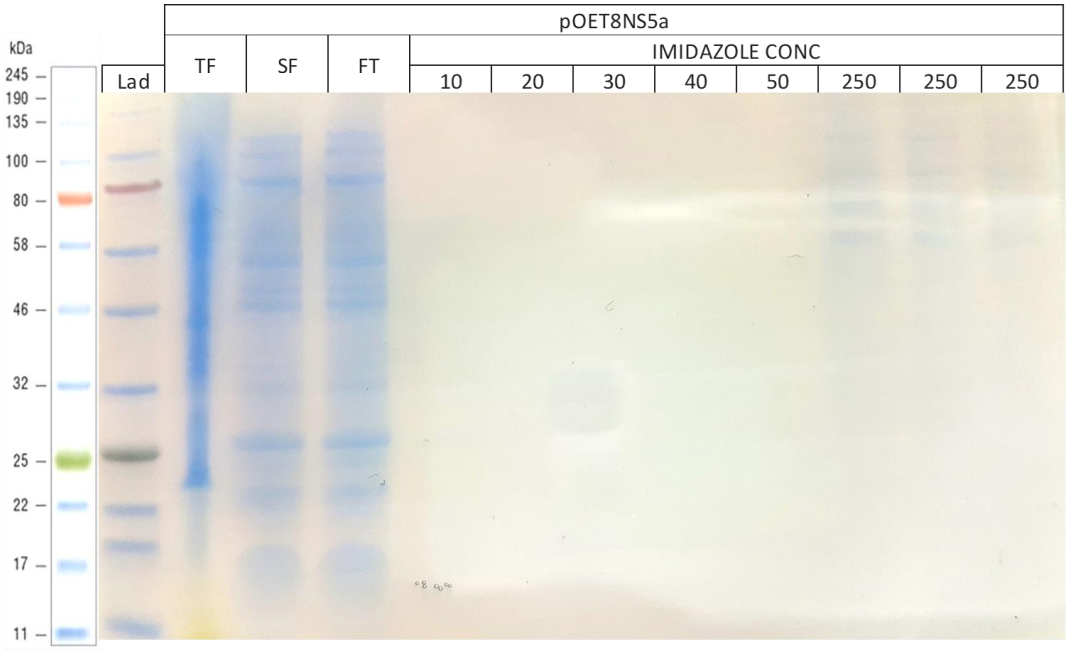

Figure 81 SDS-PAGE gel image of High NaCL HISTag purification products from pOET8NS5a Rc virus expression. NuPage 4-12% Bis-Tris PAGE gel run for 200V for 35 minutes, post electrophoresis stained with InstantBlue. Image taken with digital camera. Loading order: Lad = Protein size ladder; TF = Total fraction, SF = Soluble fraction, FT = Full transfer, 10 - 50 = 5 Washes in imidazole gradient from 10-50mM, E1-E3 = 3 X 250mM imidazole elutions. Lack of any band around the expected size of 50 kDa shows no NS5a protein was purified using the higher NaCL lysis and purification process.

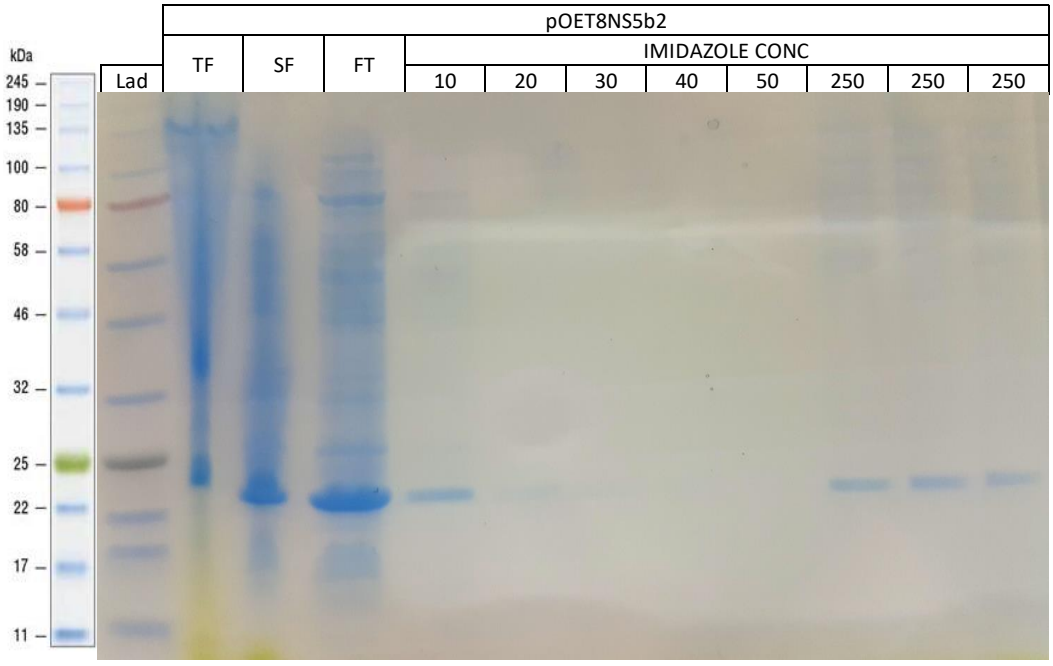

Figure 82 SDS-PAGE gel image of High NaCL HISTag purification products from pOET8NS5b2 Rc virus expression. NuPage 4-12% Bis-Tris PAGE gel run for 200V for 35 minutes, post electrophoresis stained with InstantBlue.

Image taken with digital camera. Loading order: Lad = Protein size ladder; TF = Total fraction, SF = Soluble fraction, FT = Full transfer, 10 - 50 = 5 Washes in imidazole gradient from 10-50mM, E1-E3 = 3 X 250mM imidazole elutions. Lack of any band around the expected size of 30 kDa shows no NS5b protein was purified using the higher NaCL lysis and purification process, only a band at around 25kDa can be seen showing contamination with the vankyrin expression protein.

Figure 81 and Figure 82 show the SDS page analysis for protein extraction with higher NaCL concentration and double strength benzonase nuclease, followed by a nickel coated bead HISTag purification. The lack of bands of the expected size in any of the 250 mM elutions, for either protein, show the higher salt lysis did not produce soluble protein. The only band seen in the 250 mM elutions is around 20kDa, in the pOET8NS5b1. This is the size of the vankyrin protein. This same band appeared in the cleaned up pOET8NS4 protein. As discussed before this protein has no HISTag and should not bind to the nickel coated beads, though the SDS image above clearly shows that this happened.

The next solubilisation protocols trialed were to use either urea or guanidine hydrochloride to solubilise the protein. These are both denaturing agents, with guanidine the stronger of the two. Their use may result in the expressed proteins losing some to all of their secondary structure, but to produce some soluble protein for use in an ELISA this was deemed necessary.

12.1.8.2.5UREA AND GUANIDINE SOLUBILISATION TRIAL

The first trial involved the solubilisation of the insoluble NS5a and NS5b pellets with 2M and 8M urea in phosphate-based lysis buffer as described in 11.4.6.9.2. This did not appear to solubilise either the NS5a of NS5b pellet, with SDS PAGE showing nothing in the soluble fraction.

The next trial compared both solubilisation in 8 M urea phosphate-based buffer with solubilisation with 6M guanidine hydrochloride as described in 11.4.6.9.2. The reducing agent β-mercaptoethanol was added to each buffer at a final concentration of 10mM. Solubilisation with 8M urea was followed with washing and elution steps using hybrid denaturing conditions as described in 11.4.6.9.3. The hybrid protocol solubilises the protein to allow binding of the HISTag to the nickel coated beads but finishes with standard washes to allow to protein to be cleaned up and eluted in a less denaturing environment. Final elution was performed in standard 250 mM imidazole elution buffer.

Solubilisation with 6 M guanidine hydrochloride was followed by washing and elution steps under full denaturing conditions as described in 11.4.6.9.4. All wash and elution buffers contained 8M urea including final elution buffer giving full denaturing conditions throughout the HISTag purification.

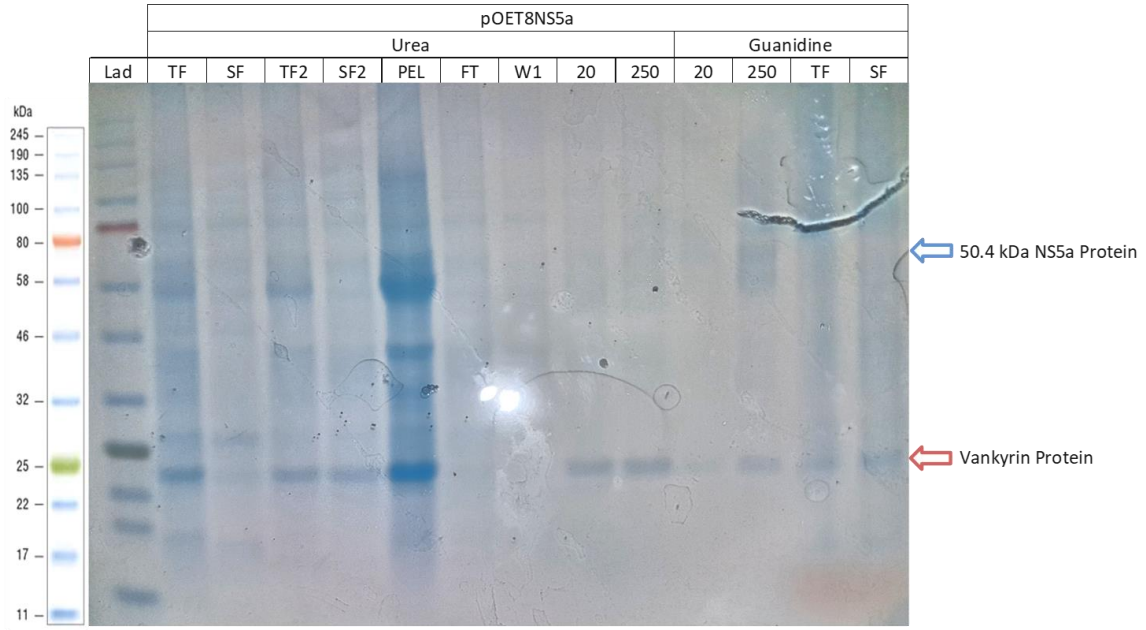

Figure 83 SDS-PAGE gel image of 8M urea and 6M guanidine hydrochloride denatured and HISTag purified products under denaturing conditions from pOET8NS5a Rc virus expression. NuPage 4-12% Bis-Tris PAGE gel run for 200V for 35 minutes, post electrophoresis stained with InstantBlue. Image taken with digital camera. Loading order: Lad = Protein size ladder; Urea denatured products TF = Total fraction, SF = Soluble fraction, TF2 = Urea denatured full transfer, SF2 = Urea denatured soluble fraction, PEL = Urea denatured pellet, FT= Full transfer, W1 = non-imidazole urea wash buffer, 20 = 20mM imidazole urea denaturing wash buffer, 250 = 1 X 250mM imidazole urea denaturing elution buffer; Guanidine denatured products, 20 = urea denaturing wash buffer, 250 = 1 X 250mM imidazole urea denaturing elution buffer. No band is seen in the expected size of the urea denatured solution fraction or the 250mM elution, there is a band at around 58 kDa in the guanidine 250 denaturing elution, suggesting the NS5a protein is solubilised with 6M guanidine hydrochloride and is HISTag purified under denaturing conditions.

Figure 83 shows the results of the urea and guanidine hydrochloride solubilisation. The urea solubilisation did not appear to work, no band could be seen in the soluble fraction even after treatment with 8 M urea, and the final 250 mM elution showed no band at the expected size. The solubilisation with 6 M guanidine hydrochloride did appear to work. There are no total fractions and soluble fractions on the image as guanidine hydrochloride cannot be run on the SDS PAGE due to precipitation when mixed with SDS buffer. Only the later wash and elution steps are shown. The 250 mM elution buffer, containing urea at 8 M, does contain a smeared band around the correct size of 50.4 kDa. This suggested the protein was solubilised in guanidine at 6 M and purified from nickel beads under denaturing conditions. This method was chosen for subsequent large-scale purification of the NS5a protein.

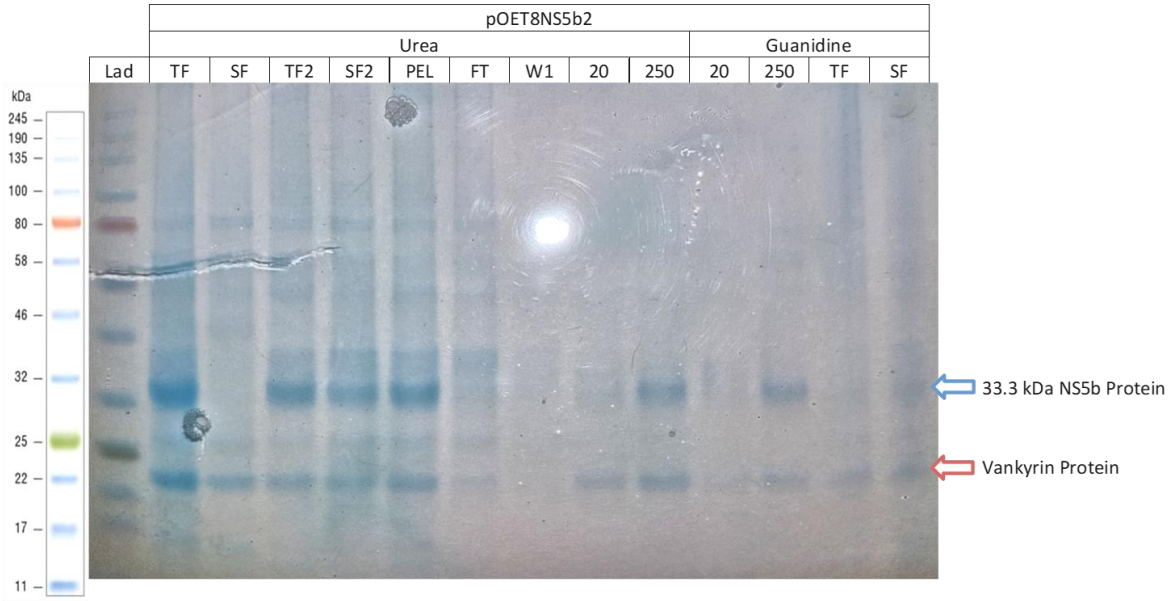

Figure 84 SDS-PAGE gel image of 8M urea and 6M guanidine hydrochloride denatured and HISTag purified products under denaturing conditions from pOET8NS5b2 Rc virus expression. NuPage 4-12% Bis-Tris PAGE gel run for 200V for 35 minutes, post electrophoresis stained with InstantBlue. Image taken with digital camera. Loading order: Lad = Protein size ladder; Urea denatured products TF = Total fraction, SF = Soluble fraction, TF2 = Urea denatured full transfer, SF2 = Urea denatured soluble fraction, PEL = Urea denatured pellet, FT= Full transfer, W1 = non-imidazole urea wash buffer, 20 = 20mM imidazole urea denaturing wash buffer, 250 = 1 X 250mM imidazole urea denaturing elution buffer; Guanidine denatured products, 20 = urea denaturing wash buffer, 250 = 1 X 250mM imidazole urea denaturing elution buffer. Band is seen at the expected size 33 kDa in the urea denatured solution fraction and the 250mM elution, there is a band of the same in the guanidine 250 denaturing elution, suggesting the NS5b protein is solubilised by both 8M urea and 6M guanidine hydrochloride and is HISTag purified under denaturing conditions.

Figure 84 shows the results of the urea and guanidine hydrochloride solubilisations for the NS5b1 protein. The protein was solubilised in both 8 M urea and 6 M guanidine hydrochloride buffers. The soluble fraction from the urea solubilisation shows a strong band at the expected size, and this band can be seen in the 250 mM elution after purification using hybrid conditions. This same band appears in the 250 mM elution following solubilisation with guanidine and purification under denaturing conditions. As the combination of solubilisation with 8 M urea and purification under hybrid conditions is less denaturing to the NS5b protein than the combination of guanidine and purification under denaturing conditions, it was decided to use this method for a large-scale purification.

In both NS5a and NS5b purifications using either urea or guanidine, an additional 2nd band was seen between 22 kDa to 25 kDa. This is the vankyrin protein discussed earlier, which again purified through the nickel bead purification process.

12.1.8.2.6NS5A LARGE SCALE SOLUBILISATION AND PURIFICATION

A large scale guanidine solubilisation and purification was performed as described in 11.4.6.9.4.

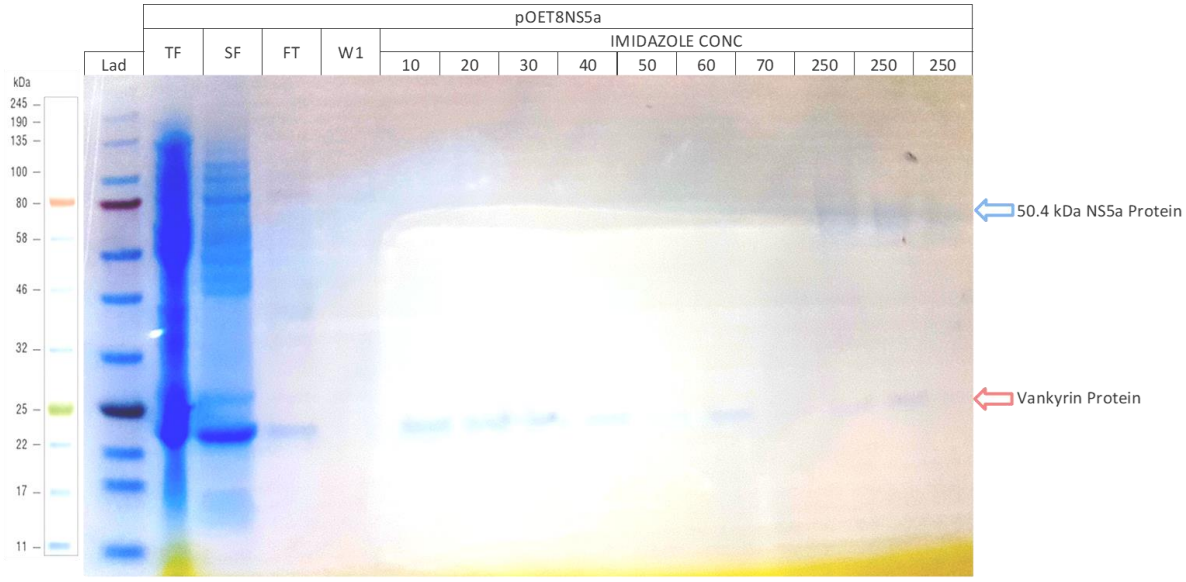

Figure 85 SDS-PAGE gel image of 6M guanidine hydrochloride denatured and HISTag purified under denaturing conditions from pOET8NS5a Rc virus expression. NuPage 4-12% Bis-Tris PAGE gel run for 200V for 35 minutes, post electrophoresis stained with InstantBlue. Image taken with digital camera. Loading order: Lad = Protein size ladder, TF = Total Fraction, SF = Soluble Fraction, FT = Full transfer, 10-60 = 10-60mM Imidazole denaturing urea washes, 250 = 3 X 250mM Imidazole denaturing 250 mM elutions. Arrow highlights strong band at 58kDa thought to be 50.4kDa NS5a protein, band at around 22 kDa is contaminating Vankyrin protein.

Figure 85 shows the success of the guanidine solubilisation and His tag purification under denaturing conditions for the NS5a protein. All 3 of the elutions collected contained a band at a size of between 58-80kDa according to the size ladder, the expected size of the protein was predicted to be 50.4kDa so although not an exact match there was a high likelihood this was the NS5a protein. In addition, there was a 2nd band around 20 kDa, again the vankyrin protein, despite higher volume washes and higher strength imidazole washes, could not be completely removed.

12.1.8.2.7NS5B1 LARGE SCALE SOLUBILISATION AND PURIFICATION

A large scale urea solubilisation and purification under hybrid denaturing conditions as described in was performed as described in 11.4.6.9.3.

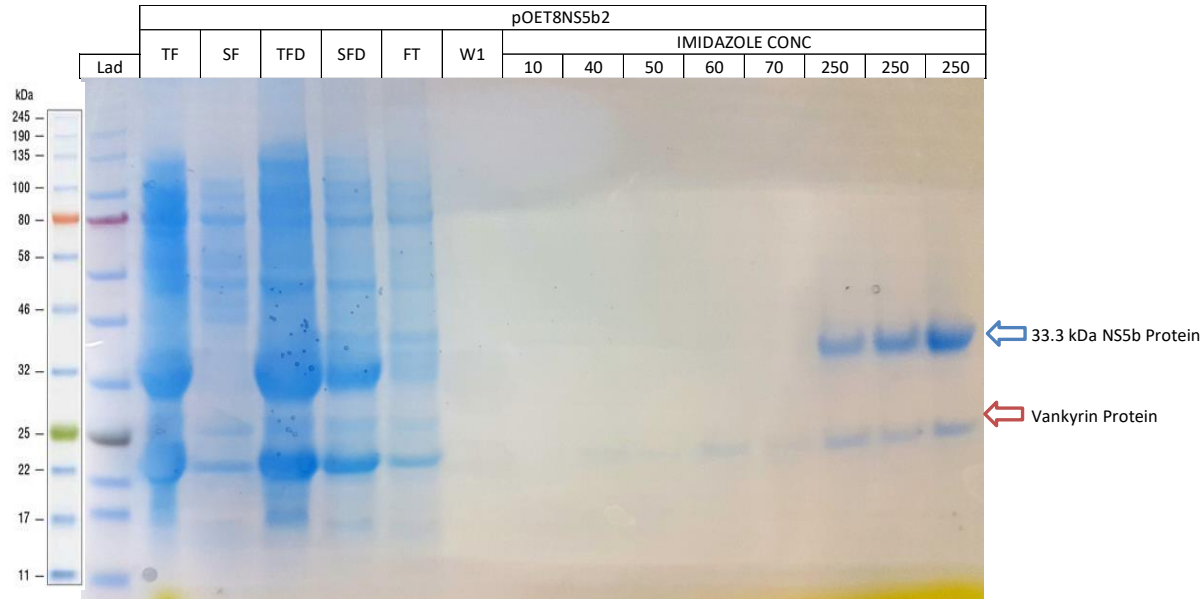

Figure 86 SDS-PAGE gel image of 8M urea denatured and HISTag purified under hybrid denaturing conditions from pOET8NS5b2 Rc virus expression. NuPage 4-12% Bis-Tris PAGE gel run for 200V for 35 minutes, post electrophoresis stained with InstantBlue. Image taken with digital camera. Loading order: Lad = Protein size ladder, TF = Total Fraction, SF = Soluble Fraction, TFD = Urea denatured total fraction, SFD = Urea denatured soluble fraction FT = Full transfer, W1 = Non-imidazole urea wash, 10 = 10mM imidazole washes, 40-70 = 40-70mM Imidazole washes, 250 = 3 X 250mM imidazole elutions. Arrow highlights strong band at 33 kDa thought to be 33.3 kDa NS5b protein, band at around 22 kDa is contaminating vankyrin protein.

Figure 86 shows the SDS page analysis of the NS5b urea solubilisation and purification under hybrid conditions. The analysis shows the protein was successfully purified using this hybrid method, with the 3 eluates all containing a strong band at the expected size of 33.3 kDa. Unfortunately, as seen with all expression using the pOET8 transfer vector, the vankyrin protein is still present between 22-25kDa, despite the use of a large number of washes and higher concentrations of imidazole wash buffer.

Final confirmation of both the NS5a and NS5b protein solubilisation and purification was performed by western blot.

12.1.8.2.8NS5A AND NS5B WESTERN BLOT

Western blot analysis was used to confirm NS5a and NS5b protein solubilisation and purification was successful.

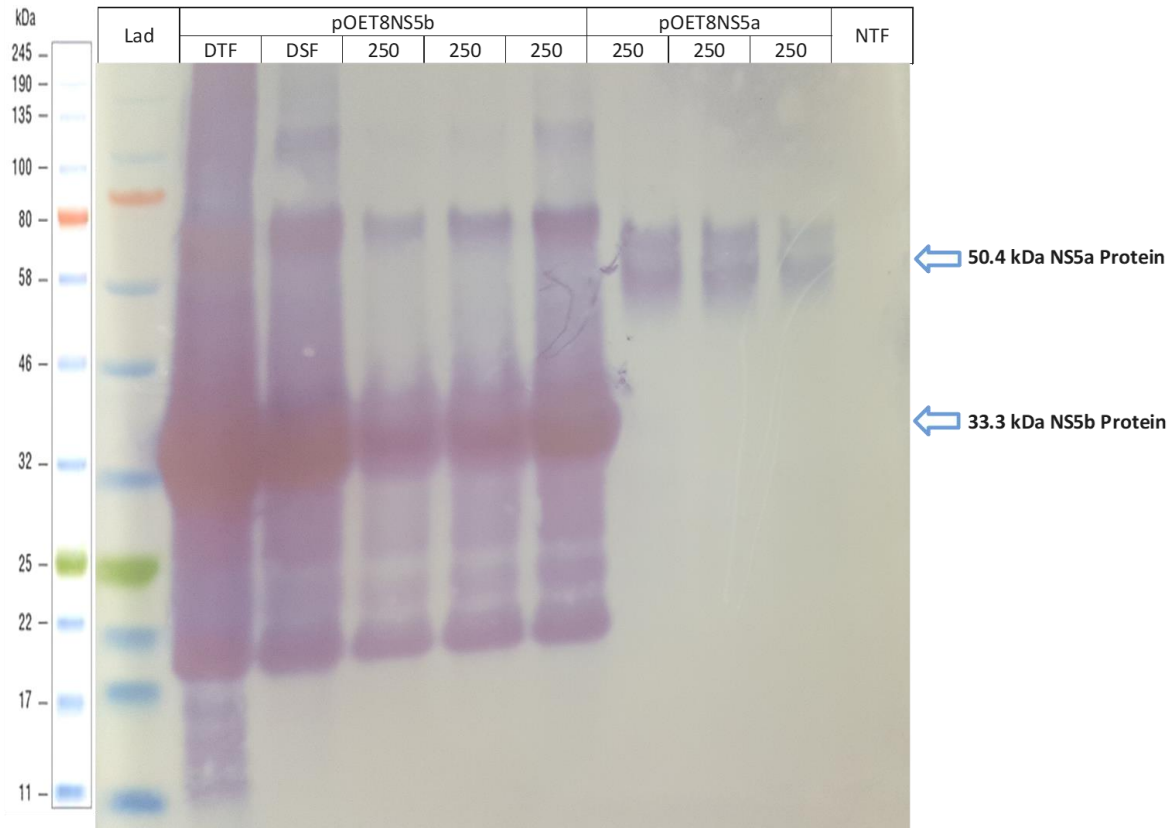

Figure 87 Western Blot of 8M Urea denatured NS5b protein HISTag purified under hybrid denaturing conditions and 6M guanidine hydrochloride NS5a protein HISTag purified under full denaturing conditions. Western blot used NuPage 4-12% Bis-Tris gels transferred to 0.45µm Nitrocellulose membrane. Primary antibody mouse mAb Anti-His (6X) at 1:1000 dilution, secondary antibody rabbit pAb-Anti-mouse IgG (HRP) used at 1:3000, substrate TMB Ultra. Image taken with digital camera. Loading order: Lad = Protein size ladder; NS5b DTF = Urea denatured total fraction, NS5b DSF = Urea denatured soluble fraction, NS5b 250 = 3 X 250mM imidazole elutions; NS5a 3 X 250 = 3 x 250mM imidazole denaturing elution buffer. NTF=Non-infected cells total fraction. All the NS5b lanes show very strong band at the expected size of 33.3kDa including the 250mM elutions confirming the purification of NS5b protein, there is also a smaller unknown band around 17 kDa and a large band around 80kDa which is possibly a dimer of the NS5b protein. The 3x250mM elutions for the NS5a protein show a strong band at around 58kDa confirming the purification of the denatured NS5a protein, it possibly appears larger than expected on the gel due to glycosylation of the expressed protein.

Figure 87 shows the western blot analysis of both the NS5b protein produced under hybrid denaturing conditions, and the NS5a protein produced under full denaturing conditions. The NS5b protein shows a very strong band of the expected size 33.3 kDa in the denatured total fraction, soluble fraction and all the 250mM eluates. There is also a strong band between 17-22 kDa, and a relatively strong band between 58-80Kda. It is not known what the lower strong band is, though it is not the vankyrin protein between (22-25 kDa) as it was smaller (17-22 kDa). The larger band seen between 58-80 kDa could be a dimer of the purified NS5b protein.

The total and soluble fractions from the NS5a solubilisation and purification are missing due to the presence of guanidine hydrochloride. The three 250 mM eluates are shown, each with a strong band matching the size of band seen previously by SDS PAGE analysis.

The western blot analysis proves the solubilisation and purification of both the NS5a and NS5b proteins.

12.1.8.3 FINAL TABLE EXPRESSED PROTEINS

Table 21 below lists all the proteins successfully expressed and purified using the *flash*BAC ultra system.

HCV Protein	Transfer Vector	Purification
Core	pOET1	HISTag Purified
NS3	pIEx-Bac3	HISTag Purified
NS4	pOET8	Denatured 8M urea/HISTag Hybrid Conditions
NS5a	pOET8	Denature 6M Guanidine/ HISTag Denature Conditions
NS5b	pOET8	Denatured 8M urea/HISTag Hybrid Conditions

Table 21 Final Table of proteins expressed using the *flash*BAC ultra baculovirus expression system. The transfer vectors used for generation of the recombinant baculovirus and the conditions for protein purification are listed alongside each protein.

12.2 ELISA OPTIMISATION

The optimum ELISA conditions were determined for both serum and DBS samples. The primary optimisation was performed using known anti-HCV positive and negative serum samples, to select a secondary antibody, primary and secondary antibody dilutions, optimum TMB reaction time, optimum incubation temperature and optimum coating concentration for each HCV protein. A further optimisation was performed separately for DBS samples to select the optimum primary antibody dilution. All tests were performed in duplicate and a mean average calculated.

12.2.1 SECONDARY ANTIBODY SELECTION

A comparison was performed between 2 separate secondary antibodies. The first was a rabbit polyclonal anti-Human IgG antibody, the second was a mouse monoclonal anti-Human IgG antibody. Both were conjugated with Horse radish peroxidase (HRP). The comparison was performed as described in section 11.6.1.1.

			Rabbit pAb Anti-Human IgG HRP			Mouse mAb Anti-Human IgG HRP		
2nd Antibody Dilution	**NS3 Antigen Conc. µg/ml**	**Serum Dilution**	**POS Signal OD***	**NEG Signal OD***	**POS/ NEG**	**POS Signal OD***	**NEG Signal OD***	**POS/ NEG**
1:10000	**10**	**1:40**	2.46	0.32	7.65	2.61	0.21	12.56
	5		1.35	0.22	6.10	1.43	0.16	8.91
	10	**1:80**	1.83	0.19	9.45	1.75	0.12	14.92
	5		0.92	0.14	6.63	0.95	0.10	9.55
1:20000	**10**	**1:40**	1.32	0.20	6.52	1.54	0.12	12.96
	5		0.73	0.14	5.26	0.79	0.09	8.73
	10	**1:80**	0.98	0.13	7.62	0.93	0.08	11.60
	5		0.52	0.10	5.46	0.47	0.07	7.17
1:40000	**10**	**1:40**	0.75	0.12	6.49	0.85	0.08	10.80
	5		0.60	0.09	6.92	0.47	0.07	6.66
	10	**1:80**	0.56	0.08	7.00	0.56	0.06	8.81
	5		0.29	0.06	4.63	0.31	0.06	5.46
1:80000	**10**	**1:40**	0.41	0.07	5.53	0.45	0.06	7.50
	5		0.21	0.07	3.16	0.27	0.06	4.93
	10	**1:80**	0.28	0.06	4.86	0.32	0.05	6.46
	5		0.16	0.06	2.84	0.19	0.05	3.88

Table 22 Comparison of Rabbit pAb anti-Human IgG HRP with Mouse mAb anti-Human IgG HRP Secondary Antibodies. NS3 antigen was coated at 10 and 5 µg/ml concentrations, Anti-HCV positive and Anti-HCV negative serum samples were run at 1:40 and 1:80 dilutions, 2nd antibody run at 1:10000 – 1:80000 dilutions, substrate TMB stopped with 0.5M sulphuric acid and read at 450nm. *OD signal minus the blank reading, average of duplicate test results. Mouse mAb Anti-Human IgG (HRP) demonstrated lower background and higher positive/negative ratio compared to rabbit pAb Anti-Human IgG (HRP).

Table 22 above shows the results from the secondary antibody comparison. The results from the mouse mAb show a consistently lower negative sample value while maintaining a higher positive sample value, across both antigen and serum concentrations, and all secondary antibody dilutions. This can be seen with the higher positive/negative ratios for the mouse mAb when compared to the rabbit pAb. It was for this reason the mouse monoclonal antibody was chosen for all subsequent experiments.

12.2.2 PRIMARY AND SECONDARY DILUTION

The dilution factor for both the primary and secondary antibodies were optimised as described in section 11.6.1.2

		1: 5000 mAb Anti-Human IgG					1:10000 mAb Anti-Human IgG				
NS3 Antigen µg/ml	**Serum Dilution**	**Blank**	**POS Signal OD***	**NEG Signal OD***	**POS/NEG**	**POS-NEG**	**Blank**	**POS Signal OD***	**NEG Signal OD***	**POS/NEG**	**POS-NEG**
10	**1:10**	0.04	2.96	1.08	**2.7**	**1.9**	0.04	2.96	0.66	**4.5**	**2.3**
5		0.04	2.96	0.70	**4.2**	**2.3**	0.04	2.96	0.48	**6.2**	**2.5**
10	**1:20**	0.04	2.96	0.68	**4.3**	**2.3**	0.04	2.96	0.47	**6.3**	**2.5**
5		0.04	2.96	0.49	**6.1**	**2.5**	0.04	2.46	0.30	**8.3**	**2.2**
10	**1:40**	0.04	2.96	0.34	**8.7**	**2.6**	0.04	2.27	0.20	**11.1**	**2.1**
5		0.04	2.19	0.15	**15.1**	**2.0**	0.04	1.33	0.09	**15.0**	**1.2**
10	**1:80**	0.04	1.97	0.18	**10.7**	**1.8**	0.04	1.13	0.11	**10.0**	**1.0**
5		0.04	1.10	0.08	**13.4**	**1.0**	0.04	0.66	0.05	**14.7**	**0.6**
		1: 20000 mAb Anti-Human IgG					**1:40000 mAb Anti-Human IgG**				
10	**1:10**	0.04	2.96	0.28	**10.5**	**2.7**	0.04	1.95	0.15	**13.0**	**1.8**
5		0.05	1.71	0.14	**12.6**	**1.6**	0.04	0.92	0.09	**10.3**	**0.8**
10	**1:20**	0.04	2.50	0.19	**13.5**	**2.3**	0.04	1.25	0.09	**14.0**	**1.2**
5		0.05	1.20	0.09	**14.1**	**1.1**	0.04	0.69	0.05	**14.1**	**0.6**
10	**1:40**	0.04	1.37	0.11	**12.4**	**1.3**	0.04	0.71	0.05	**13.4**	**0.7**
5		0.05	0.69	0.04	**19.1**	**0.7**	0.04	0.41	0.03	**13.7**	**0.4**
10	**1:80**	0.04	0.66	0.07	**9.6**	**0.6**	0.04	0.31	0.03	**9.7**	**0.3**
5		0.05	0.35	0.02	**23.2**	**0.3**	0.04	0.16	0.02	**10.9**	**0.1**

Table 23 Optimisation of primary (serum) and secondary antibody dilutions. NS3 antigen was coated at 10 and 5 µg/ml concentrations. Optimisation of primary antibody was performed by testing Anti-HCV positive and Anti-HCV negative serum samples at doubling dilutions from 1:10 to 1:80. Optimisation of secondary antibody was performed by testing mAb Anti-Human IgG (HRP) was doubling dilutions from 1:5000 – 1:40000. Substrate was TMB stopped with 0.5M sulphuric acid and read at 450nm. *OD signal minus the blank reading, average of duplicate test results. The combination of primary antibody (serum) diluted 1:20 and mAb Anti-Human IgG run at 1:2000 gave the highest combined positive to negative ratio and positive minus negative readings.

Results in Table 23 show the combination of a primary antibody (serum) dilution of 1:20, combined with a secondary antibody dilution of 1:20000, gave the highest combination of positive/negative ratio and the positive-negative reading. This combination of dilutions was chosen for all future experiments using serum samples.

12.2.3 BLOCKING BUFFER SELECTION

A comparison was performed between 1% BSA and 5% FCS based blocking buffer and diluent, as described in section 11.6.1.3.

	1% BSA				5% FCS			
Serum Sample	**Signal OD***	**Average**	**Av Pos/Neg**	**Av. Pos - Neg**	**Signal OD***	**Average**	**Pos/Neg ratio**	**Av. Pos - Neg**
POS1	2.96	2.55	22.49	2.44	1.66	1.66	14.91	1.55
POS2	2.96				1.96			
POS3	1.32				0.86			
POS4	2.96				2.14			
NEG1	0.04	0.11			0.05	0.11		
NEG2	0.10				0.12			
NEG3	0.23				0.20			
NEG4	0.09				0.08			
Blank	0.04				0.04			

Table 24 Comparison of 1% BSA and 5% FCS used as blocking buffer and diluent for NS3 Antigen ELISA. NS3 antigen was coated at 5 µg/ml concentrations. Comparison of 1% BSA and 5% FCS was performed by testing 4 Anti-HCV positive serum and 4 Anti-HCV negative serum then comparing the average results. NS3 antigen was coated at 5 µg/ml concentration, serum was used at 1:20 dilution, secondary antibody was used at 1:20000 dilution, substrate was TMB ultra stopped with 0.5M sulphuric acid and read at 450nm. *OD signal minus the blank reading, average of duplicate test results given for each sample, overall average for positive and negative Anti-HCV samples and used to calculate average positive/negative ratio and average positive-negative value. The use of 1% BSA as blocking buffer produced higher positive readings combined with similar background readings to give overall higher average positive to negative ratio and positive minus negative values.

Table 24 shows the results of the comparison. The average signal from the 4 anti-HCV positive samples and from the 4 anti-HCV negative samples was calculated and used to generate an average positive/negative ratio and positive minus negative reading. The table clearly shows a higher average signal using 1% BSA compared to 5% FCS, while maintaining a similar low background level. Therefore 1% BSA based blocking buffer and diluent were used for all subsequent optimisations and validations.

12.2.4 TEMPERATURE OPTIMISATION

To help further reduce the background signal, and improve consistency, a temperature optimisation was performed, comparing incubating all steps at room temperature with incubation at 25°C, as described in section 11.6.1.4

	RT				25°C			
Serum Sample	Signal OD*	Average	Av. Pos/Neg	Av. Pos - Neg	Signal OD*	Average	Av. Pos/Neg	Av. Pos - Neg
POS3	0.85	1.72	16.72	1.62	0.90	1.79	18.93	1.70
POS4	2.13				2.30			
POS5	1.96				1.98			
POS6	1.96				1.98			
NEG2	0.04	0.10			0.04	0.09		
NEG3	0.11				0.10			
NEG4	0.07				0.06			
NEG5	0.19				0.17			
Blank	0.05				0.05			

Table 25 Comparison of incubation at room temperature and 25°C for NS3 Antigen ELISA. Comparison of performing all incubations a room temperature or 25°C was performed by testing 4 Anti-HCV positive serum and 4 Anti-HCV negative serum then comparing the average results. NS3 antigen was coated at 5 µg/ml concentration, serum was used at 1:20 dilution, secondary antibody was used at 1:20000 dilution, substrate was TMB ultra stopped with 0.5M sulphuric acid and read at 450nm. *OD signal minus the blank reading, average of duplicate test results given for each sample. Duplicate average values used to calculate overall average for positive and negative Anti-HCV samples then used to calculate average positive/negative ratio and average positive-negative value. The results showed very little difference between incubations and room temperatures and 25°C, with the latter giving slightly higher average positive to negative ration and average positive minus negative value.

Table 25 shows the results of the temperature optimisation. The results between the 2 temperatures were not very different. The 25°C gave a slightly higher positive to negative ratio. It was decided to use a temperature of 25°C to improve consistency and overcome the variability in room temperature seen day to day.

12.2.5 TIME OPTIMISATION

A time optimisation was performed for the substrate reaction time, timed from the addition of TMB reagent to the addition of stopping solution, as described in section 11.6.1.5.

	10 minutes				20 minutes				30 Minutes			
Serum Sample	Signal OD*	Average	Av . Pos/Neg	Av. Pos - Neg	Signal OD*	Average	Av. Pos/Neg	Av. Pos - Neg	Signal OD*	Average	Av. Pos/Neg	Av. Pos - Neg
POS5	1.87	1.22	11.13	1.11	2.95	2.14	14.38	1.99	2.95	2.38	13.31	2.20
POS6	0.68				1.18				1.47			
POS7	1.11				2.29				2.74			
NEG2	0.09	0.11			0.13	0.15			0.15	0.18		
NEG3	0.14				0.21				0.25			
NEG4	0.10				0.11				0.14			
Blank	0.04				0.05				0.05			

Table 26 Comparison of TMB substrate reaction time for NS3 Antigen ELISA. Comparison of TMB substrate reaction time performed by testing by testing 3 Anti-HCV positive serum and 3 Anti-HCV negative serum then comparing the average results. NS3 antigen was coated at 5 µg/ml concentration, serum was used at 1:20 dilution, blocking buffer was 1% BSA, secondary antibody was used at 1:20000 dilution, substrate was TMB ultra stopped with 0.5M sulphuric acid and read at 450nm, all incubations were 60 minutes at 25°C except for final substrate reaction. *OD signal minus the blank reading,

average of duplicate test results given for each sample. Duplicate average values used to calculate overall average for positive and negative Anti-HCV samples then used to calculate average positive/negative ratio and average positive-negative value. The TMB substrate 20-minute incubation gave the highest average positive to negative ratio and average positive minus negative value.

Table 26 above shows the results of the TMB substrate reaction time optimisation. The 10 minute reaction time was too short. The 20 minute and 30 minute reactions were better, the 30 minute giving slightly higher signal readings but with increased backgrounds. It was decided to use a 20 minute reaction time as this gave a slightly higher positive to negative ratio.

12.2.6 ANTIGEN COATING CONCENTRATION

Multiple ELISA plates were run to find the optimum coating concentration for each HCV antigen, as described in section 11.6.1.6.

NS3

NS3 Antigen µg/ml	Serum Sample	Signal OD*	Signal OD*	Pos/Neg ratio	Av. Pos - Neg
10	POS6	2.95	2.95	7.59	2.56
	POS7	2.95			
	POS8	2.95			
	NEG5	0.49	0.39		
	NEG6	0.47			
	NEG7	0.20			
	Blank	0.05			
5	POS6	1.90	2.60	19.50	2.47
	POS7	2.95			
	POS8	2.95			
	NEG5	0.21	0.13		
	NEG6	0.13			
	NEG7	0.06			
	Blank	0.05			

Table 27 Optimisation of NS3 antigen coating concentration. Optimal NS3 antigen concentration determined by coating at 10 and 5 µg/ml and tested with 3 Anti-HCV positive and 3 Anti-HCV negative serum. Serum was used at 1:20 dilution, blocking buffer was 1% BSA, secondary antibody was used at 1:20000 dilution, substrate was TMB ultra stopped with 0.5M sulphuric acid and read at 450nm, all incubations were 60 minutes at 25°C except for 20-minute final substrate reaction. *OD signal minus the blank reading, average of duplicate test results given for each sample. Duplicate average values used to calculate overall average for positive and negative Anti-HCV samples then used to calculate average positive/negative ratio and positive-negative value. The NS3 antigen coating concentration of 5µg/ml gave the more than double average positive to negative ratio and similar average positive minus negative values.

All the previous optimisations described above used the NS3 antigen ELISA coated a final concentration of either 10 or 5 µg/ml. As these concentrations had been shown to perform well, a

full NS3 antigen dilution series was not required. Instead a final comparison using these 2 antigen coating concentrations was performed, with 3 anti-HCV positive and 3 anti-HCV negative samples.

Table 27 shows the results of this comparison. The background of the 10 µg/mL concentration was relatively high compared to the 5 µg/mL concentration, giving a much lower average positive to negative ratio. For this reason, a NS3 antigen coating concentration of 5 µg/mL was chosen.

CORE

Core Antigen µg/ml	Serum Sample	Signal OD*	Average	Pos/Neg ratio	Av. Pos - Neg
10	POS6	1.53		5.01	1.18
	POS7	1.34	1.47		
	POS8	1.56			
	NEG5	0.43			
	NEG6	0.29	0.29		
	NEG7	0.17			
	Blank	0.05			
5	POS6	1.61		7.14	1.18
	POS7	1.14	1.38		
	POS8	1.38			
	NEG5	0.28			
	NEG6	0.14	0.19		
	NEG7	0.16			
	Blank	0.05			
2.5	POS6	0.77		4.86	0.49
	POS7	0.51	0.62		
	POS8	0.59			
	NEG5	0.22			
	NEG6	0.07	0.13		
	NEG7	0.10			
	Blank	0.05			
1.25	POS6	0.43		4.97	0.26
	POS7	0.25	0.33		
	POS8	0.31			
	NEG5	0.15			
	NEG6	0.03	0.07		
	NEG7	0.03			
	Blank	0.05			

Table 28 Optimisation of Core antigen coating concentration. Optimal Core antigen concentration determined by coating at 4 dilutions from 10 to 1.25 µg/ml and tested with 3 Anti-HCV positive and 3 Anti-HCV negative serum. Serum was used at 1:20 dilution, blocking buffer was 1% BSA, secondary antibody was used at 1:20000 dilution, substrate was TMB ultra stopped with 0.5M sulphuric acid and read at 450nm, all incubations were 60 minutes at 25°C except for 20-minute

final substrate reaction. *OD signal minus the blank reading, average of duplicate test results given for each sample. Duplicate average values used to calculate overall average for positive and negative Anti-HCV samples then used to calculate average positive/negative ratio and positive-negative value. The Core antigen coating concentration of 5µg/ml gave the highest combined positive/negative ratio and positive minus negative value.

Table 28 shows the results of the Core antigen coating optimisation. The antigen was coated at 4 different concentrations, from 10 µg/mL down to 1.25 µg/mL. The optimum concentration chosen was 5 µg/mL which produced the best average positive/negative signal ratio.

NS4

NS4 Antigen µg/ml	Serum Sample	Signal OD*	Average	Pos/Neg ratio	Av. Pos - Neg
10	POS6	1.31	1.77	2.16	0.95
	POS7	1.08			
	POS8	2.93			
	NEG5	1.08	0.82		
	NEG6	0.89			
	NEG7	0.49			
	Blank	0.08			
5	POS6	1.20	1.68	2.27	0.94
	POS7	0.90			
	POS8	2.95			
	NEG5	0.83	0.74		
	NEG6	0.59			
	NEG7	0.81			
	Blank	0.06			
2.5	POS6	0.88	0.77	6.33	0.65
	POS7	0.19			
	POS8	1.25			
	NEG5	0.20	0.12		
	NEG6	0.09			
	NEG7	0.08			
	Blank	0.06			
1.25	POS6	0.15	0.39	4.95	0.31
	POS7	0.26			
	POS8	0.74			
	NEG5	0.15	0.08		
	NEG6	0.05			
	NEG7	0.04			
	Blank	0.05			

Table 29 Optimisation of NS4 antigen coating concentration. Optimal NS4 antigen concentration determined by coating at 4 dilutions from 10 to 1.25 µg/ml and tested with 3 Anti-HCV positive and 3 Anti-HCV negative serum. Serum was used at 1:20 dilution, blocking buffer was 1% BSA, secondary antibody was used at 1:20000 dilution, substrate was TMB

ultra stopped with 0.5M sulphuric acid and read at 450nm, all incubations were 60 minutes at 25°C except for 20-minute final substrate reaction. *OD signal minus the blank reading, average of duplicate test results given for each sample. Duplicate average values used to calculate overall average for positive and negative Anti-HCV samples then used to calculate average positive/negative ratio and positive-negative value. The NS4 antigen coating concentration of 2.5µg/ml gave the highest combined positive/negative ratio and positive minus negative value.

Table 29 shows the results of the NS4 antigen coating optimisation. The antigen was coated at 4 different concentrations, from 10 µg/mL down to 1.25 µg/mL. The optimum concentration chosen was 2.5 µg/mL.

NS5A

NS5a Antigen µg/ml	Serum Sample	Signal OD*	Average	Pos/Neg ratio	Av. Pos - Neg
10	POS8	2.44	2.78	4.76	2.20
	POS9	2.95			
	POS10	2.95			
	NEG6	0.20	0.58		
	NEG7	0.39			
	NEG8	1.17			
	Blank	0.08			
5	POS8	1.98	2.63	7.46	2.27
	POS9	2.95			
	POS10	2.95			
	NEG6	0.11	0.35		
	NEG7	0.23			
	NEG8	0.72			
	Blank	0.06			
2.5	POS8	1.03	2.32	9.00	2.06
	POS9	2.96			
	POS10	2.96			
	NEG6	0.19	0.26		
	NEG7	0.12			
	NEG8	0.46			
	Blank	0.06			
1.25	POS8	0.80	2.24	13.57	2.07
	POS9	2.96			
	POS10	2.96			
	NEG6	0.12	0.17		
	NEG7	0.06			
	NEG8	0.32			
	Blank	0.05			

Table 30 Optimisation of NS5a antigen coating concentration. Optimal NS5a antigen concentration determined by coating at 4 dilutions from 10 to 1.25 µg/ml and tested with 3 Anti-HCV positive and 3 Anti-HCV negative serum. Serum was

used at 1:20 dilution, blocking buffer was 1% BSA, secondary antibody was used at 1:20000 dilution, substrate was TMB ultra stopped with 0.5M sulphuric acid and read at 450nm, all incubations were 60 minutes at 25°C except for 20-minute final substrate reaction. *OD signal minus the blank reading, average of duplicate test results given for each sample. Duplicate average values used to calculate overall average for positive and negative Anti-HCV samples then used to calculate average positive/negative ratio and positive-negative value. The NS5a antigen coating concentration of 1.25µg/ml gave the highest combined positive/negative ratio and positive minus negative value.

Table 30 shows the results of the NS5a antigen coating optimisation. The antigen was coated at 4 different concentrations, from 10 µg/mL down to 1.25 µg/mL. The optimum concentration chosen was 1.25 µg/mL.

NS5B

NS5b Antigen µg/ml	Serum Sample	Signal OD*	Average	Pos/Neg ratio	Av. Pos - Neg
10	POS8	2.66	1.99	5.72	1.64
	POS9	2.94			
	POS10	0.36			
	NEG6	0.26	0.35		
	NEG7	0.35			
	NEG8	0.43			
	Blank	0.08			
5	POS8	2.56	1.80	6.28	1.52
	POS9	2.57			
	POS10	0.29			
	NEG6	0.17	0.29		
	NEG7	0.30			
	NEG8	0.39			
	Blank	0.06			
2.5	POS8	1.18	0.97	5.27	0.78
	POS9	1.60			
	POS10	0.12			
	NEG6	0.15	0.18		
	NEG7	0.10			
	NEG8	0.30			
	Blank	0.06			
1.25	POS8	0.80	0.68	4.30	0.53
	POS9	1.18			
	POS10	0.08			
	NEG6	0.10	0.16		
	NEG7	0.08			
	NEG8	0.30			
	Blank	0.05			

Table 31 Optimisation of NS5b antigen coating concentration. Optimal NS5b antigen concentration determined by coating at 4 dilutions from 10 to 1.25 µg/ml and tested with 3 Anti-HCV positive and 3 Anti-HCV negative serum. Serum was used at 1:20 dilution, blocking buffer was 1% BSA, secondary antibody was used at 1:20000 dilution, substrate was TMB ultra stopped with 0.5M sulphuric acid and read at 450nm, all incubations were 60 minutes at 25°C except for 20-minute final substrate reaction. *OD signal minus the blank reading, average of duplicate test results given for each sample. Duplicate average values used to calculate overall average for positive and negative Anti-HCV samples then used to calculate average positive/negative ratio and positive-negative value. The NS5b antigen coating concentration of 5µg/ml gave the highest combined positive/negative ratio and positive minus negative value.

Table 31 shows the results of the NS5b antigen coating optimisation. The antigen was coated at 4 different concentrations, from 10 µg/mL down to 1.25 µg/mL. The optimum concentration chosen was 5 µg/mL.

NS4 PrSpc Antigen µg/ml	Serum Sample	Signal OD*	Average	Pos/Neg ratio	Av. Pos - Neg
5	POS6	2.93		2.47	1.52
	POS7	1.82	2.56		
	POS8	2.93			
	NEG5	1.54			
	NEG6	0.49	1.04		
	NEG7	1.08			
	Blank	0.08			
2.5	POS6	2.50		3.28	1.45
	POS7	0.81	2.08		
	POS8	2.94			
	NEG5	1.01			
	NEG6	0.30	0.64		
	NEG7	0.60			
	Blank	0.06			
1.25	POS6	1.99		8.38	1.51
	POS7	0.22	1.72		
	POS8	2.94			
	NEG5	0.27			
	NEG6	0.29	0.20		
	NEG7	0.06			
	Blank	0.06			
0.625	POS6	0.52		7.28	0.78
	POS7	0.06	0.90		
	POS8	2.12			
	NEG5	0.22			
	NEG6	0.11	0.12		
	NEG7	0.05			
	Blank	0.05			

Table 32 Optimisation of NS4 PrSpc antigen coating concentration. Optimal NS4 PrSpc antigen concentration determined by coating at 4 dilutions from 10 to 1.25 µg/ml and tested with 3 Anti-HCV positive and 3 Anti-HCV negative serum. Serum was used at 1:20 dilution, blocking buffer was 1% BSA, secondary antibody was used at 1:20000 dilution, substrate was TMB ultra stopped with 0.5M sulphuric acid and read at 450nm, all incubations were 60 minutes at 25°C except for 20-minute final substrate reaction. *OD signal minus the blank reading, average of duplicate test results given for each sample. Duplicate average values used to calculate overall average for positive and negative Anti-HCV samples then used to calculate average positive/negative ratio and positive-negative value. The NS4 PrSpc antigen coating concentration of 1.25µg/ml gave the highest combined positive/negative ratio and positive minus negative value.

Table 32 shows the results of the commercially purchased NS4 PrSPc protein. As only 1 mg of antigen was purchased the antigen dilution series was started lower and ran from 5 µg/ml down to 0.625 µg/mL. The optimum concentration chosen was 1.25 µg/mL.

12.2.7 DBS PRIMARY ANTIBODY DILUTION OPTIMISATION

The primary antibody dilution optimisation was repeated for DBS samples, as described in section 11.6.1.7.

To find the optimum dilution for DBS samples, both the NS3 and NS5a ELISAs were tested with multiple samples and the optimum dilution across the 2 assays chosen.

Antigen	DBS Dilution Factor	DBS Sample	Signal OD*	Average	Pos/Neg ratio	Av. Pos - Neg
NS3 Gt1a	1	DBS POS1	0.79	1.30	11.49	1.19
		DBS POS2	0.41			
		DBS POS3	2.70			
		DBS NEG 1	INS	0.11		
		DBS NEG 2	0.11			
		DBS NEG 3	0.12			
	2	DBS POS1	0.42	1.18	15.99	1.11
		DBS POS2	0.56			
		DBS POS3	2.57			
		DBS NEG 1	0.06	0.07		
		DBS NEG 2	0.07			
		DBS NEG 3	0.09			
	5	DBS POS1	0.22	0.80	13.33	0.74
		DBS POS2	0.38			
		DBS POS3	1.81			
		DBS NEG 1	0.05	0.06		
		DBS NEG 2	0.07			
		DBS NEG 3	0.07			
	10	DBS POS1	0.16	0.69	13.07	0.64
		DBS POS2	0.14			
		DBS POS3	1.77			
		DBS NEG 1	0.05	0.05		
		DBS NEG 2	0.06			
		DBS NEG 3	0.06			
	20	DBS POS1	0.08	0.62	11.82	0.57
		DBS POS2	0.06			
		DBS POS3	1.73			
		DBS NEG 1	0.05	0.05		
		DBS NEG 2	0.06			
		DBS NEG 3	0.06			
	Blank		0.04			

Table 33 Optimisation of DBS Sample dilution using the NS3 ELISA.. Optimisation of DBS dilution was performed by testing Anti-HCV positive and Anti-HCV negative serum samples at dilutions from neat to 1:20. NS3 antigen was coated at 5 µg/ml concentration, blocking buffer was 1% BSA, secondary antibody was used at 1:20000 dilution, substrate was TMB ultra stopped with 0.5M sulphuric acid and read at 450nm, all incubations were 60 minutes at 25°C except for 20-minute final substrate reaction. *OD signal minus the blank reading, average of duplicate test results given for each sample. Duplicate average values used to calculate overall average for positive and negative Anti-HCV samples then used to calculate average positive/negative ratio and positive-negative value for each DBS dilution. The DBS dilution of 1:2 gave the highest combined positive/negative ratio and positive minus negative value.

Antigen	DBS Dilution Factor	DBS Sample	Signal OD*	Average	Pos/Neg ratio	Av. Pos - Neg
NS5a Gt1a	1	DBS POS4	2.96	2.96	15.26	2.77
		DBS POS5	2.96			
		DBS POS6	2.96			
		DBS NEG 4	0.08	0.19		
		DBS NEG 5	0.17			
		DBS NEG 6	0.34			
	2	DBS POS4	2.96	2.81	27.43	2.71
		DBS POS5	2.50			
		DBS POS6	2.96			
		DBS NEG 4	0.06	0.10		
		DBS NEG 5	0.09			
		DBS NEG 6	0.15			
	5	DBS POS4	2.34	2.14	22.55	2.05
		DBS POS5	1.13			
		DBS POS6	2.96			
		DBS NEG 4	0.05	0.10		
		DBS NEG 5	0.09			
		DBS NEG 6	0.14			
	10	DBS POS4	1.20	1.66	23.00	1.58
		DBS POS5	0.81			
		DBS POS6	2.96			
		DBS NEG 4	0.05	0.07		
		DBS NEG 5	0.07			
		DBS NEG 6	0.10			
	20	DBS POS4	0.27	1.11	16.94	1.05
		DBS POS5	0.11			
		DBS POS6	2.96			
		DBS NEG 4	0.05	0.07		
		DBS NEG 5	0.06			
		DBS NEG 6	0.09			
	Blank		0.04			

Table 34 Optimisation of DBS Sample dilution using the NS5a ELISA. Optimisation of DBS dilution was performed by testing Anti-HCV positive and Anti-HCV negative serum samples at dilutions from neat to 1:20. NS5a antigen was coated at 1.255 µg/ml concentration, blocking buffer was 1% BSA, secondary antibody was used at 1:20000 dilution, substrate was TMB ultra stopped with 0.5M sulphuric acid and read at 450nm, all incubations were 60 minutes at 25°C except for 20-minute final substrate reaction. *OD signal minus the blank reading, average of duplicate test results given for each sample. Duplicate average values used to calculate overall average for positive and negative Anti-HCV samples then used to calculate average positive/negative ratio and positive-negative value for each DBS dilution. The DBS dilution of 1:2 gave the highest combined positive/negative ratio and positive minus negative value.

Table 33 shows the results of the DBS sample dilution optimisation using the NS3 ELISA, Table 34 shows the results using the NS5a ELISA. From the 2 sets of results it was decided to use a dilution of 1:2 for DBS samples, as this gave the highest signal while maintaining a low background.

12.3 ELISA VALIDATION

12.3.1 SERUM RESULTS

For validation with serum samples a total of 95 anti-HCV positive, 92 anti-HCV negative and 1 anti-HCV equivocal samples were tested. Of the 95 anti-HCV positive samples, 50 were HCV RNA positive and 45 were HCV RNA negative. Of the HCV RNA positive samples, 38 were genotype 1, 3 were genotype 2, 48 were genotype 3, 2 were genotype 4, 1 was genotype 6 and 3 were mixed 1/3 genotypes. The single anti-HCV equivocal sample was HCV RNA negative.

Samples were tested with each assay using the optimised antigen coating concentration and optimised procedure described in 11.7.1.1. Results produced in each assay were put through ROC analysis as described in 11.7.2. For a full list of the HCV antigen results for each serum sample see Appendix, Table 51.

12.3.1.1 CORE

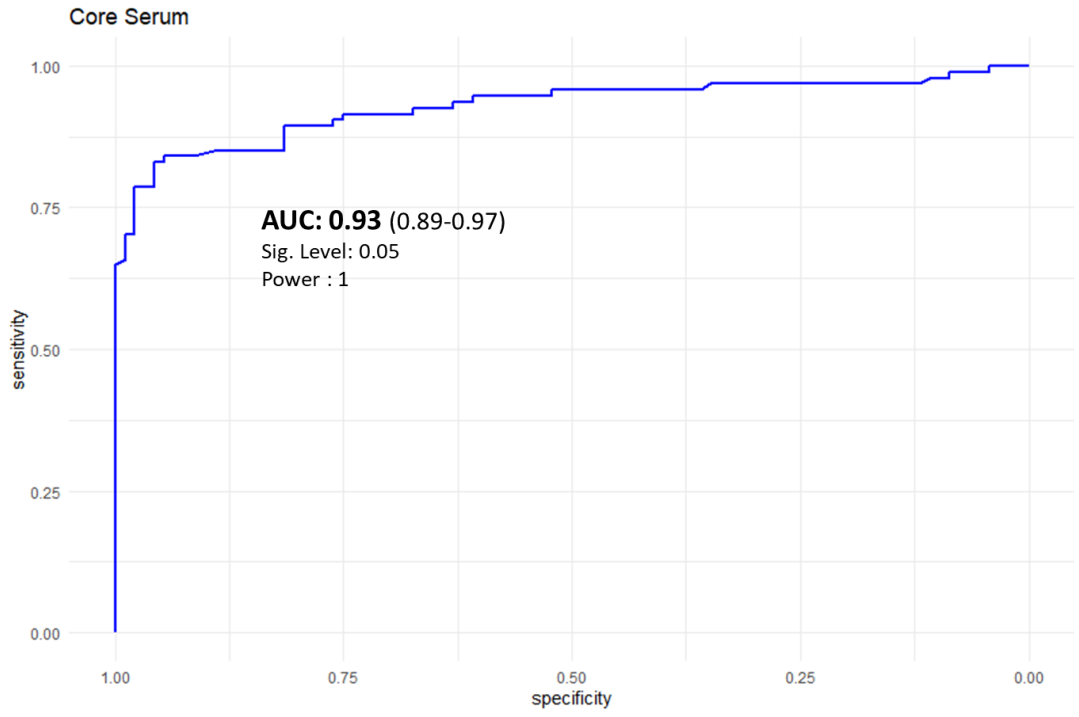

Figure 88 ROC curve produced from testing panel of anti-HCV positive and negative serum samples with Core antigen ELISA. The AUC value (95% C.I.), significance and statistical power are listed below the ROC curve.

Positive Cut-Off Method	Positive Cut Off ≥	Sensitivity %	Specificity %
Max. Specificity	0.99	64.9	100
Youden	0.63	82.98	95.65
Closest Top Left	0.62	84.04	94.56

Table 35 The 3 different positive cut-off threshold values calculated using maximum specificity, Youden and closest top left with the corresponding sensitivity and specificities for the Core antigen ELISA with serum samples.

Figure 88 shows the ROC curve and AUC value produced from the analysis of results for testing the panel of serum samples with the HCV Core antigen ELISA, Table 35 lists the 3 different positive cut-off thresholds determined by maximum specificity, Youden index and closest top left methods, with the corresponding sensitivities and specificities. The curves produced from ROC analysis and the corresponding AUC are an indicator of test performance, a perfect assay has a completely square plot and an AUC value of 1, while a high performing assay has an AUC value ≥ 0.9. An assay which performs no better than chance has a plot with diagonal line through the middle and an AUC value of 0.5. Overall, the optimised Core antigen assay performed highly with serum samples, indicated with an AUC value of 0.93, significance level of 0.05 and a statistical power of 1. Despite this the background of the assay was higher than desired, requiring a positive cut-off value to be set ≥0.99 to achieve a specificity of 100%. At this level of specificity 64.9% of samples were detected with the Core antigen assay. Alternative ways of setting a positive cut-off value with ROC analysis include the Youden index, and the closest top left analysis. Using the Youden index gave a positive cut-off value of ≥0.63, which increased the sensitivity to 82.98% while reducing the specificity to 95.65%. Closest top left analysis gave a very similar positive cut-off of ≥0.62, with sensitivity of 84.04% and specificity of 94.56%. Overall, these show a high level of reactivity in anti-HCV positive samples for the Core antigen.

12.3.1.2 NS3

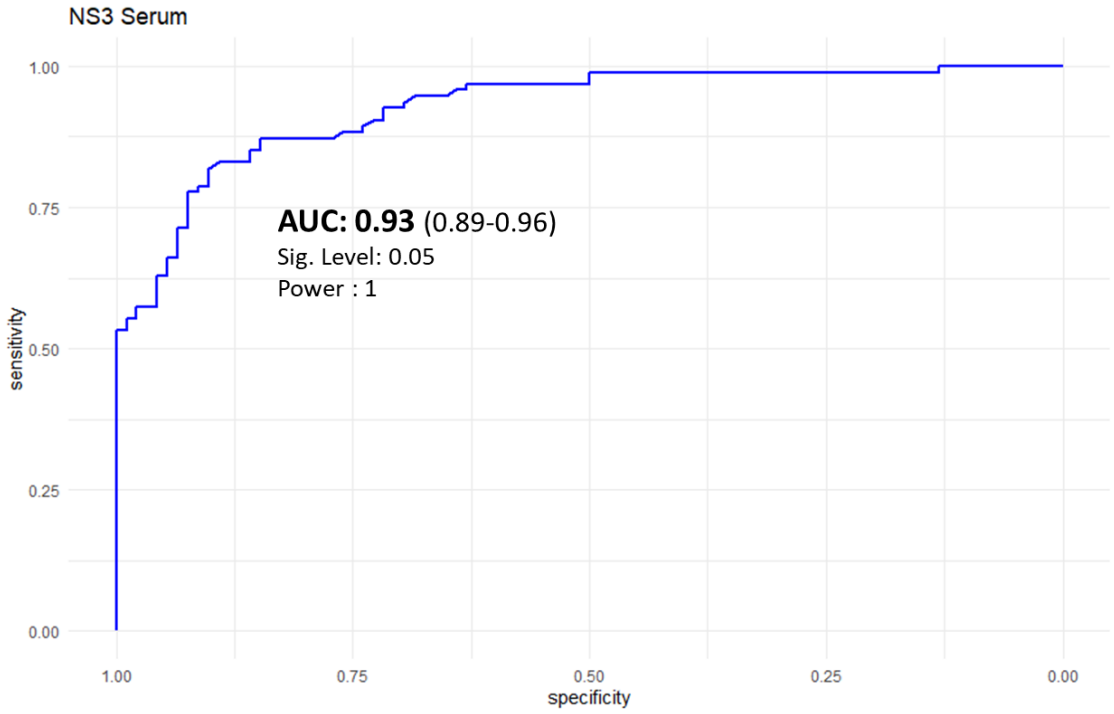

Figure 89 ROC curve produced from testing panel of anti-HCV positive and negative serum samples with the NS3 antigen ELISA. The AUC value (95% C.I.), significance and statistical power are listed below the ROC curve.

Positive Cut-Off Method	Positive Cut Off ≥	Sensitivity %	Specificity %
Max. Specificity	0.62	53.19	100
Youden	0.25	81.91	90.21
Closest Top Left	0.2	87.2	84.78

Table 36 The 3 different positive cut-off threshold values calculated using maximum specificity, Youden and closest top left with the corresponding sensitivity and specificities for the NS3 antigen ELISA with serum samples.

Figure 89 above shows the ROC curve produced from the analysis of results from testing the panel of serum samples with the HCV NS3 antigen ELISA, with an AUC of 0.93 at a significance level of 0.05 and a statistical power of 1. The 3 different positive cut-off values and corresponding sensitivity and specificities are listed in Table 36. The ROC curve shows a similar overall shape to the HCV core ROC curve with an identical AUC of 0.93, indicating an assay giving a similar overall level of performance. The NS3 antigen showed a lower background in anti-HCV negative serum samples than the Core assay, but was still high, with a cut-off of ≥0.62 required to achieve a specificity of 100%. At this specificity 53.7% of samples were positive, showing positive reactivity in a lower proportion

of samples than with the HCV core assay. Using the Youden index gave a positive cut-off value of ≥0.25, which increased the sensitivity to 81.91% while reducing the specificity to 90.21%. Closest top left analysis gave a positive cut-off of ≥0.2, with sensitivity of 87.2% but an even lower specificity of 84.78%. Overall, the Core assay showed a lower background level than with the core assay and a lower overall reactivity level.

12.3.1.3 NS4

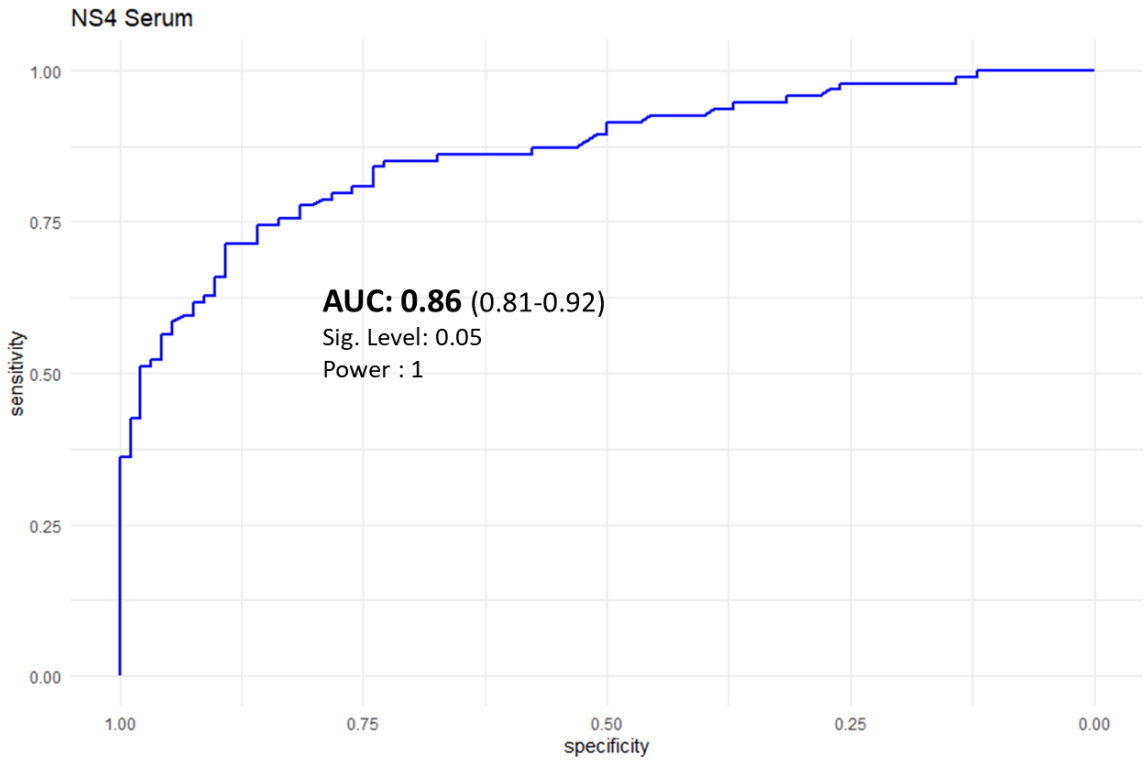

Figure 90 ROC curve produced from testing panel of anti-HCV positive and negative serum samples with the NS4 antigen ELISA. The AUC value (95% C.I.), significance and statistical power are listed below the ROC curve.

Positive Cut-Off Method	Positive Cut Off ≥	Sensitivity %	Specificity %
Max. Specificity	1.01	36.17	100
Youden	0.4	71.28	89.13
Closest Top Left	0.34	77.66	81.52

Table 37 The 3 different positive cut-off threshold values calculated using maximum specificity, Youden and closest top left with the corresponding sensitivity and specificities for the NS4 antigen ELISA with serum samples.

Figure 90 shows the ROC curve produced from the analysis of results from testing the panel of serum samples with the HCV NS4 antigen ELISA, with an AUC of 0.86 at a significance level of 0.05 and a statistical power of 1. Table 37 lists the 3 different positive cut-off values and the corresponding sensitivity and specificities. Overall, the NS4 antigen performed less well than either the Core or NS3 assays, with a lower AUC value of 0.86. The background level in anti-HCV negative serum was again high, with a positive cut-off value of ≥1 required to produce a specificity of 100%, giving a sensitivity of only 33.7%. Using the Youden analysis lowered the positive cut-off to 0.4, increasing the sensitivity to 71.28% but dropping the specificity to 89.23%. Closest top left analysis produced an even lower positive cut-off value of 0.34, which further increased sensitivity to 77.66% but further decreasing specificity to 81.52%.

12.3.1.4 NS5A

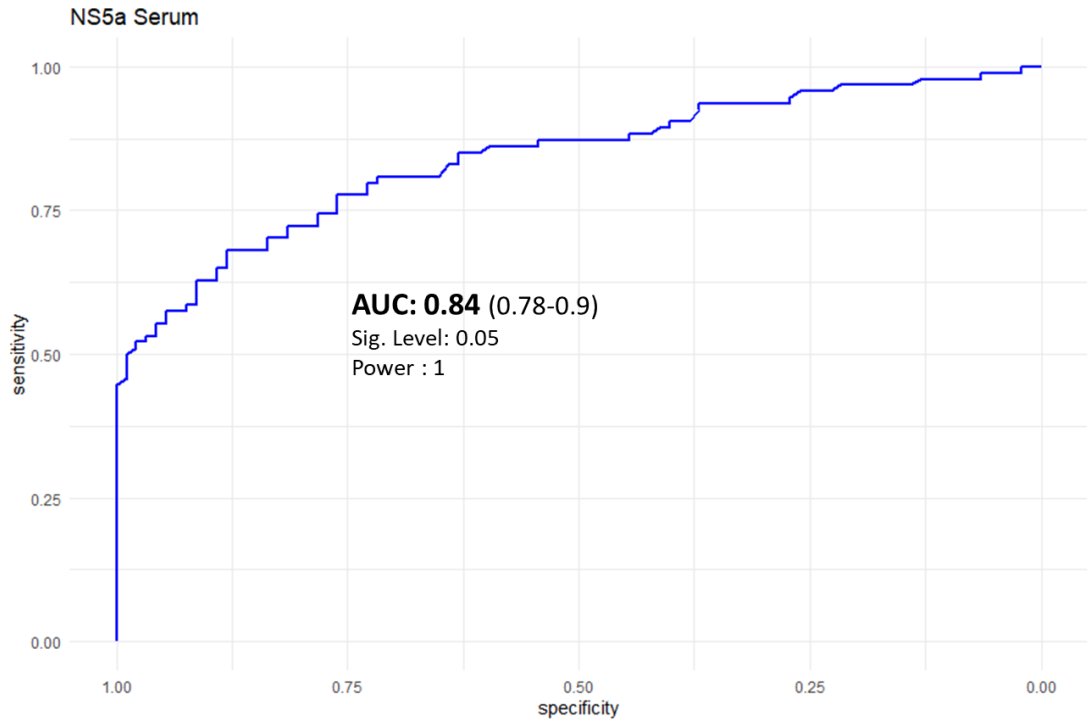

Figure 91 ROC curve produced from testing panel of anti-HCV positive and negative serum samples with the NS5a antigen ELISA. The AUC value (95% C.I.), significance and statistical power are listed below the ROC curve.

Positive Cut-Off Method	Positive Cut Off ≥	Sensitivity %	Specificity %
Max. Specificity	0.34	44.7	100
Youden	0.17	68.09	88.04
Closest Top Left	0.11	77.66	76.09

Table 38 The 3 different positive cut-off threshold values calculated using maximum specificity, Youden and closest top left with the corresponding sensitivity and specificities for the NS5a antigen ELISA with serum samples.

Figure 91 shows the ROC curve produced from the analysis of results from testing the panel of serum samples with the HCV NS5a antigen ELISA, with an AUC of 0.84 at a significance level of 0.05 and a statistical power of 1. Table 38 lists the 3 different positive cut-off values and the corresponding sensitivity and specificities. Overall, the background level seen with the NS5a assay in anti-HCV negative serum samples was lower than the assays described above. A specificity of 100% was achieved with a positive cut-off of ≥0.34, with 44.2% of positive samples reactive at this level. Though the background level was improved overall, the proportion of anti-HCV positive samples reactive with the NS5a assay was lower than with the Core or NS3 assays. Using the Youden and Closest top left analysis lowered the positive cut-ff off values further, to 0.17 and 0.11, respectively. These increased the sensitivities to 68.09% and 77.66% but lowered the specificities to 88.04% and 76.09%.

12.3.1.5 NS5B

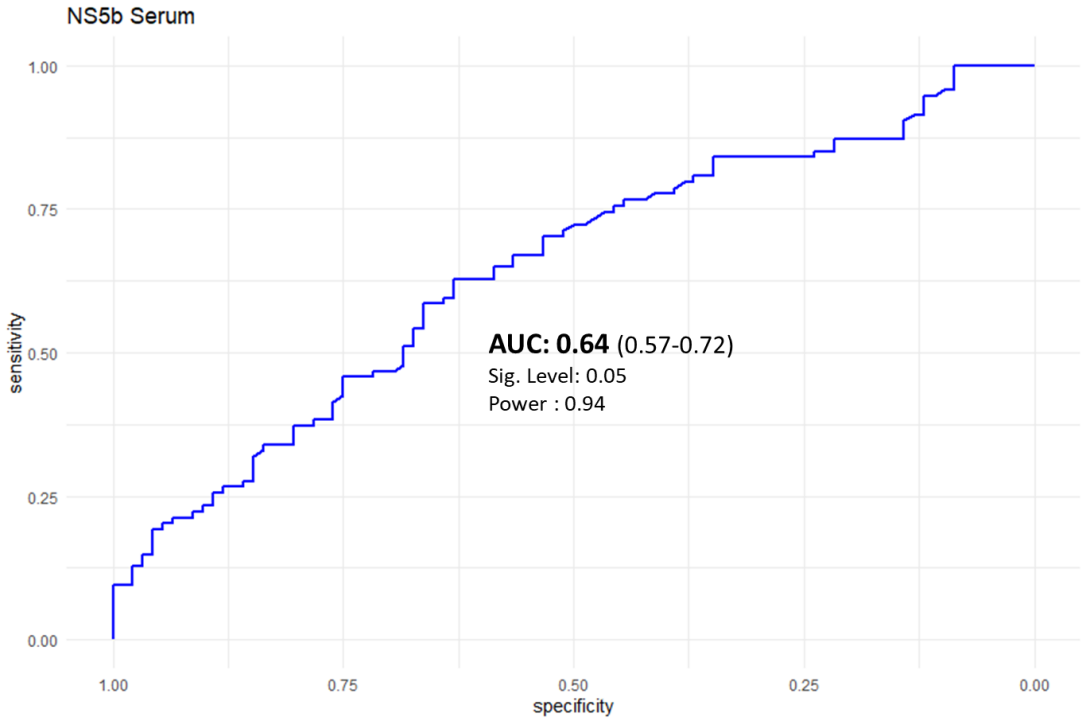

Figure 92 ROC curve produced from testing panel of anti-HCV positive and negative serum samples with the NS5b antigen ELISA. The AUC value (95% C.I.), significance and statistical power are listed below the ROC curve.

Positive Cut-Off Method	Positive Cut Off ≥	Sensitivity %	Specificity %
Max. Specificity	1.61	9.57	100
Youden	0.15	63.04	62.76
Closest Top Left	0.15	63.04	62.76

Table 39 The 3 different positive cut-off threshold values calculated using maximum specificity, Youden and closest top left with the corresponding sensitivity and specificities for the NS5b antigen ELISA with serum samples.

Figure 92 shows the ROC curve produced from the analysis of results from testing the panel of serum samples with the HCV NS5b antigen ELISA. The AUC was low at 0.64 and at a significance level of 0.05 the statistical power was 0.94, as opposed to 1 for all previous ROC analysis. Table 39 lists the positive and negative cut-off values for the 3 different methods and the corresponding sensitivities and specificities. The ROC curve shows the NS5b assay did not work very well, as the ROC curve is a diagonal line just above the middle of the plot area combined with a low AUC value of 0.64 shows an assay only just working better than chance. The background level was very high, requiring a positive cut-off value of ≥1.5 to achieve a specificity of 100%. At this cut-off value only 10.5% of

samples were positive. Using Youden and Closest top left analysis both determined a positive cut-off value of 0.15, which at this level increased the sensitivity to 63.04% but this was combined with a low specificity of 62.76%.

12.3.1.6 NS4 PR SPC

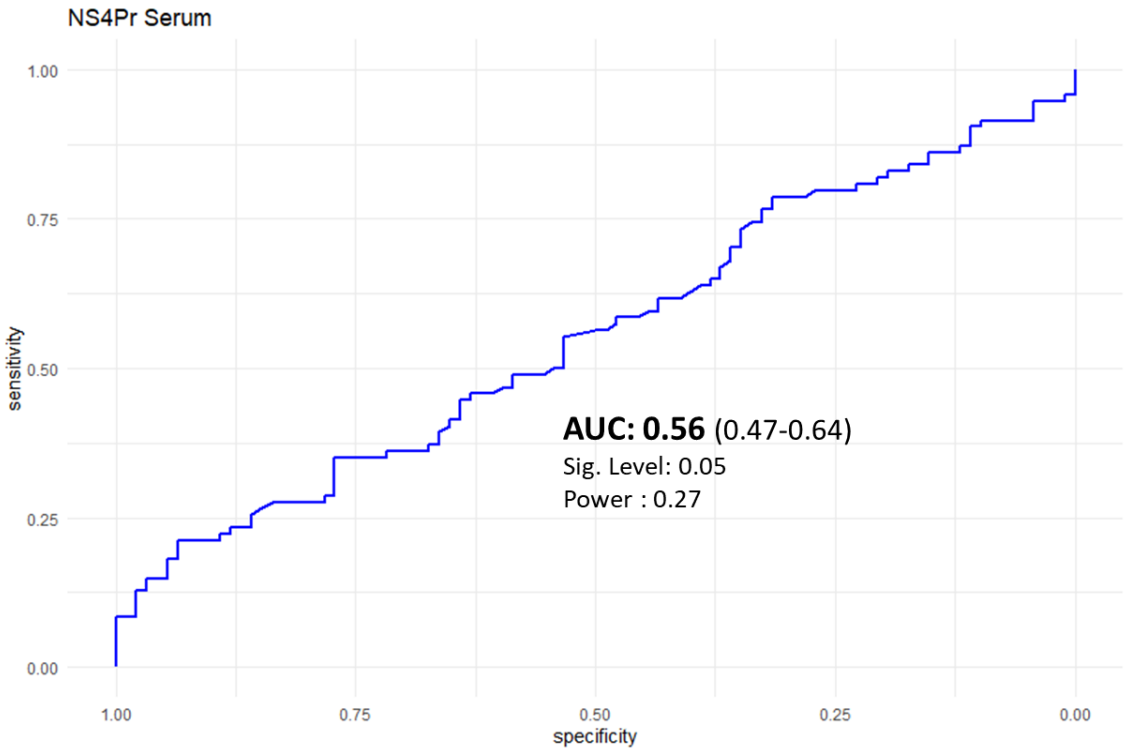

Figure 93 ROC curve produced from testing panel of anti-HCV positive and negative serum samples with the NS4 PrSPc antigen ELISA. The AUC value (95% C.I.), significance and statistical power are listed below the ROC curve.

Positive Cut-Off Method	Positive Cut Off ≥	Sensitivity %	Specificity %
Max. Specificity	2.7	8.5	100
Youden	0.47	21.27	93.47
Closest Top Left	0.19	55.32	53.26

Table 40 The 3 different positive cut-off threshold values calculated using maximum specificity, Youden and closest top left with the corresponding sensitivity and specificities for the NS4Pr antigen ELISA with serum samples.

Figure 93 shows the ROC curve produced from the analysis of results from testing the panel of serum samples with the HCV NS4PrSpc antigen ELISA. The AUC was very low at 0.56 and at a significance level of 0.05 the statistical power was only 0.27, showing a ROC analysis which was not statistically valid. Table 40 lists the positive and negative cut-off values for the 3 different methods and the

corresponding sensitivities and specificities. The ROC curve shows the NS4PrSpc assay was poor, the AUC as the ROC curve is a diagonal line through the middle of the plot area combined with a low AUC value of 0.56 shows an assay working no better than chance. The main issue with the assay was the background level in anti-HCV negative sample, requiring a positive cut-off value of ≥2.7 to achieve a specificity of 100%. As the maximum optical reading is 3.0 it made it impossible to reliably distinguish between positive and negative result. Using Youden analysis dropped this positive cut-off to 0.47, but even at this level only 21.27% of samples were reactive with a specificity of 93.47%, and as the original ROC analysis was not statistically valid this is an unreliable way to set a positive cut-off value. Using closest top-left analysis further dropped to positive cut-ff level further but dropped the specificity to a level which was no better than chance, 53.26%.

12.3.2 DBS RESULTS

For validation with DBS samples a total of 95 anti-HCV positive, 92 anti-HCV negative and 1 anti-HCV equivocal samples were tested. Of the 95 anti-HCV positive samples, 50 were HCV RNA positive and 45 were HCV RNA negative. Of the HCV RNA positive samples, 38 were genotype 1, 3 were genotype 2, 48 were genotype 3, 2 were genotype 4, 1 was genotype 6 and 3 were mixed 1/3 genotypes. The single anti-HCV equivocal sample was HCV RNA negative.

Samples were tested with each assay using the optimised antigen coating concentration and optimised procedure described in section 11.7.1.1. Results produced in each assay underwent ROC analysis as described in section 11.7.2. For a full list of the HCV antigen results for each serum sample see Appendix, Table 52.

12.3.2.1 CORE

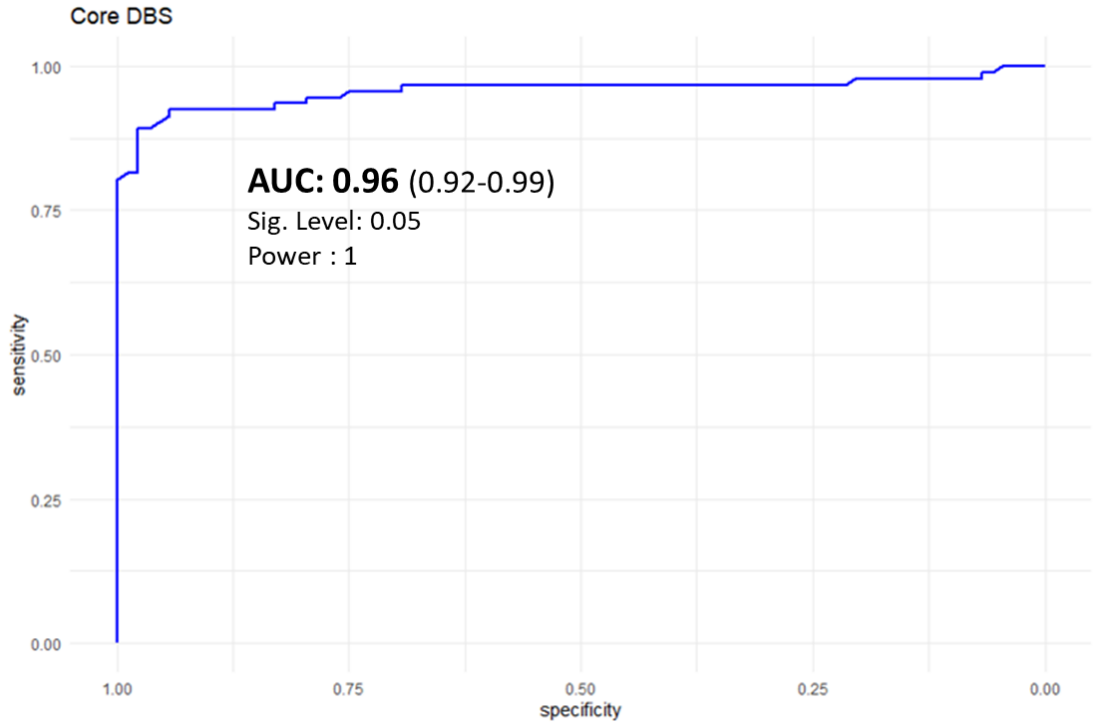

Figure 94 ROC curve produced from testing panel of anti-HCV positive and negative DBS samples with the Core antigen DBS ELISA. The AUC value (95% C.I.), significance and statistical power are listed below the ROC curve.

Positive Cut-Off Method	Positive Cut Off ≥	Sensitivity %	Specificity %
Max. Specificity	0.26	79.3	100
Youden	0.2	89.1	97.7
Closest Top Left	0.17	92.4	94.3

Table 41 The 3 different positive cut-off threshold values calculated using maximum specificity, Youden and closest top left with the corresponding sensitivity and specificities for the Core antigen ELISA with DBS samples.

Figure 94 shows the ROC curve produced from the analysis of results from testing the panel of DBS samples with the HCV Core antigen ELISA, with an AUC of 0.96 at a significance level of 0.05 and a statistical power of 1. The 3 different positive cut-off values and corresponding sensitivity and specificities are listed in Table 41. The shape of the ROC curve and the AUC value of 0.96 shows a high performing assay. The sample background was much lower than previously seen when testing serum samples with the HCV core antigen assay, a positive cut-off of ≥0.26 gave a specificity of 100%, with a sensitivity of 79.3%. Using Youden method to set the threshold dropped the positive cut-ff to 0.2, increasing the sensitivity to 89.1% while maintaining a high specificity of 97.7%. Closest

top left analysis dropped the cut-off further to 0.17, giving a sensitivity of 92.4% with a specificity of 94.3%.

12.3.2.2 NS3

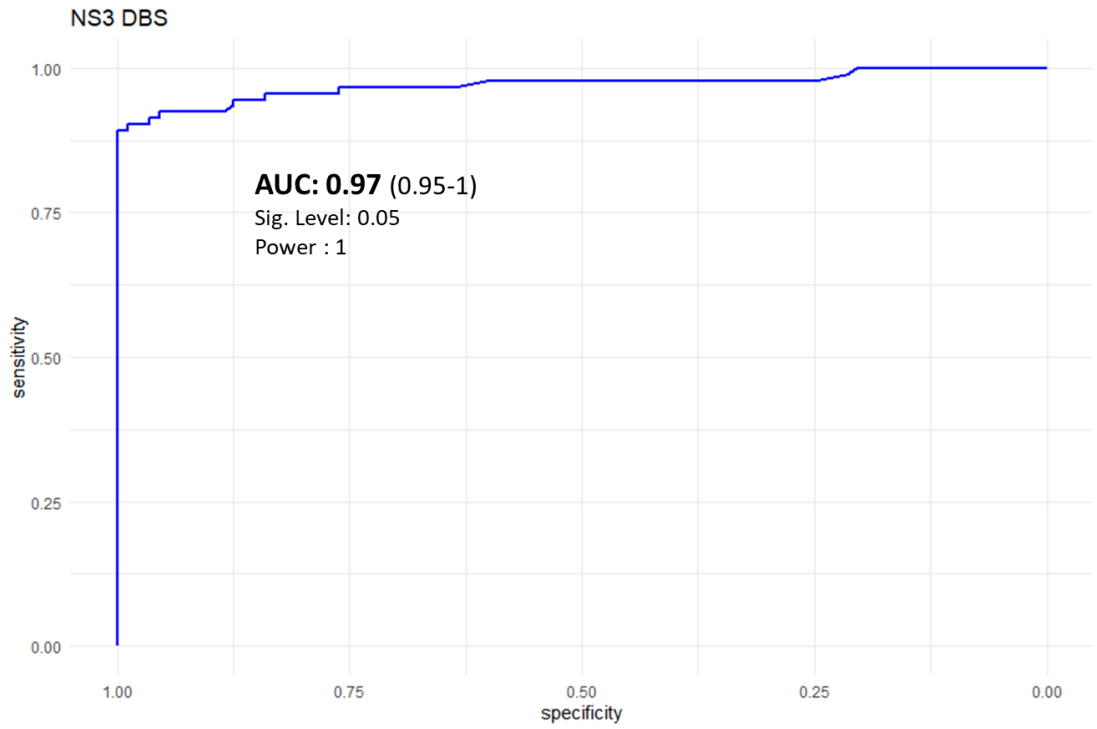

Figure 95 ROC curve produced from testing panel of anti-HCV positive and negative DBS samples with the NS3 antigen DBS ELISA. The AUC value (95% C.I.), significance and statistical power are listed below the ROC curve.

Positive Cut-Off Method	Positive Cut Off ≥	Sensitivity %	Specificity %
Max. Specificity	0.19	89.1	100
Youden	0.19	89.1	100
Closest Top Left	0.14	92.4	95.45

Table 42 The 3 different positive cut-off threshold values calculated using maximum specificity, Youden and closest top left with the corresponding sensitivity and specificities for the NS3 antigen ELISA with DBS samples.

Figure 95 shows the ROC curve produced from the analysis of results from testing the panel of DBS samples with the NS3 antigen ELISA, with an AUC of 0.97 at a significance level of 0.05 and a statistical power of 1. The 3 different positive cut-off values and corresponding sensitivity and specificities are listed in Table 42. The level of performance is similar to the Core assay, with an AUC value of 0.97 and a much lower background level than experienced with serum samples. A positive

cut-off of ≥0.26 was required to achieve a specificity of 100% with 88% of samples reactive, higher than with the core antigen assay. Using the Youden method to calculate the positive cut-off gave exactly the same threshold. Using closest top left dropped the threshold slightly to 0.14, increasing the sensitivity further to 92.4% but lowering the specificity to 95.45%.

12.3.2.3 NS4

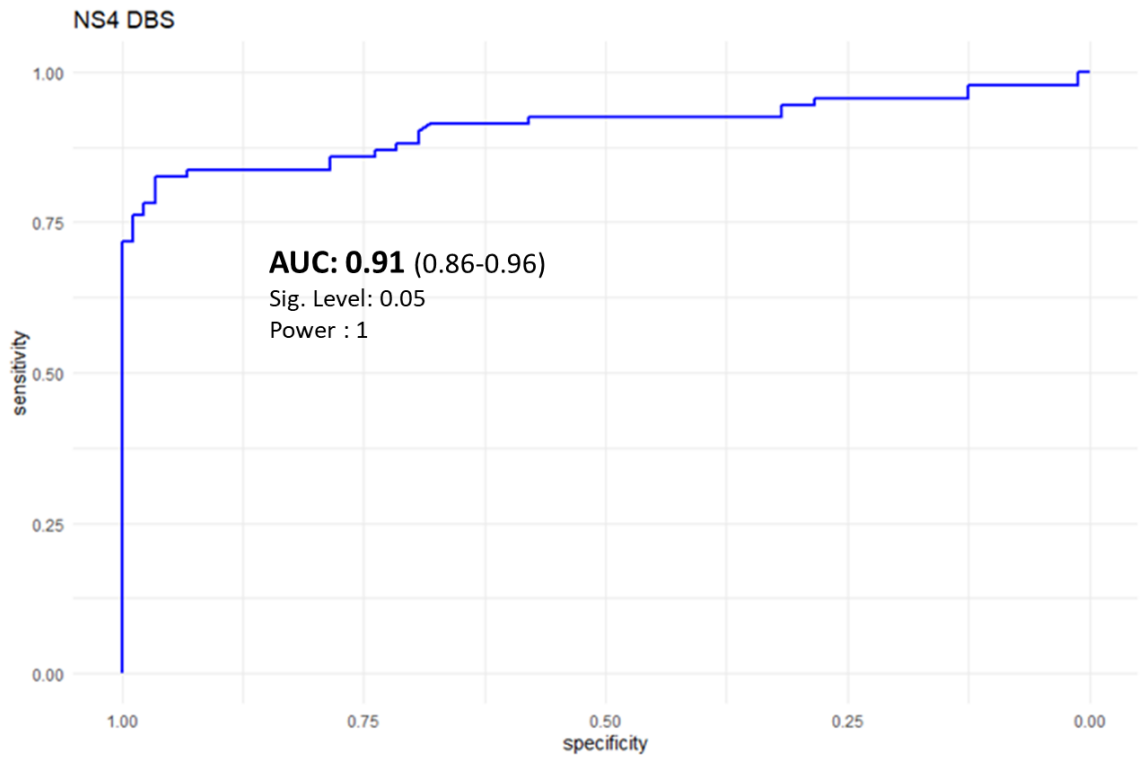

Figure 96 ROC curve produced from testing panel of anti-HCV positive and negative DBS samples with the NS4 antigen DBS ELISA. The AUC value (95% C.I.), significance and statistical power are listed below the ROC curve.

Positive Cut-Off Method	Positive Cut Off ≥	Sensitivity %	Specificity %
Max. Specificity	0.46	71.7	100
Youden	0.33	82.6	96.6
Closest Top Left	0.31	83.7	93.18

Table 43 The 3 different positive cut-off threshold values calculated using maximum specificity, Youden and closest top left with the corresponding sensitivity and specificities for the NS4 antigen ELISA with DBS samples.

Figure 96 shows the ROC curve produced from the analysis of results from testing the panel of DBS samples with the NS4 antigen ELISA, with an AUC of 0.91 at a significance level of 0.05 and a statistical power of 1. Table 43 lists the different positive cut-off thresholds with sensitivities and

specificities. The NS4 antigen assay produced a high performing assay with DBS samples with an AUC value of 0.91, though it performed less well than either the Core or NS3 assays. The background was also higher than either of those 2 assays, requiring a positive cut-off of 0.46 to achieve a specificity of 100%. with a sensitivity of 71.7% at this level. Both Youden and closest top left analysis set similar cut off levels of 0.33 and 0.31, increasing the sensitivities to above 80% while maintaining specificities above 90%.

12.3.2.4 NS5A

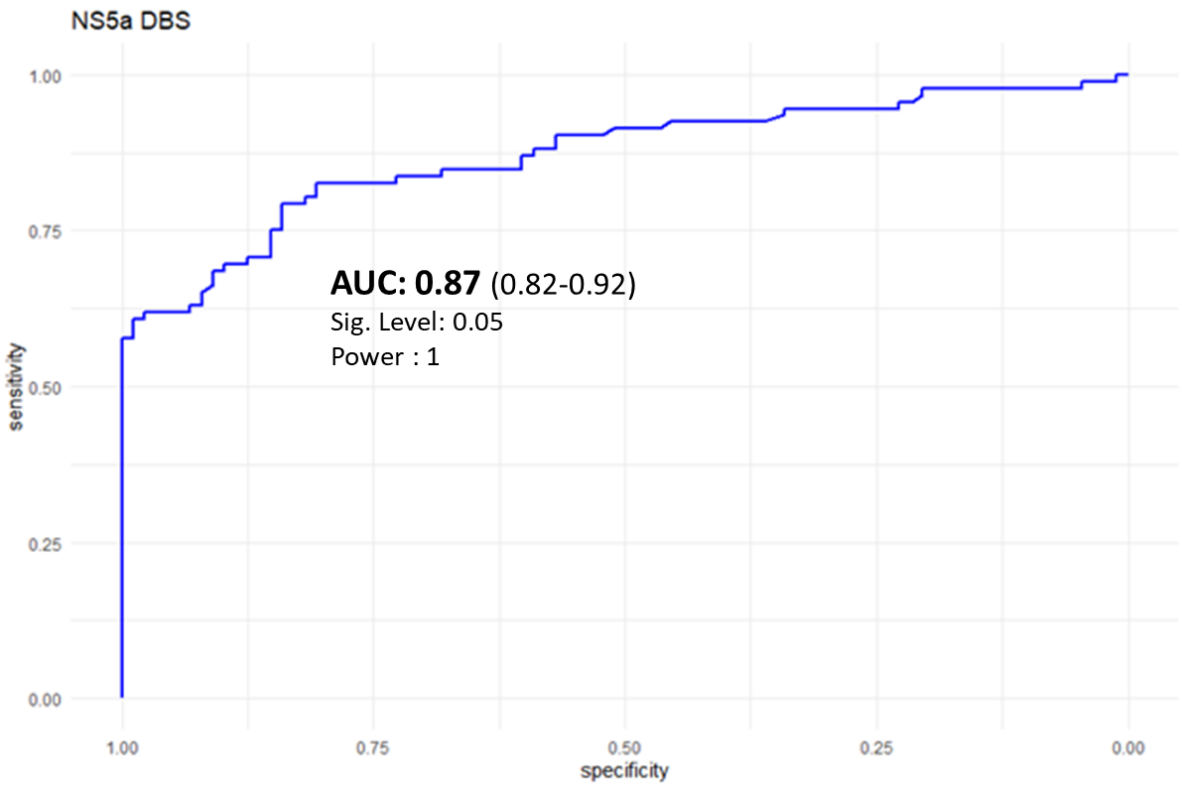

Figure 97 ROC curve produced from testing panel of anti-HCV positive and negative DBS samples with the NS5a antigen DBS ELISA. The AUC value (95% C.I.), significance and statistical power are listed below the ROC curve.

Positive Cut-Off Method	Positive Cut Off ≥	Sensitivity %	Specificity %
Max. Specificity	0.22	57.6	100
Youden	0.11	79.35	84.1
Closest Top Left	0.1	82.61	80.68

Table 44 The 3 different positive cut-off threshold values calculated using maximum specificity, Youden and closest top left with the corresponding sensitivity and specificities for the NS5a antigen ELISA with DBS samples.

Figure 97 shows the ROC curve produced from the analysis of results from testing the panel of DBS samples with the NS5a antigen ELISA, with an AUC of 0.87 at a significance level of 0.05 and a statistical power of 1. Table 44 shows the different positive cut-off thresholds with sensitivities and specificities. Overall, the assay performed slightly worse than the previous listed assays with DBS, giving an AUC value of 0.87. The background level in anti-HCV negative samples was again much lower than with serum samples, requiring a positive cut-off level of ≥0.22 to achieve of specificity of 100%, though with a sensitivity of 57.6% at this level he overall level of reactivity in anti-HCV positive samples was less than seen with the core, NS3 and NS4 antigens. Using Youden analysis to lower the positive cut-off to 0.11 increased this reactivity to 79.35% but the specificity dropped down to 84.1%. Using closest top left analysis produced similar results, with a positive cut-off level of 0.1 combined with a sensitivity of 82.61% and a specificity of 80.68%.

12.3.2.5 NS5B

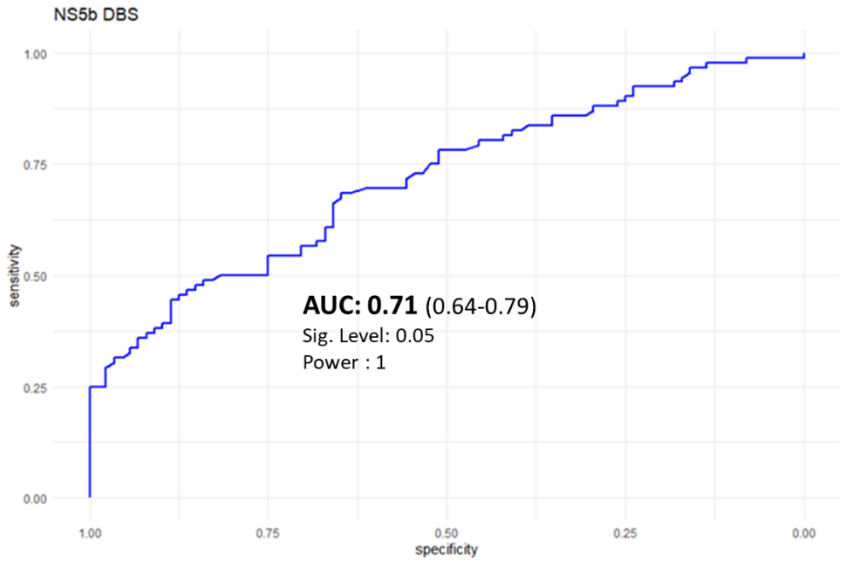

Figure 98 ROC curve produced from testing panel of anti-HCV positive and negative DBS samples with the NS5b antigen DBS ELISA. The AUC value (95% C.I.), significance and statistical power are listed below the ROC curve.

Positive Cut-Off Method	Positive Cut Off ≥	Sensitivity %	Specificity %
Max. Specificity	0.43	25	100
Youden	0.19	68.48	64.77
Closest Top Left	0.19	68.48	64.77

Table 45 The 3 different positive cut-off threshold values calculated using maximum specificity, Youden and closest top left with the corresponding sensitivity and specificities for the NS5b antigen ELISA with DBS samples

Figure 98 shows the ROC curve produced from the analysis of results from testing the panel of DBS samples with the NS5b antigen ELISA, with an AUC of 0.71 at a significance level of 0.05 and a statistical power of 1. Table 45 shows the different positive cut-off thresholds with sensitivities and specificities. This NS5b antigen assay did not work at all when testing serum samples. With DBS samples the assay performed slightly better, but the ROC curve produced was still a diagonal line slightly above the middle of the plot area with an AUC value of 0.71. The background level was higher than with the other assays when testing DBS samples, requiring a positive cut-off of ≥0.43 to achieve a specificity of 100%. At this level only 25% of samples were reactive. Decreasing the positive cut-off value with both Youden and closest top left methods have the same value of 0.19, which increased the sensitivity to 68.58% but this was combined with a large drop in specificity down to 64.77%.

12.3.2.6 NS4 PR SPC

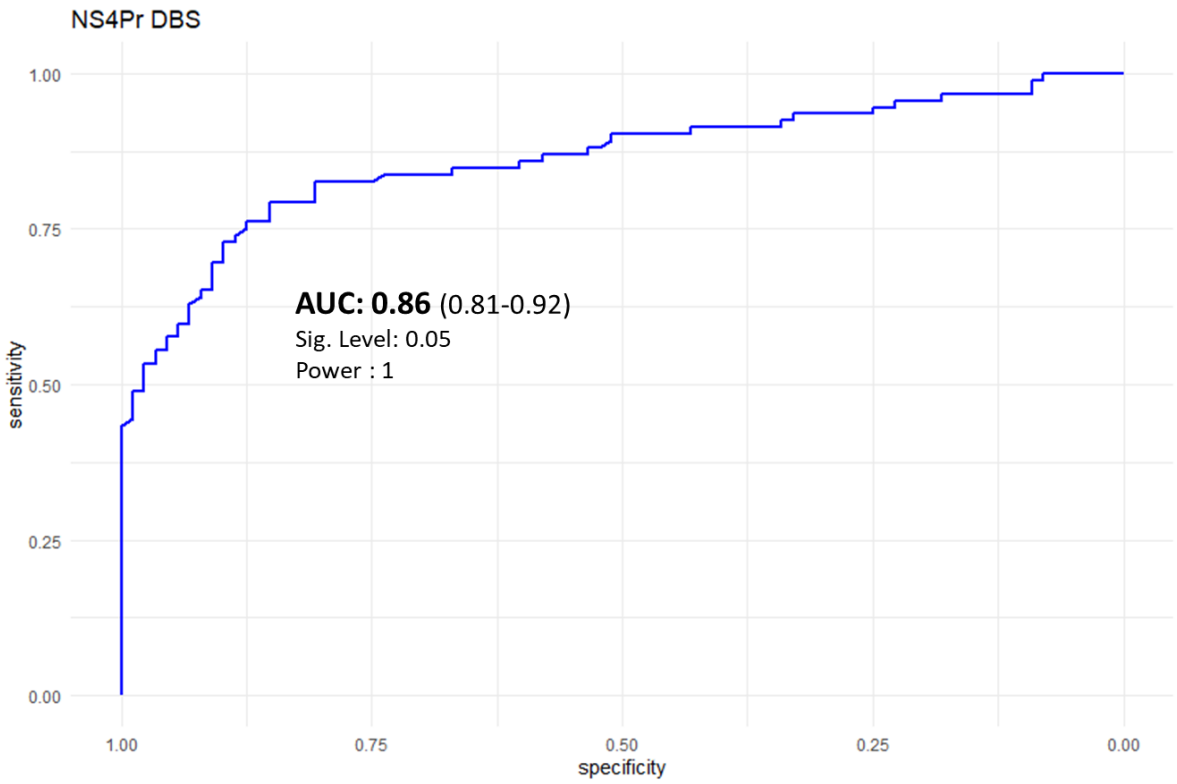

Figure 99 ROC curve produced from testing panel of anti-HCV positive and negative DBS samples with the NS4 PrSpc antigen DBS ELISA. The AUC value (95% C.I.), significance and statistical power are listed below the ROC curve.

Positive Cut-Off Method	Positive Cut Off ≥	Sensitivity %	Specificity %
Max. Specificity	0.35	43.47	100
Youden	0.16	85.2	79.4
Closest Top Left	0.16	85.2	79.4

Table 46 The 3 different positive cut-off threshold values calculated using maximum specificity, Youden and closest top left with the corresponding sensitivity and specificities for the NS4Pr antigen ELISA with DBS samples.

Figure 99 shows the ROC curve produced from the analysis of results from testing the panel of DBS samples with the NS4PrSpc antigen ELISA, with an AUC of 0.86 at a significance level of 0.05 and a statistical power of 1. Table 46 shows the different positive cut-off thresholds with sensitivities and specificities. The NS4 PrSpc antigen assay did not work with serum samples due to a very high background level. However, with DBS samples a working assay was produced with a statistically valid AUC value of 0.86 and a much lower background level, requiring a positive cut-off value of ≥.35 to achieve a specificity of 100%, with a sensitivity of 43.5% at this level. Both Youden and closest top left methods determined an optimum cut-off of 0.16, which increased sensitivity to 85.2% but this dropped the specificity to 79.4%.

12.3.3 COMPARISON ROC CURVES

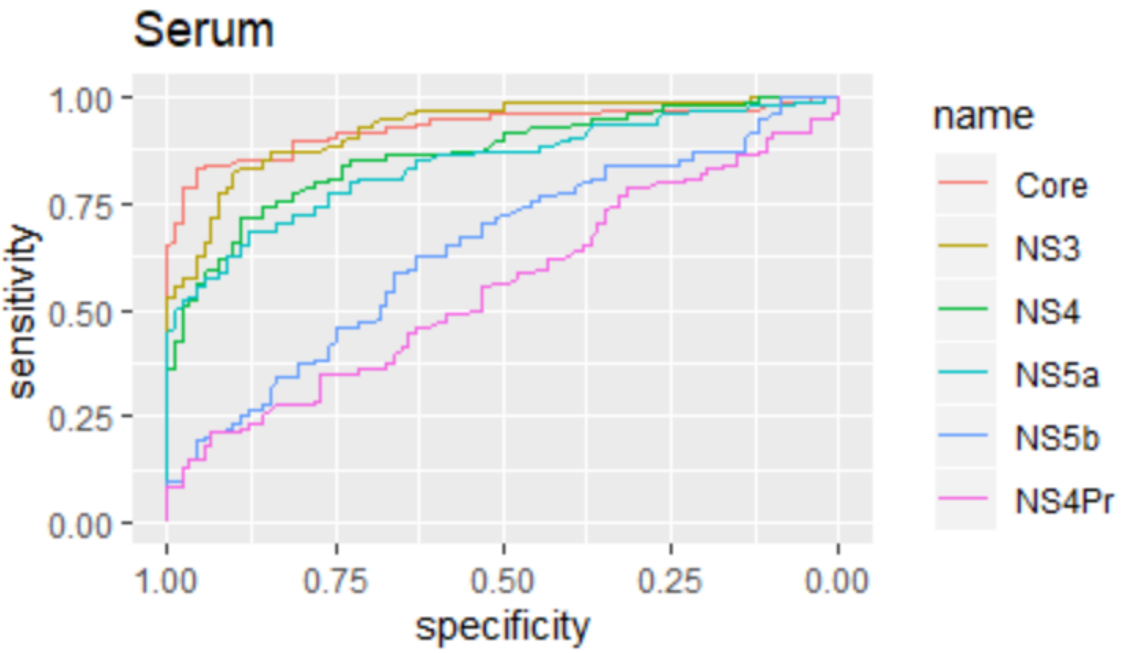

Figure 100 Comparison of HCV Antigen ELISA ROC Curves generated from testing Serum Samples. The Core and NS3 antigen assay ROC the best ROC curves with the highest AUC, followed by the NS4 and NS5a. The NS5b and NS4Pr shows poor ROC curves through the middle area of the chart area.

Sample Type	Assay	AUC (95% CI)	pAUC (95% CI)
Serum	Core	0.93 (0.89-0.97)	0.079 (0.045-0.066)
	NS3	0.93 (0.89-0.96)	0.065 (0.052-0.079)
	NS4	0.86 (0.81-0.92)	0.054 (0.042-0.068)
	NS5a	0.84 (0.78-0.9)	0.055 (0.045-0.066)
	NS5b	0.64 (0.57-0.72)	0.017 (0.009-0.027)
	NS4PrSpc	0.56 (0.47-0.64)	0.015 (0.008-0.025)

Table 47 List of AUC (95%CI) and pAUC(95%CI) for all HCV antigen assays with Serum Samples. The full shape ROC curve is represented with the AUC value, the higher the value the better performing the assay. The pAUC value represents just the high specific area of the curve and enables comparisons between two similar assay, again the higher the value the better performing the assay.

Figure 100 plots each of the ROC curves generated from testing serum samples with HCV antigen ELISAs against each other. From the figure it is clear the Core and NS3 assays are the best performing, followed by the NS4 and NS5a assays, with finally the NS5b performing poorly and the NS4PrSpc not working at all.

Table 47 below lists the AUC and pAUC for each curve, calculated as described in section 11.7.2.1. The AUC enables a comparison between the ROC curves produced by each assay but can struggle to detect a significant difference between two comparable assays. The pAUC, which has been calculated just to include the area above a high specificity of ≥90%, can enable a more discriminating comparison between 2 assays which appear to be performing equally.

The two best performing assays, the Core and NS3, both give the same total AUC so unsurprisingly there is no significant difference between the two assays, p-value 0.97. However, when only the high specificity area above 90% is used to compare the assays through the pAUC, a significant difference is detected between the better performing Core assay and the NS3 assay, p-value 0.04.

Both the NS4 assay, with an AUC of 0.86, and the NS5a assay, with an AUC of 0.84, performed significantly worse than the highest performing Core assay when comparing the total AUC, p-value 0.01 and 0.03 respectively. Their overall performance was so similar there was no significant difference between the two assays when comparing the total AUC, p-value 0.47, or even the high specificity pAUC, p-value 0.89.

Both the NS5b and NS4PrSpc assays performed very poorly. The NS5b was significantly worse than next lowest performing assay, the NS5a, p-value 3.39 $X10^{-6}$. The NS4PrSpc as explained before did not produce a working assay, the ROC curve produced was not statistically valid and produced an assay working no better than chance.

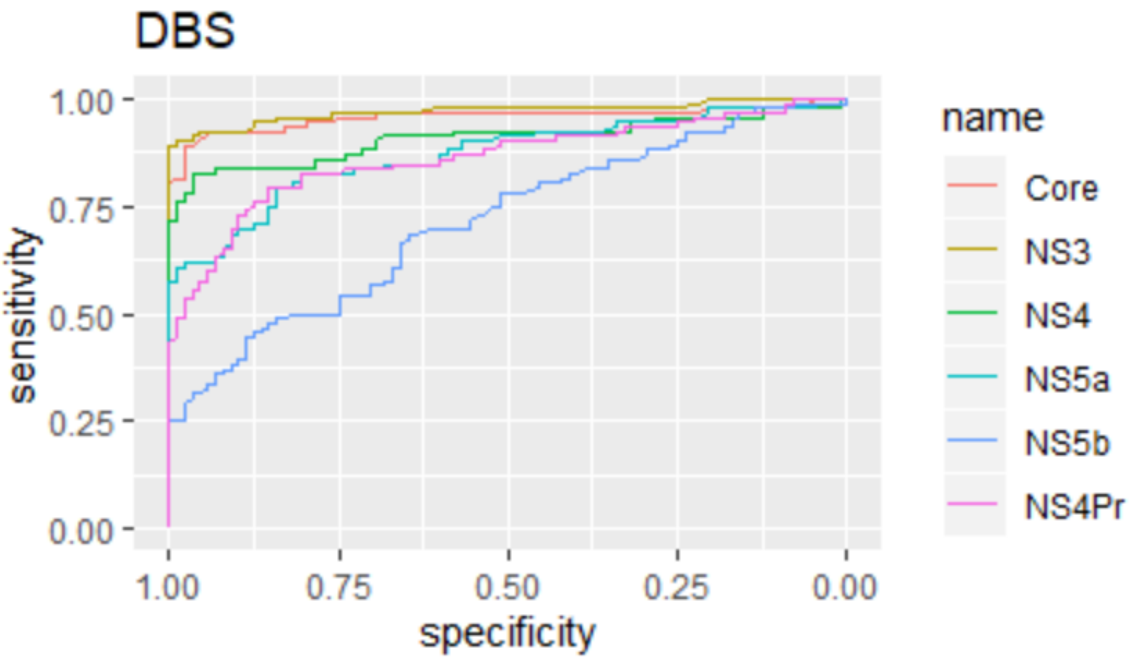

Figure 101 Comparison of HCV Antigen ELISA ROC Curves generated from testing DBS Samples. The Core and NS3 antigen assay ROC the best ROC curves with the highest AUC, followed by the NS4, NS5a and NS4Pr. Only the NS5b antigen assay produced a poor ROC curve.

Sample Type	Assay	AUC (95% CI)	pAUC (95% CI)
DBS	Core	0.96 (0.92-0.99)	0.089 (0.082-0.095)
	NS3	0.97 (0.95-1)	0.091 (0.085-0.096)
	NS4	0.91 (0.86-0.96)	0.08 (0.072-0.088)
	NS5a	0.87 (0.82-0.92)	0.062 (0.052-0.073)
	NS5b	0.71 (0.64-0.79)	0.032 (0.023 - 0.044)
	NS4PrSpc	0.86 (0.81-0.92)	0.057 (0.052-0.073)

Table 48 List of AUC (95%CI) and pAUC(95%CI) for all HCV antigen assays with DBS Samples. The full shape ROC curve is represented with the AUC value, the higher the value the better performing the assay. The pAUC value represents just the high specific area of the curve and enables comparisons between two similar assays, again the higher the value the better performing the assay.

Figure 101 plots each of the ROC curves generated from testing DBS samples with HCV antigen ELISAs against each other. As seen with the serum samples the two clearest best performing assays are the Core and NS3, which have a very similar ROC curve profile.

Table 48 lists both the AUC and pAUC (for 90% specificity and above) for all the ROC curves. The Core has an AUC of 0.96 and the NS3 an AUC of 0.97, insignificantly different to each other, p-value 0.42. Looking at the ≥90% specificity area of the curve with the calculated pAUC the Core scores 0.089 and the NS3 slightly higher 0.091. As a perfect score for the pAUC is 0.1 they both show good performance in this high specific area, the NS3 scoring slightly higher than the core but not a significance difference, p-value 0.51.

From the ROC curve profiles in Figure 101 and the AUC values in Table 48 the next best performing assay with DBS samples was the NS4 antigen. This performed significantly less well than the NS3 assay, p-value 0.01, but not significantly better than the other NS4 assay using the commercially purchased, *E.coli* derived NS4PrSpc. Only when comparing the pAUC was the 0.08 of the NS4 significantly better than the 0.057 of the NS4PrSpc, p-value 0.003. The NS5a assay performance was similar to both these assays, with a significant difference with the NS4 assay only between the pAUC of 0.062 of the NS5a and NS4 pAUC of 0.08, p-value 0.003.

Easily the worst performing assay with DBS samples was the NS5b assay, with a clear difference in the ROC curve compared to the other assays, and a significantly worse AUC value of 0.71 compared to the next lowest performing NS4PrSpc assay with an AUC value of 0.86, p-value 7.2×10^{-5}.

The AUC and pAUC values were also used to compare the performance of each antigen assay with serum and DBS samples. The Core assay performed better with DBS samples compared to serum samples, but there was only a significant difference when comparing the pAUC 0.089 for DBS with the pAUC of 0.079 for serum, p-value 0.09. The NS3 assay showed a significant difference in the AUC values, with 0.97 with DBS samples better than the 0.93 with serum samples by a significance of p-value 0.05. The NS4 only showed a significant difference comparing the pAUC values of 0.08 with DBS samples and 0.053 with serum samples, p-value 0.0006. The most dramatic difference in performance between DBS and serum samples was with the NS4PrSpc antigen, with serum samples the assay did not work giving an AUC of 0.56, but with DBS samples produced a significantly better assay with an AUC of 0.86, p-value of 1.7×10^{-7}. The NS5a assay performed slightly better with DBS samples compared to serum samples but this was not significantly different looking at either AUC or pAUC. The final NS5b assay performed poorly with both DBS and serum samples, though was significantly better with DBS samples if the pAUC values of 0.032 and 0.017 were compared, p-value 0.03.

12.3.4 OVERALL VALIDATION RESULTS

		Sample Type	Serum					DBS				
		No. Pos	95					92				
		No. Neg	92					88				
		No. Equiv.	1					7				
		Antigen	Core	NS3	NS4	NS5a	NS5b	Core	NS3	NS4	NS5a	NS5b
		Pos Cut-Off	0.99	0.62	1.01	0.34	1.61	0.26	0.19	0.46	0.22	0.43
No. Positive Antigens	≥ 1	**Sensitivity %**	**91.6**					**100.0**				
		Specificity %	**100.0**					**100.0**				
	≥ 2	**Sensitivity %**	**63.2**					**93.5**				
		Specificity %	**100.0**					**100**				
	≥ 3	**Sensitivity %**	**34.7**					**72.8**				
		Specificity %	**100.0**					**100**				
	≥ 4	**Sensitivity %**	**12.6**					**41.3**				
		Specificity %	**100.0**					**100**				
	≥ 5	**Sensitivity %**	**3.3**					**14.1**				
		Specificity %	**100.0**					**100**				

Table 49 Overall sensitivity and specificity results combining Core, NS3, NS4, NS5a and NS5b assays. The positive cut-off threshold determined by maximum specificity is listed for each antigen assay. Results for serum and DBS samples are shown in separate columns. The column on the left shows the number of antigens positive, and the corresponding sensitivity and specificity. Overall testing of DBS samples performed higher than testing serum samples, with a 100% of DBS samples positive in at least 1 antigen assay, and 93.5% of samples positive in 2 antigen assays.

Table 49 shows the overall results of testing panels of serum and DBS samples. All assays using baculovirus expressed antigens were included, the ELISA using the commercially purchased NS4 PrSpc was excluded, giving a total of 5 separate antigens tested for each sample. The positive cut-off value for each antigen assay was set at the minimum level required to achieve a specificity of 100%. The column on the left of the table shows the required number of positive antigens for a sample to be considered as testing anti-HCV positive with the antigen panel. For instance, 91.6% of known anti-HCV positive serum samples were positive with at least one antigen assay, giving an overall combined sensitivity of 91.6% combined with a specificity of 100%. The sensitivity drops to 63.2% for samples testing positive with a minimum of 2 antigens, and down to 34.7 % of samples with at least 3 antigens positive. The right-hand column in the table shows the results from testing DBS samples. This shows a higher level of overall sensitivity than with serum samples. Every known anti-HCV positive DBS sample was detected with at least one antigen, giving an overall combined sensitivity of 100%. This only drops to 93.5% for positivity with 2 antigens, and 72.8% with a minimum of 3 antigens positive.

The overall conclusion from Table 48 is the better performance of the HCV antigen assays with DBS samples compared to serum samples. The positive cut-off values shown in the table show a much higher value required to achieve a specificity of 100% when testing serum samples, demonstrating

a high background in the assays with this sample type. This makes it very difficult to differentiate between positive and negative samples and leads to lower sensitivity overall. The DBS samples showed a much lower level of background. This lower background enabled much better differentiation between positive and negative results and gave a higher sensitivity overall.

12.3.4.1 ANTI-HCV EQUIVOCAL SAMPLES

Anti-HCV equivocal samples are serum and DBS samples which previously tested anti-HCV positive with the Roche Elecsys assay but negative with the Ortho assay. It has previously been demonstrated, see section 11.5.1, that the Roche Elecsys anti-HCV II assay is more sensitive than the Ortho anti-HCV assay. This leads to a number of anti-HCV equivocal results profiles, in which genuine anti-HCV positive and possible false positive results cannot be differentiated.

One serum sample and seven DBS samples with anti-HCV equivocal results profiles were tested with the developed assays.

Study No.	Sample Type	Roche Elecsys Anti-HCV II	Ortho Anti-HCV	HCV PCR	Core	NS3	NS4	NS5a	NS5b
M18.190	Serum	P	N	N	0.152	0.093	0.098	0.065	0.087
M18.281	DBS	P	N	N	0.116	0.047	0.042	0.051	0.087
M18.282	DBS	P	N	P	0.145	0.055	**1.057**	0.093	0.184
M18.283	DBS	P	N	N	0.168	**0.231**	**0.613**	0.167	0.168
M18.284	DBS	P	N	N	0.057	0.03	**0.879**	0.042	0.062
M18.285	DBS	P	N	N	0.124	0.095	0.252	0.031	0.088
M18.288	DBS	P	N	N	0.083	0.116	**0.743**	0.021	0.186
M18.289	DBS	P	N	N	**0.275**	0.174	**0.538**	0.028	0.377

Table 50 Results from Anti-HCV Equivocal samples. Positive signals are highlighted in blue. The single serum Anti-HCV equivocal sample tested was negative in all assays. Of the 7 Anti-HCV equivocal DBS samples 5 were positive in a least one assay, and 2 were positive in 2 assays.

In Table 50 above the results of testing the signal for each individual ELISA are shown, with signals above the positive cut-off value shown in blue. The serum anti-HCV equivocal sample was negative in all assays. However, in the 7 DBS anti-HCV equivocal samples 5 were reactive in at least one assay, with 2 samples reactive in 2 assays. The most commonly reactive antigen was the NS4 assay, with one additional NS3 positive and one additional core positive. This demonstrates a higher performance of the combined antigen assays with DBS samples than was achieved with the Ortho anti-HCV assay, almost matching the performance of the Roche Cobas anti-HCV II assay.

12.3.4.2 COMPARISON CHARTS

The original test value (in RLU) for each DBS sample when tested with the Roche Cobas anti-HCV II assay was plotted against the OD signal from each DBS sample when tested with individual ELISAs.

This was produced for each of the baculovirus expressed antigen assays. This is not a direct comparison as the signal from the Cobas anti-HCV II assay does not differentiate the HCV antigens it is reactive against. It also only contains HCV core, NS3 and NS4 antigens, with no NS5 antigen. The R^2 values are generally quite low but the comparison does highlight the range and spread of the signal strength recorded for each individual antigen with DBS samples.

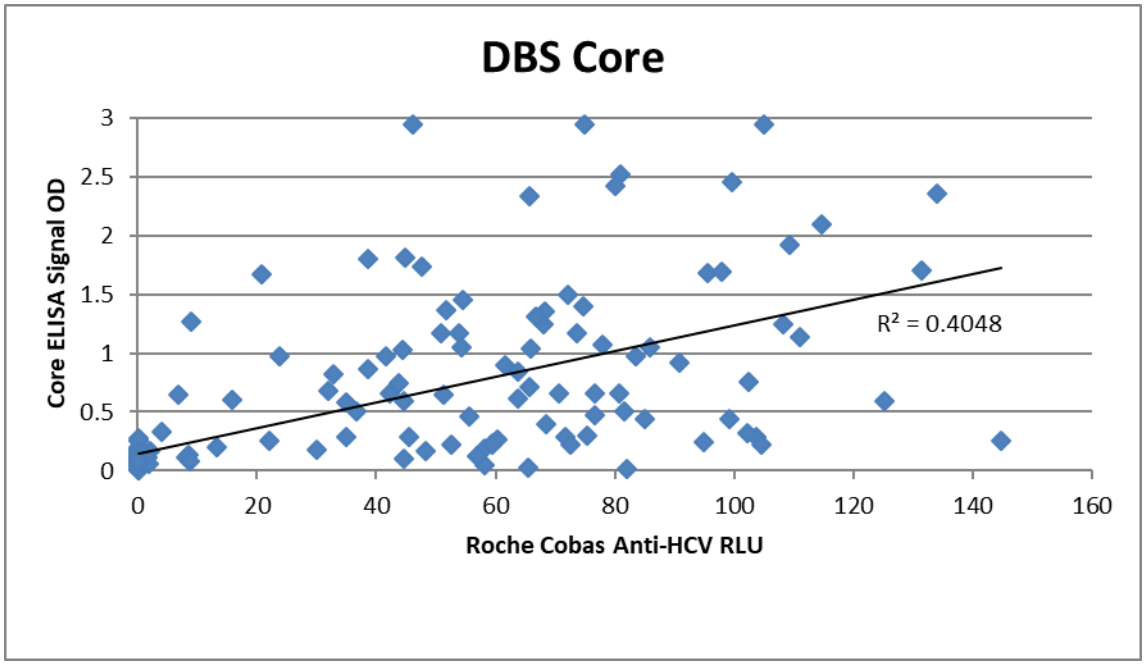

Figure 102 Graph of Roche Cobas anti-HCV II RLU value plotted against CORE ELISA Signal OD for DBS samples. The liner trendline and corresponding R2 correlation value are shown.

Figure 102 shows the core antigen assay plotted against the Cobas anti-HCV II assay. The positive cut-off value for the Roche Cobas assay is ≥0.5 RLU, so the data points spread across the chart represent anti-HCV positive samples. The signal OD for the Core ELISA assay correlates in some samples with the Cobas anti-HCV value, but many other samples are only weakly reactive even if the Cobas value is high. This leads to an overall R^2 coefficient value of 0.4048, higher than the other assays but still a weak overall correlation. Very few of the signal ODs reach the maximum level of 3, with most values below an OD of 2.

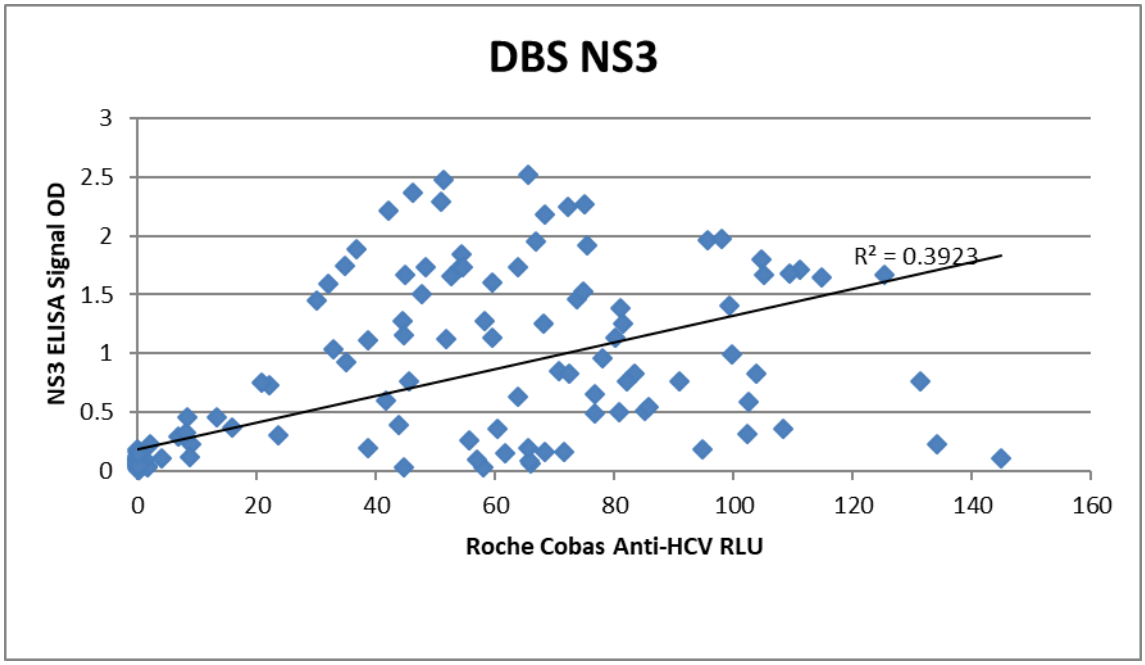

Figure 103 Graph of Roche Cobas anti-HCV II RLU value plotted against NS3 ELISA Signal OD for DBS samples. The liner trendline and corresponding R2 correlation value are shown.

Figure 103 shows the NS3 antigen assay plotted against the Cobas anti-HCV II assay. Again, the correlation between the 2 assays is fairly weak, with an R value of 0.3923, similar to that seen with the core assay. The spread of positive values for the NS3 assays is similar to the core, though the highest signal strengths are lower, with no maximum OD values were 3 recorded.

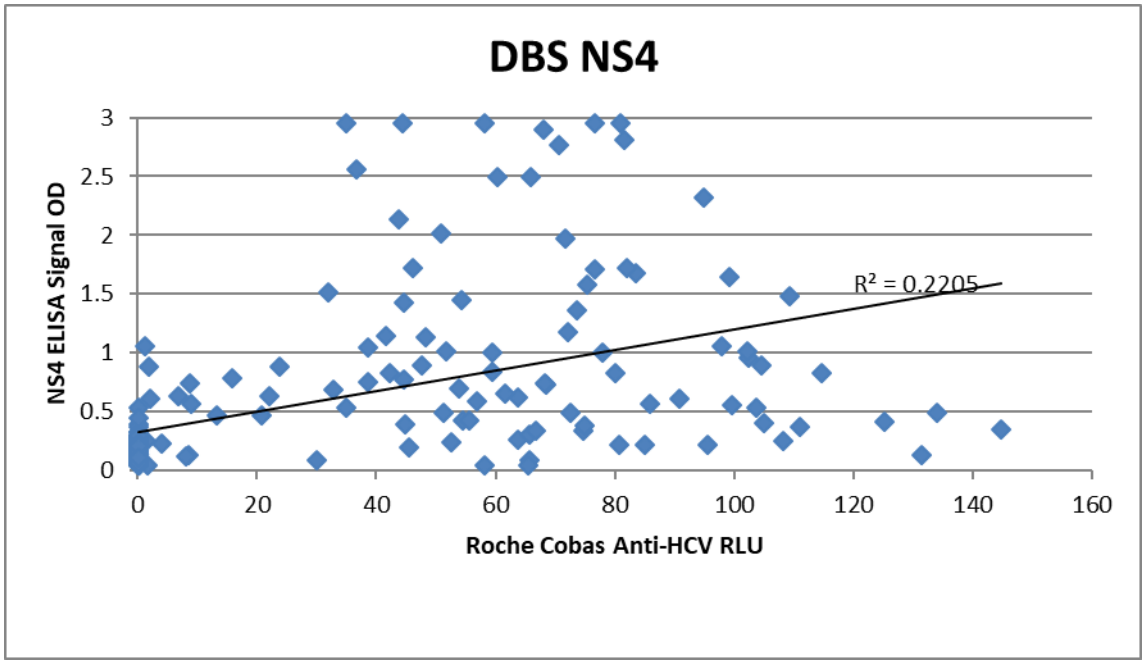

Figure 104 Graph of Roche Cobas anti-HCV II RLU value plotted against NS4 ELISA Signal OD for DBS samples. The liner trendline and corresponding R2 correlation value are shown

Figure 104 shows the NS4 antigen assay plotted against the Cobas anti-HCV II assay. The overall correlation is lower than seen with the other assays, with an R^2 value of 0.2205. This is a reflection of the overall lower reactivity in positive anti-HCV samples with the NS4 antigen assay compared to the Core and NS3 assays. The other thing to highlight from the chart is the overall higher signal OD. This applies to the anti-HCV negative sample seen as the blue points on the y-axis, which rises higher than with the other assays representing an increased background. It is also seen with the anti-HCV positive samples, with a higher number of maximum or nearly maximum signal OD values.

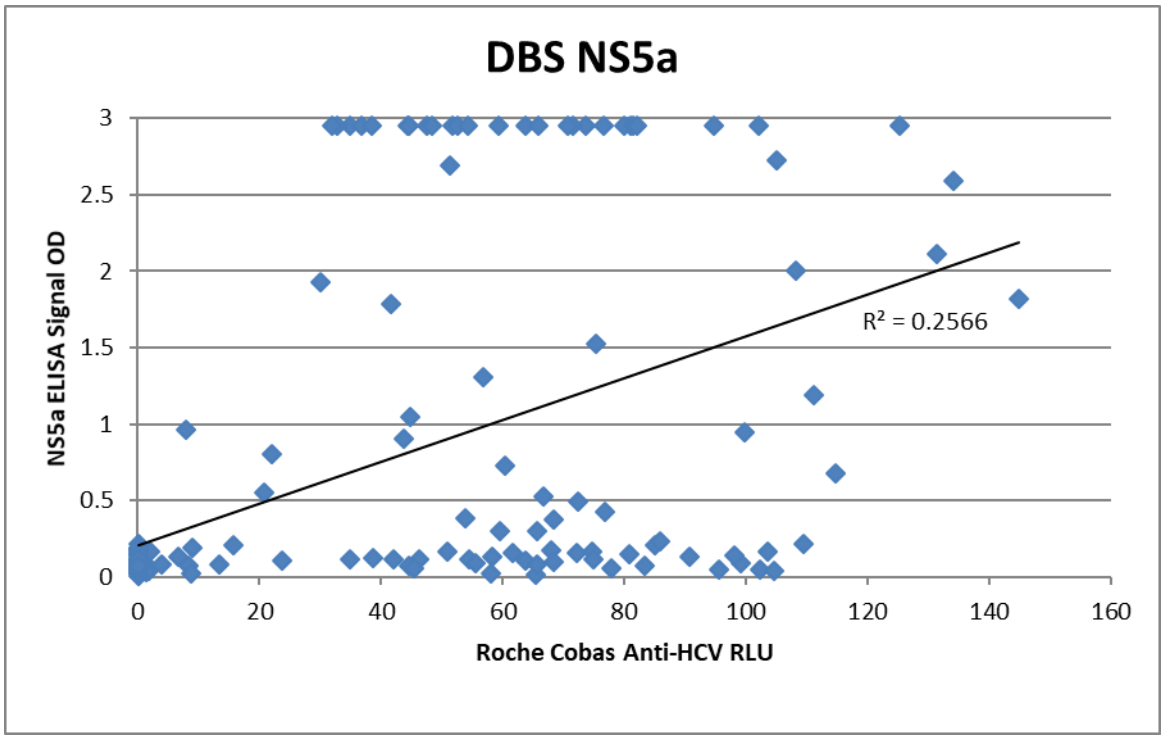

Figure 105 Graph of Roche Cobas anti-HCV II RLU value plotted against NS5a ELISA Signal OD for DBS samples. The liner trendline and corresponding R2 correlation value are shown.

Figure 105 shows the NS5a antigen assay results plotted against the Cobas anti-HCV II assay results. The correlation is still low with an R2 value of 0.2566, slightly higher than the NS4 value. The most striking aspect of the chart is the separation between low and high signal values. Though a lower proportion of anti-HCV positive samples tested positive with the NS5a antigen assay compared to the Core, NS3 and NS4, the signal OD of the samples which did test positive are generally much higher. The majority of samples react with a high OD value or not at all, with a smaller proportion of results in the middle of the chart area.

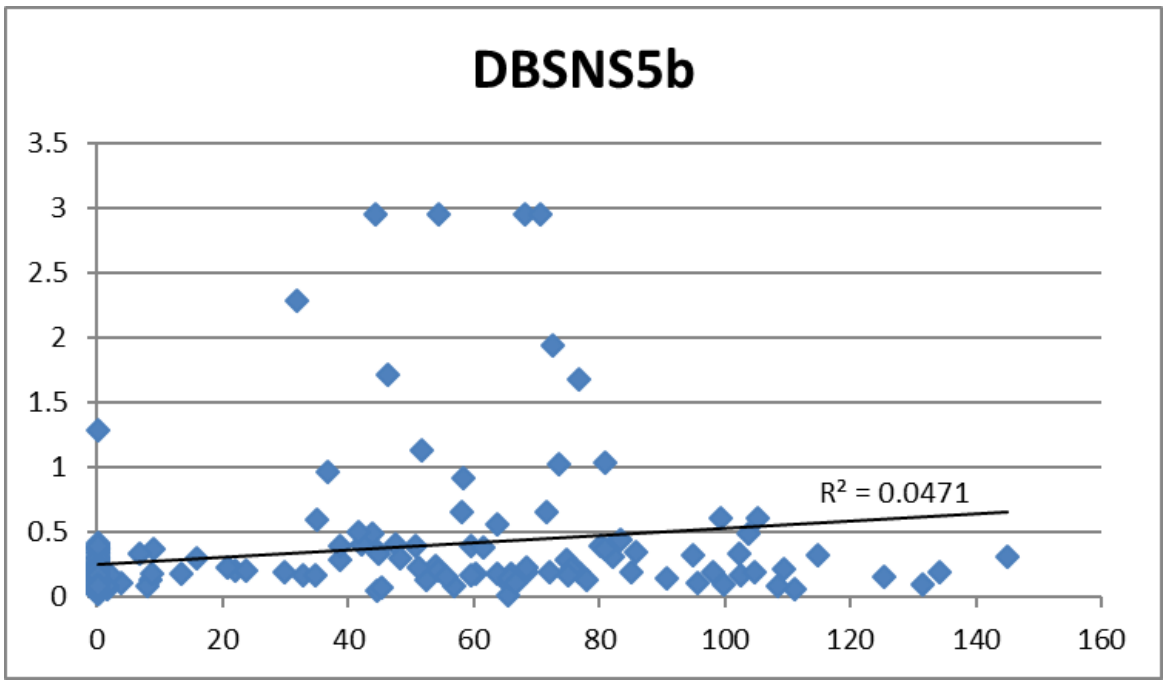

Figure 106 Graph of Roche Cobas anti-HCV II RLU value plotted against NS5b ELISA Signal OD for DBS samples. The liner trendline and corresponding R2 correlation value are shown.

Figure 106 shows the NS5b antigen assay results plotted against the Cobas anti-HCV II assay results. The R^2 correlation value is low for the NS5b assay. This was the poorest performing of the various antigen assays, which is reflected with the lowest correlation. The majority of anti-HCV positive samples recorded low values with the NS5b assay, and the anti-HCV negative background level seen on the Y axis is relatively high. A small number of samples, 4, did react strongly giving maximum OD values of 3.

12.4 OVERALL ELISA RESULTS

The five HCV antigens produced and purified from baculovirus based expression systems were optimised in individual ELISA assays. In addition to the baculovirus expressed HCV antigens, a commercially purchased NS4 antigen produced in *E. coli* was purchased. The optimised individual ELISA were then validated with panels of serum and DBS samples of known HCV antibody status.

The best performing antigens were the Core and NS3 antigens, showing the highest reactivity across anti-HCV positive samples. The NS4 performed adequately but produced high assay background levels, particularly with serum samples. The NS5a assay was reactive in a lower percentage of samples but when positive it reacted strongly. The NS5b assay was the poorest performing of the baculovirus expressed antigens, not really working with serum samples and performing only slightly better with DBS samples. The ELISA optimised with the commercially purchased NS4PrSpc antigen

was inferior to the baculovirus expressed NS4 antigen ELISA, giving very high background signals and overall lower reactivity in samples.

Overall, the results from testing DBS samples were better than the results from testing serum samples. The higher background seen when testing serum samples made it difficult to differentiate between positive and negative signals. The background level in DBS samples was lower with the assays performing better with this sample type. Combining the DBS results of the 5 ELISAs using baculovirus antigens produced an assay in which 100% of known anti-HCV positive samples were reactive in least one assay, and 93.5% in at least 2, all combined with a specificity of 100%. Testing of anti-HCV equivocal samples also showed combining results of the antigen assays outperforming the commercial CE marked Orto anti-HCV assay and nearly matching the performance of the Roche Cobas anti-HCV II assay.

13 DISCUSSION

The major aim of this project was to develop a multi-analyte assay for the detection of anti-HCV from DBS samples. The multi-analyte array was designed to increase sensitivity for detecting anti-HCV in DBS samples and to enable identification of acute cases of hepatitis C virus infection based upon the differential response to individual HCV antigens. Due to time pressures and initial delays in protein production the end goal of a multi-analyte array was not realized. However, the proteins to be used in this array were produced and validated in individual ELISAs, and results combined to produce a profile like that produced by a multi-analyte array.

The first stage in developing a new diagnostic assay for detection of anti-HCV is to choose the most suitable HCV antigens to express, and subsequently use as a capture antigen in an immunoassay. As the diagnostic assay was being designed specifically for the alternative sample type DBS, which intrinsically provides a lower sensitivity than that available from serum, it was important to select antigens that would maximize the sensitivity of the assay. As described in the introduction, HCV has 10 proteins, 3 structural and 7 non-structural, which could potentially be used as a capture antigen. Studies determining the antibody responses to each HCV protein do not always give consistent findings, with the earliest antibodies detected targeting the HCV core[366], to the NS3[310] or the NS4[366]. However, despite differences in the timing and level of detection, these 3 proteins were detected in the majority of the patients tested, and therefore should form the basis of any screening assay. Detection of the NS5 was less consistent and was completely absent in a proportion of patients.

Most modern anti-HCV assays use the same or very similar antigens. The original patent of the Chiron Corporation resulted in diagnostic licensing of the use of synthetic peptides and recombinant antigens from Chiron and led to similar recombinant proteins being used in different commercial assays. The patent was relaxed in the USA in 2004, before expiry in 2015, and expiry in Europe in October 2013[367]. As described in the introduction (section 1.4.1), the performance of these modern anti-HCV assays is universally good, giving sensitivities and specificities close to 100%[283]. When all the assays listed above were compared (except the Murex Liaison XL anti-HCV) the Elecsys® anti-HCV II was the most sensitive, with the shortest seroconversion detection time[283]. The data information sheet for the Elecsys anti-HCV II states that it uses Core, NS3 and NS4 based antigens but does not define if these are peptides or recombinant antigens and does not specify how they are produced. Two assays, the Vitrios anti-HCV and the ADVIA Centaur include an NS5 antigen produced in yeast, though for the Vitrios anti-HCV this has been shown to decrease the specificity slightly without necessarily increasing the sensitivity[368]. The most recently released assay, the Diasorin Murex Liaison XL anti-HCV, uses the same core, NS3 and NS4 targets, but unlike the other assays the HCV core antigen is produced in a Baculovirus expression system. In a recent comparison it proved equal to the

performance of the Abbott Architect anti-HCV assay[369]. One notable characteristic of both assays was the lower S/Co positive signal values recorded for genotype 3a samples compared to the other HCV genotypes. This is in part a reflection of the fact that all the expressed antigens/peptides used in anti-HCV assays are based on the sequence of genotype 1 isolates. Despite this lower reactivity this does not seem to lead to false negative results. HCV antigens notable by their absence from any of the current anti-HCV assays are the two envelope glycoproteins, E1 and E2. The high variability found in these proteins and the genotype bias in reactivity[370] would make it difficult to produce an antigen sufficiently conserved across genotypes to be used successfully in a screening assay.

Taking into account all these factors, the essential antigens required for a diagnostic screening assay to detect anti-HCV appear to be the HCV core, NS3 and NS4. In addition to these, the NS5 is a possible antigen for inclusion as a means of improving overall performance. A wider range of antigens in a screening assay, particularly when used on a multi-analyte platform which can identify the reactivity of individual antigens, may open up the possibility of identifying acute HCV infection through the pattern of results given in the array.

As explained in section 1.2.5. HCV antigens for use in a multi-analyte array can be produced using a variety of different expression methods. The simplest approach is to purchase commercially produced peptides. These peptides are short chains of amino acids typically ranging in length from 10-20aa long. The peptide chains are produced synthetically with the addition of one amino acid to another. The advantage of this approach is the relative simplicity of production, enabling several peptides to be used in an assay. The disadvantage is the peptide is a simple sequence of amino acids which has not gone through any of the post translational modifications native HCV proteins undergo when they are produced in an HCV infected human hepatocyte. HCV proteins undergo a wide range of post translational modifications[371] and these changes have been shown to be important in the immunoreactivity of expressed HCV proteins[372][371] In addition the short length of the peptides restricts the potential number of immuno-reactive epitopes compared to a fuller length expressed protein, and have been shown to decrease immune reactivity compared to a full recombinant protein[366].

To produce a protein close to its native form bacterial expression systems, generally in *E.coli*, can be used. These expression systems have been extensively studied and remain the most commonly used systems for protein expression with large quantities of protein produced relatively easily[201]. Unlike peptides, proteins produced using bacteria expression systems will have undergone some post translational modifications. However as bacteria are prokaryotes these post translational modifications are relatively simple and do not include the N- and O- linked glycosylation, fatty acid acylation, phosphorylation and disulphide-bond formation produced in higher eukaryotic cell lines[202]. An alternative eukaryotic system to bacteria is the use of yeasts. They are similar to *E.coli* in their

ease of use and cost but have the added advantage of performing additional post translational modifications[203], though as a lower eukaryotic organism these modifications do not include all the modifications found in eukaryotes such as the formation of N- and O- linked oligosaccharide structures[202]. These can only be achieved through the use of higher eukaryotic cell lines. Expression in mammalian cells offers the advantage of the highest accuracy in protein synthesis, though high level protein production is difficult to achieve[204]. The protein expression system chosen for this study was baculovirus expression in insect cells as this offers the advantages of N and O glycosylation and other post-translation modification of expressed proteins to accurately replicate the post translational modifications found in HCV proteins[371] in a simpler and safer expression system compared to mammalian cells combined with the potential for high level expression[373]

As described in section 1.2.8. baculoviruses are a group of arthropod insect viruses. The predominant strain used for protein production is *Autographa Californica* nuclear polyhedrosis virus (AcMNPV) and its infection of lepidopteran host species. The baculovirus expression life cycle undergoes 4 separate stages and produces the final virion in 2 forms, budded and occluded. The occluded form is composed of virions surrounded by large amounts of a polyhedrin and p10 protein in a polyhedral structure[213]. In the wild this very stable form enables virus to survive in soil and on the surface of leaves until taken up by a host caterpillar species. The budded form of the virus which replicates cell to cell does not require this protein mix. As the polyhedron and p10 proteins are produced in large amounts in stage 4 of the life cycle and are not essential for virus replication in cell culture conditions, they can be hijacked for production of large amounts of protein.

Since its first use in the 1980s for protein expression baculovirus based systems have been developed to increase reliability, production and ease of use (section 1.2.9). Two baculovirus based expression systems were used in this study. The first was the InsectDirect™ system. The system does not involve a baculovirus life cycle. It uses the transcriptional elements ie1 and Hr5 to promote endogenous insect transcriptional enzymes to express the gene of interest[258]. As no life cycle is involved, the system is extremely rapid producing protein in as little as 48 hours.

The first protein chosen for expression was the HCV core, a version of which is universally included in all screening assays for anti-HCV. The core is a 191 amino acid protein split into 3 domains. The first 118 amino acids make up the hydrophilic C terminus domain, amino acids 119-169 make up the more hydrophobic central domain, and amino acids 170-190 make up the very hydrophobic domain 3[10]. This final very hydrophobic domain is removed from the final version of the mature protein.

A study using short peptides to probe the entire protein revealed 3 predominant immunoreactive regions, from amino acids 1-38, 51-78 and 101-118[374]. Of these regions 1-38 contains 3 antibody

binding sites, 51-78 contains 2 binding sites and 101-118 contains 1 binding site. It is obviously important to replicate these 3 regions, especially the first 28 amino acids, in any anti-HCV screening assay.

Approaches to replicating the core in a diagnostic assay include the use of a relatively long peptide; see the C22-3 peptide above, or as an expressed protein. Anti-HCV assays and HCV antigen assays from Abbott Diagnostics use a fusion protein combining the core and NS3 regions, expressed as a single protein in *E.coli*. The Murex Liaison XL assays use the full core protein expressed in a Baculovirus based system. Use of a full recombinant protein should give better immune reactivity than a peptide[366] and baculovirus expression systems have been described for the production of HCV core[375] with both systems leading to the production of self-assembled virus like particles (VLPs), and successful detection of anti-HCV in six HCV RNA positive patients negative by other anti-HCV assays. It was for these reasons HCV core protein was produced in a baculovirus expression system, with the hope of producing HCV core protein in sufficient quantity to use as the first antigen in the anti-HCV diagnostic screening assay. The first baculovirus expression system trialed was the InsectDirect™ system, which promised the advantages of expression in a baculovirus system in a fast and simple procedure[258].

The DNA sequence representing aa1-124 sequence was made synthetically and inserted directly into the InsectDirectTM compatible pIEx plasmid vector (Eurofins Germany). The pIEx plasmid has a minimal nucleic acid sequence. It includes 2 baculovirus derived promoters, the hr5 enhance and IE1 (immediate early) promoter. These promoters are different to the widely used p10 or polyhedrin promoters used in the majority of baculovirus transfer vectors and are both activated early in the baculovirus life cycle. However, as mentioned earlier, the InsectDirect system does not produce a complete baculovirus life cycle. The pIEx plasmid is transfected into the cells, upon which, the promoters direct expression of the downstream protein sequence. This system is fast, going from plasmid transfection of Sf9 cells to protein expression in 48 hours. Unfortunately, the results of using this system for expression of the HCV core protein were disappointing. After 48 hours the Sf9 cells used for expression showed little evidence of infection, though as no baculovirus life cycle is produced this was to be expected. Unfortunately, all subsequent analysis using SDS PAGE and western blotting gave no evidence of HCV core production. The western blot analysis using an HCV Core monoclonal antibody showed a possible, very weak, band of the expected size of the core protein. It was predicted that the InsectDirect system would not produce the large amounts of protein, but it was hoped that enough would be produced to prove the production of HCV Core for initial confirmation experiments. Due to the uncertain low-level production using this system it was decided to move to a different baculovirus expression system.

The alternative baculovirus expression system used was the *flash*BAC™ ULTRA system, described in section 1.2.9. This is one of the later developments of baculovirus expression systems which includes modifications to simplify production of recombinant baculovirus and improve expression of protein[215]. The system uses a baculovirus genome missing the essential ORF 169 gene. Without this gene the baculovirus cannot complete its life cycle and will not replicate. The essential ORF gene is stored in a *flash*BAC™ compatible transfer vector. In addition to the essential gene, the transfer vector includes a baculovirus promoter (usually either p10 or polyhedron) upstream of a cloning site for insertion of the desired protein sequence. The vector also includes sequences to allow homologous recombination with the baculovirus genome. When both incomplete baculovirus genome and transfer vector are transfected into an insect cell at the same time, the transfer vector and baculovirus genome undergo homologous recombination transferring both the ORF essential gene and the desired protein sequence into the baculovirus genome. The completed genome will now undergo a full life cycle within insect cells and produce viable recombinant virus to infect other cells and to express the desired protein. As only the genome which has undergone homologous recombination with the transfer vector can produce a full replication cycle this acts as a selection step for the recombinant virus. In addition to efficient homologous recombination production of recombinant baculovirus the *flash*BAC™ ULTRA system includes multiple modifications to the baculovirus genome including deletions of 5 genes, *chiA*, *cath*, *p10*, *p74* and *p26*, to increase protein and yield[257] and deletion of the *chitinase* (*chiA*) and *v-cathepsin* (*cath*) genes to increase protein stability[252].

This *flash*BAC™ system was used as an alternative system for expression of the HCV Core protein. A *flashBAC*™ ULTRA compatible transfer vector, the Novagen pIEx-Bac3 LIC plasmid from Merck was used. This plasmid contains the IE promoter and a p10 late promoter plus the *flash*BAC™ ULTRA compatible homologous recombination sequences. The IE promoter starts expression of the protein early in the baculovirus life cycle while the p10 promoter ensures high level expression in the later stages of the life cycle. The "LIC" in the naming of the plasmid refers to ligation independent cloning, a type of cloning which does not require the use of restriction enzymes and ligation stages[376]. Instead primers are designed with compatible tails at the 5' end, when the target sequence is amplified the tails are inserted onto the end. The plasmid contains compatible sequences to those found on the primers. Treating the primers with a 5'exonuclease in the presence of dATP bases creates 5' ends on the PCR product which are compatible with the plasmid. The tails on the product are different so they will be inserted into the plasmid in the correct orientation. Primers were designed to amplify the HCV Core sequence from the pIEx plasmid with the necessary tails at the end. This was successfully cloned into the pIEx Bac 3 plasmid before transforming into *E. coli*. The plasmid also contains an ampicillin resistance gene so culture on an ampicillin containing nutrient agar plate selects out for successfully

cloned and transformed *E. coli.* A Qiagen plasmid preparation kit was then used to purify the plasmid, and nucleotide sequencing used to confirm the presence of the HCV core gene.

The finalised HCV Core pIExBac 3 plasmid was used in combination with *flash*BAC™ ULTRA to generate a recombinant baculovirus containing the HCV Core protein sequence. Generation of recombinant baculovirus involved the transfection of rapidly proliferating Sf9 cells with both the HCV Core pIExBac3 plasmid and the *flashBAC*™ ULTRA bacmid. Recombinant virus was successfully generated and amplified for a week in Sf9 cells. To quantitate the virus quantitative real-time PCR was performed using a previously published set of primers[357]. The quantitative PCR used 2 previously quantitated recombinant baculoviruses (by Oxford Expressions Ltd.) to produce a standard curve calibrated to give results in pfu/ml. Virus amplification was deemed a success if the level reached greater than 1x 10^7 pfu/ml. For all protein expression work Hi5 cells were used. These are derived from a *Trichoplusia ni* cell line, rather than the *Spodoptera frugiperda* derived Sf9 cells used for virus generation and recombination. The Hi5 cells were not used for virus generation or recombination as the virus has a higher mutation rate in this cell line, however protein expression has been shown to be higher in this cell line compared to Sf9 cells[377]. The protein optimisation experiments involved the infection of Hi5 cells with a recombinant virus at a range of MOI. This was performed in small scale 2 mL adherent cultures in 6 well plates. Protein expression was run for 72 hours, after which cells showed widespread evidence of virus infection with shrunken cells, deteriorated cell walls and reduced cell numbers.

Insect cells are eukaryotic cells lacking a tough cell membrane or cell wall making them relatively easy to lyse with a mild non-ionic detergent such as Triton X-100 with minimal damage to proteins[378]. For all protein extraction procedures, a gentle phosphate-based lysis buffer was used to lyse the cells, with 1% Triton x-100 detergent and NaCl at 150mM. Protease inhibitors were added to inhibit protein degradation and benzonase was added to digest nucleic acid. Collected cells were lysed in a small volume of this lysis buffer on ice, then centrifuged at high speed to separate the total and soluble fractions. After separation the fractions were analysed by SDS PAGE with Coomassie blue staining. The SDS PAGE analysis showed the protein expression had worked, with a strong band at the expected size which could not be seen in the negative control. Unfortunately, the band was only seen in the total fraction, and was completely missing from the soluble fraction suggesting the protein was insoluble. An insoluble protein will not purify through subsequent protein expression and cannot be used in an ELISA, so it was vital the protein was produced in a soluble form. To confirm if any soluble protein was produced a His-tag purification was performed followed by western blot.

The His-tag purification process is a form of immobilised metal ion affinity chromatography (IMAC) which utilises the high affinity of histidine residues for nickel ions in the form of Ni(II)-nitrilotriacetic

acid (Ni-NTA). The His-tag is composed of a minimum of 6 his-residues expressed at the N-termini of the protein, which will bind to Ni-NTA immobilised on agarose beads. Washes can then be performed on the beads to remove any unwanted material before a final elution step to collect the purified protein. Advantages of this approach include the small size of the His-tag, high capacity binding, mild and flexible elution conditions and the possibility of purifying under denaturing conditions[379]. In this study the protein fraction was incubated with pre-washed Ni-NTA beads for 2-3 hours at 4°C to maximise binding followed by washing and elution steps. Imidazole was used in the buffers at varying concentrations for washing and elution. Imidazole competes for the nickel binding sites, when used at lower concentrations (10-50mM) it will act as an effective wash buffer removing non-specifically bound contaminants, when used at a higher concentration (250mM) the buffer acts as an elution buffer displacing the His-tag from nickel coordination, freeing the His-tagged proteins. The decision to use the core protein soluble fraction despite the absence of a clear band in SDS PAGE analysis was to concentrate and purify any low-level soluble protein. A western blot was performed on the same aliquots used for the SDS PAGE analysis as an extra check for protein in the soluble form. This more sensitive analysis would identify any soluble protein even if it was only there in very low amounts. The western blot analysis confirmed the expression of HCV Core protein but also confirmed it was only produced in an insoluble form. Proteins can be solubilised by using a stronger detergent in the lysis buffer but this denatures the protein losing the native form and with it some of the advantages of producing the protein in a higher eukaryotic insect cell line[380]. The core protein is the main structural protein of HCV so it was deemed important to try and replicate the native form of the protein as accurately as possible. Therefore, the use of denaturing detergents was to be avoided if possible in the production of this protein.

To try and produce HCV Core protein in a soluble form it was decided to change the amino acids expressed. The original pIEx Core plasmid was designed using the first 124 amino acids of the core sequence. The total core sequence is 190 amino acids long, with the first 118 amino acids making the hydrophilic C terminus domain, amino acids 119-169 making up the more hydrophobic central domain, and amino acids 170-190 making up the very hydrophobic domain 3 which is removed during final processing of the protein. The more hydrophobic regions were removed from the original synthetic core design as it was thought this would increase solubility without removing major immune-reactive regions, and previous studies suggested less issue with using this shortened sequence compared to expression of the full 179aa[381]. The full core sequence has successfully been expressed in other studies using a baculovirus expression system[382] the primers were designed to amplify the full 179aa region of the HCV Core protein. Unfortunately, the primer starting at amino acid 1 did not produce a functioning PCR so the actual end PCR product started at amino acid 3. The primers were designed for cloning into a pOET1 plasmid. The original pIEx-Bac 3 *flash*BAC™ ULTRA

compatible transfer vector became unavailable from the commercial supplier mid-way through the project, so an alternative transfer vector was used. The pOET1 plasmid chosen was a *flash*BAC™ ULTRA compatible transfer vector produced by Oxford Expressions limited. The plasmid uses a polyhedron baculovirus promoter for high level expression and includes a 6XHisTag at the N terminus, similar to the pIExBac-3 plasmid. Unlike cloning into the pIExBac-3 plasmid cloning into the pOET1 plasmid required the use of conventional cloning with restriction enzymes. Snapgene software was used to simulate cloning into the pOET 1 plasmid so that compatible restriction enzymes could be chosen; in this instance XBa1 for the forward primer and BglII for the reverse primer. The primers were used to successfully amplify the Core sequence and after clean up were cloned into competent *E. coli* cells. As with all the transfer vector plasmids nucleotide sequencing was used to confirm the correct insertion of the desired sequence.

Production of recombinant virus and subsequent amplification was performed as for the previous core experiment. Protein optimisation was performed in Hi5 cells followed by cell lysis and SDS page analysis. The gel electrophoretic analysis showed successful expression of the full length HCV Core protein in the total fraction but yet again the soluble fraction did not have a clear band at the expected size. A HISTag purification was performed as described for the shorter length core protein. This time SDS page did show a band around the expected size in the elutions from the HISTag purification suggesting the soluble HCV Core protein was present. This was confirmed with anti-HCV core antibody by western blot analysis. After the successful expression and purification of HCV Core protein was confirmed, larger scale purification was performed to produce sufficient protein for use in an ELISA. The results demonstrate the improved solubility of the HCV core protein when expressing a fuller length version of the protein, as opposed to the shorter length protein trialed previously. This is despite in the inclusion of the hydrophobic terminus which had been predicted to reduce solubility.

The second protein produced using the *flash*BAC™ ULTRA system was the HCV NS3 protein. This is a HCV protease and some representation of this protein is found in all HCV commercial assays. Production of NS3 protein has been described before using a baculovirus expression system and was used successfully for serological detection[383]. Production of the NS3 protein was the most straightforward of all the HCV proteins. At the time this protein was expressed, sufficient pIEXBac3 transfer vector remained for cloning experiments, so primers were designed to include ligation independent cloning tags and the main immune-reactive region of the NS3 protein, 1225-1456 of the HCV genome[384]. The ligation independent cloning technique made cloning the amplified PCR product easy, with correct insertion confirmed by nucleotide sequencing. After successful recombinant virus generation and amplification, protein expression was again optimised in Hi5 cells. The SDS page analysis showed high level expression of NS3 protein at all MOI trialled. This included protein seen in both the total and soluble fractions. Protein purification followed by western blot analysis confirmed

the expression of soluble NS3 protein at a high level. Following confirmation, a large scale protein extraction and purification was performed to produce enough protein for use in an ELISA.

Another protein expressed with a combination of the pIExBac-3 transfer vector and the *flash*BAC™ ULTRA system was the NS4 protein. In nature NS4 is cleaved into the NS4a and b proteins. The NS4a forms a heterodimeric protein with the NS3 protein. The NS4b protein forms part of the viral replication complex in infected cells and is highly hydrophobic in nature[385]. A form of the NS4 protein is present in all commercial anti-HCV assays, expressed in either *E. coli* or yeast, but examples of expression in baculovirus have been described.[386] Primers were designed and used to amplify the most immune-dominant regions of the NS4a and NS4b protein[387–389], with LIC tags included to enable cloning into the pIEx-Bac3 plasmid. Recombinant virus was successfully generated and amplified but after protein expression experiments it was unclear if any protein expression had occurred. Protein purification and western blot analysis of the collected eluates failed to show any evidence of protein expression. Western blot analysis was first performed with a mouse anti-HCV mAb but this failed to detect any protein. To rule out the possibility of the anti-NS4 mAb not detecting the NS4 protein a repeat western blot was performed using a mouse anti-HIS mAb. This mAb which will detect any expressed protein via the N-termini HISTags encoded in the pIEx-Bac3 transfer vector. The previously expressed HCV Core protein with an N-terminus HISTag was run alongside as a positive control. The western blot image was blank for all the NS4 wells, including the total and soluble fraction from the lysed cells and the eluates from the HISTag purification process. This confirmed the absence of any expression of the NS4 protein.

It was unclear why expression of the NS4 protein was not successful. As highlighted before successful expression of NS4 protein has been described using baculovirus[386]. The same pIExBac-3 transfer vector had been used to express detectable levels of protein with both the Core and NS3 proteins. The transfer vector was nucleotide sequenced in two directions to ensure the NS4 gene had been cloned successfully and no stop codons were present in the sequence. Snapgene software was used to simulate protein expression from the sequenced region and highlighted no issues. A PCR was performed on a nucleic extract of the recombinant virus using transfer vector targeting primers, to ensure the NS4 gene was present in the recombinant virus and that no mutations had occurred after recombinant virus generation. The generated recombinant virus had amplified successfully to a high level of 3.28×10^7 pfu/mL and protein expression experiments showed widespread effects of baculovirus infection compared to healthy non-infected cells after 72 hours, proving the NS4 recombinant virus was viable and replicating well. Increasing the expression time to 96 hours did not have any beneficial effect. There was a possibility a mutation had occurred in a site outside of the cloning insertion area which was not sequenced that could have prevented expression. To rule this out, the entire process from transfection of Sf9 cells, generation of recombinant virus, virus

amplification and finally protein expression optimisation was repeated but again no visible protein expression was detected. Expression levels using baculovirus does vary for different proteins[215]. There is no recognised codon bias with baculovirus other than with GC rich viruses[390], but as the NS4 has a GC content of 60% this should not present an issue. It is possible the protein degraded although as described previously the *flash*BAC™ ULTRA system includes deletions of both the chitinase and cathepsin genes to aid in stability of expressed proteins[252,253]. Another possible loss of protein can occur during cell lysis due to the action of proteinases, generally these are physically in subcellular compartments but the lysis process can release these into solution where they can act on and degrade the expressed protein[391]. To overcome this potential issue a protease inhibitor cocktail was included in the lysis. This same issue of low or little protein expression was experienced with the NS5 proteins. The NS5 protein is composed of the NS5a and NS5b. The NS5a is an essential replication cofactor[23] and the NS5b is the RNA dependent RNA polymerase used for replicating the viral genome[30]. Only a small number of assays include any form of the NS5 protein, mostly as a single protein produced in *E.coli*. The decision was made to separate out the NS5 protein into its two component parts as they are both distinct large proteins with important roles in the cell cycle[41], and the NS5a in particular has been shown to be one of the dominant immunogenic HCV proteins[386] with a higher number of immune reactive sites compared to the NS5b[388]. At this point in the project there was no pIEx-Bac 3 transfer vector remaining for use to express the NS5 proteins. The alternative pOET1 transfer vector which had been used to express the full Core protein was used in its place. The NS5a protein was amplified, covering the immunodominant regions[392], and conventionally cloned using restriction enzymes into the pOET1 vector. The NS5b gene sequence, which was larger at 1800 bp, was amplified but could not be successfully cloned into the pOET1 plasmid. Various PCR insert to vector concentrations were tried, the restriction enzyme and ligation incubation steps increased and the number of plasmid preparations screened increased but none showed successful insertion of the NS5b sequence. To overcome the issue with cloning the full NS5b gene was sent for synthesis and the synthetic sequence cloned into the pOET1 plasmid by Eurofins. Recombinant virus was again successfully generated for both the NS5a and NS5b proteins but protein expression optimisation experiments failed to produce any detectable protein, through either SDS page analysis or western blot analysis with mouse anti-HIS mAb. The possible reasons for this low protein expression are similar to those outlined for the NS4 protein above, though the exact reason was never determined.

To overcome the difficulties in expressing the NS4, NS5a and NS5b proteins, an alternative transfer vector was used, the pOET8 vector produced by Oxford Expressions Ltd. The vector is similar to the pOET1 vector with a polyhedron promoter controlling protein expression and a HISTag, this time an 8XHIS, at the N-terminus of the protein. In addition, the vector includes some modifications to improve protein expression and purification. The most important of these and the reason this transfer

vector was chosen, was the inclusion of a vankyrin expression cassette under the control of a p10 baculovirus promoter. The vankyrin expression cassette includes a P-vank-1 gene encoding an anti-apoptotic protein, derived from the insect polydnavirus, *Campoletis somorensis ichnovirus*[393] Expression of the protein delays lysis of the baculovirus infected insect cells for up to several days, possibly through modulation of the immune response to viral infection, and with this delay been shown to increase protein yield [394].

Another modification in the pOET8 vector is the inclusion of a melittin bee peptide sequence to be expressed upstream of the 8XHISTag and expressed protein. The melittin bee sequence expresses a short signal peptide which increases excretion of expressed protein from the infected insect cell[395]. The transfer vector was not selected for this modification but did offer the potential advantage of simplified protein purification.

To transfer the NS4, NS5a and NS5b sequences from their respective transfer vectors into the pOET vector PCR amplification was used with primers containing compatible restriction enzyme sites. The NS4 and NS5a sequences were amplified and cloned into the pOET8 plasmid. The NS5b sequence proved more difficult to amplify. This could have been due to the larger size of the NS5b sequence. Only a smaller PCR amplicon representing a 240 amino acid portion of the NS5b, including several immune-reactive regions, could be successfully cloned. This amplified successfully and was cloned into the pOET8 plasmid. After generation and amplification of recombinant viruses all 3 proteins in the pOET8 plasmids were expressed in Hi5 cells. All expressions were run for 96 hours to take advantage of the delayed cell lysis induced by the anti-apoptotic protein. All 3 showed similar results with SDS page analysis. There was high level protein expression in all, with large bands in the total fractions for each protein at the expected size. This showed the increased protein yield as a result of the delayed cell lysis. However, in none of these proteins was the band seen in the soluble fraction. Even after protein purification and western blot analysis there was still no visible protein in a soluble form. Analysis of the Hi5 media showed no evidence any of the proteins had been secreted into the media via the melittin bee peptide, which was not surprising as the analysis showed the protein was expressed in an insoluble form.

Possible options to overcome these solubility issues were to change the expressed sequence to include some type of solubility tag[396], or solubilise the protein using a stronger denaturing detergent. As there was not time to redesign plasmids with added solubility tags it was decided to attempt to solubilise the protein using a denaturing detergent, with possible options including urea or guanidine hydrochloride[397]. As guanidine hydrochloride has been shown to be a stronger denaturing agent compared to urea[398] this was used as second option only when treatment with urea had failed to solubilise the protein. In addition to urea or guanidine the reducing agent β-mercaptoethanol was

included, which acts to break disulfide linkages aiding in the denaturing process[399]. An advantage of IMAC purification procedure with HIS tagged proteins is the option to purify in denaturing conditions[397] so solubilisation of the proteins still allowed purification with this procedure.

As the NS4 protein is a highly hydrophobic protein it was not surprising that when expressed the protein exhibited poor solubility. The previously mentioned study which claimed expression of the NS4 protein in a baculovirus system makes no mention of insolubility issues with this protein, but as the commercially purchased NS4 produced in *E. coli* was provided in a solution containing urea this obviously suggests a general issue with low solubility. The first increased solubility protocol tried with the NS4 protein was a hybrid-denaturing protocol. Cells were lysed using the same Triton X-100 based lysis buffer as used before. After the total and soluble fractions had been separated by centrifugation the remaining insoluble pellet was solubilised in 8 M urea buffer. After solubilising for 30 minutes the mixture was added to nickel coated beads which had been pre-washed in a urea containing phosphate buffer. The hybrid method used two washes in urea phosphate-based wash buffer, followed by subsequent washes in imidazole non-denaturing wash buffer containing no urea. This utilised the same imidazole concentration gradient (10-50 mM) as was used previously, followed by elution in 250 mM imidazole elution buffer. This hybrid method solubilises the protein initially but then produces a final protein which is not eluted into harsh, urea containing, elution buffer, thereby preventing further protein denaturation and degradation. The removal of the denaturing agent from the final elution buffer also allows the possibility of the protein refolding naturally[400]. This hybrid method was used successfully for the NS4 protein. The SDS page analysis showed solubilisation of the protein and 8M urea buffer followed by purification with the hybrid method gave a final protein in standard elution buffer. This was confirmed with subsequent western blot analysis.

The NS5a and NS5b proteins are both involved in the replication of the viral genome and are nucleic acid binding proteins. In the standard lysis and protein extraction, benzonase nuclease was included to degrade any nucleic acid present in the sample. It is possible that the NS5a and NS5b proteins still bound to nucleic acid despite the presence of benzonase and this may contribute to poor solubility. The first attempt to overcome this involved a standard non-denaturing protein extraction and purification in the presence of increased NaCl, increased from the 150 mM concentration used in the standard non-denaturing lysis buffer. Generally, the higher the NaCl concentration, the lower the binding affinity of the HISTAg to the nickel coated beads used in the purification process[401]. The original 150 mM NaCl concentration used represents a compromise between preventing the binding of contaminating proteins without lowering the binding of HISTag proteins to the nickel coated beads. This NaCl concentration was increased with the NS5a and NS5b proteins to dissociate any bound nucleic acid from the proteins without reducing affinity for the nickel coated beads, 300 mM NaCl was chosen. Unfortunately, the increased NaCl trial did not increase the solubility to a level that made any

soluble protein detectable. Trials with urea-based phosphate buffers demonstrated successful solubilisation of the NS5b pellet using a combination of 8M urea and the reducing agent β-mercaptoethanol at a final concentration of 10mM. As with the NS4 protein a hybrid method could be used combining solubilisation of the insoluble pellet followed by washing and elution using a non-denaturing imidazole gradient. Western blot analysis with an anti-HIS mAb was used to confirm the purification of the urea solubilised NS5b protein.

The most difficult of the expressed proteins to solubilise was the NS5a protein. The urea based hybrid denaturing protocol successfully used with NS4 and NS5b was unsuccessful with the NS5a protein. The protein did not solubilise with 8M urea buffer so guanidine hydrochloride was used. This is an ionic detergent which has been shown to be a stronger denaturing agent than urea[398]. The guanidine solubilisation buffer included β-mercaptoethanol at a final concentration of 10mM. The guanidine containing soluble fraction could not be run through SDS PAGE as the guanidine precipitates out in the SDS loading buffer. Purification of the guanidine solubilised NS5a protein was performed in full denaturing conditions, with all wash buffers and elution buffers containing urea at 8M. Using this method, a soluble form of the NS5a protein was purified, and confirmed as NS5a by western blot analysis.

The pOET8 transfer vector increased the yield of protein expressed, overcoming the issue of no to low protein expression for the NS4, NS5a and NS5b proteins. However, use of the transfer vector had produced an unexpected issue when purifying the proteins. This was the contamination of the purified eluate with an unwanted protein. This protein could be seen in the final eluates for all 3 pOET8 expressed proteins with SDS page analysis. It is thought this is the anti-apoptotic protein encoded by the vankyrin expression cassette. The protein is the same size as predicted for the vankyrin expression cassette protein and as it is under the control of a baculovirus p10 promoter it was expressed in high amounts. The vankyrin expression cassette in the pOET8 vector does not contain a HISTag coding sequence. The protein was only seen with SDS page analysis and not western blot analysis using anti-HIS mAb. Despite the lack of any HISTag the protein still purified through the nickel affinity process purification procedure. The IMAC process is not completely specific for HIS residues; other proteins can bind to the nickel coated beads[402]. The use of imidazole in the binding buffer and imidazole wash buffers should remove proteins which bind to the nickel with low affinity and leave behind the high affinity bound HIS tagged proteins. To try and improve the purity of the final eluate, two modifications of the purification process were tried. As the vankyrin protein was expressed in large amounts it was possible the contamination in the final eluate was not due to non-specific binding to nickel but was the result of a very high concentration of protein. To help overcome this potential issue the volume of the non-imidazole washes and 10mM washes was increased to 5ml. The 2nd modification was to increase the concentration of the imidazole gradient in

the wash buffer to a final concentration of 70mM thereby increasing the stringency of the wash steps. Despite these measures the protein can still be seen in the final eluates by SDS page analysis, the band is relatively weak but still present. As there was not time to attempt alternate protein purification methods it was decided to use the proteins in the ELISA with this low-level contaminant. Future work, see below, would include the use of additional purification steps to ensure removal of the vankyrin protein.

In total 5 proteins were produced in baculovirus expression systems for use in the final ELISAs. Both the core and NS3 proteins were expressed and purified in their native form. The NS4 and NS5b were solubilised in urea and purified under hybrid conditions to produce a final protein in standard elution buffer. The NS5a protein required solubilisation in guanidine hydrochloride and purification under 8 M urea denaturing conditions. In addition to the baculovirus expressed proteins a commercial NS4 protein was purchased from ProSpec Bio. The protein was purchased as a back-up in case the baculovirus expressed NS4 protein could not be solubilised and purified and to enable a comparison between an *E. coli* expressed protein and a baculovirus expressed protein.

A total of 6 proteins were used in individual ELISAs. The first stage of the optimisation process used the NS3 antigen. This antigen was chosen because it was expressed and purified in the highest amount and was known to be a commonly reactive antigen. The NS3 antigen was used to create a standard ELISA. The NS3 antigen acted as a capture antigen for any hepatitis C virus antibodies directed against the NS3 antigen to bind to. Detection of any bound antibody was achieved using an anti-human IgG secondary antibody conjugated with HRP in combination with TMB substrate, using sulphuric acid to stop the reaction. Each aspect of the ELISA was optimised using the NS3 antigen to select the blocking buffer, secondary antibody, primary and secondary antibody dilutions, incubation temperatures and substrate reaction times. Once these had been selected the other antigens were then trialed and the optimum antigen coating concentration chosen. A final optimisation was performed for DBS samples, where a different primary antibody dilution was used from that used for serum.

Samples used in the optimisation and validation were previously tested using 2 commercial anti-HCV assays. The Roche Cobas anti-HCV II assay is an electrochemiluminescence assay which includes the HCV antigens Core, NS3 and NS4. The second confirmation assay, the Ortho anti-HCV assay, is a standard plate based ELISA which incorporates the Core, NS3, NS4 and NS5 antigens. Both assays are CE marked for use with serum samples, but not DBS samples. A previous optimisation and validation for these assays had been performed for use with DBS samples. The positive: negative cut-off value from each of these assays was lowered using ROC analysis to increase sensitivity while maintaining specificity. Overall, the assays worked well with DBS samples, with the Roche Cobas anti-

HCV II assay being the more sensitive of the two, detecting more samples known to be anti-HCV positive compared to the Ortho anti-HCV assay.

The samples used for the validation had been pre-tested using the commercial assays outlined above and shown to be anti-HCV positive or anti-HCV negative. In addition, the HCV RNA status of the anti-HCV positive samples was determined. What remained unknown was the exact antigen/s anti-HCV positive samples had reacted against. Anti-HCV negative samples were known to be non-reactive for any HCV antigen in commercial assays. A possible option would have been to use a HCV recombinant immunoblot (RIBA) to confirm the presence of individual antibodies in an anti-HCV positive sample, this combines the HCV Core c22p peptide,c33c NS3 antigen, NS4 5-1-1p and c100p peptides, and NS5 antigen[403]. However, although the same antigens are represented in the RIBA, the y are not an exact match for the antigens produced in baculovirus in this study. For instance, the Core and NS4 are both short peptides, not the larger proteins produced in baculovirus, and the NS5 was produced as a whole protein and not as individual NS5a and NS5b proteins produced in this study. In addition the RIBA assay is known to be relatively insensitive when compared to ELISA[404]. An anti-HCV positive sample was therefore chosen arbitrarily for use in the optimisation, if this showed no difference in signal strength from that of an anti-HCV negative sample it was assumed to be non-reactive for that antigen and another positive sample was chosen.

Initial optimisation experiments with the NS3 antigen ELISA resulted in a high background in anti-HCV negative samples. The aim of the optimisation process was to maximise the difference in signal strength between known anti-HCV positive samples and known anti-HCV negative samples. Keeping the background signal strength in known anti-HCV negative samples to a minimum was essential. The choice of secondary antibody and the dilution used were both critical. To overcome the initial high background seen in the NS3 antigen ELISA a comparison was performed between a rabbit polyclonal anti-Human IgG antibody and a mouse monoclonal anti-Human IgG antibody. Both antibodies were conjugated with horseradish peroxidase for detection with TMB substrate. The comparison of the two antibodies showed the monoclonal anti-IgG antibody to be the better performing of the two. The lower background seen when using a monoclonal antibody is not surprising, targeting of a single epitope should give lower non-specific cross reaction than a polyclonal antibody containing a mixture of antibodies targeting different epitopes. The potential disadvantage of the monoclonal antibody is an overall drop in the positive signal strength compared to the polyclonal. The results of the comparison between the 2 assays showed a slight reduction in the positive signal strength, but this was more than compensated for with the lower background level. It was decided to use the monoclonal antibody for all further optimisation work.

The next component to optimise was the blocking buffer. A blocking buffer is used after the coating of antigen to the well. The blocking buffer will bind to any space left on the ELISA well surface which has not already been filled with antigen. The binding of these sites with the blocking buffer prevents subsequent primary and secondary antibodies from non-specifically binding to the surface. The two blocking buffers compared in this optimisation were BSA and FCS. Both were used at standard concentrations of 1% for the BSA in PBS and 5% for the FCS in PBS. In addition to the blocking stage the blocking buffer also forms the base of the sample diluent, used for diluting the primary and secondary antibodies. This is prepared using the same concentrations as the blocking buffer in PBS but with the addition of Tween at 0.05%. The results of the comparison were quite close, but overall the bovine serum albumin gave a slightly higher ratio between the positive and negative signals and so was chosen for all future work.

After the secondary antibody and blocking buffer were selected, the next optimisation steps were to determine the optimum primary and secondary antibody dilutions. The primary antibody in this case is the serum sample, potentially containing HCV antibodies. The secondary antibody was the previously chosen mAb anti-Human IgG HRP. The primary antibody in an ELISA sample was diluted, the majority of commercial assays use a primary antibody dilution of 1:10. Selecting the primary antibody dilution is a balance between maximising sensitivity while maintaining specificity. Multiple anti-HCV positive and anti-HCV negative samples were tested. The optimisation results showed the ideal dilution was between the 1:20 and 1:40. The same procedure was repeated to determine the optimum secondary antibody dilution. A range of dilutions from 1:5000 to 1:40000 were evaluated and an optimum dilution of 1:20000 was used in further experiments.

To determine optimum antigen concentration, concentrations of 10ng/µl down to 1.25ng/µl were coated on plates. The commercially purchased NS4 PrSpc antibody was used in a dilution series from 5ng/µl to 0.625 ng/µL. Multiple anti-HCV positive and anti-HCV negative samples were used to optimise the coating concentration of each expressed protein. All expressed HCV antigens worked in the initial antigen coating optimisation experiments, giving a definitive signal difference between anti-HCV positive and anti-HCV negative samples. The final concentrations chosen were all at 5 ng/µL or below. The commercially produced NS4PrSpc antibody gave very high backgrounds at the higher coating a concentration so was diluted to 0.625 ng/mL.

After optimisation with serum samples a final re-optimisation was performed for DBS samples. The samples used in this validation process were previously eluted DBS samples prepared by washing 4 spots (each 25 µL in size) in 1.5 mL of PBS/Tween. The DBS samples had already been diluted more than 10 fold relative to a serum sample. A dilution of 1:2, was chosen as the optimum dilution for DBS samples.

The fully optimised ELISA assays were then tested with a range of anti-HCV negative and anti-HCV positive serum and DBS samples. Receiver operating characteristic (ROC) analysis was used to set the positive cut-off threshold value for each ELISA and for comparison of the performance of each assay. Determination of the positive cut-off threshold is more commonly determined for an ELISA by assuming normal distribution and a cut-off of the mean of a negative reference plus two standard deviations designed to encompass the 95% normal range of negative samples. Disadvantages of this approach include a presumption that data are normally distributed[405]. An alternative to this approach is the use of ROC analysis, which enables the selection of a positive cut-off threshold value taking into consideration both sensitivity and specificity and is not sensitive to deviations from a non-normal distribution[406]. In addition ROC analysis can be used to assess the accuracy of a diagnostic test and to compare this accuracy between different tests[407]. ROC analysis was first used in the 1950s in signal detection analysis[362] it was then adapted for use in clinical diagnostic testing[408409]. In ROC analysis a reference test, in this case the Roche Cobas anti-HCV II assay, was used to assign a sample as a case (anti-HCV positive) or a control (anti-HCV negative). As outlined previously, the pattern of antibody reactivity to individual HCV antigens in Cobas anti-HCV positive samples was not known, so the comparison between each individual ELISA and the Cobas anti-HCV II cannot be said to be a like for like comparison. However, the fact anti-HCV negative samples can be considered negative for all the antigens tested in the ELISA does make the comparison worthwhile and the use of the Cobas anti-HCV II results as the reference assay justifiable. The analysis plots the sensitivity of the assay as the y coordinate against specificity for the x-coordinate[410] for each operating point, i.e. each optical density recorded for each sample tested. The generated ROC curve could then be used to determine the positive cut-off threshold and also to compare each assay. Determination of the positive cut-off threshold for ROC analysis includes methods such as the Youden Index [360] or the closest top left[361]. The Youden index uses the diagonal line through the middle of the ROC plot area, the point at which a diagnostic test works no better than chance and selects the threshold as the point furthest away from this diagonal line. The closest top left method determines the point on the ROC curve closest to the top left of the ROC plot area, the area of maximum sensitivity and specificity. Of the 2 methods the Youden index is thought to produce the more optimal cut-off for maximising accuracy[361], though both these methods were used to pick potential positive cut-off values for each HCV antigen ELISA. In addition to these 2 established methods a third method was used, which determined the lowest positive cut-off threshold which gave a maximum specificity of 100%. All ROC analysis was performed using the pROC package[359] in R statistical software. This is a comprehensive ROC statistical package that enabled the generation of a ROC curve, determination of the positive cut-off thresholds using the three listed methods, determination of the sensitivity and specificity at these thresholds and determination of the area under the curve (AUC). The AUC provides an assessment of the performance of an assay, a perfect assay has an AUC of 1, an assay delivering results no better than

a 50:50 chance has an AUC value of 0.5. Within this range a general guide is that an assay is defined as accurate if the AUC value is above 0.9, moderately accurate if between 0.7-0.9 and of low accuracy when <0.7[411]. The pROC package calculated the AUC using a previously described method[362], and determined the statistical power at a statistical significance of 0.05. In addition to giving an overall indication of the accuracy of an individual assay, the AUC value can be used to compare different assays, a function within the pROC package. For comparison of the total AUC value the non-parametric Delong method[363] for comparing paired diagnostic tests, as in tested on the same sample set, was used to determine any statistically significant difference between two assays. However, comparison of the total AUC has been shown to miss a potentially significant difference in two diagnostics assays with comparable performance when the only difference is in the high sensitivity and specificity regions of the ROC curve[359]. An alternative in these instances is the use of the partial area under the curve, pAUC, which has been shown to detect significant differences in highly comparable assays[364] and can be determined using pROC software. For comparison of assays when no significant difference was detected using the total AUC, the pAUC was calculated and compared using a bootstrapping method[412] calculated in pROC software. The pAUC was set to include only the area of high specificity above 90%. Confidence intervals for the AUC were calculated using Delong method[363] and for pAUC using a bootstrapping method[413].

Overall, the results of validation of the ELISAs with serum samples were mixed. Despite optimisation of each component of the assays, the background level in anti-HCV negative was relatively high in some assays and so high in other assays to make them unusable. The HCV Core assay performed relatively well though there was still an issue with high background levels with HCV negative samples. The ROC curve filled the majority of the plot area giving an AUC value of 0.93 identifying the assay as accurate although using the maximum specificity method to assign the positive cut-off required a threshold value of ≥0.99 to achieve a specificity of 100%. At this level just over half of the samples, 63.2%, were positive. Using the alternative Youden method to assign the positive cut-off value reduced the threshold to 0.63, at which the sensitivity increased to 82.98% but the specificity dropped to 95.65%. Using the closest top left method gave a very similar threshold of 0.62, with a sensitivity of 84.04% and a specificity of 94.56%. Despite the higher than ideal background level the results show a high level of reactivity for the Core antigen in anti-HCV positive samples.

The NS3 assay produced the same AUC value of 0.93 as the Core assay when testing the panel of serum samples. The background was slightly lower with a positive Cut-off of >0.62 giving a specificity of 100%, but this was still higher than initially aimed for. The number of samples showing reactivity to the NS3 was lower than the core, at 53.7% sensitivity when combined with 100% specificity. Both the Youden and closest top left methods dropped the threshold to 0.25 and 0.2 respectively. While this increased the sensitivity to 81.91% and 87.2%, the specificities dropped a large amount to

90.21% and 84.78% respectively an unsuitable level for a diagnostic assay. Unsurprisingly, a comparison of the Core and NS3 assay showed no statistical difference between the two when using total AUC, but as mentioned previously the total AUC can erroneously assign significance difference between 2 comparable assays. Repeating the comparison with the calculated pAUC, 0.079 for the Core and 0.065 NS3, did produce a significant difference in the high specificity areas, with a p-value of 0.04 for the Core slightly outperforming the NS3 assay.

The NS4 assay was blighted by even higher background levels, at a level which made the assay almost unusable. The ROC plot showed an assay which worked with mediocre accuracy, AUC value 0.86, but the very high background level meant a positive cut-off threshold of ≥1.1 was required to achieve a specificity of 100%. As the range for optical density results for the ELISA only went up to a maximum of 3, and the original target value for the background was around 0.1, this was much higher than aimed for during the ELISA optimisation. Using the maximum specificity threshold level only 33% of anti-HCV positive samples were reactive. Using the Youden and closest top left analysis again dropped the threshold, to 0.4 and 0.34, and increased the sensitivity to 71.28% and 77.66%, but both specificities dropped to below 90% at 89.13% and 81.52% Comparison of the total AUC with the Core assay proved an assay performing significantly worse, p=value 0.01.

The NS5a assay gave a lower background level than with the other proteins, requiring a positive cut-off value ≥0.34 to achieve a specificity of 100%. Although the background level was lower, the overall proportion of anti-HCV positive samples reactive with the NS5a assay was lower than with the Core and NS3 and around the same level as the NS4. The AUC value of 0.84 was just lower than the NS4 assay and not statistically different. Even repeating the comparison with the pAUC gave very similar values, 0.054 for the NS4 and 0.055 for the NS5a, with no significant difference two assays, p-value 0.89. As with the other assays use of the Youden and closest top left methods to set the positive cut-off reduced the thresholds but specificity for both dropped below 90%.

The NS5b assay did not work well with serum samples. The ROC plot produced an AUC value of 0.64, showing the assay was working with low accuracy and statistically inferior to the NS5a assay, p-value 3.39 $X10^{-6}$. The NS5b assay with serum samples was one of only 2 assays which did not give a statistical power of 1, for a significance of 0.05 when the power test was performed during ROC curve generation. The background level was very high, a positive cut-off of ≥1.61 was required to achieve a specificity of 100%, with only 9.6% of samples reactive at that level. Using the Youden and closest top left methods produced the same much lower threshold of 0.15, which increased sensitivity to 63.04% but dropped the specificity to an unusable level of 62.76%.

The one commercial protein trialed in the project, the *E. coli* expressed NS4 protein, failed to produce a working ELISA when tested with serum samples. This can be seen with the diagonal line through the middle of the ROC plot and an AUC value of 0.563 showing the assay was working no better than chance. The statistical power test at a significance of 0.05 for the ROC curve gave a power of only 0.27, identifying the ROC curve as not statistically valid. As with the NS5b assay the background level was so high it made identifying any positive samples difficult. Two anti-HCV negative samples gave very high signal readings, meaning a positive cut-off of ≥2.7 was required to achieve a specificity of 100%. This was almost the maximum possible OD reading detected in anti-HCV negative samples. Dropping the specificity to 94.6% did drop the positive cut-off down to ≥0.56, but at this level only 18% of anti-HCV positive samples were identifiable.

Overall, the results produced when testing serum samples with the individual ELISAs were mixed. The Core and NS3 antigens produced accurate assays, even though the background was higher than originally aimed for. The NS4 and NS5a produced working assays with mediocre accuracy and higher than ideal background levels in the anti-HCV negative sample, particularly the NS4 assay. The NS5b and the *E.coli* expressed NS4 did not produce working ELISAs, the background level was so high they were unusable. The reason for the overall high background level seen with serum samples may have been the dilution the samples were used at. Original optimisation experiments had shown the optimum dilution across each ELISA to be 1:20. After testing a much larger panel of samples across all the ELISA it seems this dilution factor was too low, and the serum samples should have been diluted more to 1:40 or 1:80 to help reduce the background level in anti-HCV negative samples.

Performance of the ELISA was improved when testing DBS samples. This was due to a lower background level when testing anti-HCV negative DBS sample, enabling much lower positive cut-off values to be set. Both the Core and NS3 assays performed well, giving AUC values of 0.96 and 0.97 respectively, close to a perfect score of 1. Both required similar positive cut-off values to achieve a specificity of 100%, ≥0.26 for the Core producing a positive result in 79.3% of samples and ≥0.19 for NS3 producing a positive result in 89.1% of samples. For the Core using the Youden index dropped the threshold to 0.2, giving a sensitivity of 89.1% combined with a specificity of 97.7%. Using top left closest method dropped the threshold further to 0.17, further increasing sensitivity to 92.4% but dropping the specificity to 94.3%. For the NS3 assay the Youden index gave the same threshold as for maximum specificity, 0.19, maintaining the same sensitivity and specificity. The closest top left dropped the threshold slightly to 0.14, increasing specificity to 92.4% with a specificity of 95.45%. Both these sets of results show a high level of reactivity in anti-HCV positive samples for both the Core and NS3 antigens. Unsurprisingly there was no significant difference between the assays when comparing the total AUC. When the pAUC was calculated for the 90% and above specificity area, the core gave a value of 0.089 and the NS3 value of 0.091. A perfect score for the pAUC is 0.1,

demonstrating good performance for both assays in this high specificity area, with no significant difference found between the two, p-value 0.51.

The NS4 assay experienced a slightly higher than ideal background level requiring a positive cut-off value of ≥0.46 to achieve a specificity of 100%, at which 71.7% of samples were reactive. Using the Youden index dropped the threshold to 0.33, with a sensitivity of 82.6% and a specificity of 96.6%. Closest top left analysis produced a threshold of 0.31, with a sensitivity of 83.7% and a specificity of 93.18%. The overall AUC value of 0.91 was a slightly lower than observed with the highest performing NS3 assay, p-value 0.01, but still represents a highly accurate assay.

The NS5a assay had a low background level overall but this was matched with a lower overall reactivity than with the other antigens, with 57.6% of samples positive at the maximum 100% specificity. Using the Youden and closest top left analysis dropped the threshold to 0.11 and 0.1, increasing sensitivity to 79.35% and 82.61% but dropping the specificity to 84.1% and 80.68% respectively. The overall AUC value was 0.87, suggesting an assay with mediocre accuracy but it was not statistically inferior to the NS4 assay. Only using pAUC, 0.08 for the NS4 assay and 0.062 for the NS5a assay, could determine a significant difference, p-value 0.003. The NS5a tended to produce a high differentiation between negative and positive samples. Though the overall proportion of samples reactive was lower, when samples were positive the signal strength tended to be very high, generally recording the maximum signal strength of 3.

The NS5b assay was the poorest performing of the baculovirus expressed proteins with an AUC value of 0.71, significantly worse than the next lowest performing assay with DBS samples, the NS4PrSpc, p-value $7.2 \times 10^{-5.}$ The overall background level was better than with serum samples but still quite high at ≥0.43 to achieve a specificity of 100% and this was combined with a very low overall reactivity, just 25% of samples were positive at this specificity. Youden and closest top left analysis produced the same lower threshold of 0.19, increasing the reactivity to 68.48% but dropping the specificity to a low 64.77%. Both the results for the serum and DBS samples show a very low overall reactivity. This could be due to a low proportion of anti-HCV samples containing antibodies directed against the NS5b protein or could be due to the truncated nature of the baculovirus expressed NS5b protein used in this assay. As there are a lower number of reactive antigenic epitopes in the NS5b protein compared to the NS5a protein [388] it is possible that this shortened protein just did not contain enough reactive epitopes to form a well performing assay.

Previous studies of commercial assays using an NS5 antigen, a full NS5 recombinant protein incorporating both the NS5a and NS5b components, have found reduced specificities compared to assays without a representation of this antigen[368]. From our findings it would suggest the NS5b component is potentially the cause of the lower specificity. The NS5a antigen assay in this study

showed a lower overall reactivity than the other antigens but a very low background and high specificity, while the NS5b did show a higher overall background level in both serum and DBS anti-HCV samples. This suggests the inclusion of a NS5a antigen as opposed to a full NS5 antigen would be more beneficial for an anti-HCV assay.

The biggest improvement between assays when testing serum and DBS samples was with the commercially purchased NS4 PrSpc protein. This had not produced a working assay with serum samples but did produce one with DBS samples, with a much reduced background. The positive cut-off threshold was slightly high at 0.35 to achieve a specificity of 100%. This was similar to the background level of the baculovirus expressed NS4 protein, but the overall reactivity was lower. Only 43.47% of samples were reactive when the specificity was set at 100%. Both Youden and closest top left analysis dropped the threshold to 0.16, increasing the sensitivity substantially to 85.2% but dropping the specificity to a low 79.4%. When compared to the baculovirus produced NS4 protein, the total AUC of the NS4PrSpc of 0.86 was lower than the 0.91 for the NS4 assay but not significantly different. It was only through comparison of the pAUC, 0.08 for the baculovirus NS4 assay compared to 0.057 for the NS4PrSpc assay, that a significant difference was detected, p-value 0.003. Despite this similarity, the overall reactivity of the baculovirus produced NS4 assay was high, with a sensitivity of 71.7% when specificity was set at 100%, compared to 43.47% for the NS4PrSpc assay.

Several findings from the ROC analysis and comparison stood out. Of the 3 methods compared for setting the positive cut-off threshold the most reliable and consistent was using a maximum specificity of 100%. The Youden index and closest top left methods generally assigned lower thresholds, with closest top left the lower of the two, which in turn increased sensitivity but decreased specificity even further. With some assays, for example the Core assay with DBS samples, this difference was relatively small, increasing the sensitivity while maintaining a specificity close to 95%. For other assays this difference was more marked. For example, with the NS5a assay with DBS samples the lower Youden index threshold increased the sensitivity to 79.35% from an original 57.6% with the maximum specificity method, but the specificity dropped to 84.1%. Using the closest top left method increased the sensitivity even more to 82.61% but dropped the specificity further to 82.61%. A specificity of this level is unacceptable for a diagnostic anti-HCV test. All current commercial anti-HCV assay have specificities greater than 99%[368], dropping to such a low level of specificity would produce an unacceptable level of false positive results for routine diagnostic use. It was for this reason that for the subsequent overall sensitivity and specificity calculations discussed below the maximum specificity cut-off was used.

Plotting the relative light units produced by the Cobas anti-HCV II assay versus the OD signal of the individual ELISA gave some indication of the spread of the signal strengths of the positive result. As described previously, this is not a direct like for like comparison as the reactivity of the individual

antigens in the Cobas anti-HCV II assay are unknown, but it does give an overall picture of the signal strengths produced by each individual ELISA and their correlation. The Core antigen assay had a mixture of signal strengths, with the majority in the middle of the possible signal range. The NS3 antigen assay, though having an overall higher percentage of reactivity in samples, produced lower overall signal strength than the Core with no samples giving a maximum value. The NS4 had a greater range of signal strengths, with several samples giving a maximum value with little correlation to the Cobas RLU. The NS5a antigen assay was reactive in just over half the samples, lower than the other antigens, but a higher proportion of the samples reactive gave the maximum signal strength. The signal strength had little correlation with that given by the Cobas anti-HCV II assay, given the assay does not contain a NS5a antigen. The results seem to suggest that although a lower proportion of those infected produce an immune reaction to the NS5a antigen, when a reaction is produced it is very strong. The NS5b assay had the lowest correlation of all the assays, not surprisingly as this was the poorest performing antigen among all the assays. Despite this, a small number of samples did give a very strong reaction.

Overall, the performance of the assays was good with DBS samples. The original aim of this project was to produce a single multi-analyte array composed of the individual antigens produced using baculovirus for use with DBS samples. Due to issues and delays in protein production the endpoint of a single well multi-analyte array assay could not be tested. However, the results of each baculovirus antigen assay could be combined to give a multi-analyte array result profile for each sample. If a sample was defined as anti-HCV positive, if at least one of the individual antigens was positive, then an overall sensitivity and specificity of 100% was achieved. This is a high level of performance for an anti-HCV assay. The Roche Cobas anti-HCV assay is the most sensitive anti-HCV assay on the market[283] so to achieve comparable performance with a plate based ELISA approach demonstrates the antigens were performing well. The Cobas anti-HCV assay has several technological advantages not available with conventional plate-based ELISA. Firstly, the use of antigen coated microparticle beads increases the available binding surface area compared to a plate-based ELISA. Secondly, the Cobas anti-HCV assay uses ECL detection which increases sensitivity compared to colorimetric detection used in conventional plate based ELISA assays[414]. Transferring these antigens into an ECL based multi-analyte array style platform such as the MSD could improve performance further.

In 93.5% of the anti-HCV positive DBS samples at least 2 antigens were positive, and in 72.8% 3 antigens were positive. Knowing the number of antigens positive for each sample has advantages over the result given by a standard anti-HCV immunoassay such as the Cobas assay. One of these is the removal of the need for anti-HCV confirmation testing. It is current best practice to confirm initial anti-HCV positive results using a second different anti-HCV assay. This is performed to detect possible false positive result from the initial screening assay, potentially produced by a non-specific reaction

with one of the antigens. This 2nd confirmation test increases the overall time to produce a result and increases the cost. With the multi-analyte array result the number of antigens positive can be identified. A sample reactive with more than one antigen is far less likely to be a false positive as the chances of a non-specific reaction with 2 antigens is reduced. If that was the case 93.5% of samples would not require further confirmation testing. This could be made more stringent by setting the number of reactive antigens to a minimum of 3, even at this level 72.8% of anti-HCV positive DBS samples would not require further confirmatory testing.

Another issue with anti-HCV confirmation testing, apart from the increased time and cost, is the difference in sensitivity between the screening assay and the confirmation assay. The confirmation assay used for the positive samples included in this validation was the Ortho anti-HCV 3.0 assay. This is a plate-based ELISA which includes a form of Core, NS3 and NS4 antigens found in the Cobas assay plus the addition of an NS5a assay. The Ortho anti-HCV assay is less sensitive than the Cobas assay, in-house validations performed in our laboratory show a 64 fold reduction in end point sensitivity. In the present assay validation, 7 equivocal anti-HCV samples were included, with Cobas anti-HCV positive results but negative Ortho anti-HCV results. Six of the 7 samples were HCV RNA negative. The samples with an equivocal anti-HCV profile combined with an HCV RNA negative results could represent samples with waning antibody levels after clearance of HCV infection but could also be false positive results produced by the Cobas anti-HCV assay. One of the samples was HCV RNA positive, this was highly likely to be a sample from a patient acutely infected with HCV, as the PCR is detected first followed by a rising anti-HCV level. Of the 7 anti-HCV equivocal samples, 5 were reactive with at least one antigen, 2 samples were reactive with 2 antigens. This demonstrates a superior performance of the combined antigen result compared to the Ortho anti-HCV assay, and confirms at least 5 of the samples as genuine positives detected by the Cobas assay but missed with the Ortho assay. In all 5 of the equivocal samples detected, the NS4 antigen was reactive. This potentially suggests the NS4 antigen is the longest lasting of the NS4 antibodies after clearance of HCV infection, and possibly the first to appear. The small number of results with equivocal samples precludes definitive conclusions but this would be something to investigate in future work.

From the individual antigen ELISA results it was difficult to determine any effect of the contaminating vankyrin protein. The 3 antigens contaminated with this protein were the NS4, NS5a and NS5b. The NS4 did produce a very high background level with serum samples and a still higher than ideal background level with DBS samples which could potentially be due to the contaminating vankyrin protein. However, the NS5a had the same contaminating vankyrin protein but produced the lowest background level of all the antigens suggesting the vankyrin protein had little effect. The NS5a antigen was used at 1.25ng/µl compared to the 2.5 ng/µl with the NS4 antigen which may partly explain a reduction in the background level if this was due to the contaminating vankyrin protein, but

this is difficult to determine. In future work it would be desirable to produce purified antigens without this contaminating protein.

The effect of denaturing the NS4, NS5a and NS5b proteins was also difficult to determine without a non-denatured protein to compare them to. Denaturing of a protein with urea or guanidine can disrupt the tertiary structure but retain elements of secondary structure with hydrophobic surfaces which are usually buried partially or fully exposed[380].The NS4 and NS5b antigens were purified using a combination hybrid method solubilising in urea but giving a final protein in standard non denaturing elution buffer. The removal or urea during this process and final elution in non-denaturing conditions does leave the possibility of the protein partially or fully reordering into its native state[400], though the use of the reducing agent β-mercaptoethanol to disrupt disulphide bridges may limit the refolding[380]. A full refolding process could have been performed using specific refolding buffers[400] but due to time pressures and the limited amount of protein to work with it was decided to use the NS4 and NS5b proteins in partially denatured state.

The NS5a antigen proved the most difficult protein to solubilise and stronger guanidine solubilisation buffer with wash and final elution steps under denaturing conditions in urea containing buffers was used. This would have denatured the protein and left no possibility of refolding. Despite this the antigen was very reactive with a proportion of samples suggesting the immune-reactive epitopes were maintained. The NS5b antigen was the poorest performing of all the antigens but this was as likely to do with the very truncated final protein as it was to do with denaturation. It must be remembered though that both the 2 best performing antigens, the Core and NS3, were both produced in a form most closely resembling that found in an HCV infected human hepatocyte. It is possible the other denatured proteins would have performed even better if they could be produced in a native soluble form.

An *E. coli* produced NS4 antigen was purchased to enable a direct comparison between a baculovirus and *E. coli* produced HCV antigen. It should be noted the commercially purchased NS4 antigen was provided in a urea containing buffer, suggesting the production suffered from the same solubility issues experienced with the baculovirus production. This is not surprising with such a highly hydrophobic protein. A direct comparison in serum samples was not possible due to the very high background produced with the *E. coli* NS4 protein. This was improved when testing DBS samples, but the *E. coli* NS4 protein was reactive in a lower proportion of samples, 43.47% compared to 71.7% and gave a significantly lower pAUC value than the better performing baculovirus produced NS4 protein This despite urea solubilisation which would be predicted to affect tertiary structure as outlined above. This suggests that despite this denaturation process enough of the post translational modifications remain to give a usable antigen, and one more closely resembling the native wild type protein, compared to a protein produced in *E. coli*.

Overall, in this study HCV Core, NS3, NS4, N5a and NS5b antigens were successfully expressed using a baculovirus based expression system. Problems with low expression levels were overcome using the *flash*BAC™ ULTRA expression system combined with a variety of compatible transfer vectors. Low solubility issues were overcome for the NS4, NS5a and NS5b proteins using urea or guanidine based solubilisation procedures. Each antigen was optimised in individual ELISAs, separately for serum and DBS samples. Each ELISA was validated with a panel of serum and DBS samples, and the overall results combined to give a total multi-analyte array profile. Combined results for testing serum samples produced a working assay but several antigens suffered with high background levels. Combining the results for DBS samples produced a very sensitive and specific assay, matching the performance of the current best performing commercial anti-HCV assay. Potential advantages of this multi-analyte array approach include the removal of the need for anti-HCV confirmation testing in the vast majority of samples, and the identification of individual antigen reactivity gives the possibility of identifying acute infection or to investigate a vaccine response.

13.1 FUTURE WORK

Protein production could be improved from the methods described in this study in several ways. The first possible option would be to remove the affinity tag and melittin bee sequence from the remaining protein. All 3 insoluble proteins were expressed in the pOET8 plasmid, which contains an 8 X HIStag and melittin bee signal sequence at the N' termini, with a human rhinovirus 3C (HRV-3C) protease cleavage spacer between the tags and the expressed proteins. The cleavage site opens up the possibility of removing both the HIS Tag and melittin sequence from the final protein using an HRV-3C protease step. Due to time pressures and the need to purify enough protein to perform the validation ELISA's this step was not performed. The HISTag is not predicted to affect the solubility of a protein[415] and this was seen with both the Core or NS3 proteins which remained soluble without its removal. However neither of these proteins contained the melittin bee signal sequence and as affinity tags have variable effects on the proteins they are attached to, including a change in the solubility[416], it is possible the affinity tag encoded in the pOET8 transfer vector contributed to the insolubility.

If removing these tags did not have the desired effect of increasing solubility another option would be the addition of a solubility tag. Solubility tags are peptides or proteins fused to the expressed proteins which increase the overall solubility. The most commonly used tags are maltose-binding protein (MBP), glutathione-S-transferase (GST), N-utilisation substance A (NusA) and thioredoxin (Trx), with MBP and GST doubling up as affinity tags[396]. Most experience of solubility tags has been gained through use with *E.coli* based expression systems which suffer from poor solubility compared to eukaryotic expression systems[379] but solubility tags such as GST can be used in baculovirus based systems[417]. As the effectiveness of these solubility tags varies between proteins a number of different

tags may need to be trialed, possibly doubling these up as an affinity tag before removal from the final protein[379]. Another option to increase solubility would be the use of the CamSol method. This uses software based calculations to predict the solubility of thousands of variants of the desired protein, identifying a final sequence which maximises the solubility while maintaining the native form[418]**.** The modified sequence can then be produced synthetically for future expression experiments. The use of this approach promises to save a large amount of experimental time by replacing it with computational predictions. Unfortunately, this method was not available until the end of this project but all future potential fusion protein sequences should be analysed with this *in silico* approach to identify solubility issues before practical experimentation.

Another issue in the expression of the proteins was the contamination of the NS4, NS5a and NS5b purified protein solutions with the product of the vankyrin expression cassette. The vankyrin product contaminated all proteins expressed using the pOET 8 transfer vector. The delayed cell lysis induced by the vankyrin protein enabled higher expression of protein and helped produce protein in sufficient amount for subsequent experiments, but the IMAC purification procedure was unable to remove all the vankyrin protein from the final protein solution. To fully remove this contaminating protein an additional purification step, termed a polishing step, will be required. A recommended additional purification step for IMAC purified proteins is ion exchange chromatography (IEC)[402]. This is one of the most commonly used methods for the separation of proteins, based on the binding of proteins to positively or negatively charged groups which are immobilised on a stationary phase[419]. The expressed Vankyrin protein is 171 aa long, with a molecular weight of 19.4KDa, and a predicted isolelectric point of 6.71. The expressed NS4 protein was 379 aa long, with a molecular weight of 40kDa and a predicted isoelectric point of 6.97; the expressed NS5a protein was 457aa, a molecular weight of 50kDa, and a predicted isolelectric point of 6.59 and the expressed NS5b protein was 364 aa, with a molecular weight of 40kDa and an predicted isoelectric point of 8.19. These are estimations of the isoelectric point which can vary depending on the method used to calculate them[420] so may vary when the actual ion exchange chromatography is performed. As the isoelectric points of NS4 and NS5a are close to the predicted vankyrin protein isoelectric point a high resolution separation would need to be performed using a linear NaCL gradient[421] to achieve a good separation. Even using this approach it is possible the close predicted isoelectric points mean a high degree of separation cannot be achieved to separate the vankyrin protein from these 2 proteins. Alternative approaches to ion exchange would include size exclusion chromatography[422]. As the vankyrin has a predicted molecular weight of 19.4 kDa, compared to NS4 with a molecular weight of 40kDa and the NS5a with a predicted molecular weight of 50kDa, this represents a good separation in size.

A final approach to remove the vankyrin protein would be the use of hydrophobic interaction chromatography. This uses the absorption of hydrophobic regions on a protein to immobilised

hydrophobic ligands at high salt concentrations, with a following descending salt gradient to elute the proteins separately[423]. As the vankyrin was soluble, as seen in all soluble fractions after purification, and the hydrophobic NS4, NS5a and NS5b proteins were not, this would be a good approach to vankyrin protein removal. Separation of proteins bound to the stationary phase is achieved through the use of ionic or pH based concentration gradients. Advantages of this method include the high capacity and selectivity. To be used successfully, several steps must be optimised including the choice of stationary phase resin plus the pH and counter ion concentrations used in the load, wash and elution buffers[424]. Once optimised the selectivity offered with this technique should enable the separation of the expressed HCV protein from the contaminating vankyrin protein more successfully than was achieved with IMAC alone, giving a higher purity protein for use in immunoassays.

In this study the results from the individual ELISA were combined to give a multi-analyte array result profile. The initial aim of the study was to combine all the antigens into a multi-analyte array such as that offered by MSD technology. Developing an assay on this platform would give a full array profile but from a single well. The platform uses ECL technology which would further increase the performance of the assay compared to the standard enzymatic based detections used in this study. This multi-analyte array would give a full result profile, eliminating the need for anti-HCV confirmation testing in the majority of samples. Another addition to the multi-analyte array could be the development of an HCV antigen screen, to run alongside the anti-HCV assay. This could identify active HCV infection from the same sample, potentially speeding up the diagnosis and reducing the cost of detecting active infection compared to the current use of PCR for the detection of HCV RNA.

Future studies could use a multi-analyte array to determine the specificity of the antibody response in acute infections, to determine if there is a pattern to the results which could be used to reliably identify acute infection. Identification of acute infection is important in enabling intervention to prevent ongoing transmission and help to identify geographic areas in which testing and treatment should be concentrated, a necessary step if HCV is to be successfully eliminated. The multi-analyte array could also be used to monitor the immune response in patients who clear HCV infection, compared to those who become chronically infected, to gain a more in depth understanding of an effective immune response and provide useful information for any ongoing vaccine development studies.

14 REFERENCES

1. Alter, H., Holland, P., Purcell, R. & Popper, H. Transmissible agent in non-A, non-B hepatitis. *Lancet* (1978).
2. Choo, Q. L. *et al.* Isolation of a cDNA clone derived from a blood-borne non-A, non-B viral hepatitis genome. *Science* **244**, 359–62 (1989).
3. Blach, S. *et al.* Global prevalence and genotype distribution of hepatitis C virus infection in 2015: a modelling study. *Lancet Gastroenterol. Hepatol.* **2**, 161–176 (2017).
4. Ashfaq, U. A., Javed, T., Rehman, S., Nawaz, Z. & Riazuddin, S. An overview of HCV molecular biology, replication and immune responses. *Virol. J.* **8**, 1–10 (2011).
5. Moradpour, D., Penin, F. & Rice, C. M. Replication of hepatitis C virus. *Nat. Rev. Microbiol.* **5**, 453–63 (2007).
6. Penin, F., Dubuisson, J., Rey, F. a, Moradpour, D. & Pawlotsky, J.-M. Structural biology of hepatitis C virus. *Hepatology* **39**, 5–19 (2004).
7. Kaito, M. *et al.* Hepatitis C virus particle detected by immunoelectron microscopic study. *J. Gen. Virol.* **75 (Pt 7)**, 1755–60 (1994).
8. Kolykhalov, A. A., Feinstone, S. M. & Rice, C. M. Identification of a highly conserved sequence element at the 3' terminus of hepatitis C virus genome RNA. *J. Virol.* **70**, 3363–3371 (1996).
9. Santolini, E., Migliaccio, G. & La Monica, N. Biosynthesis and biochemical properties of the hepatitis C virus core protein. *J. Virol.* **68**, 3631–3641 (1994).
10. Hope, R. G. & McLauchlan, J. Sequence motifs required for lipid droplet association and protein stability are unique to the hepatitis C virus core protein. *J. Gen. Virol.* **81**, 1913–25 (2000).
11. Bartosch, B., Dubuisson, J. & Cosset, F.-L. Infectious Hepatitis C Virus Pseudo-particles Containing Functional E1-E2 Envelope Protein Complexes. *J. Exp. Med.* **197**, 633–642 (2003).
12. Falkowska, E., Kajumo, F., Garcia, E., Reinus, J. & Dragic, T. Hepatitis C virus envelope glycoprotein E2 glycans modulate entry, CD81 binding, and neutralization. *J. Virol.* **81**, 8072–9 (2007).
13. Helle, F. *et al.* Role of N-linked glycans in the functions of hepatitis C virus envelope proteins incorporated into infectious virions. *J. Virol.* **84**, 11905–15 (2010).
14. Luik, P. *et al.* The 3-dimensional structure of a hepatitis C virus p7 ion channel by electron microscopy. *Proc. Natl. Acad. Sci. U. S. A.* **106**, 12712–6 (2009).
15. Steinmann, E. *et al.* Hepatitis C virus p7 protein is crucial for assembly and release of infectious virions. *PLoS Pathog.* **3**, e103 (2007).
16. Griffin, S. D. C. *et al.* The p7 protein of hepatitis C virus forms an ion channel that is blocked by the antiviral drug, Amantadine. *FEBS Lett.* **535**, 34–38 (2003).
17. Lorenz, I. C., Marcotrigiano, J., Dentzer, T. G. & Rice, C. M. Structure of the catalytic domain of the hepatitis C virus NS2-3 protease. *Nature* **442**, 831–5 (2006).
18. Halfon, P. & Locarnini, S. Hepatitis C virus resistance to protease inhibitors. *J. Hepatol.* **55**, 192–206 (2011).
19. Li, K. *et al.* Immune evasion by hepatitis C virus NS3/4A protease-mediated cleavage of the Toll-like receptor 3 adaptor protein TRIF. *Proc. Natl. Acad. Sci. U. S. A.* **102**, 2992–2997 (2005).

20. Lundin, M., Monne, M., Widell, A., von Heijne, G. & Persson, M. A. A. Topology of the Membrane-Associated Hepatitis C Virus Protein NS4B. *J. Virol.* **77**, 5428–5438 (2003).

21. Egger, D. *et al.* Expression of Hepatitis C Virus Proteins Induces Distinct Membrane Alterations Including a Candidate Viral Replication Complex Expression of Hepatitis C Virus Proteins Induces Distinct Membrane Alterations Including a Candidate Viral Replication Complex. *J. Virol.* **76**, 5975–5984 (2002).

22. Jones, D. M., Patel, A. H., Targett-Adams, P. & McLauchlan, J. The hepatitis C virus NS4B protein can trans-complement viral RNA replication and modulates production of infectious virus. *J. Virol.* **83**, 2163–77 (2009).

23. Huang, L. *et al.* Hepatitis C virus nonstructural protein 5A (NS5A) is an RNA-binding protein. *J. Biol. Chem.* **280**, 36417–28 (2005).

24. Tellinghuisen, T. L., Marcotrigiano, J., Gorbalenya, A. E. & Rice, C. M. The NS5A protein of hepatitis C virus is a zinc metalloprotein. *J. Biol. Chem.* **279**, 48576–87 (2004).

25. Penin, F. *et al.* Structure and function of the membrane anchor domain of hepatitis C virus nonstructural protein 5A. *J. Biol. Chem.* **279**, 40835–43 (2004).

26. Appel, N., Pietschmann, T. & Bartenschlager, R. Mutational Analysis of Hepatitis C Virus Nonstructural Protein 5A : Potential Role of Differential Phosphorylation in RNA Replication and Identification of a Genetically Flexible Domain Mutational Analysis of Hepatitis C Virus Nonstructural Protein 5A : P. *J. Virol.* **79**, 3187–3194 (2005).

27. Neddermann, P. *et al.* Reduction of Hepatitis C Virus NS5A Hyperphosphorylation by Selective Inhibition of Cellular Kinases Activates Viral RNA Replication in Cell Culture Reduction of Hepatitis C Virus NS5A Hyperphosphorylation by Selective Inhibition of Cellular Kinases Activ. *J. Virol.* **78**, 13306–13314 (2004).

28. Tellinghuisen, T. L., Foss, K. L., Treadaway, J. C. & Rice, C. M. Identification of residues required for RNA replication in domains II and III of the hepatitis C virus NS5A protein. *J. Virol.* **82**, 1073–83 (2008).

29. Appel, N. *et al.* Essential role of domain III of nonstructural protein 5A for hepatitis C virus infectious particle assembly. *PLoS Pathog.* **4**, e1000035 (2008).

30. Bressanelli, S. *et al.* Crystal structure of the RNA-dependent RNA polymerase of hepatitis C virus. *Proc. Natl. Acad. Sci. U. S. A.* **96**, 13034–9 (1999).

31. Lesburg, C. A. *et al.* Crystal structure of the RNA-dependent RNA polymerase from hepatitis C virus reveals a fully encircled active site. *Nat. Struct. Biol.* **6**, 937–943 (1999).

32. Lee, K. J., Choi, J., Ou, J., Michael, M. C. & Lai, M. M. C. The C-Terminal Transmembrane Domain of Hepatitis C Virus (HCV) RNA Polymerase Is Essential for HCV Replication In Vivo The C-Terminal Transmembrane Domain of Hepatitis C Virus (HCV) RNA Polymerase Is Essential for HCV Replication In Vivo. *J. Virol.* **78**, 3797–3802 (2004).

33. Quinkert, D., Bartenschlager, R. & Lohmann, V. Quantitative Analysis of the Hepatitis C Virus Replication Complex Quantitative Analysis of the Hepatitis C Virus Replication Complex. *J. Virol.* **79**, 13694–13605 (2005).

34. Bressanelli, S., Tomei, L., Rey, F. A. & Francesco, R. De. Structural Analysis of the Hepatitis C Virus RNA Polymerase in Complex with Ribonucleotides. *J. Virol.* **76**, 3482–3492 (2002).

35. Chinnaswamy, S., Murali, a, Li, P., Fujisaki, K. & Kao, C. C. Regulation of de novo-initiated RNA synthesis in hepatitis C virus RNA-dependent RNA polymerase by intermolecular interactions. *J. Virol.* **84**, 5923–35 (2010).

36. Blaising, J. & Pécheur, E.-I. Lipids: a key for hepatitis C virus entry and a potential target for antiviral strategies. *Biochimie* **95**, 96–102 (2013).

37. Maillard, P. *et al.* Nonenveloped Nucleocapsids of Hepatitis C Virus in the Serum of Infected Patients Nonenveloped Nucleocapsids of Hepatitis C Virus in the Serum of Infected Patients. *J. Virol.* **75**, 8240–8250 (2001).

38. P. André, F. Komurian-Pradel, S. Deforges, M. Perret, J. L. Berland, M. Sodoyer, S. Pol, C. Bréchot, G. P.-B. and V. L. Characterization of Low- and Very-Low-Density Hepatitis C Virus RNA-Containing Particles. *J. Virol.* **76**, 6919–6928 (2002).

39. Alvisi, G., Madan, V. & Bartenschlager, R. Hepatitis c virus and host cell lipids: An intimate connection. *RNA Biol.* **8**, 258–269 (2011).

40. Helle, F. & Dubuisson, J. Hepatitis C virus entry into host cells. *Cell. Mol. Life Sci.* **65**, 100–12 (2008).

41. Bartenschlager, R., Cosset, F.-L. & Lohmann, V. Hepatitis C virus replication cycle. *J. Hepatol.* **53**, 583–5 (2010).

42. Rehermann, B. Hepatitis C virus versus innate and adaptive immune responses: a tale of coevolution and coexistence. *J. Clin. Invest.* **119**, 1745–1754 (2009).

43. Oliviero, B. *et al.* Natural killer cell functional dichotomy in chronic hepatitis B and chronic hepatitis C virus infections. *Gastroenterology* **137**, 1151–60, 1160.e1–7 (2009).

44. Jo, J. *et al.* Analysis of CD8+ T-cell-mediated inhibition of hepatitis C virus replication using a novel immunological model. *Gastroenterology* **136**, 1391–401 (2009).

45. Jinushi, M. *et al.* Modulation of Dendritic Cell Functions in Chronic Hepatitis C. *J. Immunol.* **173**, 6072–6081 (2004).

46. Farci, P. *et al.* Prevention of hepatitis C virus infection in chimpanzees after antibody-mediated in vitro neutralization. *Proc. Natl. Acad. Sci. U. S. A.* **91**, 7792–6 (1994).

47. Cooper, S. *et al.* Analysis of a successful immune response against hepatitis C virus. *Immunity* **10**, 439–49 (1999).

48. Post, J. J. *et al.* Clearance of hepatitis C viremia associated with cellular immunity in the absence of seroconversion in the hepatitis C incidence and transmission in prisons study cohort. *J. Infect. Dis.* **189**, 1846–55 (2004).

49. Duffy, S., Shackelton, L. a & Holmes, E. C. Rates of evolutionary change in viruses: patterns and determinants. *Nat. Rev. Genet.* **9**, 267–76 (2008).

50. Farci, P. The Outcome of Acute Hepatitis C Predicted by the Evolution of the Viral Quasispecies. *Science (80-.).* **288**, 339–344 (2000).

51. Thimme, R. *et al.* Determinants of viral clearance and persistence during acute hepatitis C virus infection. *J. Exp. Med.* **194**, 1395–406 (2001).

52. Lechner, F. *et al.* Analysis of successful immune responses in persons infected with hepatitis C virus. *J. Exp. Med.* **191**, 1499–512 (2000).

53. Shoukry, N. H. *et al.* Memory CD8+ T cells are required for protection from persistent hepatitis C virus infection. *J. Exp. Med.* **197**, 1645–55 (2003).

54. Gerlach, J. T. *et al.* Recurrence of hepatitis C virus after loss of virus-specific CD4(+) T-cell response in acute hepatitis C. *Gastroenterology* **117**, 933–41 (1999).

55. Bowen, D. G. & Walker, C. M. Mutational escape from CD8+ T cell immunity: HCV evolution, from chimpanzees to man. *J. Exp. Med.* **201**, 1709–14 (2005).

56. Bowen, D. G. & Walker, C. M. Adaptive immune responses in acute and chronic hepatitis C virus infection. *Nature* **436**, 946–52 (2005).

57. Bucks, C. M., Norton, J. a, Boesteanu, A. C., Mueller, Y. M. & Katsikis, P. D. Chronic antigen stimulation alone is sufficient to drive CD8+ T cell exhaustion. *J. Immunol.* **182**, 6697–708

(2009).

58. Mueller, S. N. & Ahmed, R. High antigen levels are the cause of T cell exhaustion during chronic viral infection. *Proc. Natl. Acad. Sci. U. S. A.* **106**, 8623–8 (2009).

59. Joyce, M. a *et al.* HCV induces oxidative and ER stress, and sensitizes infected cells to apoptosis in SCID/Alb-uPA mice. *PLoS Pathog.* **5**, e1000291 (2009).

60. Deng, L. *et al.* Hepatitis C virus infection induces apoptosis through a Bax-triggered, mitochondrion-mediated, caspase 3-dependent pathway. *J. Virol.* **82**, 10375–85 (2008).

61. Joyce, M. a & Tyrrell, D. L. J. The cell biology of hepatitis C virus. *Microbes Infect.* **12**, 263–71 (2010).

62. Rehermann, B. Pathogenesis of chronic viral hepatitis: differential roles of T cells and NK cells. *Nat. Med.* **19**, 859–68 (2013).

63. Ivanov, A. V. *et al.* Oxidative stress, a trigger of hepatitis C and B virus-induced liver carcinogenesis. *Oncotarget* **8**, 3895–3932 (2017).

64. Wiese, M., Berr, F., Lafrenz, M., Porst, H. & Oesen, U. Low frequency of cirrhosis in a hepatitis C (genotype 1b) single-source outbreak in germany: a 20-year multicenter study. *Hepatology* **32**, 91–6 (2000).

65. Bonis, P. a. Clinical outcomes after hepatitis C infection from contaminated anti-D immune globulin. *N. Engl. J. Med.* **341**, 763 (1999).

66. Subjects, S. Prevalence and clinical outcome of hepatitis C infection in children who underwent cardiac surgery before the implementation of blood-donor screening. *Clin. Pediatr. (Phila).* **39**, 249 (2000).

67. Rodger, a J. *et al.* Assessment of long-term outcomes of community-acquired hepatitis C infection in a cohort with sera stored from 1971 to 1975. *Hepatology* **32**, 582–7 (2000).

68. Gerlach, J. T. *et al.* Acute hepatitis C: high rate of both spontaneous and treatment-induced viral clearance1 1The Bundesministerium für Bildung und Forschung and the European Union, as sponsors of the study, had no role in study design, data collection, analysis, or interpret. *Gastroenterology* **125**, 80–88 (2003).

69. Hofer, H. *et al.* Spontaneous viral clearance in patients with acute hepatitis C can be predicted by repeated measurements of serum viral load. *Hepatology* **37**, 60–4 (2003).

70. Grant, W. *et al.* Hepatitis C in Asymptomatic Blood Donors. *Hepatology* **26**, 29S (1997).

71. Villano, S. A., Vlahov, D., Nelson, K. E., Cohn, S. & Thomas, D. L. Persistence of viremia and the importance of long-term follow-up after acute hepatitis C infection. *Hepatology* **29**, 908–914 (1999).

72. Factors, E. *et al.* The Natural History of Hepatitis C Virus Infection. *Jama* **284**, 450–456 (2000).

73. Lee, M.-H., Yang, H.-I. & Chen, C.-J. Long-term health outcomes of chronic hepatitis C patients: A review of findings from REVEAL-HCV cohort study. *BioMedicine* **2**, 99–107 (2012).

74. Micallef, J. M., Kaldor, J. M. & Dore, G. J. Spontaneous viral clearance following acute hepatitis C infection : a systematic review of longitudinal studies. *J. Viral Hepat.* **13**, 34–41 (2006).

75. Cox, A. L. *et al.* Prospective evaluation of community-acquired acute-phase hepatitis C virus infection. *Clin. Infect. Dis.* **40**, 951–8 (2005).

76. Kamal, S. M. *et al.* Pegylated interferon alpha therapy in acute hepatitis C: relation to hepatitis C virus-specific T cell response kinetics. *Hepatology* **39**, 1721–31 (2004).

77. Maheshwari, A., Ray, S. & Thuluvath, P. J. Acute hepatitis C. *Lancet* **372**, 321–32 (2008).

78. Poynard, T., Bedossa, P. & Opolon, P. Natural history of liver fibrosis progression in patients with chronic hepatitis C. *Lancet* **349**, 825–832 (1997).

79. Poynard, T. *et al.* Rates and risk factors of liver fibrosis progression in patients with chronic hepatitis c. *J. Hepatol.* **34**, 730–9 (2001).

80. Ikeda, K. *et al.* Antibody to hepatitis B core antigen and risk for hepatitis C-related hepatocellular carcinoma: A prospective study. *Ann. Intern. Med.* **146**, 649–656 (2007).

81. Romeo, R. *et al.* Hepatitis C is more severe in drug users with human immunodeficiency virus infection. *J. Viral Hepat.* **7**, 297–301 (2000).

82. Chen, C.-L. *et al.* Metabolic factors and risk of hepatocellular carcinoma by chronic hepatitis B/C infection: a follow-up study in Taiwan. *Gastroenterology* **135**, 111–21 (2008).

83. Lok, A. S. *et al.* Incidence of Hepatocellular Carcinoma and Associated Risk Factors in Hepatitis C-Related Advanced Liver Disease. *Gastroenterology* **136**, 138–148 (2009).

84. Freeman, a J., Law, M. G., Kaldor, J. M. & Dore, G. J. Predicting progression to cirrhosis in chronic hepatitis C virus infection. *J. Viral Hepat.* **10**, 285–93 (2003).

85. Fattovich, G. *et al.* Morbidity and Mortality in Compensated Cirrhosis Type C : A retrospective follow-up study of 384 patients. *Gastroenterology* **112**, 463–472 (1997).

86. Ferri, C. *et al.* Mixed cryoglobulinemia: Demographic, clinical, and serologic features and survival in 231 patients. *Semin. Arthritis Rheum.* **33**, 355–374 (2004).

87. Fernandez-Soto, L. *et al.* Increased risk of autoimmune thyroid disease in hepatitis C vs hepatitis B before, during, and after discontinuing interferon therapy. *Arch. Intern. Med.* **158**, 1445–8 (1998).

88. Petti, S., Rabiei, M., De Luca, M. & Scully, C. The magnitude of the association between hepatitis C virus infection and oral lichen planus: meta-analysis and case control study. *Odontology* **99**, 168–78 (2011).

89. Petta, S. *et al.* Carotid atherosclerosis and chronic hepatitis C: a prospective study of risk associations. *Hepatology* **55**, 1317–23 (2012).

90. Richard J. Johnson, David R. Gretch, Hideaki Yamabe, Jamie Hart, Carlos Bacchi, Peter Hartwell, William G. Couser, Lawrence Corey, Mark H. Wener, C. E. A. and R. W. Membranoproliferative glomeruloephritis associated with hepatitis c virus infection. *N. Engl. J. Med.* **328**, 465–70 (1993).

91. McAndrews, M. P. *et al.* Prevalence and significance of neurocognitive dysfunction in hepatitis C in the absence of correlated risk factors. *Hepatology* **41**, 801–8 (2005).

92. Lavanchy, D. The global burden of hepatitis C. *Liver Int. Off. J. Int. Assoc. Study Liver* **29 Suppl 1**, 74–81 (2009).

93. Gower, E., Estes C, C., Hindman, S., Razavi-Shearer, K. & Razavi, H. Global epidemiology and genotype distribution of the hepatitis C virus. *J. Hepatol.* **61**, S45–S57 (2014).

94. World Health Organization. *Global Hepatitis Report, 2017. (2017). Available at https://www.who.int/hepatitis/publications/global-hepatitis-report2017/en/. Accessed 07/10/2019.* doi:10.1149/2.030203jes.

95. Annemarie Wasley, M. J. A. Epidemiology of Hepatitis C: Geographic Differences and Temporal Trends. *Semin Liver Dis* **20**, 0001–0016 (2000).

96. James G. Donahue,Alvaro Munoz, Paul M. Ness, Donald E. Brown, David H. Yawn, Hugh A. McAlllister, B. A. R. and K. E. N. The declining risk of post-transfusion Hepatitis C Virus Infection. *N. Engl. J. Med.* **327**, 369–373 (1992).

97. Shepard, C. W., Finelli, L. & Alter, M. J. Global epidemiology of hepatitis C virus infection. *Lancet Infect. Dis.* **5**, 558–67 (2005).

98. Hagan, L. M. & Schinazi, R. F. Best strategies for global HCV eradication. *Liver Int.* **33**, 68–79 (2013).

99. Frank, C. *et al.* The role of parenteral antischistosomal therapy in the spread of hepatitis C virus in Egypt. *Lancet* **355**, 887–91 (2000).

100. *World Health Organization. Blood Safety. Fact Sheet No. 279. (2011). Available at https://www.who.int/worldblooddonorday/media/who_blood_safety_factsheet_2011.pdf. Accessed 03/03/2014*. doi:10.3201/eid0403.980317.

101. Pépin, J., Chakra, C. N. A., Pépin, E., Nault, V. & Valiquette, L. Evolution of the global burden of viral infections from unsafe medical injections, 2000-2010. *PLoS One* **9**, 1–8 (2014).

102. Terrault, N. A. Sexual activity as a risk factor for hepatitis C. *Hepatology* **36**, S99–S105 (2002).

103. *Public Health England. Hepatitis C in the UK 2019. Working to eliminate hepatitis as a major public health threat. (2019).Available at https://assets.publishing.service.gov.uk/government/uploads/system/uploads/attachment_data/file/831155/Hepatitis_C_in_th*.

104. Public Health England. Annual report from the sentinel surveillance of blood borne virus testing in England: data for January to December 2017. (2018). Available at https://assets.publishing.service.gov.uk/government/uploads/system/uploads/attachment_data.

105. Public Health England. Hepatitis C in England 2019. Working to eliminate hepatitis C as a major public health threat. Available at https://assets.publishing.service.gov.uk/government/uploads/system/uploads/attachment_data/file/855064/HCV_in_England_2019.p.

106. Uddin, G. *et al.* Prevalence of chronic viral hepatitis in people of south Asian ethnicity living in England: the prevalence cannot necessarily be predicted from the prevalence in the country of origin. *J. Viral Hepat.* **17**, 327–335 (2010).

107. Harris, R. J. *et al.* Hepatitis C prevalence in England remains low and varies by ethnicity: an updated evidence synthesis. *Eur. J. Public Health* **22**, 187–92 (2012).

108. Public Health England. Shooting Up Infections among people who injected drugs in the UK 2015:November 2016 update (2016). Available at https://assets.publishing.service.gov.uk/government/uploads/system/uploads/attachment_data/file/567232/PHE_Briefing_on_S.

109. *Public Health England. Hepatitis C in England 2018 Report.(2018). Available at https://assets.publishing.service.gov.uk/government/uploads/system/uploads/attachment_data/f ile/732469/HCV_IN_THE_UK_2018_UK.pdf A. Accessed 08/10/2019.*

110. *Unlinked anonymous HIV and viral hepatitis monitoring among PWID: 2018 report. Public Health England. (2018). Available at https://assets.publishing.service.gov.uk/government/uploads/system/uploads/attachment_data/file/729614/hpr2718_uam-pwid.pdf. Accesse*. vol. 12 (2018).

111. Turner, K. M. E. *et al.* The impact of needle and syringe provision and opiate substitution therapy on the incidence of hepatitis C virus in injecting drug users: pooling of UK evidence. *Addiction* **106**, 1978–88 (2011).

112. Price, H. *et al.* Hepatitis C in men who have sex with men in London--a community survey. *HIV Med.* **14**, 578–580 (2013).

113. Hosein, S. R. & Wilson, D. P. HIV, HCV, and drug use in men who have sex with men. *Lancet* **382**, 1095–6 (2013).

114. *Public Health England. Hepatitis C in the UK 2014 Report. (PHE Publications, 1-103, 2014)*. (2014).

115. Public Health England. Hepatitis C in England 2017 report. Available at. (2017).

116. *Combating hepatitis B and C to reach elimination by 2030. Available at*. *World Health Organization* https://www.who.int/hepatitis/publications/hep-elimination-by-2030-brief/en/.Accessed 08/10/2019. (2016).

117. Stanaway, J. D. *et al.* The global burden of viral hepatitis from 1990 to 2013: findings from the Global Burden of Disease Study 2013. *Lancet* **388**, 1081–1088 (2016).

118. Manns, M. P. *et al.* Peginterferon alfa-2b plus ribavirin compared with interferon alfa-2b plus ribavirin for initial treatment of chronic hepatitis C: a randomised trial. *Lancet* **358**, 958–65 (2001).

119. Fried, M.W. Shiffman, M.L. Reddy, R. Smith, C. Marinos, G. Goncales, F.L. Haussinger, D. Diago, M. Carosi, G. Dhumeaux, D. Craxi, A. Lin, A. Hoffman, J. Yu, J. Peginterferon Alfa-2a plus ribavirin for chronic hepatitis C virus infection in HIV-infected patients. *N. Engl. J. Med.* **347**, 975–982 (2002).

120. NHS England. *National Partnership Agreement Between : NOMS , NHS England and Public Health England for the Co-Commissioning and Delivery of Healthcare Services in Prisons in England*. https://assets.publishing.service.gov.uk/government/uploads/system/uploads/attachment_data/file/460445/national_partnership_agreement_commissioning-delivery-healthcare-prisons_2015.pdf. Accessed 05/04/2014. (2013).

121. Public Health England. *Summary report : National event for early lessons learnt from the opt-out blood-borne virus (BBV) testing policy in prisons , 2017. Available at*. https://assets.publishing.service.gov.uk/government/uploads/system/uploads/attachment_data/file/455531/BBV_event_report_21_May_2015.pdf. Accessed 10/09/2019.

122. Poynard, T. *et al.* Meta-analysis of interferon randomized trials in the treatment of viral hepatitis C: Effects of dose and duration. *Hepatology* **24**, 778–789 (1996).

123. Schalm, S. W. *et al.* Interferon-Ribavirin for Chronic Hepatitis C With and Controlled Trials. *Gastroenterology* **117**, 408–413 (1999).

124. Lohmann, V. Replication of Subgenomic Hepatitis C Virus RNAs in a Hepatoma Cell Line. *Science (80-.).* **285**, 110–113 (1999).

125. Lindenbach, B. D. *et al.* Complete replication of hepatitis C virus in cell culture. *Science* **309**, 623–6 (2005).

126. Zhong, J. *et al.* Robust hepatitis C virus infection in vitro. *Proc. Natl. Acad. Sci. U. S. A.* **102**, 9294–9 (2005).

127. Wakita, T. *et al.* Production of infectious hepatitis C virus in tissue culture from a cloned viral genome. *Nat. Med.* **11**, 791–6 (2005).

128. Hinrichsen, H. *et al.* Short-term antiviral efficacy of BILN 2061, a hepatitis C virus serine protease inhibitor, in hepatitis C genotype 1 patients. *Gastroenterology* **127**, 1347–1355 (2004).

129. Reiser, M. *et al.* Antiviral efficacy of NS3-serine protease inhibitor BILN-2061 in patients with chronic genotype 2 and 3 hepatitis C. *Hepatology* **41**, 832–5 (2005).

130. Bisceglie, A. M. Di *et al.* Telaprevir for previously untreated chronic hepatitis C virus infection. *N. Engl. J. Med.* **364**, 2405–16 (2011).

131. Marcellin, P. *et al.* Boceprevir for previously treated chronic hepatitis C virus genotype 1 infection. *J. R. Coll. Physicians Edinb.* **41**, 122–3 (2011).

132. Lawitz, E. *et al.* Telaprevir for retreatment of HCV infection. *N. Engl. J. Med.* **364**, 2417–28 (2011).

133. Lawitz, E., Forns, X. & Zeuzem, S. Simeprevir (TMC435) With Peginterferon/Ribavirin for Treatment of Chronic HCV Genotype 1 Infection in Patients Who Relapsed After Previous Interferon-Based Therapy: Results from PROMISE, a Phase III trial. *AGA Abstr.* **144**, S-151 (2013).

134. Jacobson, I. *et al.* 1425 Simeprevir (Tmc435) With Peginterferon/Ribavirin for Chronic Hcv Genotype-1 Infection in Treatment-Naïve Patients: Results From Quest-1, a Phase Iii Trial. *J. Hepatol.* **58**, S574 (2013).

135. Zeuzem, S. *et al.* Simeprevir increases rate of sustained virologic response among treatment-experienced patients with HCV genotype-1 infection: A phase IIb trial. *Gastroenterology* **146**, 430–441 (2014).

136. Fried, M., Buti, M., Dore, G. & Flisiak, R. Once daily simeprevir (TMC435) with pegylated interferon and ribavirin in treatment-naïve genotype 1 hepatitis C: The randomized PILLAR study. *Hepatology* **58**, 1918–1929 (2013).

137. Berger, K. L. *et al.* Baseline hepatitis C virus (HCV) NS3 polymorphisms and their impact on treatment response in clinical studies of the HCV NS3 protease inhibitor faldaprevir. *Antimicrob. Agents Chemother.* **58**, 698–705 (2014).

138. Majumdar, A., Kitson, M. T. & Roberts, S. K. Systematic review: Current concepts and challenges for the direct-acting antiviral era in hepatitis C cirrhosis. *Aliment. Pharmacol. Ther.* **43**, 1276–1292 (2016).

139. Hezode, C. *et al.* Daclatasvir, an NS5A Replication Complex Inhibitor, Combined With Peginterferon Alfa-2a and Ribavirin in Treatment-Naive HCV-Genotype 1 or 4 Patients: Phase 2b COMMAND-1 SVR12 Results. *Hepatology* **56**, 553A-554A (2012).

140. Dore, G. J. *et al.* Daclatasvir Combined With Peginterferon Alfa-2a and Ribavirin for 12 or 16 Weeks in Patients With Hcv Genotype 2 or 3 Infection: Command Gt2/3 Study. *J. Hepatol.* **58**, S570-571 (2013).

141. Lawitz, E. *et al.* Sofosbuvir in combination with peginterferon alfa-2a and ribavirin for non-cirrhotic, treatment-naive patients with genotypes 1, 2, and 3 hepatitis C infection: a randomised, double-blind, phase 2 trial. *Lancet. Infect. Dis.* **13**, 401–8 (2013).

142. Zeuzem, S. *et al.* Simeprevir increases rate of sustained virologic response among treatment-experienced patients with HCV genotype-1 infection: a phase IIb trial. *Gastroenterology* **146**, 430–41.e6 (2014).

143. Afdhal, N. *et al.* Ledipasvir and Sofosbuvir for Untreated HCV Genotype 1 Infection. *N. Engl. J. Med.* 1889–1898 (2014) doi:10.1056/NEJMoa1402454.

144. Sulkowski, M. S. *et al.* Daclatasvir plus sofosbuvir for previously treated or untreated chronic HCV infection. *N. Engl. J. Med.* **370**, 211–21 (2014).

145. Pawlotsky, J. M. *et al.* EASL Recommendations on Treatment of Hepatitis C 2018. *J. Hepatol.* **69**, 461–511 (2018).

146. Simmons, R. *et al.* Establishing the cascade of care for hepatitis C in England—benchmarking to monitor impact of direct acting antivirals. *J. Viral Hepat.* **25**, 482–490 (2018).

147. World Health Organisation (WHO). Action plan for the health sector response to viral hepatitis in the WHO European Region. **27**, 12–15 (2016).

148. Baumert, T. F., Fauvelle, C., Chen, D. Y. & Lauer, G. M. A prophylactic hepatitis C virus vaccine: A distant peak still worth climbing. *J. Hepatol.* **61**, S34–S44 (2014).

149. Hahn, J. a. *et al.* Potential impact of vaccination on the hepatitis C virus epidemic in injection drug users. *Epidemics* **1**, 47–57 (2009).

150. Podevin, P. *et al.* Production of infectious hepatitis C virus in primary cultures of human adult hepatocytes. *Gastroenterology* **139**, 1355–64 (2010).

151. *Institute of Medicine of the National Acadamies. Chimpanzees in Behavioral Research Biomedical and Assessing the Necessity*. *National Academy of Sciences* www.iom.edu/chimpstudy (2011).

152. Mercer, D. F. *et al.* Hepatitis C virus replication in mice with chimeric human livers. *Nat. Med.* **7**, 927–33 (2001).

153. Bukh, J. Animal models for the study of hepatitis C virus infection and related liver disease. *Gastroenterology* **142**, 1279-1287.e3 (2012).

154. Dorner, M. *et al.* A genetically humanized mouse model for hepatitis C virus infection. *Nature* **474**, 208–11 (2011).

155. Simmonds, P. Genetic diversity and evolution of hepatitis C virus--15 years on. *J. Gen. Virol.* **85**, 3173–88 (2004).

156. Choo, Q. L. *et al.* Vaccination of chimpanzees against infection by the hepatitis C virus. *Proc. Natl. Acad. Sci. U. S. A.* **91**, 1294–8 (1994).

157. Frey, E.S. Houghton, M. Coates, S. Abrignani, S. Chien, D. Rosa, D. Pileri, P. Ray, R. Di Bisceglie, A. Rinella, P. Hill, H. Wolff, M.C. Schultze, V. Han, J.H. Scharschmidt, B. Belshe, R. B. Safety and Immunogenicity of HCV E1E2 Vaccine Adjuvanted with MF59 Administered to Healthy Adults. *Vaccine* vol. 31 6367–6373 (2010).

158. Ray, R. Meyer, K. Banerjee, A. Basu, A. Coates, S. Abrignani, S. Houghton, M. Frey, E.S. Belse, R. B. Characterization of antibodies induced by vaccination with hepatitis C virus envelope glycoproteins. *J. Infect. Dis.* **202**, 862–866 (2010).

159. Law, M. *et al.* Broadly neutralizing antibodies protect against hepatitis C virus quasispecies challenge. *Nat. Med.* **14**, 25–7 (2008).

160. Liang, T. J. Current progress in development of hepatitis C virus vaccines. *Nat. Med.* **19**, 869–78 (2013).

161. Rollier, C. S., Reyes-Sandoval, A., Cottingham, M. G., Ewer, K. & Hill, A. V. S. Viral vectors as vaccine platforms: deployment in sight. *Curr. Opin. Immunol.* **23**, 377–82 (2011).

162. Bråve, A., Ljungberg, K., Wahren, B. & Liu, M. a. Vaccine delivery methods using viral vectors. *Mol. Pharm.* **4**, 18–32 (2007).

163. Barnes, E., Folgori, A., Capone, S., Swadling, L. & Aston, S. Novel adenovirus-based vaccines induce broad and sustained T cell responses to HCV in man. *Sci Transl Med* **4**, 1–22 (2012).

164. Folgori, A. *et al.* A T-cell HCV vaccine eliciting effective immunity against heterologous virus challenge in chimpanzees. *Nat. Med.* **12**, 190–7 (2006).

165. Swadling, L. *et al.* A Human Vaccine Strategy Based On Chimpanzee Adenoviral and MVA Vectors That Primes , Boosts and Sustains Functional HCV Specific T-Cell Memory *. *Sci Transl Med* **6**, (2014).

166. Houghton, M. Prospects for prophylactic and therapeutic vaccines against the hepatitis C viruses. *Immunol. Rev.* **239**, 99–108 (2011).

167. Yalow, R. & Berson, S. Immunoassay of endogenous plasma insulin in man. *Clin Invest* **39**,

1157–75 (1996).

168. Ekins R.P. The Estimation of Thyroxine in human plasma by an electrophoretic technique. *Clin. Chim. Acta* **5**, 453–459 (1959).

169. Andreotti, P. E. *et al.* Immunoassay of infectious agents. *Biotechniques* **35**, 850–9 (2003).

170. B.K. Van Weemen, A. H. W. M. S. Immunoassay using Antigen-Enzyme Conjugates. *FEBS Letts* **15**, 232–236 (1971).

171. Engvall, E. & Perlmann, P. Enzyme-linked immunosorbent assay (ELISA). Quantitative assay of immunoglobulin G. *Immunochemistry* **8**, 871–4 (1971).

172. Lautier, F., Razafitsalama, D. & Lavillaureix, J. Comparison of the reversed passive hemagglutination with the electroimmunodiffusion method for hepatitis B antigen. *Experientia* **33**, 131 (1977).

173. G, Wolters, L.P.C. Kuijpers, J. Kacaki, A. H. W. M. S. Enzyme-Imunoassay for HBsAg. *Lancet* **308**, 690 (1976).

174. Andreasson, U., Portelius, E., Pannee, J., Zetterberg, H. & Blennow, K. Multiplexing and multivariate analysis in neurodegeneration. *Methods* **56**, 464–70 (2012).

175. Santhanam, K. & Bard, A. Chemiluminescence of Electrogenerated 9, 10-Diphenylanthracene Anion Radical1. *J. Am. Chem. …* **86**, 5350–51 (1965).

176. Visco, R. & Chandross, E. Electroluminescence in solutions of aromatic hydrocarbons. *J. Am. Chem. …* **87**, 139–40 (1964).

177. Tokel-Takvoryan, N.E. Hemingway, R.E. Bard, A. J. Electrogenerated chemiluminescence. XIII. Electrochemical and electrogenerated chemiluminescence studies of ruthenium chelates. *J. Am. …* **840**, 6582–6589 (1973).

178. Richter, M. M. Electrochemiluminescence (ECL). *Chem. Rev.* **104**, 3003–36 (2004).

179. Noffsinger, J. & Danielson, N. Generation of chemiluminescence upon reaction of aliphatic amines with tris (2, 2′-bipyridine) ruthenium (III). *Anal. Chem.* **59**, 865–868 (1987).

180. Wightman, R. M., Forry, S. P., Maus, R., Badocco, D. & Pastore, P. Rate-Determining Step in the Electrogenerated Chemiluminescence from Tertiary Amines with Tris (2 , 2 ′ -bipyridyl) ruthenium (II). *J. Phys. Chem. B* **108**, 19119–19125 (2004).

181. Pastore, P., Badocco, D. & Zanon, F. Influence of nature, concentration and pH of buffer acid–base system on rate determining step of the electrochemiluminescence of Ru(bpy)32+ with tertiary aliphatic amines. *Electrochim. Acta* **51**, 5394–5401 (2006).

182. Miao, W., Choi, J. & Bard, A. J. Electrogenerated Chemiluminescence 69 : The Tri-n-propylamine (TPrA) System Revisited s A New Route Involving TPrA • + Cation Radicals. *J. Am. Chem. Soc.* **124**, 14478–14485 (2002).

183. Blackburn, G. F. *et al.* Electrochemiluminescence Detectionfor Developmentof Immunoassaysand DNA Probe Assaysfor ClinicalDiagnostics. *Clin. Chem.* **37**, 1534–1539 (1991).

184. Deaver, D. A new non-isotopic detection system for immunoassays. *Nature* **377**, 758–760 (1995).

185. Steinkamp JA, Wilson JS, Saunders GC, S. C. Phagocytosis: Flow Cytometric Quantitation with Fluorescent Microspheres. *Science (80-.).* **215**, 64–66 (1982).

186. Lisi, P. J., Huang, C. W. & Hoffman, R. A. A fluorescence immunoassay for soluble antigens employing flow cytometric detection. **120**, 171–179 (1982).

187. McHugh, T. & Miner, R. Simultaneous detection of antibodies to cytomegalovirus and herpes simplex virus by using flow cytometry and a microsphere-based fluorescence immunoassay.

J. Clin. Microbiol. **26**, 1957 (1988).

188. Scillian, J. J. *et al.* Early detection of antibodies against rDNA-produced HIV proteins with a flow cytometric assay. *Blood* **73**, 2041–8 (1989).

189. Fulton, R. J., Mcdade, R. L., Smith, P. L., Kienker, L. J. & Jr, J. R. K. Advanced multiplexed analysis with the FlowMetrix TM system. *Clin. Chem.* **43**, 1749–1756 (1997).

190. Vignali, D. a. Multiplexed particle-based flow cytometric assays. *J. Immunol. Methods* **243**, 243–55 (2000).

191. Houser, B. Bio-Rad's Bio-Plex® suspension array system, xMAP technology overview. *Arch. Physiol. Biochem.* **118**, 192–6 (2012).

192. Köhler, G. & Milstein, C. Continuous cultures of fused cells secreting antibody of predefined specificity. *Nature* **256**, 495–497 (1975).

193. Smith, G. P. Filamentous fusion phage: novel expression vectors that display cloned antigens on the virion surface. *Science* **228**, 1315–7 (1985).

194. Better, M., Chang, C. P., Robinson, R. R. & Horwitz, a H. Escherichia coli secretion of an active chimeric antibody fragment. *Science* **240**, 1041–3 (1988).

195. J. McCafferty, A.D. Griffiths, G. Winter, D. J. C. Phage antibodies: filamentous phage displaying antibody variable domains. *Nature* **348**, 552–551 (1990).

196. Irving, M. B., Pan, O. & Scott, J. K. Random-peptide libraries and antigen-fragment libraries for epitope mapping and the development of vaccines and diagnostics. *Curr. Opin. Chem. Biol.* **5**, 314–24 (2001).

197. C. Tuerk, L. G. Systematic Evolution of Ligands by Exponential Enrichment : RNA Ligands to Bacteriophage El-T. *Science (80-.).* **249**, 505–510 (1990).

198. Jayasena, S. D. Aptamers: an emerging class of molecules that rival antibodies in diagnostics. *Clin. Chem.* **45**, 1628–50 (1999).

199. Jenison, R. D., Gill, S. C., Pardi, a & Polisky, B. High-resolution molecular discrimination by RNA. *Science* **263**, 1425–9 (1994).

200. Ruckman, J. 2'-Fluoropyrimidine RNA-based Aptamers to the 165-Amino Acid Form of Vascular Endothelial Growth Factor (VEGF165). *J. Biol. Chem.* **273**, 20556–20567 (1998).

201. Higgins, S.J. Hames, B. D. *Protein Expression. A Practical Approach. (Oxford University Press 1999)*.

202. Yin, J., Li, G., Ren, X. & Herrler, G. Select what you need: a comparative evaluation of the advantages and limitations of frequently used expression systems for foreign genes. *J. Biotechnol.* **127**, 335–47 (2007).

203. Mattanovich, D. *et al. Recombinant Gene Expression*. vol. 824 (Humana Press, 2012).

204. Verma, R., Boleti, E. & George, a J. Antibody engineering: comparison of bacterial, yeast, insect and mammalian expression systems. *J. Immunol. Methods* **216**, 165–81 (1998).

205. van Oers MM, V. J. Baculovirus genomics. *Curr Drug Targets* **8**, 1051–68 (2007).

206. Herniou, E. a, Olszewski, J. a, Cory, J. S. & O'Reilly, D. R. The genome sequence and evolution of baculoviruses. *Annu. Rev. Entomol.* **48**, 211–34 (2003).

207. Jehle, J. a *et al.* On the classification and nomenclature of baculoviruses: a proposal for revision. *Arch. Virol.* **151**, 1257–66 (2006).

208. Zanotto, P. de A., Kessing, B. & Maruniak, J. Phylogenetic interrelationships among baculoviruses: evolutionary rates and host associations. *J. Invertebr. Pathol.* **62**, 147–64 (1993).

209. Monsma, S. a, Oomens, a G. & Blissard, G. W. The GP64 envelope fusion protein is an essential baculovirus protein required for cell-to-cell transmission of infection. *J. Virol.* **70**, 4607–16 (1996).

210. IJkel, W. F. *et al.* A novel baculovirus envelope fusion protein with a proprotein convertase cleavage site. *Virology* **275**, 30–41 (2000).

211. Pearson, M. N., Groten, C. & Rohrmann, G. F. Identification of the lymantria dispar nucleopolyhedrovirus envelope fusion protein provides evidence for a phylogenetic division of the Baculoviridae. *J. Virol.* **74**, 6126–31 (2000).

212. Rohrmann, G. F. *Baculovirus Molecular Biology: Second Edition [Internet]. Bethesda (MD): National Center for Biotechnology Information (US)*. (2011).

213. Blissard, G. W. & Rohrmann, G. F. Baculovirus diversity and molecular biology. *Annu. Rev. Entomol.* **35**, 127–55 (1990).

214. Ayres, M., Howard, S. & Kuzio, J. The Complete DNA Sequence of Autographa californica Nuclear Polyhedrosis Virus. *Virology* **202**, 586–605 (1994).

215. van Oers, M. M. Opportunities and challenges for the baculovirus expression system. *J. Invertebr. Pathol.* **107 Suppl**, S3-15 (2011).

216. Rohrmann, G. F. *Rohrmann, G. F. Baculovirus Molecular Biology. (National Center for Biotechnology Information US, 2008).* (2008).

217. Passarelli AL, G. LA. Baculovirus late and very late gene regulation. *Curr Drug Targets.* **8**, 1103–15 (2007).

218. Kovacs, R., Graham, B. L. & Summers, M. A. X. D. Identifications of Spliced Baculovirus RNAs Expressed Late in Infection. *Virology* **183**, 633–643 (1991).

219. Guarino, L. a & Summers, M. D. Functional mapping of a trans-activating gene required for expression of a baculovirus delayed-early gene. *J. Virol.* **57**, 563–71 (1986).

220. Hoopes, R. R. & Rohrmann, G. F. In vitro transcription of baculovirus immediate early genes: accurate mRNA initiation by nuclear extracts from both insect and human cells. *Proc. Natl. Acad. Sci. U. S. A.* **88**, 4513–7 (1991).

221. Kool, M. Ahrens, C.H. Vlak, J. M. R. G. F. Review Artcile: Replication of baculovirus DNA. *J. Gen. Virol.* **76**, 2103–2118 (1995).

222. Guarino, L. a, Xu, B., Jin, J. & Dong, W. A virus-encoded RNA polymerase purified from baculovirus-infected cells. *J. Virol.* **72**, 7985–91 (1998).

223. Todd, J. W., Passarelli, A. L. & Miller, L. K. Eighteen baculovirus genes, including lef-11, p35, 39K, and p47, support late gene expression. *J. Virol.* **69**, 968–974 (1995).

224. Lu, a & Miller, L. K. The roles of eighteen baculovirus late expression factor genes in transcription and DNA replication. *J. Virol.* **69**, 975–82 (1995).

225. Kool, M., Ahrens, C. H., Goldbach, R. W., Rohrmann, G. F. & Vlak, J. M. Identification of genes involved in DNA replication of the Autographa californica baculovirus. *Proc. Natl. Acad. Sci. U. S. A.* **91**, 11212–6 (1994).

226. Rohrmann, G. F. Polyhedrin structure. *J. Gen. Virol.* **67 (Pt 8)**, 1499–513 (1986).

227. Russell, R. L., Pearson, M. N. & Rohrmann, G. F. Immunoelectron microscopic examination of Orgyia pseudotsugata multicapsid nuclear polyhedrosis virus-infected Lymantria dispar cells: time course and localization of major polyhedron-associated proteins. *J. Gen. Virol.* **72 (Pt 2)**, 275–83 (1991).

228. Ooi, B. G., Rankin, C. & Miller, L. K. Downstream sequences augment transcription from the essential initiation site of a baculovirus polyhedrin gene. *J. Mol. Biol.* **210**, 721–36 (1989).

229. McLachlin, J. R. & Miller, L. K. Identification and characterization of vlf-1, a baculovirus gene involved in very late gene expression. *J. Virol.* **68**, 7746–56 (1994).

230. Yang, S. & Miller, L. K. Activation of baculovirus very late promoters by interaction with very late factor 1. *J. Virol.* **73**, 3404–9 (1999).

231. Mistretta, T. & Guarino, L. A. Transcriptional Activity of Baculovirus Very Late Factor 1. *J. Virol.* **79**, 1958–1960 (2005).

232. Smith, G. E., Vlak, J. M. & Summers, M. D. Physical Analysis of Autographa californica Nuclear Polyhedrosis Virus Transcripts for Polyhedrin and 10,000-Molecular-Weight Protein. *J. Virol.* **45**, 215–25 (1983).

233. Akihiro Usami, Takeo Suzuki, Hidekazu Nagaya, H. K. and S. I. Silkworm as a Host of Baculovirus Expression. *Curr. Pharm. Biotechnol.* **11**, 246–250 (2010).

234. Smith, G. E., Summers, M. D. & Fraser, M. J. Production of human beta interferon in insect cells infected with a baculovirus expression vector . Production of Human Beta Interferon in Insect Cells Infected with a Baculovirus Expression Vector. *Mol. Cell. Biol.* **3**, 2156–2165 (1983).

235. van Rijn, P. a, van Gennip, H. G. & Moormann, R. J. An experimental marker vaccine and accompanying serological diagnostic test both based on envelope glycoprotein E2 of classical swine fever virus (CSFV). *Vaccine* **17**, 433–40 (1999).

236. Harper, D. M. *et al.* Sustained efficacy up to 4.5 years of a bivalent L1 virus-like particle vaccine against human papillomavirus types 16 and 18: follow-up from a randomised control trial. *Lancet* **367**, 1247–55 (2006).

237. Kantoff, P. & Higano, C. Sipuleucel-T immunotherapy for castration-resistant prostate cancer. *N. Engl. J. Med.* **363**, 411–422 (2010).

238. Rivera-Gonzalez, G. C., Swift, S. L., Dussupt, V., Georgopoulos, L. J. & Maitland, N. J. Baculoviruses as gene therapy vectors for human prostate cancer. *J. Invertebr. Pathol.* **107 Suppl**, S59-70 (2011).

239. Smith, G. E., Fraser, M. J. & Summers, M. D. Molecular Engineering of the Autographa californica Nuclear Polyhedrosis Virus Genome: Deletion Mutations Within the Polyhedrin Gene. *J. Virol.* **46**, 584–593 (1983).

240. Kitts, P. A., Ayres, M. D. & Possee, R. D. Linearization of baculovirus DNA enhances the recovery of recombinant virus expression vectors. *Nucleic Acids Res.* **18**, 5667–5672 (1990).

241. Machesky, L. & Insall, R. WASP homology sequences in baculoviruses. *Trends Cell Biol.* **11**, 286–287 (2001).

242. Goley, E. D. *et al.* Dynamic nuclear actin assembly by Arp2/3 complex and a baculovirus WASP-like protein. *Science* **314**, 464–7 (2006).

243. Kitts PA, P. R. A method for producing recombinant baculovirus expression vectors at high frequency. *Biotechniques* **14**, 810–7 (1993).

244. Patel, G., Nasmyth, K. & Jones, N. A new method for the isolation of recombinant baculovirus. *Nucleic Acids Res.* **20**, 97–104 (1992).

245. Luckow, V. a, Lee, S. C., Barry, G. F. & Olins, P. O. Efficient generation of infectious recombinant baculoviruses by site-specific transposon-mediated insertion of foreign genes into a baculovirus genome propagated in Escherichia coli. *J. Virol.* **67**, 4566–79 (1993).

246. Airenne, K. & Peltomaa, E. Improved generation of recombinant baculovirus genomes in Escherichia coli. *Nucleic Acids Res.* **31**, 1–6 (2003).

247. McCarthy, C. B. & Romanowski, V. A simplified method for the extraction of baculoviral DNA for PCR analysis: a practical application. *J. Virol. Methods* **148**, 286–90 (2008).

248. Hitchman, R. B., Possee, R. D. & King, L. A. Expression Systems: Methods Express. CHAPTER 9 Improved baculovirus expression vectors. 147–168 (2007).

249. Possee, R. D. *et al.* Generation of baculovirus vectors for the high-throughput production of proteins in insect cells. *Biotechnol. Bioeng.* **101**, 1115–22 (2008).

250. Li, G., Wang, J., Deng, R. & Wang, X. Characterization of AcMNPV with a deletion of ac68 gene. *Virus Genes* **37**, 119–27 (2008).

251. Wang, Y. *et al.* ac18 is not essential for the propagation of Autographa californica multiple nucleopolyhedrovirus. *Virology* **367**, 71–81 (2007).

252. Kaba, S. a, Salcedo, A. M., Wafula, P. O., Vlak, J. M. & van Oers, M. M. Development of a chitinase and v-cathepsin negative bacmid for improved integrity of secreted recombinant proteins. *J. Virol. Methods* **122**, 113–8 (2004).

253. Hawtin, R. E. *et al.* Liquefaction of Autographa californica nucleopolyhedrovirus-infected insects is dependent on the integrity of virus-encoded chitinase and cathepsin genes. *Virology* **238**, 243–53 (1997).

254. Carpentier, D. C. J., Griffiths, C. M. & King, L. a. The baculovirus P10 protein of Autographa californica nucleopolyhedrovirus forms two distinct cytoskeletal-like structures and associates with polyhedral occlusion bodies during infection. *Virology* **371**, 278–91 (2008).

255. Kuzio, J., Jaques, R. & Faulkner, P. Identification of ~ 74 , a Gene Essential for Virulence of Baculovirus Occlusion Bodies A region of the genome of Autographa californica nuclear polyhedrosis virus (AcNPV ; family Baculoviri- dae) comprising adjacent HindIll-C ? and -P fragments very la. *Virology* **763**, 759–763 (1989).

256. Rodems, S. M. & Friesen, P. D. The hr5 transcriptional enhancer stimulates early expression from the Autographa californica nuclear polyhedrosis virus genome but is not required for virus replication. *J. Virol.* **67**, 5776–85 (1993).

257. Hitchman, R. B. *et al.* Genetic modification of a baculovirus vector for increased expression in insect cells. *Cell Biol. Toxicol.* **26**, 57–68 (2010).

258. Loomis, K. H. *et al.* InsectDirect System: rapid, high-level protein expression and purification from insect cells. *J. Struct. Funct. Genomics* **6**, 189–94 (2005).

259. Kuo, G. *et al.* An assay for circulating antibodies to a major etiologic virus of human non-A, non-B hepatitis. *Science* **244**, 362–4 (1989).

260. Contreras, M., Barbara, J. & Cash, J. Screening for hepatitis C virus antibody. *Lancet* **26**, 505 (1989).

261. Ebeling, F., Naukkarinen, R. & Leikola, J. Recombinant immunoblot assay for hepatitis C virus antibody as predictor of infectivity. *Lancet* **335**, 982–3 (1990).

262. Poel, C. Van der & Reesink, H. Anti-HCV and transaminase testing of blood donors. *Lancet* **336**, 187–188 (1990).

263. Kato, N. *et al.* Molecular cloning of the human hepatitis C virus genome from Japanese patients with non-A, non-B hepatitis. *Proc. Natl. Acad. Sci. U. S. A.* **87**, 9524–8 (1990).

264. Choo, Q. L. *et al.* Genetic organization and diversity of the hepatitis C virus. *Proc. Natl. Acad. Sci. U. S. A.* **88**, 2451–5 (1991).

265. Ogata, N., Alter, H. J., Miller, R. H. & Purcell, R. H. Nucleotide sequence and mutation rate of the H strain of hepatitis C virus. *Proc. Natl. Acad. Sci. U. S. A.* **88**, 3392–6 (1991).

266. Takeuchi, K. *et al.* Nucleotide sequence of core and envelope genes of the hepatitis C virus genome derived directly from human healthy carriers. *Nucleic Acids Res.* **18**, 4626 (1990).

267. Takamizawa, A. *et al.* Structure and organization of the hepatitis C virus genome isolated

from human carriers. *J. Virol.* **65**, 1105–1113 (1991).

268. Okamoto, H. *et al.* Nucleotide sequence of the genomic RNA of hepatitis C virus isolated from a human carrier: comparison with reported isolates for conserved and divergent regions. *J. Gen. Virol.* **72 (Pt 11**, 2697–704 (1991).

269. Alter, H. New kit on the block: Evaluation of second-generation assays for detection of antibody to the hepatitis C virus. *Hepatology* **15**, 350–353 (1992).

270. Poel, C. Van der & Reesink, H. Confirmation of hepatitis C virus infection by new four-antigen recombinant immunoblot assay. *Lancet* **337**, 317–319 (1991).

271. Okamoto, H. *et al.* Antibodies against synthetic oligopeptides deduced from the putative core gene for the diagnosis of hepatitis virus infection. *Hepatology* **15**, 180–6 (1992).

272. Jeffers, L. J. *et al.* Prevalence of antibodies to hepatitis C virus among patients with cryptogenic chronic hepatitis and cirrhosis. *Hepatology* **15**, 187–90 (1992).

273. Brown, J., Dourakis, S. & Karayiannis, P. Seroprevalence of hepatitis C virus nucleocapsid antibodies in patients with cryptogenic chronic liver disease. *Hepatology* **15**, 175–179 (1992).

274. Katayama, T. *et al.* Improved serodiagnosis of non-A, non-B hepatitis by an assay detecting antibody to hepatitis C virus core antigen. *Hepatology* **15**, 391–4 (1992).

275. Bååth, L., Widell, a & Nordenfelt, E. A comparison between one first generation and three second generation anti-HCV ELISAs: an investigation in high- and low-risk subjects in correlation with recombinant immunoblot assay and polymerase chain reaction. *J. Virol. Methods* **40**, 287–96 (1992).

276. Uyttendaele, S., Claeys, H., Mertens, W., Verhaert, H. & Vermylen, C. Evaluation of third-generation screening and confirmatory assays for HCV antibodies. *Vox Sang.* **66**, 122–9 (1994).

277. Vernelen, K., Claeys, H. & Verhaert, H. Significance of NS3 and NS5 antigens in screening for HCV antibody. *Lancet* **343**, 853–854 (1994).

278. Abdel-Hamid, M. *et al.* Comparison of second- and third-generation enzyme immunoassays for detecting antibodies to hepatitis C virus. *J. Clin. Microbiol.* **40**, 1656–1659 (2002).

279. Colin, C. *et al.* Sensitivity and specificity of third-generation hepatitis C virus antibody detection assays: An analysis of the literature. *J. Viral Hepat.* **8**, 87–95 (2001).

280. Barrera, J. M. *et al.* Improved detection of anti-HCV in post-transfusion hepatitis by a third-generation ELISA. *Vox Sang.* **68**, 15–8 (1995).

281. Kim, S., Kim, J.-H., Yoon, S., Park, Y.-H. & Kim, H.-S. Clinical performance evaluation of four automated chemiluminescence immunoassays for hepatitis C virus antibody detection. *J. Clin. Microbiol.* **46**, 3919–23 (2008).

282. Watterson, J.M. Stallcup, P. Escamille, D. Chernay, P. Reyes, A. Trevino, S. C. Evaluation of the Ortho-Clinical Diagnostics Vitros ECi Anti-HCV Test: Comparison With Three Other Methods. *J. Clin. Lab. Anal.* **21**, 71–76 (2007).

283. Esteban, J. I. *et al.* Multicenter Evaluation of the Elecsys W Anti-HCV II Assay for the Diagnosis of Hepatitis C Virus Infection. *J. Med. Virol.* **85**, 1362–1368 (2013).

284. Agency, H. P. UK Standards for Microbiology Investigations: Investigation of Hepatitis C Infection by Antibody testing or combined Antigen/Antibody Assay. *Virology* **V5**, 1–10 (2011).

285. Kashiwakuma, T. *et al.* Detection of hepatitis C virus specific core protein in serum of patients by a sensitive fluorescence enzyme immunoassay (FEIA). *J. Immunol. Methods* **190**, 79–89 (1996).

286. Orito, E. *et al.* Quantification of serum hepatitis C virus core protein level in patients chronically infected with different hepatitis C virus genotypes. *Gut* **39**, 876–80 (1996).

287. Tanaka, T. *et al.* Simple fluorescent enzyme immunoassay for detection and quantification of hepatitis C viremia. *J. Hepatol.* **23**, 742–5 (1995).

288. Aoyagi, K. *et al.* Development of a simple and highly sensitive enzyme immunoassay for hepatitis C virus core antigen. *J. Clin. Microbiol.* **37**, 1802–8 (1999).

289. Morota, K. *et al.* A new sensitive and automated chemiluminescent microparticle immunoassay for quantitative determination of hepatitis C virus core antigen. *J. Virol. Methods* **157**, 8–14 (2009).

290. Park, Y. *et al.* New automated hepatitis C virus (HCV) core antigen assay as an alternative to real-time PCR for HCV RNA quantification. *J. Clin. Microbiol.* **48**, 2253–6 (2010).

291. Ross, R. S. *et al.* Analytical performance characteristics and clinical utility of a novel assay for total hepatitis C virus core antigen quantification. *J. Clin. Microbiol.* **48**, 1161–8 (2010).

292. Mederacke, I. *et al.* Performance and clinical utility of a novel fully automated quantitative HCV-core antigen assay. *J. Clin. Virol.* **46**, 210–5 (2009).

293. Bouvier-Alias, M. *et al.* Clinical utility of total HCV core antigen quantification: a new indirect marker of HCV replication. *Hepatology* **36**, 211–8 (2002).

294. Chevaliez, S., Bouvier-Alias, M. & Pawlotsky, J.-M. Performance of the Abbott real-time PCR assay using m2000sp and m2000rt for hepatitis C virus RNA quantification. *J. Clin. Microbiol.* **47**, 1726–32 (2009).

295. EASL clinical practice guidelines: Management of hepatitis C virus infection. *Journal of Hepatology* vol. 60 392–420 (2014).

296. Peterson J, Green G, Lida K, Caldwell B, Kerrison P, Bernich S, Aoyagi K, L. S. Detection of Hepatitis C Core Antigen in the Antibody Negative ' Window ' Phase of Hepatitis C Infection. *Vox Sang* **78**, 80–85 (2000).

297. Couroucé, A. & Marrec, N. Le. Efficacy of HCV core antigen detection during the preseroconversion period. *Transfusion* **40**, 1198–1202 (2000).

298. Icardi, G. *et al.* Novel approach to reduce the hepatitis C virus (HCV) window period: Clinical evaluation of a new enzyme-linked immunosorbent assay for HCV core antigen. *J. Clin. Microbiol.* **39**, 3110–3114 (2001).

299. Lee, S. R. *et al.* Efficacy of a hepatitis C virus core antigen enzyme-linked immunosorbent assay for the identification of 'window-phase' blood donations. *Vox Sang.* **80**, 19–23 (2001).

300. Miedouge, M. *et al.* Analytical evaluation of HCV core antigen and interest for HCV screening in haemodialysis patients. *J. Clin. Virol.* **48**, 18–21 (2010).

301. Boodram, B. Hershow, R.C. Cotler, S.J. Ouellet, L. J. Chronic hepatitis C virus infection and increases in viral load in a prospective cohort of young, HIV-uninfected injection drug users. *Drug Alcohol Depend.* **119**, 166–171 (2011).

302. Deterding, K. *et al.* Delayed versus immediate treatment for patients with acute hepatitis C: a randomised controlled non-inferiority trial. *Lancet Infect. Dis.* **13**, 497–506 (2013).

303. Chau, K. H. *et al.* IgM-antibody response to hepatitis C virus antigens in acute and chronic post-transfusion non-A, non-B hepatitis. *J. Virol. Methods* **35**, 343–52 (1991).

304. Chen, P. J. *et al.* Transient immunoglobulin M antibody response to hepatitis C virus capsid antigen in posttransfusion hepatitis C: putative serological marker for acute viral infection. *Proc. Natl. Acad. Sci. U. S. A.* **89**, 5971–5 (1992).

305. Hellström, U. B., Sylvan, S. P., Decker, R. H. & Sönnerborg, a. Immunoglobulin M reactivity

towards the immunologically active region sp75 of the core protein of hepatitis C virus (HCV) in chronic HCV infection. *J. Med. Virol.* **39**, 325–32 (1993).

306. Sagnelli, E. *et al.* Diagnosis of hepatitis C virus related acute hepatitis by serial determination of IgM anti-HCV titres. *J. Hepatol.* **42**, 646–51 (2005).

307. Kanno, A. & Kazuyama, Y. Immunoglobulin G antibody avidity assay for serodiagnosis of hepatitis C virus infection. *J. Med. Virol.* **68**, 229–33 (2002).

308. Coppola, N. *et al.* Anti-HCV IgG avidity index in acute hepatitis C. *J. Clin. Virol.* **40**, 110–5 (2007).

309. Klimashevskaya, S. *et al.* Distinguishing acute from chronic and resolved hepatitis C virus (HCV) infections by measurement of anti-HCV immunoglobulin G avidity index. *J. Clin. Microbiol.* **45**, 3400–3 (2007).

310. Netski, D. M. *et al.* Humoral immune response in acute hepatitis C virus infection. *Clin. Infect. Dis.* **41**, 667–75 (2005).

311. Smith, B. D. *et al.* Evaluation of three rapid screening assays for detection of antibodies to hepatitis C virus. *J. Infect. Dis.* **204**, 825–31 (2011).

312. Smith, B. D. *et al.* Performance of premarket rapid hepatitis C virus antibody assays in 4 national human immunodeficiency virus behavioral surveillance system sites. *Clin. Infect. Dis.* **53**, 780–6 (2011).

313. Lubelchek R, Kroc K, Hota B, Sharief R, Muppudi U, Pulvirenti J, W. R. The Role of Rapid vs Conventional Human Immunodeficiency Virus Testing for Inpatients. *Arch. Intern. Med.* **165**, 1956–1960 (2005).

314. Kendrick, S. R. *et al.* Outcomes of offering rapid point-of-care HIV testing in a sexually transmitted disease clinic. *J. Acquir. Immune Defic. Syndr.* **38**, 142–146 (2005).

315. Metcalf, C. a. *et al.* Relative Efficacy of Prevention Counseling With Rapid and Standard HIV Testing: A Randomized, Controlled Trial (RESPECT-2). *Sex. Transm. Dis.* **32**, 130–138 (2005).

316. Guthrie, R. & Susi, A. A simple phenylalanine method for detecting phenylketonuria in large populations of newborn infants. *Pediatrics* **32**, 338 (1963).

317. *UK Newborn Screening Programme Centre. NHS Screening Programmes: Guidelines for Newborn Blood Spot Sampling. (UK National Screening Committee Publication, 2012)*.

318. von Schenck, H., Lönnström, L. & Engström, M. Quality control of reflectometric determinations of glucose in dried blood spots on filter paper. *Clin. Chem.* **31**, 706–9 (1985).

319. McDade TW, Burhop J, D. J. High-Sensitivity Enzymme Immunoassay for C-reactive Protein in dried Blood Spots. *Clin. Chem.* **50**, 650–2 (2004).

320. Barin, F. *et al.* Development and Validation of an Immunoassay for Identification of Recent Human Immunodeficiency Virus Type 1 Infections and Its Use on Dried Serum Spots. *J. Clin. Microbiol.* **43**, 4441–4447 (2005).

321. Turner, R. & Holman, R. Automatic lancet for capillary blood sampling. *Lancet* **30**, 1976 (1978).

322. Parker, S. P. & Cubitt, W. D. The use of the dried blood spot sample in epidemiological studies. *J. Clin. Pathol.* **52**, 633–9 (1999).

323. McDade, T., Williams, S. & Snodgrass, J. What a drop can do: dried blood spots as a minimally invasive method for integrating biomarkers into population-based research. *Demography* **44**, 899–925 (2007).

324. Stevens S, Brown S, Singleton C, M. F. *Centres for Disease Control Newborn Screening Quality Assurance Program: Filter Paper Comparison Study*. (2009).

325. Rottinghaus, E. *et al.* Comparison of Ahlstrom grade 226, Munktell TFN, and Whatman 903 filter papers for dried blood spot specimen collection and subsequent HIV-1 load and drug resistance genotyping analysis. *J. Clin. Microbiol.* **51**, 55–60 (2013).

326. Evengard B, Ehrnst A, von Sydow M, Pehrson, Pehr O, Lundbergh P, L. E. Effect of heat on extracted HIV viral infectivity and antibody activity using the filter paper technique of blood sampling. *AIDS* **3**, 591–596 (1989).

327. *World Health Organisation: Guidance on regulations for the Transport of Infectious Substances 2013-2014*. (2013).

328. McCarron, B. *et al.* Hepaots.titis C antibody detection in dried blood sp. *J. Viral Hepat.* **6**, 453–6 (1999).

329. Parker, S. P., Khan, H. I. & Cubitt, W. D. Detection of antibodies to hepatitis C virus in dried blood spot samples from mothers and their offspring in Lahore, Pakistan. *J. Clin. Microbiol.* **37**, 2061–2063 (1999).

330. A., J. *et al.* Evaluation of a modified commercial assay in detecting antibody to hepatitis C virus in oral fluids and dried blood spots. *J. Med. Virol.* **71**, 49–55 (2003).

331. *Department of Health: Hepatitis C Action Plan for England*. (2004).

332. *NHS Scotland. Hepatitis C Action Plan for Scotland - Phase I: September 2006 - August 2008 (Scottish Executive, 2006)*. (2006).

333. Craine, N., Parry, J., O'Toole, J., D'Arcy, S. & Lyons, M. Improving blood-borne viral diagnosis; clinical audit of the uptake of dried blood spot testing offered by a substance misuse service. *J. Viral Hepat.* **16**, 219–22 (2009).

334. Hickman, M. *et al.* Increasing the uptake of hepatitis C virus testing among injecting drug users in specialist drug treatment and prison settings by using dried blood spots for diagnostic testing: a cluster randomized controlled trial. *J. Viral Hepat.* **15**, 250–254 (2008).

335. Hope, V.D. Hickman, M. Ngui, S.L. Jones, S. Telfer, M. Bizzarri, M. Ncube, F. Parry, J. V. Measuring the incidence, prevalence and genetic relatedness of hepatitis C infections among a community recruited sample of injecting drug users, using dried blood spots. *J. Viral Hepat.* **18**, 262–270 (2011).

336. Parry, J., Perry, K. & Mortimer, P. Sensitive assays for viral antibodies in saliva: an alternative to tests on serum. *Lancet* 72–75 (1987).

337. Spielberg, F. *et al.* Home collection for frequent HIV testing: Acceptability of oral fluids, dried blood sports and telephone results. *AIDS* **14**, 1819–1828 (2000).

338. Donnell-Fink, L. & Arbelaez, C. fingerstick versus oral fluid rapid HIV testing: results from the universal screening for HIV infection in the emergency room (usher Phase II) randomized controlled trial. *J. Acquir. Immune Defic. Syndr.* **24**, 309–326 (2012).

339. Pfaffe, T., Cooper-White, J., Beyerlein, P., Kostner, K. & Punyadeera, C. Diagnostic potential of saliva: current state and future applications. *Clin. Chem.* **57**, 675–87 (2011).

340. Brandtzaeg, P. Fjellanger, I. Gjeruldsen, S. T. Human secretory immunoglobulins. *Scand. J. haemotology* (1970).

341. Mortimer, P. P. & Parry, J. V. Non-invasive virological diagnosis: Are saliva and urine specimens adequate substitutes for blood? *Rev. Med. Virol.* **1**, 73–78 (1991).

342. Holm-Hansen, C. & Tong, G. Comparison of oral fluid collectors for use in a rapid point-of-care diagnostic device. *Clin. Diagn. Lab. Immunol.* **11**, 909–912 (2004).

343. Cruz, H. M. *et al.* An evaluation of different saliva collection methods for detection of antibodies against hepatitis C virus (anti-HCV). *J. Oral Pathol. Med.* **41**, 793–800 (2012).

344. Yaari, A. *et al.* Detection of HCV salivary antibodies by a simple and rapid test. *J. Virol. Methods* **133**, 1–5 (2006).

345. Lee, S. R. *et al.* Evaluation of a rapid, point-of-care test device for the diagnosis of hepatitis C infection. *J. Clin. Virol.* **48**, 15–7 (2010).

346. Lee, S. R. *et al.* 696 Results of a Multi-Center Evaluation of a New Rapid Test for Detection of Hcv Infection Using Whole Blood, Serum, Plasma and Oral Fluid. *J. Hepatol.* **52**, S271 (2010).

347. Jewett, a *et al.* Field-based performance of three pre-market rapid hepatitis C virus antibody assays in STAHR (Study to Assess Hepatitis C Risk) among young adults who inject drugs in San Diego, CA. *J. Clin. Virol.* **54**, 213–7 (2012).

348. Cha, Y. J. *et al.* Performance evaluation of the OraQuick hepatitis C virus rapid antibody test. *Ann. Lab. Med.* **33**, 184–9 (2013).

349. Larrat, S. *et al.* Performance of an antigen-antibody combined assay for hepatitis C virus testing without venipuncture. *J. Clin. Virol.* **55**, 220–5 (2012).

350. Visseaux, B. *et al.* Anti-hepatitis C virus antibody detection in oral fluid: Influence of human immunodeficiency virus co-infection. *J. Clin. Virol.* **58**, 385–90 (2013).

351. Marques, B.L.C. Brandao, C.U. Silva, E.F. Marques, V.A. Villela-Nogueira, C.A. Do O, K.M.R. de Paula, M.T. Lewis-Ximenez, L.L. Lampe, E. Villar, L. M. Dried Blood Spot Samples: Optimization of Commercial EIAs for Hepatitis C Antibody Detection and Stability Under Different Storage Conditions. *J. Med. Virol.* **84**, 1600–1607 (2012).

352. Health Protection Agency. Hepatitis C in the UK Annual Report 2008. (Health Protection Agency 2008). (2008).

353. Crouch, D. J. Oral fluid collection: the neglected variable in oral fluid testing. *Forensic Sci. Int.* **150**, 165–73 (2005).

354. Novagen. pIEx-6 Vector Map.

355. Novagen. 3C / LIC Cloning Kits. User protocol TB453. 1–12 (2011).

356. Woods, C. K. *et al.* Automating HIV drug resistance genotyping with RECall, a freely accessible sequence analysis tool. *J. Clin. Microbiol.* **50**, 1936–1942 (2012).

357. Hitchman, R. B., Siaterli, E. A., Nixon, C. P. & King, L. A. Quantitative Real-Time PCR for Rapid and Accurate Titration of Recombinant Baculovirus Particles. *Biotechnol. Bioeng.* **96**, 810–814 (2007).

358. Yeagle, P. L. The Membranes of Cells Chapter 4 – Detergents (Elsevier 2016). in doi:10.1016/B978-0-12-800047-2.00004-8.

359. Turck, N. *et al.* pROC: an open-source package for R and S+ to analyze and compare ROC curves. *BMC Bioinformatics* **8**, 12–77 (2011).

360. Youden, W. J. Index for rating diagnostic tests. *Cancer* **3**, 32–35 (1950).

361. Perkins, N. J. & Schisterman, E. F. The Inconsistency of " Optimal " Cut-points Using Two ROC Based Criteria. *Am J Epidemiol* **163**, 670–675 (2006).

362. Fawcett, T. An introduction to ROC analysis. *Pattern Recognit. Lett.* **27**, 861–874 (2006).

363. Delong, E. R. & Carolina, N. Comparing the Areas under Two or More Correlated Receiver Operating Characteristic Curves : A Nonparametric Approach Author (s): Elizabeth R . DeLong , David M . DeLong and Daniel L . Clarke-Pearson Published by : International Biometric Society Stable . *Biometrics* **44**, 837–845 (2016).

364. McClish, D. K. Analyzing a Portion of the ROC Curve. *Med. Decis. Mak.* **9**, 190–195 (1989).

365. Penna, A. & Cahalan, M. Western blotting using the Invitrogen Nupage novex Bis tris MiniGels. *J. Vis. Exp.* 2–4 (2007) doi:10.3791/264.

366. Beld, M. *et al.* Quantitative antibody responses to structural (Core) and nonstructural (NS3, NS4, and NS5) hepatitis C virus proteins among seroconverting injecting drug users: impact of epitope variation and relationship to detection of HCV RNA in blood. *Hepatology* **29**, 1288–98 (1999).

367. Chiron Corp's European Patent for Methods and Compositions for Controlling Translation of HCV Proteins Expires. *Global IP News: Biotechnology Patent News* (2013).

368. Kim, S., Kim, J.-H., Yoon, S., Park, Y.-H. & Kim, H.-S. Clinical performance evaluation of four automated chemiluminescence immunoassays for hepatitis C virus antibody detection. *J. Clin. Microbiol.* **46**, 3919–23 (2008).

369. Krawczyk, A. *et al.* Clinical performance of the novel DiaSorin LIAISON® XL murex: HBsAg Quant, HCV-Ab, HIV-Ab/Ag assays. *J. Clin. Virol.* **59**, 44–49 (2014).

370. Hamed, M. R. B. *et al.* Association of antibodies to hepatitis C virus glycoproteins 1 and 2 (anti-E1E2) with HCV disease. *J. Viral Hepat.* **15**, 339–345 (2008).

371. Baumert, T. F. *et al.* Antibodies against hepatitis C virus-like particles and viral clearance in acute and chronic hepatitis C. *Hepatology* **32**, 610–617 (2000).

372. Li, P. *et al.* Engineering of N-glycosylation of hepatitis C virus envelope protein E2 enhances T cell responses for DNA immunization. *Vaccine* **25**, 1544–1551 (2007).

373. Masavuli, M. G., Wijesundara, D. K., Torresi, J., Gowans, E. J. & Grubor-Bauk, B. Preclinical development and production of virus-like particles as vaccine candidates for hepatitis C. *Front. Microbiol.* **8**, 1–11 (2017).

374. Sällberg, M., Rudén, U., Wahren, B. & Magnius, L. O. Immunodominant regions within the hepatitis C virus core and putative matrix proteins. *J. Clin. Microbiol.* **30**, 1989–94 (1992).

375. Xiang, J. *et al.* Recombinant hepatitis C virus-like particles expressed by baculovirus: utility in cell-binding and antibody detection assays. *J. Med. Virol.* **68**, 537–43 (2002).

376. Stevenson, J., Krycer, J. R., Phan, L. & Brown, A. J. A practical comparison of ligation-independent cloning techniques. *PLoS One* **8**, 8–14 (2013).

377. Krammer, F., Schinko, T., Palmberger, D. & Tauer, C. Europe PMC Funders Group Trichoplusia ni cells (High Five ™) are highly efficient for the production of influenza A virus-like particles : a comparison of two insect cell lines as production platforms for influenza vaccines. *Mol. Biotechnol.* **45**, 226–234 (2010).

378. Islam, M. S., Aryasomayajula, A. & Selvaganapathy, P. R. A review on macroscale and microscale cell lysis methods. *Micromachines* **8**, (2017).

379. Waugh, D. S. Making the most of affinity tags. *Trends Biotechnol.* **23**, 316–320 (2005).

380. Fersht, A. R. Denaturation (Proteins). *Encycl. Genet.* 529 (2001) doi:10.1006/rwgn.2001.0321.

381. Kunkel, M. *et al.* Self-Assembly of Nucleocapsid-Like Particles from Recombinant Hepatitis C Virus Core Protein. *J. Virol.* **75**, 2119–2129 (2001).

382. Chiba, J. *et al.* Serodiagnosis of hepatitis C virus (HCV) infection with an HCV core protein molecularly expressed by a recombinant baculovirus. *Proc. Natl. Acad. Sci. U. S. A.* **88**, 4641–5 (1991).

383. Choi, S. H., Kim, S. Y., Park, K. J., Kim, Y. J. & Hwang, S. B. Hepatitis C virus core protein is efficiently released into the culture medium in insect cells. *J. Biochem. Mol. Biol.* **37**, 735–40

(2004).

384. Eckels, D. D., Zhou, H., Bian, T. H. & Wang, H. Identification of antigenic escape variants in an immunodominant epitope of hepatitis C virus. *Int. Immunol.* **11**, 577–583 (1999).

385. Choi, M., Lee, S., Choi, T. & Lee, C. A hepatitis C virus NS4B inhibitor suppresses viral genome replication by disrupting NS4B's dimerization/multimerization as well as its interaction with NS5A. *Virus Genes* **47**, 395–407 (2013).

386. Sillanpää, M. *et al.* Hepatitis C virus core, NS3, NS4B and NS5A are the major immunogenic proteins in humoral immunity in chronic HCV infection. *Virol. J.* **6**, 84 (2009).

387. Chang, J. C. *et al.* Artificial NS4 mosaic antigen of hepatitis C virus. *J. Med. Virol.* **59**, 437–450 (1999).

388. Yu. E. Khudyakov, N. S. Khudyakova, D. L Jue, S. B. Lambert, S. Fang, and H. A. F. Linear B-Cell Epitopes of the NS3-NS4-NS5 Proteins of the Hepatitis C Virus as Modeled with Synthetic Peptides Yu. *Virol. J.* **206**, 666–672 (1995).

389. Chang, J. C. *et al.* Antigenic heterogeneity of the hepatitis C virus NS4 protein as modeled with synthetic peptides. *Virology* **257**, 177–190 (1999).

390. Jiang, Y., Deng, F., Wang, H. & Hu, Z. An extensive analysis on the global codon usage pattern of baculoviruses. *Arch. Virol.* **153**, 2273–2282 (2008).

391. Barry J. Ryan. Chapter 4 Avoiding proteolysis during protein chromatopraphy. in *Protein Chromatography Methods and Protocols.* 61–72 (2011). doi:10.1007/978-1-4939-6412-3_21.

392. Dou, X. G. *et al.* Antigenic heterogeneity of the hepatitis C virus NS5A protein. *J. Clin. Microbiol.* **40**, 61–67 (2002).

393. Kroemer, J. A. & Webb, B. A. Divergences in Protein Activity and Cellular Localization within the Campoletis sonorensis Ichnovirus Vankyrin Family. *J. Virol.* **80**, 12219–12228 (2006).

394. Steele, K. H. *et al.* Improving the baculovirus expression vector system with vankyrin-enhanced technology. *Biotechnol. Prog.* **33**, 1496–1507 (2017).

395. Tessier, D. C., Thomas, D. Y., Khouri, H. E., Laliberié, F. & Vernet, T. Enhanced secretion from insect cells of a foreign protein fused to the honeybee melittin signal peptide. *Gene* **98**, 177–183 (1991).

396. Esposito, D. & Chatterjee, D. K. Enhancement of soluble protein expression through the use of fusion tags. *Curr. Opin. Biotechnol.* **17**, 353–358 (2006).

397. Spriestersbach, A., Kubicek, J., Schäfer, F., Block, H. & Maertens, B. Purification of His-Tagged Proteins. *Methods Enzymol.* **559**, 1–15 (2015).

398. West, S. M., Guise, A. D. & Chaudhuri, J. B. A comparison of the denaturants urea and guanidine hydrochloride on protein refolding. *Food Bioprod. Process. Trans. Inst. Chem. Eng. Part C* **75**, 50–56 (1997).

399. Bhavagan, N. V. CHAPTER 4 - Three-Dimensional Structure of Proteins,. in *Medical Biochemistry, Academic Press* 51–65 (2002). doi:10.1016/B978-0-12-095440-7.50006-8.

400. Yamaguchi, H. & Miyazaki, M. Refolding techniques for recovering biologically active recombinant proteins from inclusion bodies. *Biomolecules* **4**, 235–251 (2014).

401. K. Tsumoto, D. Ejima, A. M. Sunczuk, Y. Kita, T. A. Effects of Salts on Protein–Surface Interactions: Applications for Column Chromatography. *J. Pharm. Sci.* **96**, 1677–1690 (2007).

402. Gräslund, S. *et al.* Protein production and purification. *Nat. Methods* **5**, 135–146 (2008).

403. Corporation, C. RIBA v3 Strip Immunoblot Assay (SIA) for the Detection of Antibodies to

Hepatitis C Virus (Anti-HCV) in Human Serum or Plasma. 1–23 (1998).

404. Kolho, E., Naukkarinen, R. & Krusius, T. Transmission of HCV infection by RIBA indeterminate and positive blood units. *Transfus. Med.* **2**, 243–248 (1992).

405. Greiner, M., Pfeiffer, D. & Smith, R. D. Principles and practical application of the receiver-operating characteristic analysis for diagnostic tests. *Prev. Vet. Med.* **45**, 23–41 (2000).

406. Hanley, J. A. The Robustness of the "Binormal" Assumptions Used in Fitting ROC Curves. *Med. Decis. Mak.* **8**, 197–203 (1988).

407. Akobeng, A. K. Understanding diagnostic tests 3: Receiver operating characteristic curves. *Acta Paediatr. Int. J. Paediatr.* **96**, 644–647 (2007).

408. Tests, D. Basic Principles of ROC Analysis. *Semin. Nucl. Med.* **VIII**, 283–298 (1978).

409. Swets, J. A. Measuring the Accuracy of Diagnostic Systems Author(s): John A. Swets Source: *Science (80-.).* **240**, 1285–1293 (1988).

410. Park, S. H., Goo, J. M. & Jo, C. H. Receiver operating characteristic (ROC) curve: Practical review for radiologists. *Korean J. Radiol.* **5**, 11–18 (2004).

411. Fischer, J. E., Bachmann, L. M. & Jaeschke, R. A readers' guide to the interpretation of diagnostic test properties: Clinical example of sepsis. *Intensive Care Med.* **29**, 1043–1051 (2003).

412. Hanley, J. A. & McNeil, B. J. A method of comparing the areas under receiver operating characteristic curves derived from the same cases. *Radiology* **148**, 839–843 (1983).

413. Carpenter, J. & Bithell, J. Bootstrap confidence intervals: When, which, what? A practical guide for medical statisticians. *Stat. Med.* **19**, 1141–1164 (2000).

414. Guglielmo-Viret, V., Attrée, O., Blanco-Gros, V. & Thullier, P. Comparison of electrochemiluminescence assay and ELISA for the detection of Clostridium botulinum type B neurotoxin. *J. Immunol. Methods* **301**, 164–172 (2005).

415. Carson, M., Johnson, D. H., McDonald, H., Brouillette, C. & Delucas, L. J. His-tag impact on structure. *Acta Crystallogr. D. Biol. Crystallogr.* **63**, 295–301 (2007).

416. Arnau, J., Lauritzen, C., Petersen, G. E. & Pedersen, J. Current strategies for the use of affinity tags and tag removal for the purification of recombinant proteins. *Protein Expr. Purif.* **48**, 1–13 (2006).

417. Lemaitre, R. P., Bogdanova, A., Borgonovo, B., Woodruff, J. B. & Drechsel, D. N. FlexiBAC: A versatile, open-source baculovirus vector system for protein expression, secretion, and proteolytic processing. *BMC Biotechnol.* **19**, 1–11 (2019).

418. Sormanni, P., Aprile, F. A. & Vendruscolo, M. The CamSol method of rational design of protein mutants with enhanced solubility. *J. Mol. Biol.* **427**, 478–490 (2015).

419. Roos, P. H. *Chapter 1 Ion Exchange Chromatography*. *Protein Liquid Chromatography. Elsevier Science.* (Elsevier B.V., 1999). doi:10.1016/S0301-4770(08)60529-1.

420. Audain, E., Ramos, Y., Hermjakob, H., Flower, D. R. & Perez-Riverol, Y. Accurate estimation of isoelectric point of protein and peptide based on amino acid sequences. *Bioinformatics* **32**, 821–827 (2016).

421. *Ion exchange chromatography and Chromatofocusing. Principles and Methods*. *GE Healthcare Bio-Sciences AB* (2010). doi:10.1515/9783110862430.1187.

422. Hong, P., Koza, S. & Bouvier, E. S. P. A review size-exclusion chromatography for the analysis of protein biotherapeutics and their aggregates. *J. Liq. Chromatogr. Relat. Technol.* **35**, 2923–2950 (2012).

423. Tomaz, C. T. & Queiroz, J. A. *Hydrophobic Interaction Chromatography*. *Liquid*

Chromatography: Fundamentals and Instrumentation (Elsevier Inc., 2013). doi:10.1016/B978-0-12-415807-8.00006-7.

424. Kelley, B. D. *et al.* High-throughput screening of chromatographic separations: IV. Ion-exchange. *Biotechnol. Bioeng.* **100**, 950–963 (2008).

15 APPENDIX

Study No.	anti-HCV	Core	NS3	NS4Pr	NS4	NS5a	NS5b
M18.006	P	1.764	0.258	0.146	1.472	0.111	0.17
M18.008	P	0.466	0.17	0.399	2.872	0.073	0.535
M18.009	P	1.496	1.166	0.472	2.956	2.955	2.955
M18.010	P	1.862	0.217	0.241	0.498	0.054	0.046
M18.011	P	2.86	0.11	0.357	0.457	0.192	1.62
M18.013	P	2.494	0.131	0.14	0.524	2.955	0.201
M18.014	P	0.74	0.877	0.5	0.885	0.272	0.175
M18.015	P	2.398	0.777	0.374	2.257	0.063	0.49
M18.016	P	2.897	0.484	0.549	0.509	0.936	0.168
M18.017	N	0.271	0.066	0.129	0.154	0.057	0.064
M18.018	N	0.215	0.047	0.172	0.192	0.068	0.592
M18.019	N	0.556	0.061	0.07	0.492	0.079	0.09
M18.020	N	0.168	0.033	0.187	0.246	0.094	0.074
M18.021	N	0.243	0.063	0.201	0.317	0.122	0.206
M18.022	N	0.282	0.131	0.252	0.291	0.306	0.208
M18.023	N	0.501	0.07	0.46	0.262	0.169	0.847
M18.024	N	0.207	0.076	0.112	0.191	0.17	0.299
M18.025	N	0.484	0.175	0.391	0.363	0.216	0.305
M18.026	N	0.116	0.037	0.112	0.231	0.066	0.067
M18.027	N	0.083	0.026	0.084	0.08	0.04	0.039
M18.028	N	0.199	0.106	0.221	0.196	0.109	0.119
M18.029	N	0.191	0.041	0.205	0.129	0.033	0.106
M18.030	P	1.251	1.612	2.953	2.956	2.955	0.094
M18.031	P	0.626	1.923	2.953	1.626	2.955	2.955
M18.032	P	1.84	2.073	2.953	1.331	2.955	0.098
M18.033	P	1.383	1.499	1.391	0.295	0.194	0.215
M18.034	P	0.187	0.086	0.274	0.668	0.176	0.548
M18.035	P	0.368	0.164	0.302	0.746	0.496	0.181
M18.036	N	0.24	0.043	0.228	0.243	0.096	0.077
M18.037	N	0.129	0.037	0.109	0.252	0.07	0.064
M18.038	N	0.095	0.033	0.24	0.105	0.037	0.162
M18.039	N	0.233	0.115	0.268	0.51	0.199	0.147
M18.040	N	0.1	0.022	0.106	0.074	0.072	0.148
M18.041	N	0.119	0.034	0.147	0.214	0.095	0.134

M18.042	N	0.167	0.048	0.253	0.234	0.115	0.199
M18.043	N	0.075	0.234	0.07	0.096	0.036	0.033
M18.044	N	0.169	0.044	0.1	0.155	0.075	0.097
M18.045	N	0.069	0.012	0.052	0.084	0.02	0.014
M18.046	N	0.294	0.096	0.303	0.333	0.2	0.154
M18.047	N	0.287	0.109	0.268	0.392	0.193	0.139
M18.048	N	0.348	0.064	0.112	0.489	0.34	0.973
M18.049	N	0.162	0.046	0.265	0.205	0.085	0.081
M18.050	N	0.193	0.031	0.063	0.278	0.115	0.06
M18.051	N	0.299	0.079	0.321	0.254	0.108	0.24
M18.052	N	0.328	0.095	0.308	0.309	0.21	0.613
M18.053	N	0.176	0.037	0.089	0.145	0.041	0.096
M18.054	N	0.108	0.049	0.296	0.165	0.068	0.091
M18.055	N	0.157	0.047	0.187	0.842	0.055	1.367
M18.056	N	0.221	0.071	0.203	0.281	0.12	1.607
M18.057	N	0.39	0.045	0.108	0.321	0.036	0.243
M18.058	N	0.146	0.03	0.148	0.133	0.055	0.046
M18.059	N	0.116	0.035	0.1	0.685	0.123	0.604
M18.060	N	0.174	0.046	0.083	0.153	0.082	0.109
M18.061	N	0.152	0.035	0.096	0.129	0.049	0.125
M18.062	N	0.14	0.028	0.036	0.129	0.014	0.029
M18.063	N	0.166	0.052	0.128	0.174	0.06	0.078
M18.064	N	0.135	0.051	0.206	0.143	0.1	0.115
M18.065	N	0.238	0.072	0.267	0.199	0.048	0.149
M18.066	N	0.19	0.041	0.216	0.106	0.088	0.066
M18.067	P	1.388	0.184	0.18	0.49	0.308	0.061
M18.068	P	2.09	0.735	0.193	0.6	0.205	0.094
M18.069	P	0.984	1.388	0.24	2.104	0.105	0.956
M18.070	P	0.686	2.101	1.15	0.965	2.955	0.112
M18.071	P	0.296	0.256	0.278	0.308	0.651	0.688
M18.072	P	0.089	0.331	0.238	0.161	0.308	0.051
M18.073	P	1.804	0.837	0.187	1.502	2.955	0.673
M18.074	P	0.318	1.101	2.953	0.923	2.955	2.955
M18.075	P	2.443	0.31	0.159	2.956	0.095	0.042
M18.076	P	0.671	0.401	0.061	0.431	0.821	0.051
M18.077	P	0.801	0.882	0.198	2.062	2.955	0.927
M18.078	P	1.286	0.874	0.179	2.956	2.955	2.955
M18.079	P	1.632	0.036	0.356	1.261	0.651	0.062
M18.080	P	1.516	0.524	0.231	2.956	0.308	0.193
M18.081	P	0.36	0.78	0.208	0.154	2.955	0.23
M18.082	P	1.912	1.254	2.953	0.42	2.955	0.07

M18.083	P	2.115	0.986	1.259	0.694	0.095	1.613
M18.084	P	1.774	1.401	2.953	0.314	0.821	0.061
M18.085	P	0.979	0.085	0.737	0.124	2.955	0.07
M18.086	P	2.74	1.227	0.109	1.863	2.955	0.043
M18.087	P	0.907	0.661	0.632	0.423	0.306	0.151
M18.088	P	0.119	0.369	0.293	0.173	0.025	0.06
M18.089	P	0.877	1.56	0.985	0.411	0.34	0.236
M18.090	P	0.429	0.367	0.131	2.746	0.091	0.138
M18.091	P	2.182	2.39	2.953	2.956	2.955	2.955
M18.092	P	1.75	1.735	0.628	1.197	1.02	0.151
M18.093	P	2.433	1.978	0.39	2.818	2.955	0.146
M18.094	P	0.652	1.404	0.242	2.956	2.955	2.955
M18.095	P	0.643	0.34	0.286	2.404	0.59	0.075
M18.096	P	2.021	1.503	2.953	0.831	2.955	0.042
M18.097	P	2.805	0.816	0.277	2.956	0.06	0.056
M18.098	P	0.112	0.342	0.227	0.151	0.018	0.043
M18.099	P	1.711	0.172	0.23	1.009	2.955	1.32
M18.100	P	2.399	0.347	0.894	0.256	2.501	0.22
M18.101	P	1.466	0.132	1.065	0.545	2.955	0.151
M18.102	N	0.519	0.184	2.441	0.359	0.106	0.271
M18.103	N	0.149	0.103	0.059	0.112	0.054	0.104
M18.104	N	0.321	0.302	0.155	0.253	0.16	0.198
M18.105	N	0.383	0.209	0.232	0.331	0.103	0.421
M18.106	N	0.673	0.282	0.145	0.397	0.072	0.203
M18.107	N	0.49	0.576	0.376	0.446	0.299	0.366
M18.108	N	0.168	0.094	0.154	0.108	0.071	0.071
M18.109	N	0.27	0.098	2.261	0.179	0.053	0.039
M18.110	N	0.527	0.499	0.224	0.381	0.265	0.477
M18.111	N	0.299	0.253	0.316	0.221	0.152	0.161
M18.112	N	0.616	0.517	0.26	0.207	0.046	0.131
M18.113	N	0.06	0.021	0.78	0.338	0.009	0.031
M18.114	N	0.391	0.357	0.187	0.245	0.147	0.194
M18.115	N	0.345	0.18	0.414	0.263	0.051	0.113
M18.116	N	0.093	0.078	0.253	0.084	0.044	0.063
M18.117	N	0.519	0.226	0.048	0.16	0.061	0.142
M18.118	N	0.504	0.128	0.381	0.372	0.043	0.427
M18.119	N	0.334	0.135	0.257	0.174	0.052	0.1
M18.120	N	0.306	0.07	0.091	0.09	0.036	0.077
M18.121	N	0.258	0.101	0.181	0.164	0.021	0.033
M18.122	N	0.228	0.103	0.439	0.129	0.055	0.108
M18.123	N	0.175	0.079	0.996	0.099	0.037	0.069

M18.124	N	0.298	0.083	0.203	0.126	0.052	0.076
M18.125	N	0.471	0.192	0.068	0.17	0.042	0.077
M18.126	N	0.184	0.061	0.153	0.086	0.041	0.106
M18.127	N	0.295	0.104	0.564	0.201	0.206	0.539
M18.128	N	0.39	0.17	0.248	0.589	0.031	0.091
M18.129	N	0.361	0.194	0.356	0.255	0.101	0.314
M18.130	N	0.508	0.192	0.049	0.228	0.085	0.132
M18.131	N	0.342	0.165	0.32	0.239	0.07	0.12
M18.132	N	0.151	0.072	0.029	0.226	0.026	0.068
M18.133	N	0.679	0.376	0.052	0.518	0.173	0.249
M18.134	N	0.251	0.121	0.878	0.144	0.053	0.059
M18.135	N	0.221	0.123	0.18	0.136	0.049	0.563
M18.136	N	0.175	0.065	0.22	0.131	0.03	0.048
M18.137	N	0.139	0.057	0.353	0.099	0.024	0.292
M18.138	N	0.979	0.405	0.036	0.309	0.097	0.125
M18.139	N	0.226	0.087	0.116	0.2	0.031	0.076
M18.140	N	0.48	0.2	0.109	0.303	0.099	0.221
M18.141	N	0.263	0.19	0.159	0.166	0.067	0.147
M18.142	N	0.18	0.087	0.176	1.006	0.035	0.04
M18.143	N	0.331	0.243	0.033	0.228	0.077	0.118
M18.144	N	0.274	0.133	0.053	0.19	0.111	0.119
M18.145	N	0.629	0.196	0.137	0.671	0.233	0.184
M18.146	N	0.242	0.2	0.409	0.16	0.076	0.173
M18.147	N	0.792	0.612	0.102	0.219	0.043	0.11
M18.148	N	0.187	0.048	0.171	0.164	0.019	0.044
M18.149	N	0.372	0.123	0.15	0.39	0.062	0.664
M18.150	P	1.391	0.36	0.15	1.456	0.108	0.221
M18.151	P	2.672	0.292	0.148	0.608	0.341	0.12
M18.152	P	0.455	2.203	0.156	0.449	0.187	0.283
M18.153	P	2.729	0.791	0.145	0.709	0.335	0.611
M18.154	P	0.398	2.137	0.101	0.306	0.526	0.124
M18.155	P	2.656	0.496	0.03	0.348	0.238	0.314
M18.156	P	1.392	2.415	0.025	0.728	0.71	0.679
M18.157	P	1.104	0.205	0.081	0.678	0.155	0.114
M18.158	P	1.341	0.219	0.132	0.2	0.115	0.138
M18.159	P	2.949	0.409	0.22	2.692	2.535	0.118
M18.160	P	2.949	2.044	0.231	1.892	0.113	0.159
M18.161	P	2.893	0.253	0.113	0.425	1.009	0.126
M18.162	P	2.934	2.167	0.092	1.971	0.107	0.164
M18.163	P	2.38	0.492	0.353	0.643	2.93	0.194
M18.164	P	2.949	2.954	0.129	0.917	2.482	0.19

M18.165	P	1.599	2.759	0.207	0.387	0.207	0.343
M18.166	P	1.001	0.358	0.046	0.33	0.203	0.188
M18.167	P	1.628	2.031	0.06	0.464	0.223	0.143
M18.168	P	0.519	0.362	0.203	1.192	0.144	0.396
M18.169	P	2.569	1.127	0.249	0.179	1.632	0.105
M18.170	P	0.919	0.304	0.289	1.128	0.042	0.181
M18.171	P	1.963	0.468	0.04	1.772	0.156	0.308
M18.172	P	0.684	0.578	0.028	0.852	0.085	0.618
M18.173	P	1.136	1.525	0.079	2.956	2.549	0.278
M18.174	P	2.872	2.624	0.153	0.386	1.905	1.068
M18.175	P	0.691	0.137	0.259	1.847	0.036	0.092
M18.176	P	0.246	1.702	0.171	0.107	0.047	0.453
M18.177	P	2.89	0.404	0.014	1.536	0.092	0.164
M18.178	P	2.758	2.26	0.098	0.765	0.204	0.227
M18.179	P	0.764	0.592	0.087	0.219	0.056	0.127
M18.180	P	1.718	2.896	0.064	0.389	0.205	0.32
M18.181	P	1.225	0.204	0.125	0.209	0.197	0.129
M18.182	P	1.097	0.275	0.195	0.703	0.134	0.58
M18.183	P	2.471	1.681	0.038	0.974	1.322	0.104
M18.184	P	0.761	0.384	0.025	0.369	0.243	0.246
M18.185	P	0.737	0.624	0.14	0.221	0.046	0.119
M18.186	P	1.23	0.949	0.114	0.208	2.271	0.108
M18.187	P	0.291	2.463	0.146	0.518	0.117	0.28
M18.188	P	2.049	2.69	0.135	0.348	0.055	0.217
M18.189	P	2.949	2.8	0.062	0.333	2.136	1.231
M18.192	P	0.631	0.121	0.201	2.319	0.118	0.347
M18.193	P	1.721	2.513	0.122	0.305	0.229	0.363
M18.194	P	0.707	0.551	0.188	0.233	0.055	0.684
M18.195	P	2.949	0.626	0.054	0.78	0.301	2.757

Table 51 ELISA results for each HCV antigen ELISA with Serum samples of known anti-HCV status. anti-HCV column is HCV status determined by Roche Cobas anti-HCVII assay, P=Positive, N=Negative, OD results – blank are given for each HCV antigen

Study No.	anti - HCV	Core	NS31a	NS4abPr	NS4ab	NS5a	NS5b
M18.196	P	2.517	1.388	0.458	2.956	2.955	1.033
M18.197	P	1.365	1.119	0.372	1.016	2.955	1.128
M18.198	P	0.286	0.824	0.49	0.538	0.162	0.486
M18.199	P	0.848	0.631	0.384	0.622	2.955	0.562
M18.200	P	0.232	1.601	2.953	1	0.301	0.398
M18.201	P	0.896	0.149	1.724	0.649	0.156	0.387
M18.202	P	0.44	1.403	0.217	1.641	0.093	0.609
M18.203	P	1.166	1.457	0.91	1.358	2.955	1.02
M18.204	P	1.251	1.258	0.321	2.893	0.174	2.955
M18.205	P	2.423	1.134	0.391	0.827	2.955	0.401
M18.206	P	0.76	0.592	0.166	0.955	0.048	0.17
M18.207	P	0.579	0.923	0.454	2.956	2.955	0.598
M18.208	P	1.172	1.722	1.07	0.695	0.38	0.237
M18.209	P	0.187	1.274	0.383	2.956	0.129	0.913
M18.210	P	1.032	1.278	0.512	2.956	2.955	2.955
M18.211	P	0.587	1.154	2.829	0.773	2.955	0.356
M18.212	P	0.823	1.032	0.55	0.686	2.955	0.17
M18.213	P	0.593	1.666	1.241	0.415	2.955	0.154
M18.214	P	1.4	1.525	0.732	0.335	0.164	0.292
M18.215	P	1.04	0.065	0.228	2.497	2.955	0.178
M18.216	P	0.867	0.199	0.268	1.047	0.125	0.286
M18.217	P	0.507	1.882	2.175	2.561	2.955	0.963
M18.218	P	0.218	1.795	0.556	0.897	0.044	0.195
M18.219	P	0.318	0.321	1.759	1.007	2.955	0.331
M18.220	P	1.738	1.504	2.953	0.894	2.955	0.403
M18.221	P	0.217	1.653	0.182	0.235	2.955	0.138
M18.222	P	0.268	0.363	0.075	2.498	0.725	0.179
M18.223	P	0.288	0.161	0.102	1.972	2.955	0.655
M18.224	P	0.681	1.594	0.554	1.512	2.955	2.286
M18.225	P	0.51	1.256	0.367	2.808	2.955	0.381
M18.226	P	0.443	0.513	0.358	0.215	0.205	0.19
M18.227	P	0.654	0.849	0.373	2.768	2.955	2.955
M18.228	P	1.801	1.107	2.186	0.751	2.955	0.395
M18.229	P	0.657	0.659	0.131	2.956	2.955	1.677
M18.230	P	0.241	0.19	0.224	2.319	2.955	0.329
M18.231	P	1.049	1.847	2.953	1.445	2.955	2.955
M18.232	P	0.97	0.829	0.109	1.675	0.077	0.449
M18.233	P	0.171	1.731	2.953	1.133	2.955	0.297

M18.234	P	0.019	0.767	0.246	1.726	2.955	0.315
M18.235	P	0.255	0.104	0.105	0.349	1.819	0.308
M18.236	P	0.106	0.03	0.034	1.422	0.07	0.053
M18.237	P	0.042	0.031	0.034	0.042	0.025	0.655
M18.238	P	1.27	0.226	0.33	0.569	0.187	0.377
M18.239	P	0.74	0.392	0.442	2.14	0.904	0.492
M18.240	P	0.472	0.496	0.231	1.709	0.426	0.194
M18.241	P	0.226	1.134	0.2	0.842	2.955	0.167
M18.242	P	1.074	0.959	0.162	1.004	0.059	0.131
M18.243	P	2.949	2.368	2.441	1.716	0.117	1.717
M18.244	P	0.292	0.763	0.059	0.198	0.058	0.079
M18.245	P	0.332	0.105	0.155	0.227	0.083	0.112
M18.246	P	1.053	0.548	0.232	0.565	0.234	0.351
M18.247	P	1.142	1.714	0.145	0.368	1.186	0.069
M18.248	P	0.657	2.216	0.376	0.832	0.116	0.41
M18.249	P	0.292	1.747	0.154	0.536	0.116	0.175
M18.250	P	0.646	2.474	2.261	0.49	2.695	0.235
M18.251	P	0.303	1.917	0.224	1.577	1.524	0.215
M18.252	P	2.949	1.672	0.316	0.403	2.722	0.606
M18.253	P	0.652	0.296	0.201	0.632	0.13	0.332
M18.254	P	2.354	0.234	0.78	0.49	2.595	0.191
M18.255	P	1.808	1.672	0.187	0.392	1.051	0.34
M18.256	P	0.615	1.729	0.414	0.259	0.107	0.187
M18.257	P	0.398	2.178	0.163	0.728	0.101	0.199
M18.258	P	0.227	0.825	0.048	0.494	0.492	1.935
M18.259	P	2.949	2.267	0.383	0.378	0.115	0.175
M18.260	P	0.132	0.453	0.257	0.127	0.073	0.131
M18.261	P	2.46	0.992	0.091	0.559	0.947	0.095
M18.262	P	0.97	0.597	0.181	1.148	1.782	0.505
M18.263	P	1.166	2.294	0.439	2.012	0.166	0.392
M18.264	P	1.701	0.768	0.996	0.128	2.115	0.096
M18.265	P	0.251	0.732	0.203	0.626	0.803	0.205
M18.266	P	0.123	0.095	0.068	0.583	1.305	0.085
M18.267	P	0.117	0.326	0.151	0.114	0.964	0.086
M18.268	P	1.241	0.362	0.574	0.252	2.003	0.084
M18.269	P	1.449	1.737	0.248	0.423	0.112	0.207
M18.270	P	1.687	1.957	0.356	0.216	0.047	0.106
M18.271	P	0.707	0.085	0.203	0.085	0.302	0.102
M18.272	P	1.672	0.756	0.32	0.468	0.552	0.226
M18.273	P	0.021	0.195	0.029	0.042	0.017	0.021
M18.274	P	1.698	1.975	0.289	1.057	0.139	0.193

M18.275	P	0.916	0.768	0.25	0.613	0.133	0.142
M18.276	P	0.977	0.309	0.18	0.879	0.107	0.201
M18.277	P	0.459	0.266	0.22	0.423	0.088	0.153
M18.278	P	0.663	0.499	0.353	0.216	0.152	0.375
M18.279	P	0.178	1.453	0.195	0.085	1.925	0.196
M18.280	P	0.203	0.459	0.116	0.468	0.08	0.177
M18.286	P	1.501	2.248	0.259	1.175	0.156	0.194
M18.287	P	2.333	2.523	0.409	0.303	0.078	0.145
M18.290	N	0.045	0.04	0.083	0.131	0.051	0.206
M18.291	N	0.037	0.025	0.087	0.211	0.065	0.156
M18.292	N	0.029	0.03	0.058	0.095	0.03	0.086
M18.293	N	0.05	0.031	0.124	0.102	0.095	0.088
M18.294	N	0.06	0.047	0.113	0.206	0.091	0.183
M18.295	N	0.005	0.008	0.023	0.043	0.01	0.031
M18.296	N	0.046	0.022	0.107	0.111	0.027	0.132
M18.297	N	0.069	0.06	0.089	0.184	0.102	0.154
M18.298	N	0.032	0.027	0.057	0.11	0.054	0.108
M18.299	N	0.118	0.075	0.118	0.215	0.171	0.184
M18.300	N	0.07	0.058	0.105	0.203	0.056	0.154
M18.301	N	0.082	0.053	0.157	0.246	0.103	0.218
M18.302	N	0.064	0.1	0.082	0.14	0.057	0.138
M18.303	N	0.042	0.032	0.048	0.098	0.059	0.085
M18.304	N	0.093	0.077	0.117	0.208	0.075	0.212
M18.305	N	0.019	0.018	0.042	0.056	0.02	0.047
M18.306	N	0.048	0.013	0.025	0.074	0.106	0.06
M18.307	N	0.063	0.044	0.063	0.141	0.079	0.18
M18.308	N	0.117	0.086	0.291	0.279	0.102	0.28
M18.309	N	0.112	0.115	0.135	0.205	0.054	0.139
M18.310	N	0.116	0.067	0.126	0.27	0.072	0.307
M18.311	N	0.151	0.069	0.155	0.241	0.181	0.25
M18.312	N	0.115	0.069	0.172	0.29	0.183	0.334
M18.313	N	0.003	0.029	0.039	0.081	0.027	0.078
M18.314	N	0.096	0.065	0.099	0.167	0.102	0.135
M18.315	N	0.1	0.091	0.128	0.194	0.135	0.262
M18.316	N	0.032	0.038	0.041	0.069	0.026	0.098
M18.317	N	0.163	0.083	0.149	0.298	0.114	0.389
M18.318	N	0.031	0.016	0.022	0.056	0.078	0.046
M18.319	N	0.058	0.027	0.066	0.133	0.081	0.145
M18.320	N	0.178	0.102	0.181	0.236	0.214	0.353
M18.321	N	0.057	0.039	0.111	0.202	0.064	0.347
M18.322	N	0.07	0.044	0.074	0.173	0.155	0.223

M18.323	N	0.049	0.045	0.101	0.212	0.092	0.245
M18.324	N	0.069	0.098	0.197	0.324	0.103	0.387
M18.325	N	0.049	0.042	0.063	0.134	0.043	0.371
M18.326	N	0.081	0.051	0.083	0.155	0.067	0.173
M18.327	N	0.056	0.034	0.091	0.121	0.073	0.128
M18.328	N	0.069	0.086	0.09	0.179	0.069	0.266
M18.329	N	0.039	0.031	0.049	0.102	0.053	0.18
M18.330	N	0.074	0.049	0.183	0.27	0.061	0.295
M18.331	N	0.187	0.107	0.242	0.395	0.162	0.31
M18.332	N	0.038	0.087	0.133	0.141	0.059	0.146
M18.333	N	0.145	0.028	0.04	0.099	0.047	0.112
M18.334	N	0.128	0.044	0.258	0.207	0.092	0.215
M18.335	N	0.153	0.091	0.161	0.305	0.179	0.423
M18.336	N	0.126	0.105	0.123	0.265	0.185	0.412
M18.337	N	0.082	0.053	0.15	0.176	0.106	0.135
M18.338	N	0.163	0.049	0.15	0.371	0.074	0.177
M18.339	N	0.202	0.112	0.148	0.325	0.138	0.286
M18.340	N	0.111	0.051	0.156	0.265	0.119	0.187
M18.341	N	0.118	0.084	0.145	0.248	0.091	0.175
M18.342	N	0.055	0.04	0.101	0.142	0.056	0.104
M18.343	N	0.012	0.013	0.03	0.044	0.076	0.041
M18.344	N	0.017	0.027	0.025	0.041	0.036	0.028
M18.345	N	0.098	0.067	0.102	0.179	0.092	0.12
M18.346	N	0.119	0.091	0.132	0.272	0.037	0.152
M18.347	N	0.142	0.168	0.22	0.288	0.065	0.197
M18.348	N	0.25	0.111	0.231	0.449	0.044	0.191
M18.349	N	0.086	0.073	0.113	0.141	0.189	0.11
M18.350	N	0.062	0.059	0.092	0.126	0.05	0.108
M18.351	N	0.078	0.05	0.353	0.139	0.031	0.124
M18.352	N	0.072	0.04	0.129	0.14	0.021	0.112
M18.353	N	0.135	0.092	0.207	0.288	0.091	0.302
M18.354	N	0.037	0.043	0.046	0.096	0.1	0.084
M18.355	N	0.075	0.045	0.06	0.169	0.15	0.158
M18.356	N	0.047	0.023	0.049	0.102	0.094	0.38
M18.357	N	*0.251*	0.181	0.249	0.156	0.033	0.395
M18.358	N	0.047	0.018	0.052	0.119	0.059	0.091
M18.359	N	0.037	0.031	0.04	0.11	0.072	0.053
M18.360	N	0.02	0.011	0.028	0.047	0.021	0.027
M18.361	N	0.095	0.065	0.079	0.28	0.091	0.288
M18.363	N	0.169	0.133	0.137	0.221	0.15	0.189
M18.364	N	0.128	0.065	0.171	0.193	0.094	0.18

M18.365	N	0.031	0.026	0.014	0.065	0.033	0.055
M18.366	N	0.102	0.045	0.098	0.223	0.059	0.187
M18.367	N	0.074	0.034	0.087	0.145	0.072	0.144
M18.368	N	0.031	0.029	0.064	0.113	0.053	0.078
M18.369	N	0.1	0.066	0.125	0.165	0.07	0.156
M18.370	N	0.046	0.029	0.036	0.112	0.031	0.064
M18.371	N	0.049	0.04	0.038	0.097	0.043	0.068
M18.372	N	0.04	0.066	0.025	0.062	0.05	0.055
M18.373	N	0.134	0.108	0.14	0.27	0.109	0.225
M18.374	N	0.153	0.167	0.114	0.231	0.114	0.24
M18.375	N	0.108	0.06	0.146	0.288	0.077	0.212
M18.376	N	0.088	0.041	0.135	0.229	0.041	0.176
M18.377	N	0.045	0.046	0.062	0.209	0.047	0.093
M18.378	N	0.076	0.153	0.062	0.106	0.073	0.091
M18.379	P	1.927	1.682	0.524	1.476	0.213	0.213
M18.380	P	0.602	0.367	0.26	0.786	0.209	0.303
M18.381	P	1.354	0.169	0.122	0.735	0.377	0.228
M18.382	P	2.0971	1.65	0.188	0.832	0.674	0.327
M18.383	P	1.315	1.95	0.054	0.341	0.527	0.111

Table 52 ELISA results for each HCV antigen ELISA with DBS samples of known anti-HCV status. anti-HCV column is HCV status determined by Roche Cobas anti-HCVII assay, P=Positive, N=Negative, OD results – blank are given for each HCV antigen.